

**DIOGO SALLES CORRÊA**

**“Methodology for Evaluating the Collective Harmonic Impact of Residential Loads in Modern Power Distribution Systems”**

*“Metodologias para a Avaliação do Impacto Harmônico Coletivo de Cargas Residenciais em Modernos Sistemas de Distribuição de Energia Elétrica”*

**Campinas**

**2012**



**Universidade Estadual de Campinas**  
**Faculdade de Engenharia Elétrica e de Computação**  
**Departamento de Sistemas de Energia Elétrica**

**DIOGO SALLES CORRÊA**

**“METHODODOLOGY FOR EVALUATING THE COLLECTIVE HARMONIC IMPACT  
OF RESIDENTIAL LOADS IN MODERN POWER DISTRIBUTION SYSTEMS”**

***“METODOLOGIAS PARA A AVALIAÇÃO DO IMPACTO HARMÔNICO COLETIVO DE  
CARGAS RESIDENCIAIS EM MODERNOS SISTEMAS DE DISTRIBUIÇÃO DE  
ENERGIA ELÉTRICA”***

Doctorate Thesis presented to the School of Electrical and Computer Engineering of University of Campinas to obtain the Ph.D. grade in Electrical Engineering

Tese De Doutorado apresentada a Faculdade de Engenharia Elétrica e Computação da Universidade Estadual de Campinas para Obtenção Do Título De Doutor em Engenharia Elétrica

**Tutor: Associate Professor Walmir de Freitas Filho**

***Orientador: Prof. Dr. Walmir de Freitas Filho***

**Campinas**

**2012**

FICHA CATALOGRÁFICA ELABORADA PELA  
BIBLIOTECA DA ÁREA DE ENGENHARIA E ARQUITETURA - BAE - UNICAMP

Sa34m	<p>Salles Corrêa, Diogo</p> <p>Metodologias para a avaliação do impacto harmônico coletivo de cargas residenciais em modernos sistemas de distribuição de energia elétrica / Diogo Salles Corrêa. -- Campinas, SP: [s.n.], 2012.</p> <p>Orientador: Walmir de Freitas Filho .</p> <p>Tese de Doutorado - Universidade Estadual de Campinas, Faculdade de Engenharia Elétrica e de Computação.</p> <p>1. Análise estocástica . 2. Harmônicos (Ondas elétricas). 3. Energia elétrica-distribuição. I. Freitas Filho, Walmir de. II. Universidade Estadual de Campinas. Faculdade de Engenharia Elétrica e de Computação. III. Título.</p>
-------	---

Título em Inglês: Methodology for evaluating the collective harmonic impact of residential loads in modern power distribution systems

Palavras-chave em Inglês: Stochastic analysis, Harmonics (Electric waves), Electric Power - Distribution

Área de concentração: Energia Elétrica

Titulação: Doutor em Engenharia Elétrica

Banca examinadora: Denis Vinicius Coury, Nelson Kagan, José Antenor Pomílio , Luiz Carlos Pereira da Silva

Data da defesa: 04-06-2012

Programa de Pós Graduação: Engenharia Elétrica

## COMISSÃO JULGADORA - TESE DE DOUTORADO


**Candidato:** Diogo Salles Corrêa

**Data da Defesa:** 4 de junho de 2012

**Título da Tese:** "Methodology for Evaluating the Collective Harmonic Impact of Residential Loads in Modern Power Distribution Systems"

Prof. Dr. Walmir de Freitas Filho (Presidente):  \_\_\_\_\_

Prof. Dr. Denis Vinicius Coury:  \_\_\_\_\_

Prof. Dr. Nelson Kagan:  \_\_\_\_\_

Prof. Dr. José Antonio Pomílio:  \_\_\_\_\_

Prof. Dr. Luiz Carlos Pereira da Silva:  \_\_\_\_\_



# Abstract

The proliferation of electronic-based residential loads has resulted in significant harmonic distortion in the voltages and currents of distribution power systems. There is an urgent need for techniques that can determine the collective harmonic impact of these modern residential loads. Such techniques can be used, for example, to predict the harmonic effects of widespread adoption of compact fluorescent lights (CFLs). In response to this need, this PhD thesis proposes a versatile Monte Carlo simulation method for evaluating the potential impact of such residential loads on the harmonic levels of power distribution systems. The method models the random harmonic current injections of residential loads by simulating their operating states. This is done by determining the switch-on probability of a residential load based on load research results. The result is a time-varying harmonic equivalent circuit representing a residential house. By combining multiple residential houses supplied from a service transformer, a probabilistic model for service transformers is also derived. Field measurement results confirmed the validity of the proposed technique. The proposed methodology is applied to a typical distribution system for evaluating the impact of residential loads on several power quality aspects. The results of different case studies proved to be valuable in answering the following questions: (1) What are the potential power quality impacts of distributed nonlinear residential loads on primary and secondary power distribution systems? The example impacts include voltage distortion, zero sequence harmonics, neutral voltage/current rise, telephone interference, metering error, increased losses, overloading of distribution transformers. (2) How serious the impacts will become when more and more energy efficient appliances and consumer electronics penetrates into the residential loads? (3) If the consequence is of concern, what are the strategies and options available for utilities to manage the problem?

**Keywords:** Distribution systems, power quality, residential loads, statistical analysis, time-varying harmonics.





# Resumo

A penetração em massa de equipamentos eletrônicos de maior eficiência energética em residências está resultando em distorções significativas das formas de onda de tensão e corrente dos modernos sistemas de distribuição. Há uma necessidade crescente de técnicas que permitam determinar o impacto coletivo destas cargas residenciais nos níveis de distorção harmônica. Tais técnicas podem ser usadas, por exemplo, para prever os impactos da adoção em massa de lâmpadas fluorescentes compactas. Nesse contexto, esta tese de doutorado propõe uma técnica probabilística para avaliação do impacto dessas cargas residenciais na qualidade de energia tanto no primário como no secundário dos sistemas de distribuição de energia elétrica. O método modela individualmente e de forma estocástica as injeções harmônicas dos típicos eletrodomésticos a partir da distribuição da probabilidade de que cada aparelho seja ligado, a qual foi obtida a partir da pesquisa de dados de comportamento de carga. O resultado é um circuito elétrico equivalente harmônico variável no tempo representando uma casa residencial. Além disso, um modelo probabilístico para transformadores de distribuição foi desenvolvido através da combinação do transformador e das casas conectadas. Resultados de medições de campo confirmaram a validade da modelagem proposta. Em seguida, a metodologia proposta foi aplicada para investigar o impacto de tais cargas residenciais sobre a qualidade de energia dos sistemas de distribuição, tanto no primário como no secundário. Impactos como distorção harmônica na tensão e corrente; carregamento do transformador; elevação da tensão e corrente do neutro; interferência telefônica foram avaliados. A evolução dos impactos ao longo dos próximos anos, a partir de dados de tendências de mercado, também foi determinada. Adicionalmente, realizaram-se estudos para verificar a eficácia de duas soluções possíveis para mitigar distorção harmônica, sendo que a primeira consistiu em adotar os limites de emissão harmônica definidos pelo guia técnico IEC; e a segunda consistiu na instalação de filtros harmônicos no primário do sistema de distribuição.

**Palavras-chave:** Análise estocástica, cargas residenciais, harmônicos, qualidade de energia, sistemas de distribuição.



*"In science one tries to tell people, in such  
a way as to be understood by everyone,  
something that no one ever knew before.  
But in poetry, it's the exact opposite.*

**- Paul Dirac**



# Acknowledgements

Let me present my acknowledgements in my native language:

- À minha família, em especial à minha mãe Silvia, por me apoiar em todos os momentos.
- Ao professor Walmir de Freitas Filho pela excelente orientação, paciência e amizade;
- Ao professor Wilsun Xu pela orientação durante meu doutorado sanduíche na Universidade de Alberta, Canadá;
- Aos professores Denis Vinícius Coury, Nelson Kagan, José Antenor Pomilio e Luiz Carlos Pereira da Silva pelas sugestões e contribuições para a melhoria dessa tese de doutorado;
- Aos professores da Faculdade de Engenharia Elétrica e Computação da UNICAMP;
- Aos colegas do Departamento de Sistemas de Energia Elétrica da UNICAMP;
- Aos colegas do *Power Disturbance and Signalling (PDS) Research Lab* da Universidade de Alberta, Canadá;
- À FAPESP, CNPq e CAPES pelo apoio financeiro.



# TABLE OF CONTENTS

Abstract.....	vii
Resumo.....	ix
Acknowledgements .....	xiii
<b>Chapter 1 INTRODUCTION .....</b>	<b>1</b>
<b>Chapter 2 MODELING AND USAGE TREND OF RESIDENTIAL LOADS .....</b>	<b>7</b>
<b>2.1. Electrical Characteristics of Residential Loads .....</b>	<b>7</b>
2.1.1. <i>Linear and Nonlinear Appliances</i> .....	11
2.1.2. <i>Modeling of Home Appliances</i> .....	15
<b>2.2. Trends in Residential Loads Usage .....</b>	<b>18</b>
2.2.1. <i>Lighting Home Appliances</i> .....	19
2.2.2. <i>Televisions</i> .....	19
2.2.3. <i>Personal Computers</i> .....	20
2.2.4. <i>Printers</i> .....	22
2.2.5. <i>Major Residential Loads</i> .....	22
2.2.6. <i>Other Residential Loads</i> .....	24
<b>Chapter 3 MODELING OF RESIDENTIAL HOUSES .....</b>	<b>25</b>
<b>3.1. Overview of the Proposed Method .....</b>	<b>25</b>
<b>3.2. Residential Load Profile Modeling.....</b>	<b>26</b>
3.2.1. <i>Daily Time of Use Probability Profiles</i> .....	27
3.2.2. <i>Appliance Duration Characteristics</i> .....	32
3.2.3. <i>Size and Occupancy Pattern of Household</i> .....	34
3.2.4. <i>Probabilistic Model of Residential Load Switching-on</i> .....	35
<b>3.3. Single House Validation Studies .....</b>	<b>41</b>
<b>3.4. Service Transformer Validation Studies .....</b>	<b>47</b>
<b>3.5. Summary.....</b>	<b>53</b>
<b>Chapter 4 MODELING AND SIMULATION OF SECONDARY DISTRIBUTION SYSTEMS.....</b>	<b>55</b>
<b>4.1. Distribution System Modeling .....</b>	<b>56</b>
4.1.1. <i>Primary System Model</i> .....	56
4.1.2. <i>Service Transformer Model</i> .....	58
4.1.3. <i>Secondary System Model</i> .....	58
<b>4.2. Simulation Technique.....</b>	<b>59</b>
<b>4.3. Model Parameters Used for Simulation Studies .....</b>	<b>61</b>
<b>4.4. Results of Interest for Secondary System Analysis.....</b>	<b>62</b>
<b>Chapter 5 MODELING AND SIMULATION OF PRIMARY DISTRIBUTION SYSTEMS.....</b>	<b>65</b>
<b>5.1. Primary System Model .....</b>	<b>66</b>
<b>5.2. Service Transformer and Secondary System Model .....</b>	<b>67</b>
<b>5.3. Simulation Procedure for Primary System Analysis.....</b>	<b>68</b>
<b>5.4. Model Parameters Used for Simulation Studies .....</b>	<b>69</b>

<b>5.5. Results of Interest for Primary System Analysis .....</b>	<b>70</b>
<b>Chapter 6 HARMONIC IMPACTS ON SECONDARY DISTRIBUTION SYSTEMS .....</b>	<b>75</b>
<b>6.1. Study Scenarios .....</b>	<b>76</b>
<b>6.2. Base Case Results .....</b>	<b>77</b>
6.2.1. <i>Voltage and current distortions in the secondary system .....</i>	77
6.2.2. <i>Neutral conductor current &amp; voltage rise .....</i>	78
6.2.3. <i>Impact of harmonics on the secondary system losses .....</i>	79
6.2.4. <i>Overloading of distribution transformers .....</i>	80
<b>6.3. Load Evolution Results.....</b>	<b>81</b>
6.3.1. <i>Harmonic voltage and current distortions.....</i>	82
6.3.2. <i>Neutral harmonic voltage and current .....</i>	84
6.3.3. <i>Power losses.....</i>	85
6.3.4. <i>Impact of harmonics on revenue meter errors.....</i>	88
6.3.5. <i>Impact on service transformer .....</i>	88
<b>6.4. Summary of Findings .....</b>	<b>90</b>
<b>Chapter 7 HARMONIC IMPACTS ON PRIMARY DISTRIBUTION SYSTEMS .....</b>	<b>93</b>
<b>7.1. Study Scenarios .....</b>	<b>93</b>
<b>7.2. Base Case Results .....</b>	<b>94</b>
7.2.1. <i>Voltage and current distortions in the primary system.....</i>	95
7.2.2. <i>Telephone interference level .....</i>	97
7.2.3. <i>Neutral conductor current/voltage rise .....</i>	99
7.2.4. <i>Harmonic-caused losses .....</i>	100
<b>7.3. Load Evolution Results.....</b>	<b>101</b>
7.3.1. <i>Harmonic voltage and current distortions.....</i>	101
7.3.2. <i>Telephone interference in the form of IT factors .....</i>	103
7.3.3. <i>Neutral conductor current/voltage rise .....</i>	104
7.3.4. <i>Harmonic-caused losses .....</i>	105
7.3.5. <i>Substation capacitor loading .....</i>	107
7.3.6. <i>Harmonic current penetration into the transmission system.....</i>	110
<b>7.4. Summary of Findings .....</b>	<b>110</b>
<b>Chapter 8 HARMONIC MITIGATION STUDIES .....</b>	<b>113</b>
<b>8.1. The Need for Mitigating Harmonics from Residential Customers .....</b>	<b>113</b>
<b>8.2. Harmonic Mitigation Using IEC Limits .....</b>	<b>115</b>
8.2.1. <i>IEC Standard 61000-3-2.....</i>	115
8.2.2. <i>Case Study Description.....</i>	117
8.2.3. <i>Results of the Secondary System .....</i>	118
<b>8.3. Harmonic Mitigation Using Passive Filters .....</b>	<b>120</b>
<b>8.4. Harmonic Mitigation Effectiveness for Primary System .....</b>	<b>123</b>
8.4.1. <i>Harmonic voltage and current distortions.....</i>	124
8.4.2. <i>Telephone interference levels .....</i>	125
8.4.3. <i>Neutral conductor current .....</i>	127
<b>8.5. Summary.....</b>	<b>127</b>
<b>Chapter 9 CONCLUSIONS AND FUTURE WORK.....</b>	<b>129</b>
<b>Chapter 10 REFERENCES .....</b>	<b>133</b>



<b>Appendix A</b>	<b>Harmonic Data of Home Appliances .....</b>	<b>141</b>
<b>Appendix B</b>	<b>V x I Characteristics of Home Appliances.....</b>	<b>143</b>
<b>Appendix C</b>	<b>Service Transformer Model.....</b>	<b>147</b>
<b>Appendix D</b>	<b>Case Study Using an Actual System.....</b>	<b>155</b>
<b>Appendix E</b>	<b>Publications .....</b>	<b>165</b>



## LIST OF TABLES

Table 2.1: Measured home appliances.....	8
Table 2.2: Harmonic magnitude characteristics of home appliances. ....	9
Table 2.3: Comparing the harmonic impact of one unit of home appliances. ....	10
Table 2.4: Linear and nonlinear appliances. ....	14
Table 2.5: Fundamental active and reactive power of the linear appliances. ....	16
Table 3.1: Appliance usage pattern for major appliances.....	33
Table 3.2: Average appliance usage pattern for other appliances. ....	34
Table 3.3: Occupancy pattern for a typical household. ....	35
Table 3.4: Simulation results of a residential house ( $I_{\text{house}}(h)$ ). ....	45
Table 3.5: Field measurement results of a residential house. ....	45
Table 3.6: Percentage of variance of the first principal component of transformer current. ....	49
Table 3.7: Standard deviation of the residue of measured and simulated fundamental and 3 <sup>rd</sup> harmonic current. ....	52
Table 3.8: Average standard deviation of higher order harmonic currents. ....	53
Table 4.1: Base case system parameters. ....	61
Table 5.1: Base case system parameters. ....	70
Table 5.2: Telephone interference factor (TIF) weighting at different frequencies [6].....	72
Table 7.1: Capacitor loading limits (related to its rating). ....	108
Table 8.1: Limits for Class A equipment.....	116
Table 8.2: Limits for Class C equipment.....	116
Table 8.3: Limits for Class D equipment.....	117
Table 8.4: Impact of IEC limits on the transformer loading.....	120
Table 8.5: Parameters of harmonic filters.....	122



## LIST OF FIGURES

Figure 1.1: Distribution system with multiple harmonic sources. ....	2
Figure 2.1: Harmonic phase characteristics of home appliances [5]. ....	11
Figure 2.2: Correlation between V and I of linear appliances. ....	12
Figure 2.3: Correlation between V and I of nonlinear appliances. ....	13
Figure 2.4: Model for linear appliances. ....	15
Figure 2.5: Model for nonlinear appliances. ....	16
Figure 2.6: Current waveform measured from CFLs of different brands. ....	18
Figure 2.7: Trends on the number of CFLs and incandescent lamps per household. ....	19
Figure 2.8: Trends on the number of CRT and LCD TVs per household. ....	20
Figure 2.9: Trend on the number of computers per household. ....	21
Figure 2.10: Trends on the number of laptops and desktops per household. ....	21
Figure 2.11: Trend on the number of printers per household. ....	22
Figure 2.12: Trends on the number of energy conservation and regular fridges per household. ....	23
Figure 2.13: Trends on the number of front-loading and top-loading washers per household. ....	24
Figure 3.1: Structure of the bottom-up model for a residential house. ....	26
Figure 3.2: Time of use probability profile for cooking activity. ....	28
Figure 3.3: Time of use probability profile for breakfast related activities. ....	28
Figure 3.4: Time of use probability profile for stove (range). ....	29
Figure 3.5: Time of use probability profile for laundry activity. ....	29
Figure 3.6: Time of use probability profile for television. ....	30
Figure 3.7: Time of use probability profile for personal computer (PC). ....	30
Figure 3.8: Time of use probability profile for bathroom lighting. ....	31
Figure 3.9: Time of use probability profile for house clean activity. ....	31
Figure 3.10: Time of use probability profile for occasional events. ....	32
Figure 3.11: Procedure to determine switch-on events of appliances. ....	37
Figure 3.12: Time of use probability profile calibration with occupancy function. ....	39
Figure 3.13: Time of use probability profile for microwave. ....	40
Figure 3.14: Time of use probability profile for different residential loads. ....	41
Figure 3.15: Power distribution system for three-wire single-phase feeding systems. ....	42
Figure 3.16: Equivalent circuit model to represent a residential house. ....	43
Figure 3.17: The simulation output $I_{\text{house}}(h)$ of a house during one day. ....	44
Figure 3.18: House total impedance. ....	46
Figure 3.19: Cumulative distribution of the house total impedance (30 days). ....	46
Figure 3.20: The equivalent service transformer circuit model. ....	47
Figure 3.21: Example of transformer current output during one weekday obtained from real field measurement. ....	48
Figure 3.22: Comparison of the first principal components (weekdays). ....	51
Figure 3.23: Comparison of the first principal components (weekends). ....	51
Figure 3.24: Probability distribution of measured and simulated residue part for weekdays. ....	52
Figure 3.25: Probability distribution curves of higher harmonics (weekdays). ....	53
Figure 4.1: Layout of a MGN distribution system. ....	56
Figure 4.2: Schematic model to study secondary distribution systems. ....	56
Figure 4.3: Equivalent MGN primary distribution system. ....	57

Figure 4.4: Multigrounded neutral ladder network.....	57
Figure 4.5: Single-phase service transformer. ....	58
Figure 4.6: Single house harmonic equivalent model.....	59
Figure 4.7: Harmonic power flow simulation procedure for the secondary system.....	61
Figure 4.8: Definition of and procedure to determine the “95% index”.....	64
Figure 5.1: Multigrounded 4-wire distribution system.....	65
Figure 5.2: Four-wire (four-phase) feeder model. ....	67
Figure 5.3: Simplified model of the service transformer and its loads.....	68
Figure 5.4: Harmonic power flow simulation procedure for the primary system. ....	69
Figure 5.5: Distribution network model for primary system analysis. ....	70
Figure 6.1: Average harmonic phase voltages of all houses.....	77
Figure 6.2: Average harmonic phase current of all houses.....	77
Figure 6.3: Average neutral to ground voltage. ....	79
Figure 6.4: Average neutral current circulating between the houses.....	79
Figure 6.5: Secondary system power losses. ....	80
Figure 6.6: Service transformer power losses.....	81
Figure 6.7: Average phase A voltage.....	83
Figure 6.8: Average phase A current. ....	83
Figure 6.9: Average neutral voltage level.....	84
Figure 6.10: Average neutral current circulating between the houses.....	85
Figure 6.11: Total fundamental power losses at the secondary system.....	86
Figure 6.12: Total harmonic power losses at the secondary system.....	87
Figure 6.13: Power loss and K-factor of service transformer.....	89
Figure 6.14: Average annual growth for main power quality indices. ....	90
Figure 7.1: Average imbalance level on the distribution network.....	95
Figure 7.2: Average dominant sequence voltage.....	96
Figure 7.3: Average zero sequence voltage. ....	96
Figure 7.4: Average dominant sequence current. ....	97
Figure 7.5: Average zero sequence current.....	97
Figure 7.6: Average individual and total IT levels at the primary system.....	98
Figure 7.7: Schematic representation of the telephone line in parallel to the primary system. ....	98
Figure 7.8: Voltage induced at the end of a telephone line. ....	99
Figure 7.9: Average neutral voltage level at the primary system. ....	99
Figure 7.10: Average neutral current level at the primary system.....	100
Figure 7.11: Daily profile of the total active power losses at the primary system. ....	100
Figure 7.12: Growth characteristics of dominant sequence voltages in the primary system.....	102
Figure 7.13: Growth characteristics of zero sequence voltages in the primary system.....	102
Figure 7.14: Growth characteristics of dominant sequence currents in the primary system. ....	103
Figure 7.15: Growth characteristics of zero sequence currents in the primary system. ....	103
Figure 7.16: Growth characteristics of IT index in the primary system. ....	104
Figure 7.17: Growth characteristics of induced voltage on a parallel conductor. ....	104
Figure 7.18: Growth characteristics of neutral voltage in the primary system. ....	104
Figure 7.19: Growth characteristics of neutral current in the primary system. ....	105
Figure 7.20: Total fundamental power losses at the primary system. ....	106
Figure 7.21: Harmonic power losses at the primary system. ....	107
Figure 7.22: Harmonic voltage and current levels at the substation capacitor. ....	109

Figure 7.23: Capacitor loading indices. ....	109
Figure 7.24: Growth characteristics of the harmonics entering into transmission system. ....	110
Figure 7.25: Average annual growth rate of key power quality indices. ....	112
Figure 8.1: Suburban residential customer clusters supplied by one distribution feeder. ....	114
Figure 8.2: Harmonic current spectrum of neighborhood loads. ....	114
Figure 8.3: Harmonic current limits of IEEE Std. 519. ....	114
Figure 8.4: Measured and modified (IEC limits) harmonic spectra for four appliances. ....	117
Figure 8.5: Impact of IEC limits on secondary system voltage. ....	118
Figure 8.6: Impact of IEC limits on phase voltage of the secondary system. ....	119
Figure 8.7: Impact of IEC limits on phase current of the secondary system. ....	119
Figure 8.8: Single tuned filter and associated frequency response. ....	120
Figure 8.9: The Yg/Δ transformer based filter. ....	121
Figure 8.10: Frequency scan for each individual tuned harmonic filter. ....	122
Figure 8.11: Feeder harmonic currents as affected by filters locations. ....	123
Figure 8.12: System and 3rd and 5th filters frequency scan. ....	123
Figure 8.13: Effects of mitigation options on feeder harmonic voltage. ....	124
Figure 8.14: Effects of mitigation options on feeder harmonic current. ....	125
Figure 8.15: Effects of mitigation options on the harmonics entering into transmission system. ....	125
Figure 8.16: Effects of mitigation options on the IT levels at the primary system. ....	126
Figure 8.17: Effects of mitigation options on the voltage induced in a parallel conductor. ....	126
Figure 8.18: Effects of installing 9th and 15th filters on telephone interference. ....	126
Figure 8.19: Effects of mitigation options on the average neutral current levels. ....	127





---

# Chapter 1

## INTRODUCTION

---

The proliferation of electronic-based modern residential loads (home appliances<sup>1</sup>) has resulted in significant harmonic distortions in the voltages and currents of residential power distribution systems [1]-[6]. These new harmonic sources have comparable sizes and are distributed all over a network. Although they produce insignificant harmonic currents individually, the collective effect of a large number of such loads can be substantial. For example, the 3<sup>rd</sup> harmonic has become a main contributor to the feeder voltage distortion [1]-[3], 9<sup>th</sup> harmonic has caused telephone interference in a number of cases [6]-[7], metering and instrumentation may be affected by harmonic components [8]-[9]. At present, there is an urgent need for techniques that can determine the collective harmonic impact of modern residential loads. Such techniques can be used, for example, to predict the harmonic effects of intensive adoption of CFLs (compact fluorescent lights) and to quantify the effectiveness of certain harmonic control measures. One such measure is to adopt the IEC device level limits<sup>2</sup> [10].

Traditional techniques for harmonic power flow analysis generally have difficulties in determining the collective impact of mass distributed harmonic sources. To make the problem manageable, some researchers have sub-divided the problem into two types. One assumes that the harmonic-producing loads are deterministic and the other that the loads vary randomly [12]-[16]. This PhD thesis deals with the second type of problem, namely the random variation of distributed harmonic loads. The problem of probabilistic harmonic distortion assessment is explained as follows.

---

<sup>1</sup>In this thesis, the terms “residential load” and “home appliance” are used interchangeably.

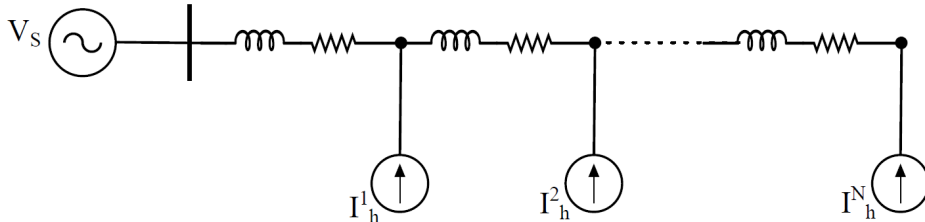
<sup>2</sup>IEEE established a task force (P1495) to build a standard establishing equipment harmonic limits, much like IEC 61000-3-2, however, currently, it is inactive and the standard project is no longer endorsed by IEEE due to lack of consensus among the various parties involved. The following text (extracted from [11]) was the initial motivation for establishing this standard “*What is found is a wide range of nonlinear devices that have been identified which collectively need to be considered for future power distribution systems. In addition, there are some newer technologies being explored which could add to the previous mix. The objective is to arrive at a reasonable set of limits for single-phase equipment such that the likelihood of a problem caused by harmonics is small.*”

Figure 1.1 illustrates a system containing distributed harmonic sources, which are represented as harmonic current sources. The current sources interact with the system impedance and produce harmonic voltages at various locations of the system. The impact of the  $i^{th}$  harmonic current source on the distortion of the bus  $k$  voltage can be determined as follows [16]:

$$V_h^k = Z_h^{ki} \times I_h^i \quad (1.1)$$

where  $V_h^k$  is the  $h^{th}$  harmonic voltage at bus  $k$ ,  $I_h^i$  is the  $h^{th}$  harmonic current injection by the harmonic-producing loads at bus  $i$  and  $Z_h^{ki}$  is the transfer impedance between buses  $i$  and  $k$  at the  $h^{th}$  harmonic frequency. The collective effect of all the sources on the bus  $k$  voltage is the phasor summation of the effect of the individual sources, as follows:

$$V_h^k = \sum_{i=1}^N V_h^{ki} = \sum_{i=1}^N Z_h^{ki} \times I_h^i = Z_h^{k1} \times I_h^1 + Z_h^{k2} \times I_h^2 + \dots + Z_h^{kN} \times I_h^N \quad (1.2)$$



**Figure 1.1: Distribution system with multiple harmonic sources.**

If one knows the magnitude of the harmonic current source accurately, the harmonic voltage can be estimated with good accuracy using the above equation. Traditional harmonic analysis methods are based on such an assumption. The common approach is that a typical harmonic source spectrum of the load is determined first by assuming there is no voltage distortion at the load bus. The spectrum is then used to construct the current sources needed for equation (1.2). Although this approach is generally acceptable for cases involving very small numbers of harmonic sources, it has been very conservative for cases with distributed harmonic sources. If the distributed harmonic sources vary randomly, one cannot use deterministic methods to find the harmonic distortion level.

The application of probabilistic methods for analyzing power system harmonic distortion commenced in the late 1960s [17]. Over the past many years, some researchers have investigated the summation of random harmonic phasors [12]-[13], the algorithms of stochastic harmonic power flows [14]-[15], and methods to predict the mean values of harmonic indices [16]. All

these works have greatly contributed to our understanding on the modeling and analysis of systems with randomly varying harmonic loads. Unfortunately, the available techniques are still not in a shape to fulfill the needs of predicting harmonic distortions caused by consumer behaviour or regulatory policy changes. In other words, using the methods of these works it is very complicated, if not impossible, to determine what will be the impact on the harmonic levels for scenarios like: (a) incandescent lamps are replaced by CFLs, (b) in the next 5 years the penetration of LCD TVs grows 10% (c) what is the effectiveness of enforcing home appliances to comply with harmonic emission levels defined by the IEC 61000-3-2 standard.

To handle this issue, this PhD thesis proposes a versatile method based on Monte Carlo simulation [17]-[18] to study the harmonic impact of residential loads on power distribution systems. The main idea is originated from the following observation: the random harmonic generation of residential loads is almost exclusively due to the random on/off states of the loads. For example, a CFL can be in an ON or OFF state randomly at any given time. But once it is turned on, its harmonic currents essentially follow a known, deterministic spectrum. Therefore, the key to develop the aforementioned harmonic assessment technique is to model the random on/off state change events of residential loads properly. Once the states of all residential loads are known, the problem becomes a deterministic harmonic power flow problem [19]-[20]. Fortunately, a body of knowledge on residential load behaviors has been developed for load research purposes [21]-[24]. These techniques can be adapted to solve the problem of predicting the operating states of residential loads. The result is a time-varying harmonic equivalent circuit representing a residential house. By combining multiple residential houses served by a service transformer, a model for service transformers is also proposed. One of the attractive characteristics of the proposed methodology is its bottom-up approach. As a result, one can simulate the effect of market trends and policy changes. For example, the harmonic impact of CFLs can be studied by adjusting the composition of lighting fixtures in the residential load database.

Then, the proposed methodology is applied to a typical distribution system for evaluating the impact of residential loads on several power quality aspects of both primary and secondary systems. As it will be shown in the following chapters, the results of different case studies proved to be valuable in answering the following questions:

- 1) *What are the potential power quality impacts of mass distributed nonlinear loads on primary and secondary power distribution systems?* The example impacts include voltage distortion, zero sequence harmonics, neutral voltage/current rise, telephone interference, metering error, increased losses, overloading of distribution transformers etc. The following is a more detailed list:
  - i. Harmonic voltage and current distortion levels in the system, in both positive and zero sequences;
  - ii. Telephone interference in the form of IT factors;
  - iii. Harmonic resonance characteristics as affected by underground cables and overhead lines;
  - iv. Neutral current/voltage rise;
  - v. Impact of harmonics on line losses;
  - vi. Impact of harmonics on revenue meter errors;
  - vii. Overloading of distribution transformers; and
  - viii. Overloading of feeder and substation capacitors (fuse blow).
- 2) *How serious the impacts may become if consumers adopt more and more energy efficient appliances and consumer electronics?* Through extensive research work, this thesis established models to represent the growth of electronic appliances in homes.
- 3) *What are the strategies and options available for utilities to manage the situation?* This thesis further investigated the impact of two harmonic management strategies: adopting the IEC standards on limiting harmonic generation from individual appliances and installing system-wide harmonic filters.

This PhD thesis is organized as follows:

- Chapter 2 presents the electrical characteristics and market trends of common home appliances. Based on the findings of previous and additional research works, harmonic models have been developed for home appliances. Through surveying and analyzing various consumer market research data, adoption or usage trends of key home appliances have been established.
- Chapter 3 presents a bottom-up probabilistic electric model for residential houses based

on the behaviours of their inhabitants and the electric characteristics of the appliances. By combining multiple residential houses served by a service transformer, a model for service transformers is also derived. These models are verified by comparing their results with real field measurements.

- Chapter 4 presents the techniques and procedures for assessing the harmonic impact of residential loads on the secondary distribution systems. Several indices are introduced to characterize the impact. Similarly, Chapter 5 presents the techniques and procedures for studying the impact on the primary distribution systems.
- Chapters 6 and 7 present the results and findings of harmonic impact study on the secondary and primary systems respectively. The evolution of home appliances as established by the market trends is taken into account and the annual growth rates of the various harmonic impacts are determined.
- Chapter 8 presents a high-level feasibility and effectiveness study on two harmonic mitigation options to deal with the harmonic distortion situation faced by power distribution systems. These options are (1) adopting the IEC device level harmonic emission limits for home appliances and (2) installing feeder level harmonic filters.
- Chapter 9 summarizes the main findings of this thesis.



---

## Chapter 2

# MODELING AND USAGE TREND OF RESIDENTIAL LOADS

---

In order to develop a tool that can evaluate the impact of distributed nonlinear residential loads on power distribution systems, the initial step is to develop an adequate model for those residential loads. There are three aspects to model a residential load, as follows:

- 1) *Electrical model*: this model is needed for conducting harmonic penetration studies;
- 2) *Usage trend model*: this model helps to predict the extent of residential loads adoption in the future;
- 3) *Status model*: This model helps to determine the operating status (ON and OFF) of a residential load.

This chapter is focused on the first and second models. The third model, which is the main part of the proposed methodology, is presented in Chapter 3.

### 2.1. Electrical Characteristics of Residential Loads

This section presents the characteristics of the currents drawn by common home appliances obtained from laboratory measurements conducted by several researchers at the *Power Disturbance & Signaling Research Laboratory* at the University of Alberta, Canada. The measured appliances commonly found in residential houses in North America are listed in Table 2.1. Codes are assigned to them for easy identification in the figures and tables shown later. This table also identifies the number of measured appliances of each type. In total, 31 types of common appliances are measured and listed. Detailed data about each appliance type are shown in Appendix A. It must be noticed that more than one piece of equipment (i.e., different brands) of the same type was measured for most of the appliances, however, for the sake of space; Appendix A shows only one a representative spectrum for each appliance type. More

measurement results can be found in [5].

**Table 2.1: Measured home appliances.**

Group	Code	Appliance Type	Number Tested
Lighting	CFL	Compact Fluorescent Lamp	12
	EBL	Electric-Ballast Fluorescent Lamp	3
	MBL	Magnetic-Ballast Fluorescent Lamp	1
	INC	Incandescent Lamp	1
Entertainment	PC	Desktop PC	3
	LCD	LCD Computer Monitor	3
	LAP	Laptop	3
	LCD TV	LCD Television	3
	CRT TV	CRT Television	2
Major Appliances	R FR	Regular Fridge	2
	ASD FR	ASD-based Fridge	3
	FRE	Freezer	1
	WSH	ASD-based Washer	1
	DRY	Regular Dryer	1
	ASD DRY	ASD-based Dryer	1
	RAN	Electric Range	3
	OVE	Electric Oven	1
Kitchen	MW	Microwave Oven	3
	TOA	Toaster	1
	COF	Coffee Maker	1
	GRI	Griddle	1
	WAF	Waffle Iron	1
	BRE	Bread Maker	1
	BLE	Blender	2
	FOO	Food Processor	1
Office	PRIN	Printer	1
	COP	Copier	1
Others	KET	Electric Kettle	2
	FUR	Furnace	1
	GAR	Garage Door	1
	VAC	Vacuum Cleaner	2

Table 2.2 shows the main electric results obtained for some of the main home appliances. Those results include the fundamental current Total Harmonic Distortion ( $THD_i$ ), fundamental power factor ( $FPF$ ) and total power factor ( $PF$ ) and, which were calculated by using the IEEE definition [25]. Some appliances have different operating cycles that exhibit different power consumption and harmonic current characteristics. For example, a washing machine can have washing, rinsing and spinning cycles. Other appliances, such as the CFLs, exhibit almost



constant power consumption. Table 2.2 presents the characteristics for the full load under normal operating conditions. The column of “Operating Power” shows the power consumption under normal operating condition. Therefore, for some appliances, the operating power is less than the rated power. For example, a washing machine may be rated as 500W but actually draws power of 180W during normal operation. In the same example, the washing machine operates most of the time in the washing condition, which is the condition corresponding to the full-load under normal operating conditions, and is also the condition in which the device draws the most distorted current.

Table 2.2 confirms that most electronic home appliances are harmonic producers. Many of the electronic appliances such as CFLs, desktop PCs and computer monitors have a THD<sub>I</sub> higher than 100%. Table 2.2 also shows that most of the appliances have reasonably high fundamental frequency power factors, and some of them have a leading power factor (indicated by “\*” in the table). Appendix A

**Table 2.2: Harmonic magnitude characteristics of home appliances.**

Appliance	THD <sub>I</sub> [%]	FPF	PF	Operating power [W]	I <sub>rms</sub> [A]	I <sub>1</sub> [A]
CFL	120	0.9*	0.6	15	0.24	0.15
EBL	140	0.96*	0.56	15	0.24	0.14
MBL	8	0.38	0.38	33	0.73	0.73
PC	112	1	0.69	100	1.30	0.88
LCD	110	0.96*	0.64	40	0.48	0.34
LAP	130	0.96*	0.58	75	1.14	0.68
LCD TV	10	0.99*	0.98	300	2.59	2.58
CRT TV	145	1	0.56	70	1.00	0.57
MW	41	0.99*	0.9	1200	11.08	10.49
ASD FR	7	0.92	0.91	170	1.6	1.6
R FR	16	0.94	0.93	150	1.30	1.27
WSH	75	0.45	0.35	180	4.20	3.36
ASD DRY	55	0.98	0.86	1000	4.90	4.30
FUR	11	0.84	0.84	500	4.85	4.82

In order to compare the harmonic impact of various home appliances, an index called Equivalent-CFL proposed in [5] is used in this thesis. This index quantifies each appliance in terms of its harmonic impact expressed as the number of CFLs it is equivalent to. This index is defined as follows. For each harmonic order  $h$ , the ratio of the appliance’s current to that of the representative CFL current is determined by using the following equation:

$$Ratio_{h\_Appliance} = \frac{I_{h\_appliance}}{I_{h\_CFL}} \quad (2.1)$$

where  $I_{h\_appliance}$  is the appliance's harmonic current at order  $h$ , and  $I_{h\_CFL}$  is the representative CFL harmonic current at order  $h$ . For example, a  $Ratio_h$  of 2 implies that the appliance generates twice as much harmonic current at order  $h$  as the representative CFL. In order to obtain a single index and compare the appliance with a representative CFL, the ratios of different harmonic orders are aggregated into one value by using a weighted average as follows [5]:

$$Equivalent-CFL_{Appliance} = \sqrt{\sum_{h=3}^H (w_h \times Ratio_{h\_Appliance})^2} = \sqrt{\frac{\sum_{h=3}^H I_{h\_Appliance}^2}{\sum_{h=3}^H I_{h\_CFL}^2}} \quad (2.2)$$

The weighting factor  $w_h$  is the individual harmonic distortion of the CFL current. This weighting factor is used because if a CFL produces more harmonic at  $h$ , the harmonics from other appliances will also be treated with more significance at the same order.

The results obtained from the calculated individual Equivalent-CFL index of all appliances are presented in Table 2.3. The results are arranged in the ascending order of the index. This table shows that a desktop PC is equivalent to 7 CFLs in terms of harmonic current injection. A microwave oven has a harmonic impact equivalent to 26.4 CFLs. The table also lists the power ratios with respect to the CFL and the harmonic current ratios from the 3<sup>rd</sup> to the 13<sup>th</sup> harmonics.

**Table 2.3: Comparing the harmonic impact of one unit of home appliances.**

Appliance type	Operating Power [W]	Power Ratio	Eq-CFL	Ratio <sub>3</sub>	Ratio <sub>5</sub>	Ratio <sub>7</sub>	Ratio <sub>9</sub>	Ratio <sub>11</sub>	Ratio <sub>13</sub>
MBL	30	2	0.42	0.56	0.02	0.11	0.08	0.12	0.06
CFL	15	1	1.00	1.00	1.00	1.00	1.00	1.00	1.00
ASD FR	170	11.3	1.14	1.03	0.28	2.74	1.23	0.89	0.60
EBL	18	1.2	1.15	0.99	1.39	1.69	0.60	0.46	1.10
LCD TV	300	20	1.32	1.34	1.56	0.88	0.89	0.58	0.95
R FR	150	10	1.35	1.22	1.33	1.44	1.92	2.08	1.54
LCD	40	2.67	2.35	2.04	3.30	1.24	0.23	1.92	2.43
FUR	500	33.33	2.53	2.68	2.72	1.71	1.26	1.67	1.76
CRT TV	70	4.67	5.81	4.93	6.77	7.02	7.37	7.15	4.42
LAP	75	5	6.15	5.37	5.66	5.57	7.97	11.38	11.05
PC	100	6.67	7.05	7.32	8.02	5.47	2.43	2.58	4.62
ASD DRY	1000	66.67	12.58	15.23	8.26	5.90	10.85	4.90	8.55
MW	1200	80	26.42	33.09	16.72	9.14	7.20	6.13	4.14

The appliances' current phasors at harmonic orders 3<sup>rd</sup>-13<sup>th</sup> are shown in Figure 2.1 [5]. The

phasors use the supply voltage angle as a reference, setting the phase angle of the fundamental frequency voltage to zero. The currents are normalized to emphasize the current harmonic angles and to improve visualization. This figure reveals the potential harmonic cancellation that might occur when 2 or more appliances are operated together. For example, the 3rd harmonic current of the LCD monitor is about  $180^\circ$  out of phase with that of the furnace. Conversely, the 3rd harmonic of the desktop PC is almost in phase ( $0^\circ$ ) with that of the CRT TV.

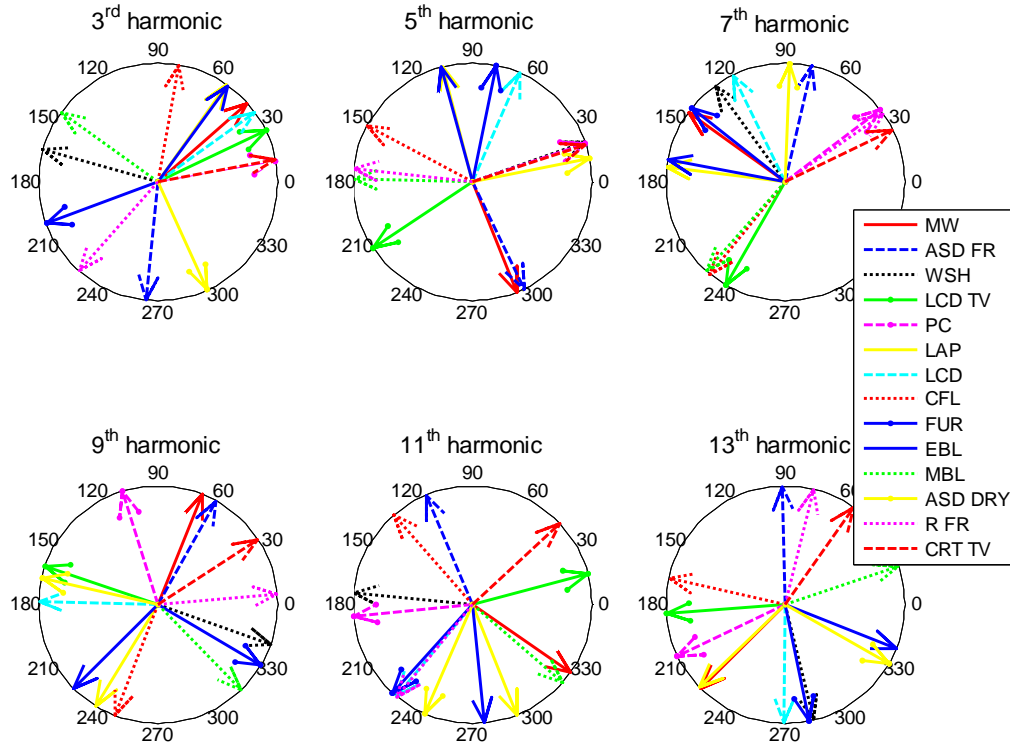
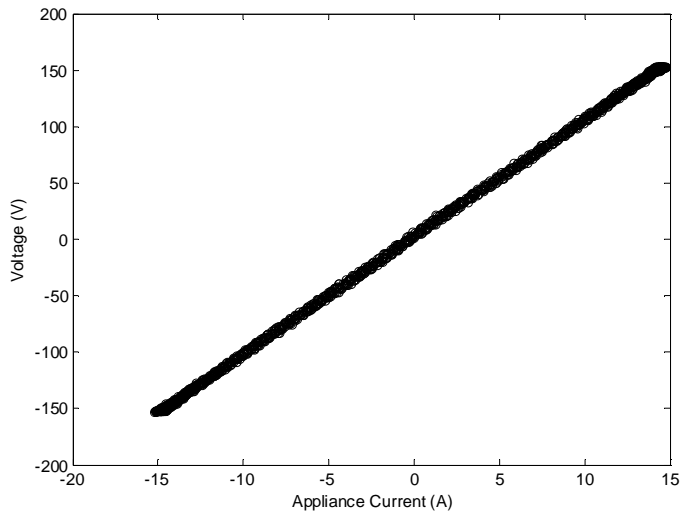


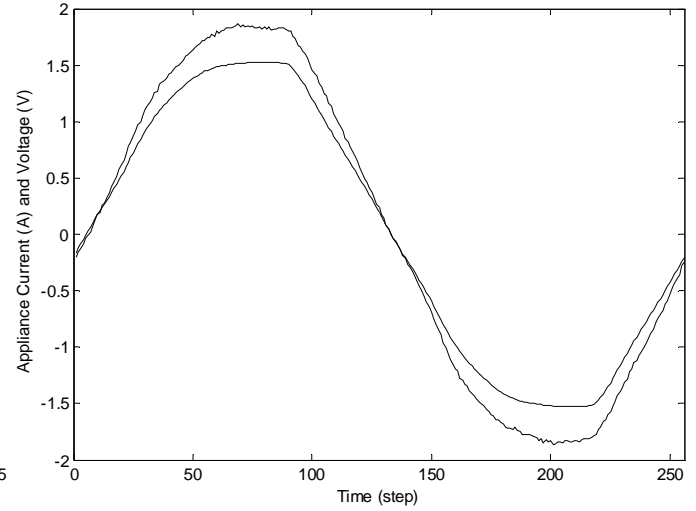
**Figure 2.1: Harmonic phase characteristics of home appliances [5].**

### 2.1.1. Linear and Nonlinear Appliances

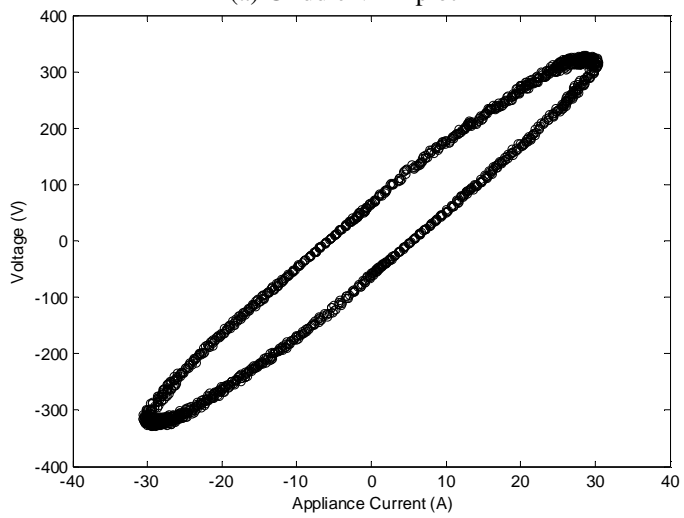
The measurement activities have identified a need to determine which residential loads are linear or nonlinear. In a distorted supply voltage scenario, even a resistive load could have distorted current waveform, appearing as a nonlinear source. In this thesis, the correlation of the instantaneous current and voltage waveforms (V-I plot) are used to separate linear loads from nonlinear loads. The method is illustrated in Figure 2.2 and Figure 2.3 for four residential loads. If the load is linear, the V-I plot is shaped either as a straight line (resistive load) or as a ring (reactive load). The voltage versus current plots for nonlinear residential loads are neither a straight line nor a ring, e.g. the microwave oven in Figure 2.3. Measurements sampling rate is 256 samples per cycle.



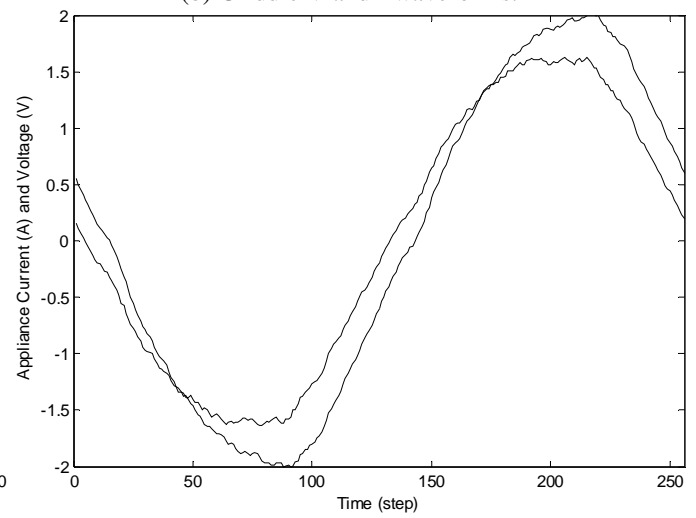
(a) Griddle V x I plot



(b) Griddle V and I waveforms.



(c) Dryer V x I plot



(d) Dryer V and I waveforms.

**Figure 2.2: Correlation between V and I of linear appliances.**

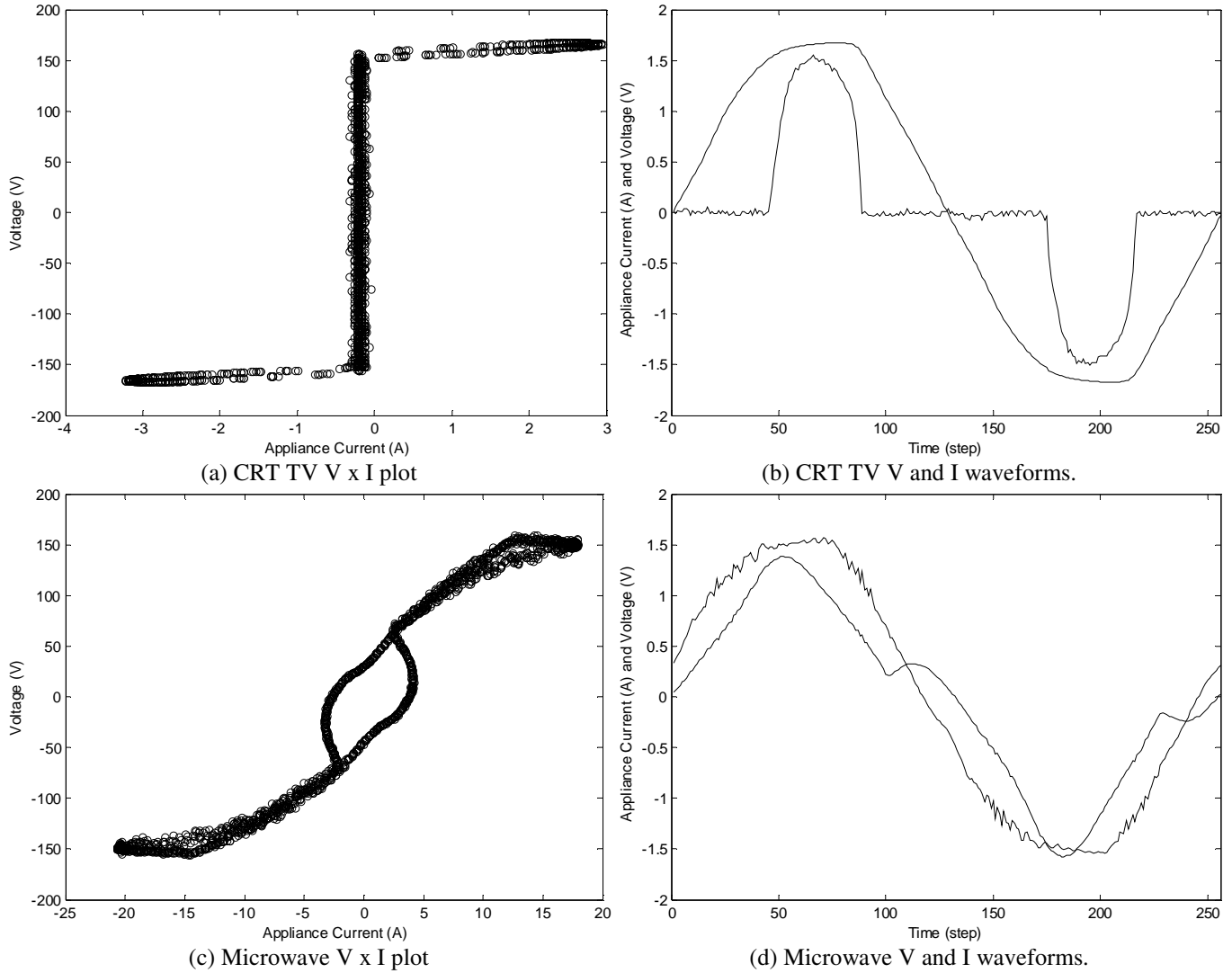


**Figure 2.3: Correlation between V and I of nonlinear appliances.**

The V x I plot for all appliances under analysis in this thesis is shown in Appendix B. Based on this analysis, each appliance is categorized as linear or nonlinear load, as shown in Table 2.4.

**Table 2.4: Linear and nonlinear appliances.**

Appliance Name	Characteristic of Appliance
Compact Fluorescent Lamp	Non-linear
Electric-Ballast Fluorescent Lamp	Non-linear
Magnetic-Ballast Fluorescent Lamp	Linear
Incandescent Lamp	Linear
Desktop PC	Non-linear
LCD Computer Monitor	Non-linear
Laptop	Non-linear
LCD Television	Non-linear
CRT Television	Non-linear
Fridge	Non-linear
Freezer	Non-linear
Washer	Non-linear
Dryer	Linear
Electric Range	Linear
Electric Oven	Linear
Microwave Oven	Non-linear
Toaster	Linear
Coffee Maker	Linear
Griddle	Linear
Waffle Iron	Linear
Bread Maker	Non-linear
Blender	Non-linear
Food Processor	Non-linear
Printer	Non-linear
Copier	Non-linear
Electric Kettle	Linear
Furnace	Non-linear
Garage Door	Non-linear
Vacuum Cleaner	Non-linear

Two observations about the results of Table 2.4 are presented as follows. We observed that the average total harmonic distortion ( $THD_I$ ) of the current measured from regular fridges was found to be around 15% and the ASD fridges around 7%. The measurements results from [4] also show distortion ( $THD_I \approx 9\%$ ) on the current drawn by fridges. The current distortion depends on the motor's design and magnetic saturation can possibly make the distortion worse.

The furnace measured is heat-pump type and the average current THD was found to be around 11%. Some heat pump models produce less harmonics than others. Harmonics are dependent on ambient indoor and outdoor conditions, and whether a heat pump is in heating or cooling mode.

### 2.1.2. Modeling of Home Appliances

As discussed earlier, residential loads are classified as two types, linear and nonlinear. In this thesis, the linear loads are modelled as constant power loads at the fundamental frequency (60Hz) and as impedance at harmonic frequencies, as shown in Figure 2.4, in accordance with [26].

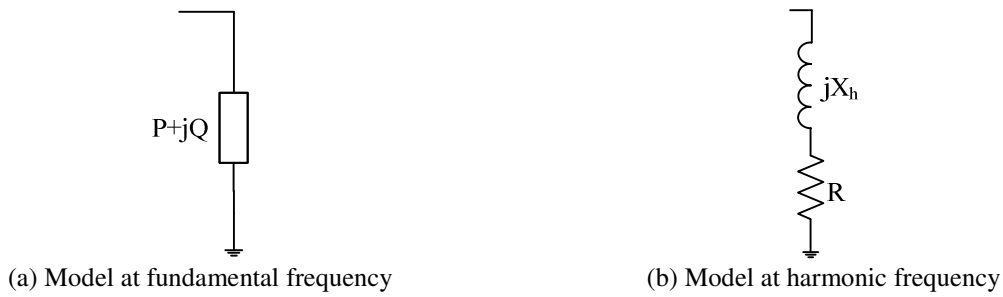


**Figure 2.4: Model for linear appliances.**

The parameters for the model of each linear appliance can be obtained from the measurements according to the following equations:

$$\begin{aligned}
 P + jQ &= V_1 \times \text{conj}(I_1) \\
 R &= \frac{V_1^2}{P} \\
 X_h &= h \times \frac{V_1^2}{Q}
 \end{aligned}
 \tag{2.3}$$

where  $V_1$  and  $I_1$  are the fundamental frequency component of the voltage and current, respectively, measured for a particular appliance.

Table 2.5 presents the active and reactive power consumed by different linear appliances. As it can be seen, the appliances are mainly resistive. The symbol ‘\*’ means that the appliance is two-phase.

**Table 2.5: Fundamental active and reactive power of the linear appliances.**

Device	Brands	P (W)	Q (var)
Magnetic-ballast Fluorescent	1	33.69	80.96
Incandescent Lamp	1	59.28	0.05
Dryer*	1	1262.70	257.15
Range*	1	993.06	6.84
Oven*	1	381.75	1.82
Toaster	1	902.68	11.31
Coffee Maker	1	919.39	11.74
Griddle	1	1384.60	7.98
Waffle Iron	1	972.27	6.56
Electric Kettle	1	1518.80	16.02
	2	1490.50	15.43

The nonlinear loads are modelled as constant power loads at the fundamental frequency (60Hz) and as current sources at harmonic frequencies, as shown in Figure 2.5 [26]. The magnitude and phase of the source is calculated from the harmonic current spectrum of the appliance using the following well-known procedure recommended in [26]:



**Figure 2.5: Model for nonlinear appliances.**

1. The harmonic-producing load is treated as a constant power load at the fundamental frequency, and the fundamental frequency power flow of the system is solved;
2. The current injected from the load to the system is then calculated and is denoted as  $I_h = I_l \angle \theta_l$ ;
3. The magnitude and phase angle of the harmonic current source representing the load are determined as follows:



$$\begin{aligned}
I_h &= I_1 \times \frac{I_{h\text{-spectrum}}}{I_{1\text{-spectrum}}} \\
\theta_h &= \theta_{h\text{-spectrum}} + h \times (\theta_1 - \theta_{h\text{-spectrum}})
\end{aligned}
\tag{2.4}$$

where subscript "spectrum" stands for the typical harmonic current spectrum (obtained from real measurements) of the load, which can be found in Appendix A. The meaning of the magnitude formula is to scale up the typical harmonic current spectrum to match the fundamental frequency power flow result ( $I_1$ ). The phase formula shifts the spectrum waveform to match the phase angle of  $\theta_1$ . Since the  $h$ -th harmonic has  $h$ -times higher frequency, its phase angle is shifted by  $h$  times of the fundamental frequency shift. This spectrum-based current source model is the most common one used in commercial power system harmonic analysis programs. The input data requirement is minimal.

When adopting the current source model for nonlinear loads, the issue of whether to include the attenuation and diversity effects has been examined. Attenuation refers to the reduction of the magnitude of harmonic currents produced by a residential load when its supply voltage is distorted [27]. Based on published research works [15], [26]-[27] and extensive lab tests conducted by [28], we concluded that the attenuation effect becomes significant only when the voltage distortion is quite high (for example, THD above 10%). We have not observed such high voltage distortion level in field nor found from simulation results. So the attenuation effect is omitted from the model proposed at present. This will lead to slightly higher harmonic levels in the system. If the need to include the effect arises, iterative harmonic power flow algorithms can be used [26], [29].

The diversity effect refers to the differences of harmonic current phase angles associated with a residential load [26]-[27]. It is common knowledge that a residential load always produces harmonic currents at the same phase angle with respect to its supply voltage (if given the same operating condition). This is why typical spectrum can be used to model a harmonic-producing load. Figure 2.6 shows the waveforms of multiple CFLs from different vendors [5]. It can be seen that the waveforms are similar, meaning the harmonic angle (and magnitude) differences are small. As a result, the random variation of phase angles from their mean values is not included in the electrical model. The variation due to different brands can be included in the Monte Carlo sampling explained later. It is important to note that the variation of phase angles caused by the variation of the phase angles of supply voltages is included through equation (2.4).

Harmonic cancellation effect caused by voltage phase differences at different points of a feeder because of the branch impedances are also modeled in the simulation through equation (2.4) and the multiphase network model.

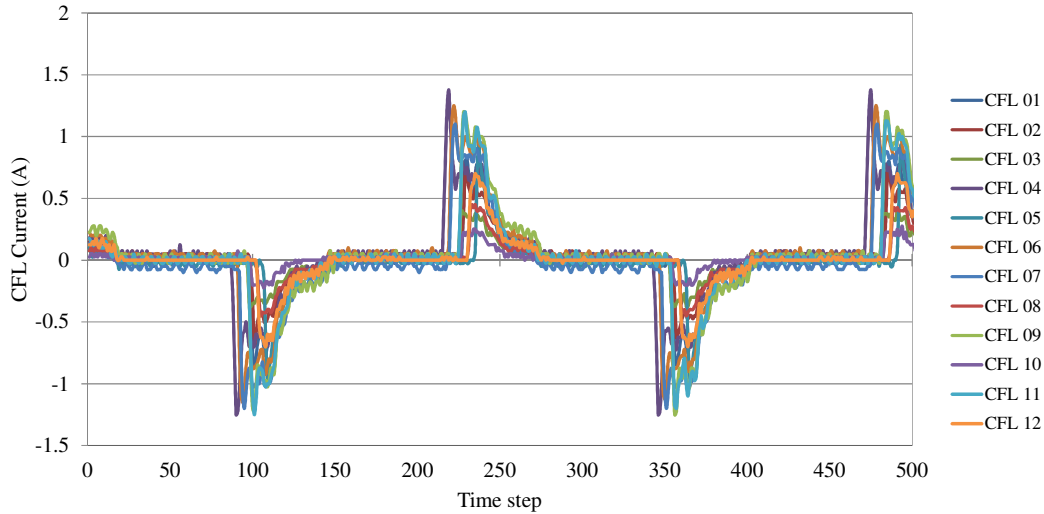


**Figure 2.6: Current waveform measured from CFLs of different brands.**

## 2.2. Trends in Residential Loads Usage

Since this PhD thesis is also concerned about how the harmonic voltage or current levels will evolve in the next 5 to 10 years, it is important to determine the usage or consumer trends of harmonic-producing home appliances. This thesis analyzed the market survey data for key consumer electronics and home appliances. Trend models have been established for them. It must be noticed that is very complicated to predict the future situation precisely based on past information, but the following results represent reasonable estimations and, more importantly, will be used to demonstrate the usefulness of the proposed methodology in Chapter 6 and Chapter 7.

It is important to note that the results reported here are based on the load composition characteristics of Canada and United States. Using these charts directly for other countries will basically depend if they have similar socio-economic scenario and government incentives stimulating the usage of certain types of residential loads. Some of the residential loads included in the methodology are not common in other countries. Results for other locations can be obtained using the proposed technique but one needs to consider relevant regional load characteristics. The main purpose of this thesis is to show how to use this information to study the evolution of the harmonic distortion in residential feeders in the coming years.

### 2.2.1. Lighting Home Appliances

Some governments around the world have passed measures to improve the energy efficiency of light bulbs used in homes and businesses. CFLs are likely to be one of the main causes of power quality concerns in residential areas in the near future [2],[30] because incandescent lamps are being banned in many countries. According to the estimation in [31], 13.5% of the residential installed lamps are CFLs and incandescent lamps will disappear by 2020 in the United States. As reported by IEA [32], it was found out that by 2002 households had on average 1 CFL and 36 Incandescent bulbs. In 2007, a large survey found an average of 3.37 CFL per household [33]. Therefore, using the data from these works [30]-[33], the average number of CFLs and incandescent bulbs was found for the next 10 years and the results are shown in Figure 2.7. It must be noticed that results shown in Figure 2.7 are based in data related to North America and it might be applied to other countries depending on the socio-economic scenario and on government politics to enforce the use of CFLs.

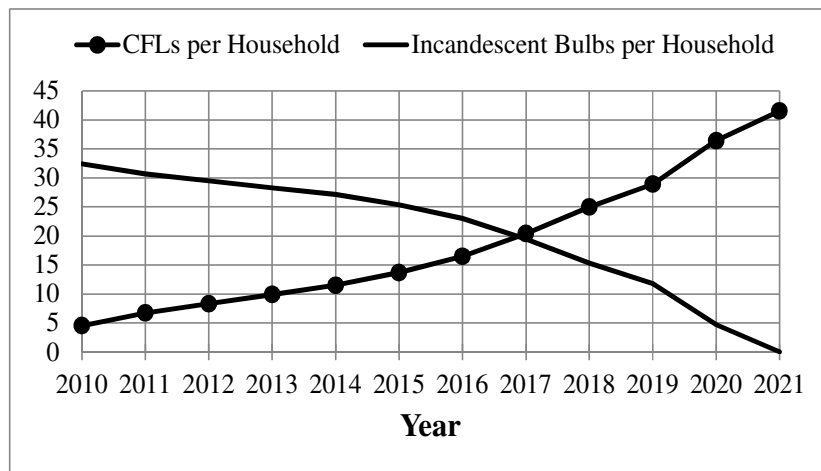


Figure 2.7: Trends on the number of CFLs and incandescent lamps per household.

### 2.2.2. Televisions

Televisions have been changing rapidly in recent years as the transition from analog broadcasting to digital broadcasting accelerates. As a result, CRTs' share has been getting smaller and replaced by LCD (including LED-backlit) and Plasma (PDP) displays, which have the nature advantage of providing digital media. According to [34], in the year of 2007, half of the market was dominated by CRT and half by LCD and Plasma. Moreover, one can observe that CRT TV will be eliminated by year 2014.

The average number of TV sets in the United States household is 2.24. The typical lifespan of television is 5 to 6 years. Assuming people would change their TV set every 6 years, the different types of TVs' penetration in one year will only be affected by the TV sales of the past 6 years. Information about the annual sales of each TV can be found on [34]. For the years after 2014, it was assumed the sales are the same as the year 2014, as predictions after this year were not found in the literature. Therefore, for each type, the number of TV per household, for year “ $i$ ”, can be calculated as follows:

$$TVH^Y(i) = \frac{STV^Y(i-5) + \dots + STV^Y(i)}{TSTV(i-5) + \dots + TSTV(i)} \times NTV \quad (2.5)$$

where

- $TVH^Y$  is the number of TVs of type  $Y$  per household;
- $NTV$  is the average number of TVs, including all types, per household;
- $STV^Y$  is the sales of TVs of type  $Y$ ;
- $TSTV$  the total sales of all types of TVs.

Therefore, according to the above equation and assuming the average number of TVs per household ( $NTV$ ) is fixed during the next 10 years, the number of LCD and CRT per household can be estimated and is shown in Figure 2.8.

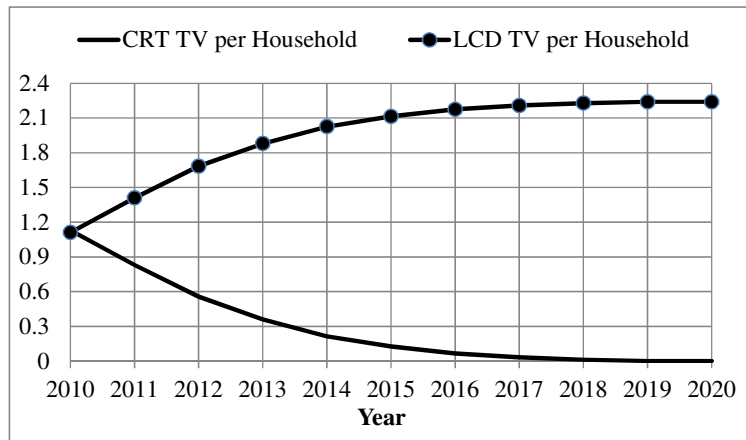


Figure 2.8: Trends on the number of CRT and LCD TVs per household.

### 2.2.3. Personal Computers

Industry practice uses the indicator of *Computer Ownership per Person* (CP) [35]-[36], instead of *Computers per Household* (CH). The indicator  $CH$  can be determined by  $CH = CP \times APH$ . The parameter  $APH$  is the average population per household, which is assumed equal to 2.72 in this thesis. According to references [35]-[36], CP was equal to 0.773 for 2006

and 0.98 in 2010 for North America. Using this data and assuming linear growth, the number of computers (laptops and desktops) per household is estimated the coming years and shown in Figure 2.9.

Regarding laptop ownership, a research done by [37] showed that laptop ownership (LP) jumped from 0.43 in 2007 to 0.59 per person in 2010, which means *Laptops per Household* (LH = LP×APH) equal to 1.17 in 2007 and 1.44 in 2010. Using this data and assuming linear growth, the number of laptops per household is estimated for the coming years and shown in Figure 2.10.

To calculate the number of desktops per household, the curve associated to laptops in Figure 2.10 is subtracted from the curve of Figure 2.9. The result is also shown in Figure 2.10.

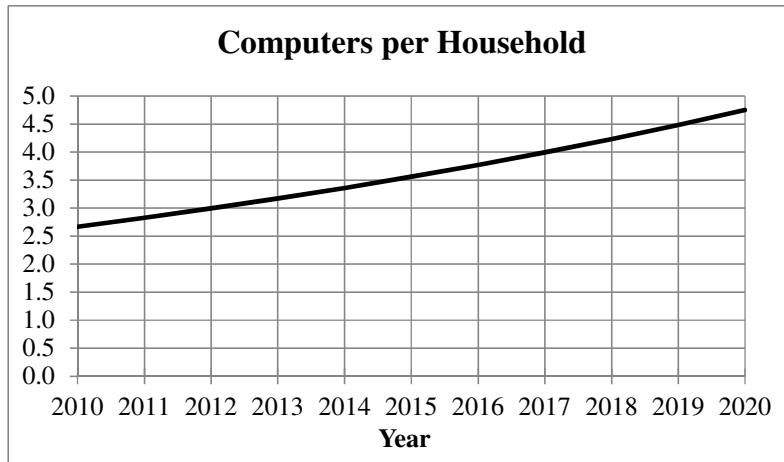


Figure 2.9: Trend on the number of computers per household.

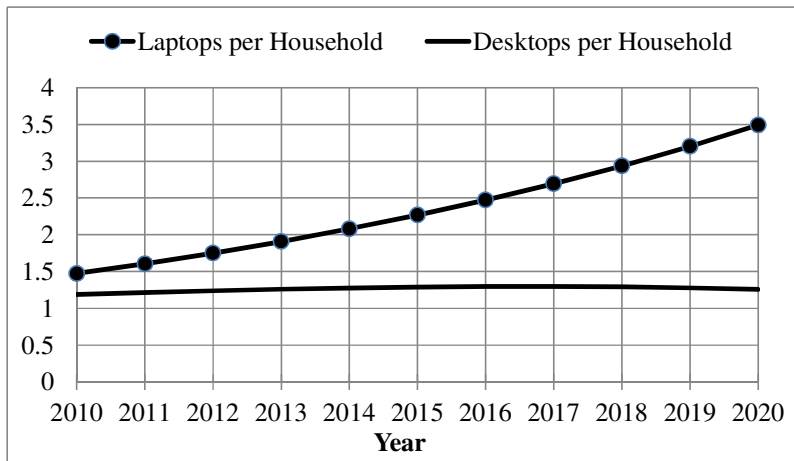


Figure 2.10: Trends on the number of laptops and desktops per household.

This indicates that desktops ownership will change slightly at around 1 per household.

According to [38], industry analysts predicted that notebooks sales would exceed desktop sales for the first time in 2008. By 2011, it expected laptops to represent 66% of corporate purchases, with 71% of consumers opting for a notebook instead of a desktop.

#### 2.2.4. Printers

Printer ownership data has not been found on the literature. However, literature search showed that printer sales in the 2<sup>nd</sup> quarter of 2006 in US were 1,763,201. Meanwhile, the PC sales in the United States in the 4<sup>th</sup> quarter of 2006 were 15,866,000 [39]. Hence, printers installed per computer (PPC) are:

$$PPC = \frac{\text{Printer Shipment}}{\text{PC Shipment}} = \frac{1763201}{15866000} = 0.11 \text{ printers per PC}$$

The above data presents a possible estimate of the printer use in homes. It is noted that printers' growth rate could be higher than PC as the above rate includes printers used for business and home. Assuming that the printers' ownership is associated with the PC ownership, the trend index *Printers per Household* (PH) is given by 0.11×CH. The resulting estimation of printers per household for the next several years is illustrated in Figure 2.11.

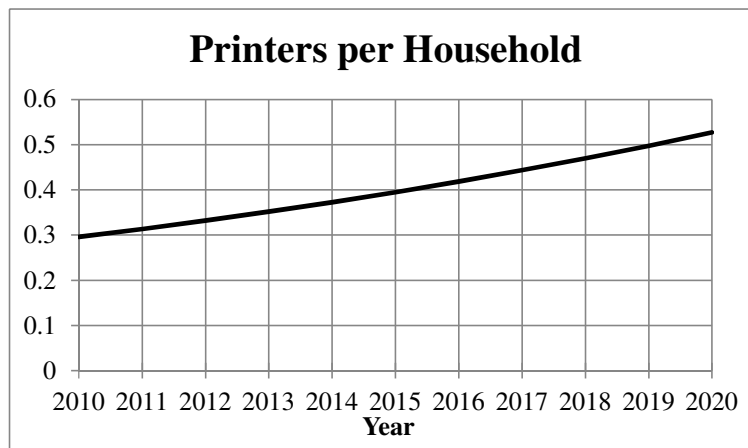


Figure 2.11: Trend on the number of printers per household.

#### 2.2.5. Major Residential Loads

In this thesis, major residential loads stand for fridge, freezer, washer, dryer and electric range. In Canada, information regarding each appliance penetration per household can be obtained from *NRCan* (Nature Resources Canada) [40]. In this research, electric dryer and range are treated as linear impedance load, so their replacement has no impact on the harmonic current

penetration. However, if the motor based appliances, such as washers, fridges and freezers, are changed to newer models, an impact on harmonic levels is expected.

With the increased usage of ASD-based (Adjustable Speed Drive) fridges, there will be a significant change in harmonic current producing due to the electronic-based drive. According to [41], the THD of current can reach as high as 136% when operated at reduced speed. If ASD-based fridge is replaced, it is expected that significant incremental harmonic currents will be injected into the distribution system.

The typical lifespan of fridge is 15 years [40], which means that the penetration of the specific fridge type in the households in a certain year is related to the last 15 years:

$$FRIH^Y(i) = \frac{SF^Y(i-15) + \dots + SF^Y(i)}{TSF(i-15) + \dots + TSF(i)} \times NFRI \quad (2.6)$$

where

- $FRIH^Y$  is the number of fridges of type  $Y$  per household;
- $NFRI$  is the average number of fridges, including all types, per household;
- $SF^Y$  is the sales of fridges of type  $Y$ ;
- $TSF$  the total sales of all types of fridges.

It is assumed that the total fridge sales every year is fixed. Fridges with energy consumption lower than 30 kwh/cu.ft. per year are categorized as energy conservation type. Based on sales information about energy conservation and regular fridges obtained from [40], the household penetration for both types of fridges was estimated and the result is shown in Figure 2.12

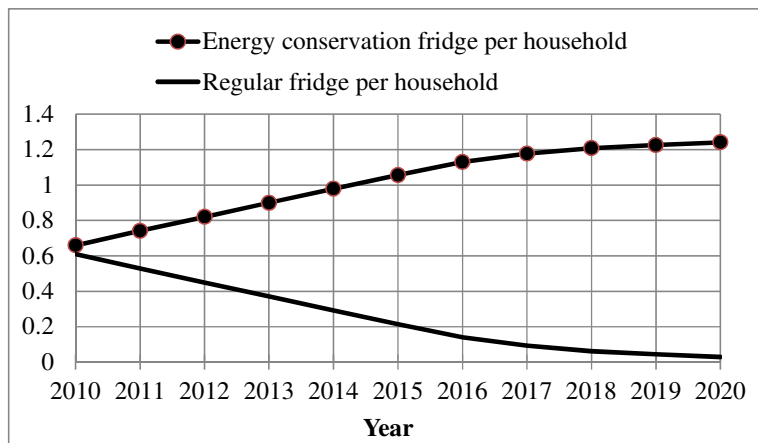


Figure 2.12: Trends on the number of energy conservation and regular fridges per household.

Currently, two types of washers are commercially available, front-loading and top-loading. In 2006, 46.9% of the clothes washers shipped in Canada were front-loading units, and they are

generally more efficient. Reference [40] also provides information regarding sales of front-loading and top-loading washers in Canada. Assuming the lifespan of washer is 10 years, which means that the penetration of the specific washer type in the households in a certain year “i” is related to the last 10 years:

$$WSH^Y(i) = \frac{SW^Y(i-10) + \dots + SW^Y(i)}{TSW(i-10) + \dots + TSW(i)} \times NWSH \quad (2.7)$$

where

- $WSH^Y$  is the number of washers of type  $Y$  (front or top-loading) per household;
- $NWSH$  is the average number of washers, including all types, per household;
- $SW^Y$  is the sales of washers of type  $Y$ ;
- $TSW$  the total sales of all types of washers.

From equation above, it is possible to estimate for the coming years the number of washers of each type per household and the results are shown in Figure 2.13.

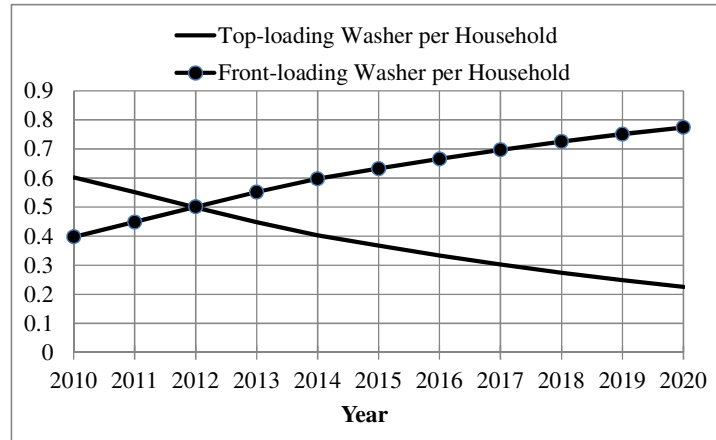


Figure 2.13: Trends on the number of front-loading and top-loading washers per household.

## 2.2.6. Other Residential Loads

There are many other harmonic producing appliances in homes. Due to the lack of market data, the usage trend of these appliances is assumed to be constant over the next several years. A list of appliances considered in this thesis was shown in Table 2.1. However, more appliances can be included using the techniques developed in this thesis. Inclusion of such loads represents location or utility specific studies.



---

## Chapter 3

# MODELING OF RESIDENTIAL HOUSES

---

In the previous chapter, it was discussed two aspects regarding the modeling of residential loads, i.e., electrical characteristics and usage trend. This chapter is focused on the third aspect, which consists of determining the operating status (ON and OFF) of a residential load. The amount of harmonic currents injected into the distribution system from residential houses depends greatly on the operating conditions of each residential load, which in turn is a function of the habits and population of a household. In order to assess the harmonic impact of various residential loads adequately, it is very important to establish the model of the appliances' operating activities in a home. The result is an electrical model of residential houses.

### 3.1. Overview of the Proposed Method

The proposed residential house modeling adopts a bottom-up approach. This is necessary since this thesis is interested in the impact of specific types of appliances. In a general way, the purpose of the bottom-up approach is to determine individual models for each component of the actual system. In the load modeling problem, this approach permits the determination of individual models that represent the behaviour of different appliances: lamps, stoves, washers, among others [42]. The structure of the bottom-up approach for load modeling is shown in Figure 3.1 [23].

On the left of Figure 3.1, there is a set of daily activity profiles, which represent the likelihood of people performing different activities at different times during a day; these profiles are assumed to be the same for all households. To the right of Figure 3.1 is an individual household. The household is assigned an active occupancy data series and a set of installed appliances. The actual operating status of each appliance is determined from its corresponding daily activity profiles. When an appliance switch-on occurs, it will be included as an operating

load. The whole household load is a random collection of operating loads, linear or nonlinear, as a function of time.

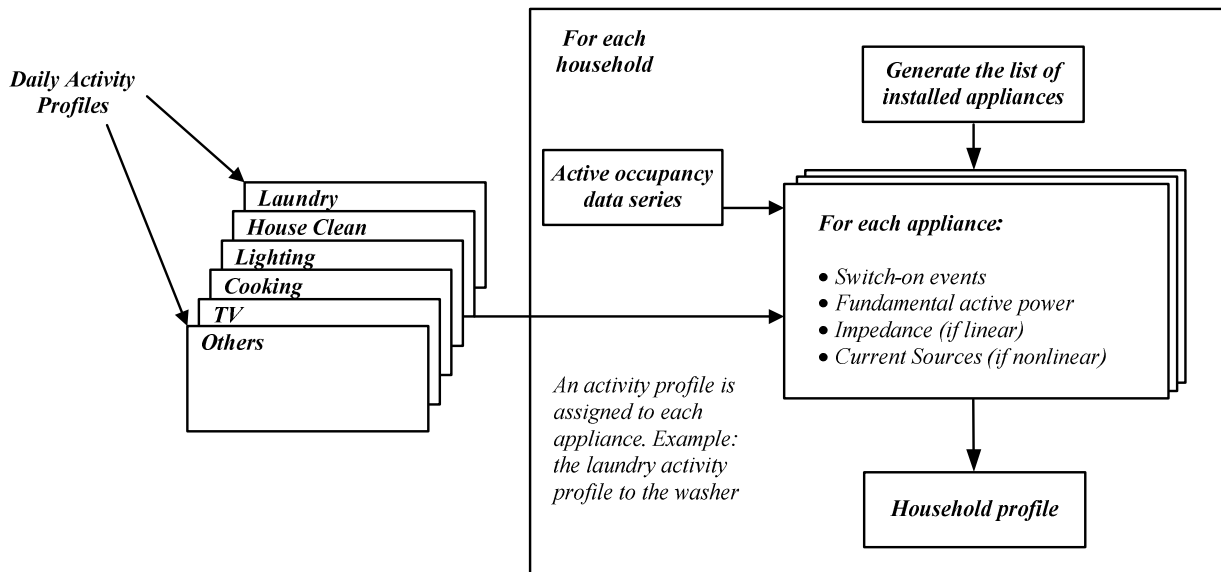


Figure 3.1: Structure of the bottom-up model for a residential house.

### 3.2. Residential Load Profile Modeling

Considerable research efforts have been made in the past on the subject of developing detailed residential electrical load profiles from limited sources of data, i.e. reconstructing the expected daily electrical loads of a household based on appliance sets, occupancy patterns, and statistical data. Based on the published works [21]-[24], the basic idea of home load profile modeling is to address three factors:

- 1) When residential load will be turned on. This can be simulated using the *Daily Time of Use Probability Profiles* of the residential loads;
- 2) How long residential load will stay on (i.e., working cycle duration). The duration can be determined from measured data and from understanding the purpose of the residential loads involved;
- 3) How to include the impact of the habits and population of a household.

A load profile is created by combining these factors. Each factor is presented in detail in the following subsections.

### 3.2.1. Daily Time of Use Probability Profiles

In 1985, Walker and Pokoski [21] constructed electric load profiles from individual appliances by introducing the concept of “availability” and “proclivity” functions to predict whether someone is available (at home and awake) and their tendency to use an appliance at any given time, respectively. Since then, many researchers [22]-[24] have investigated how to quantify the probability of the specified activity being undertaken as a function of time-of-day, which is termed as the *Time of Use Probability Profiles*. It represents the probability of a household performing a specific activity during a 24 hour period. For example, reference [43] found that the number of dwellings that have one active occupant between 08:00 and 08:10 in a weekday is 2082. The number of dwellings where the occupant is performing a cooking related activity is 288. The probability of cooking event occurs at any minute between 08:00 and 08:10 is  $288/2082 = 0.138$ . In this thesis, the residential loads’ activity profiles are mainly collected from technical articles [21]-[24] and research surveys [43]-[44].

It is important to notice that information regarding the activity profile of each residential load presented in this section is related to Canada, United States and United Kingdom. The reason is that the activity profile data is not available for all residential loads in one country only. Results for other locations can be obtained using the proposed technique but one needs to consider relevant regional load characteristics. The main purpose in this chapter is how to use this information to model the stochastic tendency to use an appliance at any given time.

#### 3.2.1.1. Cooking Activity Profile

Most of the kitchen loads are related to cooking activities. They share the same probability of switching on at a given time of the day. As shown in Figure 3.2, the curves are applied to predict the occupants’ cooking related actions and to establish the probability of a load switch-on event, such as using microwave, blender and griddle etc.

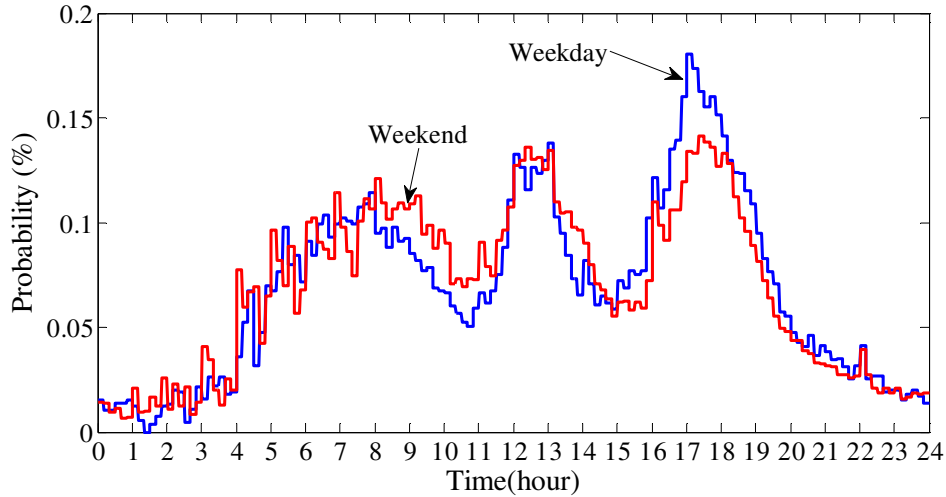


**Figure 3.2: Time of use probability profile for cooking activity.**

The probability profile is given with 1-min resolution and the higher the value in the profile. The higher the value in the profile, the higher the probability that the load switches on. For example, a microwave switch-on event would be far more likely to occur at 17:00 than at 4:00. The profile on weekends is flatter than the profile for weekdays because people tend to cook at more random times on weekends [44].

Additionally, people are more likely to use toaster and waffle iron in the morning, and range at noon and in the evening. Specific profiles for some major appliances or group of appliances, like the ones shown in Figure 3.3 and Figure 3.4 are also utilized in this thesis.

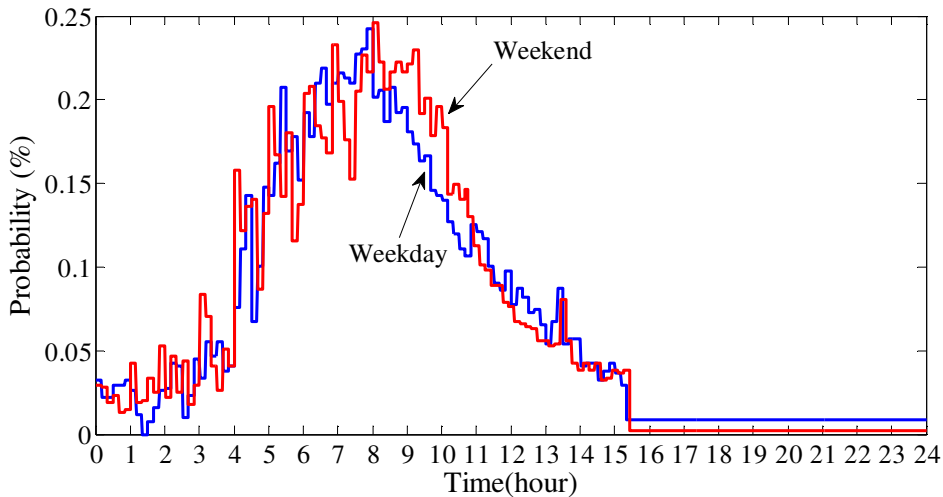


**Figure 3.3: Time of use probability profile for breakfast related activities.**

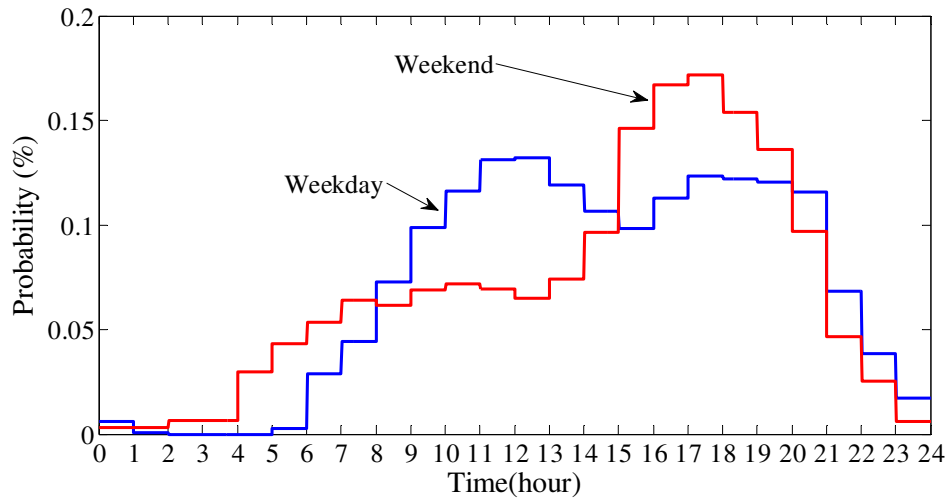


**Figure 3.4:** Time of use probability profile for stove (range).

### 3.2.1.2. Laundry Activity Profile

Daily time of use of washer machines is determined by laundry activity profile shown in Figure 3.5. The time of use profile for dryers is generally the same shape as the washer profile, and is offset from the washer profile in time. People usually turn on dryers between 10 and 30 minutes following the end of the washer cycle [44].

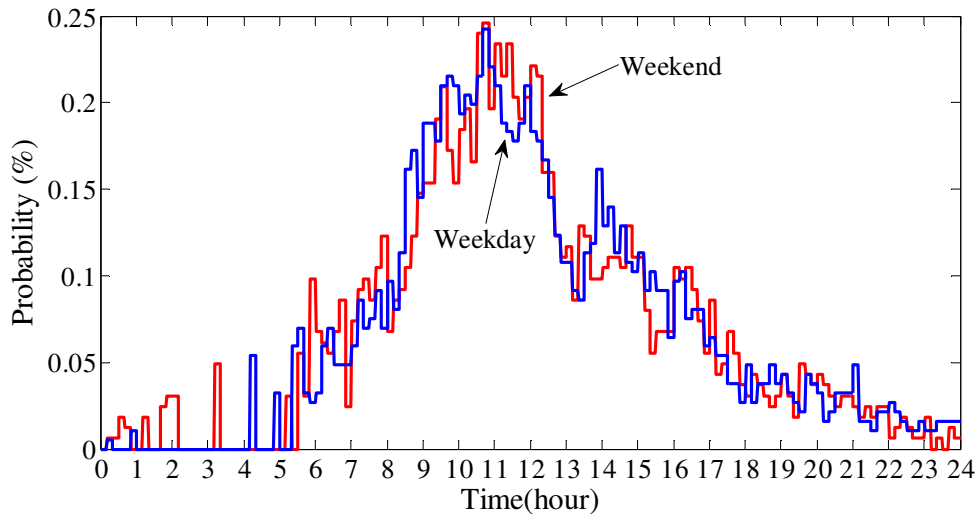


**Figure 3.5:** Time of use probability profile for laundry activity.

### 3.2.1.3. Television and Personal Computer Profile

The probability profiles of television and personal computer are shown in Figure 3.6 [44].

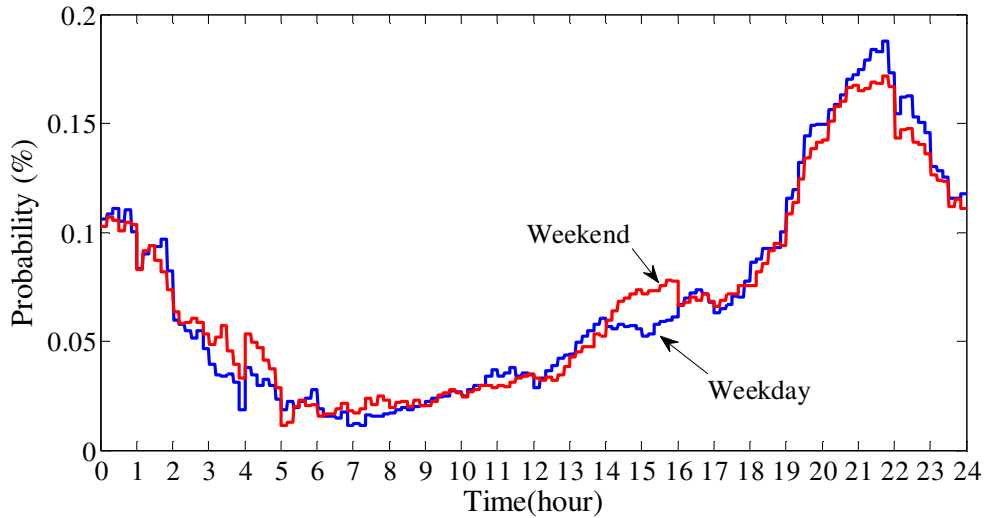


**Figure 3.6: Time of use probability profile for television.**

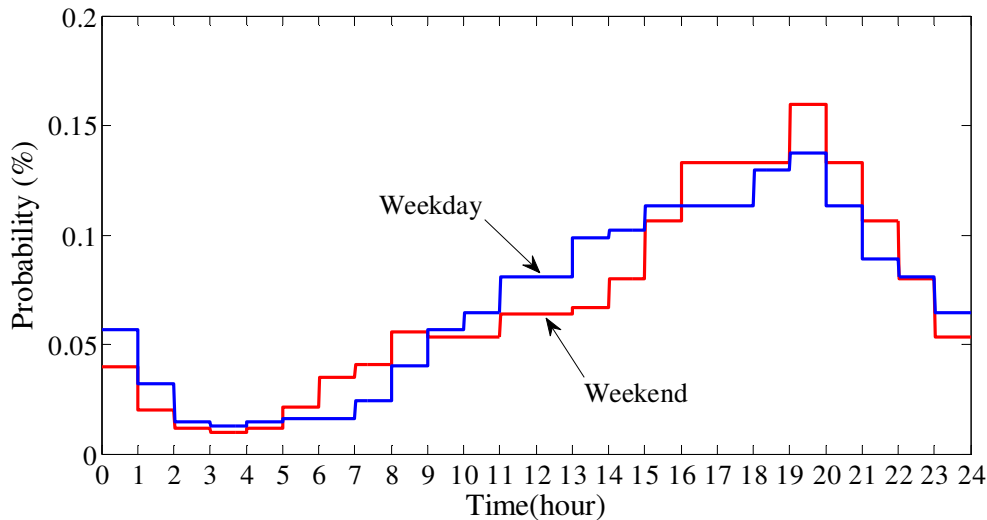


**Figure 3.7: Time of use probability profile for personal computer (PC).**

#### 3.2.1.4. Lighting Profile

Lighting can be divided into three basic categories: living room and bedroom lighting, kitchen lighting and bathroom lighting. Living room and bedroom lighting is associated with people’s occupancy, while kitchen lighting is related to cooking activity (the kitchen lighting turns on with the beginning of cooking and it turns off after some time of the ending of cooking). Bathroom lighting can also be determined from people’s occupancy; however it is more random if compared to living and bedroom lighting profiles. Bathroom lighting profile is given in Figure 3.8 [44].

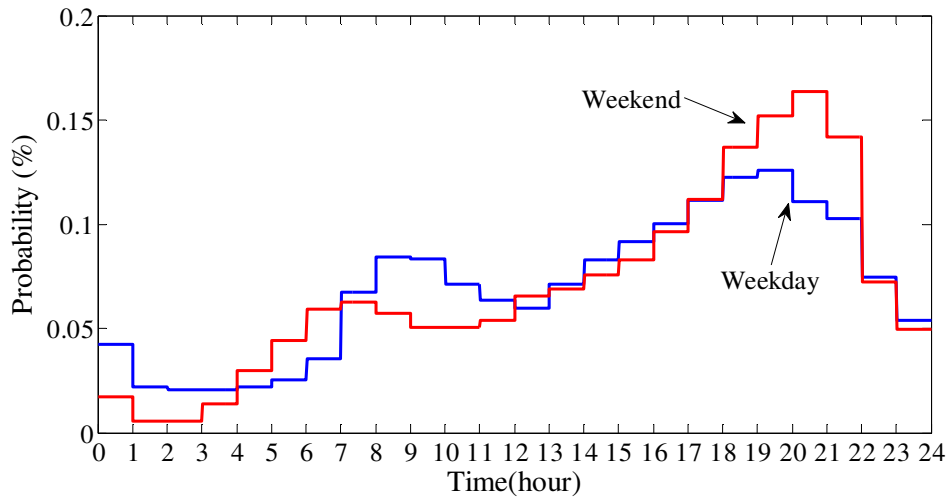


**Figure 3.8: Time of use probability profile for bathroom lighting.**

### 3.2.1.5. House Cleaning Profile

The time of use probability profile of house cleaning devices such as vacuum cleaners can be determined from Figure 3.9. Normally, the house cleaning activity is carried out from 8:00 a.m. to 06:00 p.m.

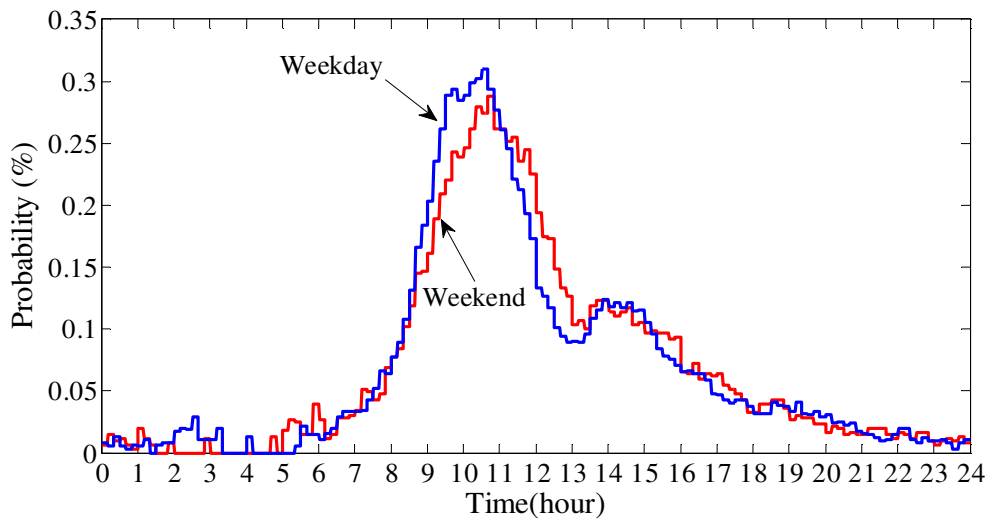


**Figure 3.9: Time of use probability profile for house clean activity.**

### 3.2.1.6. Occasional Event Profile

The occasional event time of use profile establishes the probability of a number of appliances which activate occasionally. The operating of electric kettle, motor of garage door and furnace etc. are defined as occasional event. Based on the information from [44], the profile

illustrated in Figure 3.10 is assigned to these loads.

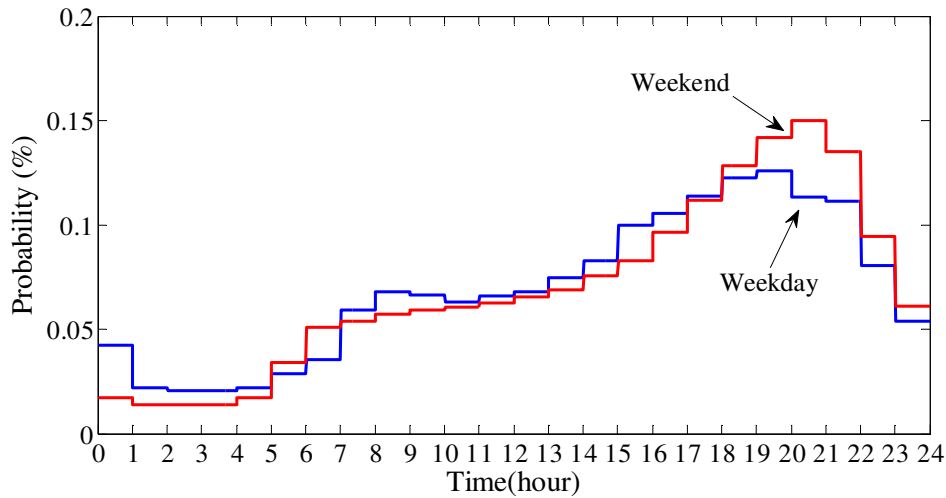


**Figure 3.10: Time of use probability profile for occasional events.**

Due to data unavailability, we do not have a specific time of use probability profile for all appliances, however, a solution for that is presented in Section 3.2.4 and is briefly exemplified as follows. For example, coffeemaker and toaster are assigned the same breakfast time of use probability profile (shown in Figure 3.3), however based on the respective average number of switch-on events per day (discussed in Section 3.2.2), the probability of coffeemaker to switch-on is normalized and, then, can be less or more than that of toaster.

### 3.2.2. Appliance Duration Characteristics

For major appliances, the working cycle duration can be established according to the measurement data from *Canadian Center for Housing Technology* (CCHT) [45]. At the CCHT, a simulated occupancy system triggers daily residential load on/off state change events in a real single detached home. The average cycles per year is derived from standard residential load test methods of the Canadian Standards Association (CAN/CSA-C373-92, CAN/CSA-C361-92 and CAN/CSA-C360 - 98) [46]-[48]. Details of some major residential loads and working cycle durations are presented in Table 3.1.



**Table 3.1: Appliance usage pattern for major appliances.**

<b>Appliance</b>	<b>Power (W)</b>	<b>Cycle Duration (min)</b>	<b>Cycles per year</b>	<b>Annual Consumption (kWh/year)</b>
Dishwasher	467	30 to 45	200 (low) 322 (medium) 418 (high)	58 (low) 94 (medium) 122 (high)
Washer	505	30 (two 15-minute cycles)	242 (low) 392 (medium) 601 (high)	61 (low) 99 (medium) 152 (high)
Dryer	4115	30 to 60	192 (low) 416 (medium) 640 (high)	593 (low) 1284 (medium) 1976 (high)
Range	1600	15 to 70	678 (low) 678 (medium) 950 (high)	769 (low) 769 (medium) 1077 (high)
Refrigerator	265 (peak)	----	----	801 (low), 801 (medium) 1602 (high: 2 fridges)
Freezer	202 (peak) 263 (peak)	----	----	0 (low), 614 (medium) 798 (high)

Information regarding the other appliances analyzed in this thesis was extracted from a series of buyers guides published by *Natural Resources Canada* [49]-[50] and from field measurements. This list of appliances with their power rating and expected hours of operation per month is presented in Table 3.2.

**Table 3.2: Average appliance usage pattern for other appliances.**

	<b>Appliances</b>	<b>Power Rating (W)</b>	<b>Average Hours per month</b>
<b>Kitchen</b>	Blender	350	3
	Coffee Maker	900	12
	Deep Fryer	1500	8
	Exhaust fan	250	30
	Electric kettle	1500	15
	Hot plate (one burner)	1250	14
	Microwave oven	1500	10
	Mixer	175	6
	Toaster	1200	4
<b>Laundry</b>	Iron	1000	12
<b>Comfort and Health</b>	Electric blanket	180	180
	Fan	120	6
	Hair dryer	1000	5
<b>Entertainment</b>	Computer (desktop)	250	240
	Computer (laptop)	30	240
	Laptop charger	100	240
	Radio	5	120
	Stereo	120	120
	Television	100	125
	VCR	40	100
<b>Outdoors</b>	Lawn mower	1000	10
<b>Tools</b>	Drill	250	4
	Circular saw	1000	6
	Table saw	1000	4
	Lathe	460	2
<b>Other</b>	Sewing Machine	100	10
	Vacuum cleaner	800	10

The above data only includes the total working hours per month. The number of switch-on events per day is determined as follows: for example, the average working hours for microwave is 10 per month per Table 3.2. If the average working cycle duration of microwave is 4 min, one can get  $m = (10 \times 60) / (30 \times 4) = 5$  switch-on events per day.

### 3.2.3. Size and Occupancy Pattern of Household

The size of household has a significant impact on daily electricity demand. In order to include the impact of different household sizes, a household size factor  $k$  is introduced. When modeling a residential house with specified number of  $n$  occupants,  $k$  is equal to the ratio

between  $n$  and the average number of people per household (assumed to be 2.5 in this thesis based on reference [51]). The value of average hours per month for each residential load provided in Table 3.2 cannot be used directly for different household sizes since, for example, a house with more people will lead to an increase in load usage. In order to take this into account, the usage times provided in Table 3.2 will be multiplied by the household size factor  $k$ .

Occupancy pattern (i.e. when occupants of a residence are at home, and using residential loads) affects the on/off state of the loads. The common factors influencing the occupancy pattern are as follows [23]: (a) the time of first person getting up in the morning and last person go to sleep, (b) the period of inactive house occupancy during working hours. Due to lack of information about house occupancy pattern, it is proposed 5 most typical scenarios of household occupancy pattern. Table 3.3 lists these possible scenarios.

**Table 3.3: Occupancy pattern for a typical household.**

Type of Day	No.	Work Type	Time of Waking up	Working Time	Time of Going to Bed
Weekday	1	Full-time	6:00 - 7:30	8:00 - 17:00	22:00 - 00:00
	2	Part-time Morning	6:00 - 7:30	8:00 - 12:00	22:00 - 00:00
	3	Part-time Afternoon	6:00 - 8:00	13:00 - 17:00	22:00 - 00:00
	4	Not Working	6:00 - 8:00	N/A	22:00 - 00:00
Weekend	5	N/A	7:00 - 9:00	N/A	22:00 - 00:00

### 3.2.4. Probabilistic Model of Residential Load Switching-on

Based on the usage pattern of residential loads discussed in the previous sections and the method of [23], a procedure to determine load switch-on events at a given time of a day (which is also called a simulation step) has been established. The procedure is a form of Monte Carlo simulation and implemented in a computer program. At each simulation step, a list of residential loads that are on is generated, which forms the load profile at that step. The simulation procedure is shown Figure 3.11 and explained below:

1. Determine the types of appliances and the number of each type in the house. This can be found using the market trends results presented in Chapter 2;
2. Choose one appliance from the house:
  - 2.1. Initialize simulation step  $t = 1$ . The time of use probability profile (Section 3.2.1) is selected according to the chosen appliance and whether it is a weekend or not; the

occupancy pattern is also selected according to the working type and whether it is a weekend or not;

- 2.2. The probability of appliance activation ( $Pr$ ) can be read from its activity profile;
- 2.3. The average number of residential load switch-on events per day ( $m$ ) (Section 3.2.2), is modified to consider household size,  $m^* = m \times k$ , where  $k$  is the household size factor;
- 2.4. The probability ( $P$ ) of a residential load to switch on at present simulation step ( $t$ ) is equal to the previous probability  $Pr$  multiplied by the modified number of appliance switch-on events ( $m^*$ ) and a calibration scalar ( $c$ ),  $P = Pr \times m^* \times c$ . A discussion of how the calibration scalar is derived is presented below;
- 2.5. The calculated probability  $P$  is compared to a normally distributed random number ( $n$ ) between 0 and 1. If  $P$  is larger than  $n$ , go to step 2.6; otherwise go to step 2.7;
- 2.6. The appliance is switched on and the present simulation time step is updated to ( $t = t + D$ ), where  $D$  is the appliance average working cycle duration. Go to step 2.8;
- 2.7. The appliance remains off and the present simulation time step is updated to ( $t = t + \Delta t$ ).  $\Delta t$  is the simulation resolution (e.g., 1 min). Go to step 2.8;
- 2.8. If current simulation step ( $t$ ) is less than final step go to step 2.2, otherwise choose another appliance and go to step 2.1.

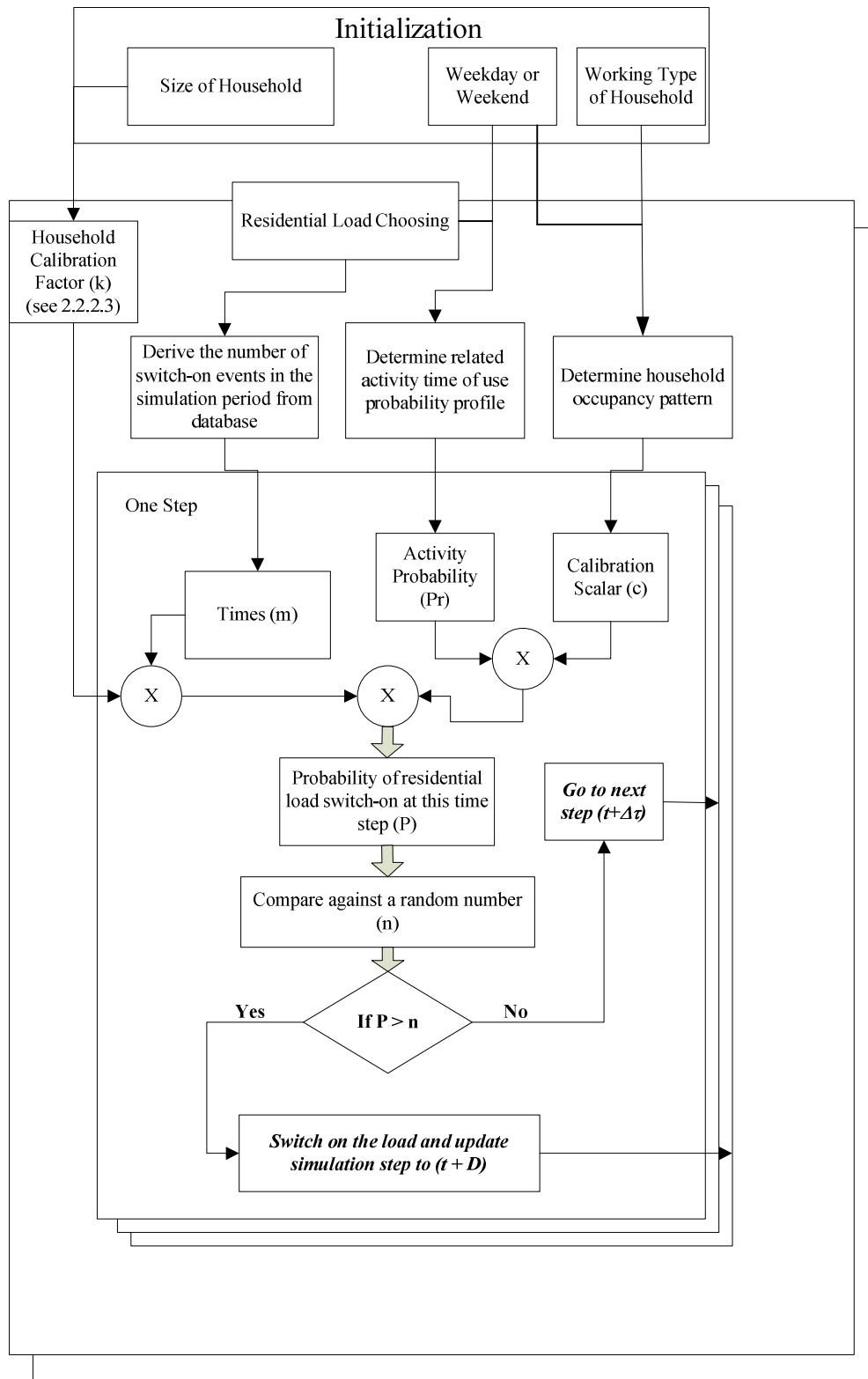


Figure 3.11: Procedure to determine switch-on events of appliances.

In step 4, the calibration scalar ( $c$ ) is introduced to reflect the influence of household occupancy pattern [23]. This paper uses occupancy function, as follows, to represent occupancy pattern.

$$OF(n) = \begin{cases} 1 & \text{when house is actively occupied (e.g., morning, evening)} \\ 0 & \text{when house is inactively occupied (e.g., daytime, midnight)} \end{cases}$$

where "inactively occupied" refers to the scenario where nobody is at home or awake.

If  $OF(n) = 0$ , the calibration scalar  $c$  is made 0 for most residential loads, which makes the probability of certain load switch-on to be zero when nobody is at home or awake. If  $OF(n) = 1$ , the calibration scalar  $c$  is introduced so as to make the mean probability of an activity taking place, when multiplied by the calibration scalar, equal to the mean probability of an load switch-on event. As shown in Figure 3.12, before calibration, we have:

$$\sum_{n=1}^N \Pr(n) = 1$$

After introducing the occupancy function and calibration scalar  $c$ :

$$\sum_{n=1}^N \Pr_c(n) = \sum_{n=1}^N c \times \Pr(n) \times OF(n) = 1 \Rightarrow c = \frac{1}{\sum_{n=1}^N \Pr(n) \times OF(n)}$$

$$c = \begin{cases} 0 & OF(n) = 0 \\ \frac{1}{\sum_{n=1}^N \Pr(n) \times OF(n)} & OF(n) = 1 \end{cases}$$

Some residential loads such as fridge, freezer and furnace etc. are independent of household occupancy, so the calibration scalar is always made equal to 1.

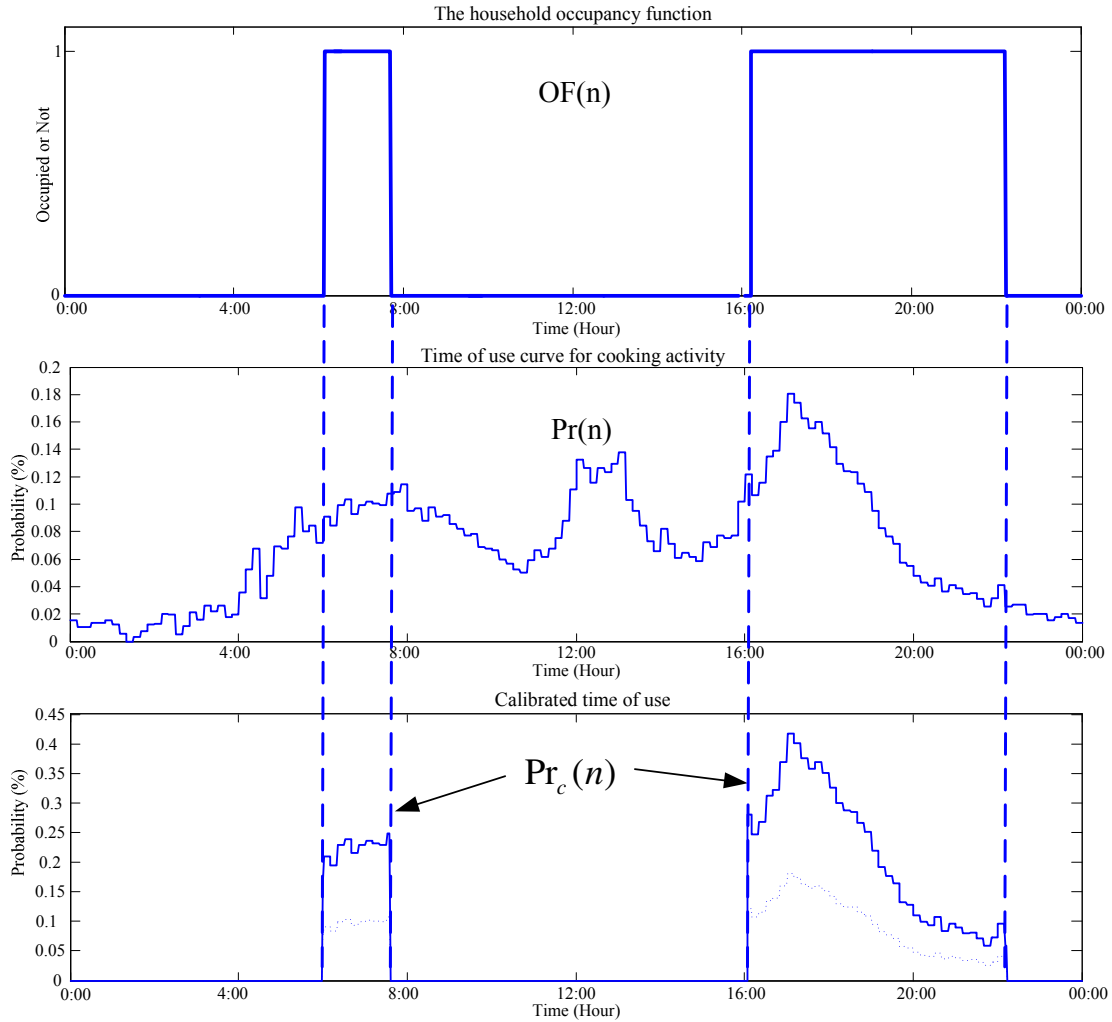


**Figure 3.12: Time of use probability profile calibration with occupancy function.**

The simulation of microwave usage is used as an example to illustrate the above procedure (Figure 3.13). The simulated household is set to have an average size and is full-time work type. The day of interest is weekday. The simulation resolution is 1-min, which means  $N = 1440$  steps in one day. As it can be seen from Figure 3.13, the time of first person waking up is 05:40, the inactive occupancy period during work is 7:28-16:58, and the time of last person going to bed is 22:36 for this randomly generated instance. If the simulation runs to the first step (00:01), the value of occupancy function is 0 and calibration scalar  $c=0$ , the resulting probability of microwave switch-on ( $P$ ) at this time step is 0, which means the microwave has no chance to switch on. However, if the time step is equal to 1200 (20:00), the value of occupancy function is 1, and calibration scalar is:

$$c = \frac{1}{\sum_{n=1}^N \Pr(n) \times OF(n)} = \frac{1}{0.43} = 2.33$$

The probability of microwave use at this step is  $\Pr = 0.06\%$  as it can be observed from Figure 3.2. According to the residential load usage characteristic, the average working cycle duration and the average working hours per month of a microwave are equal to 4 minutes and 10 hours (Table 3.2). So the number of switch-on events per day of the microwave is equal to  $m = (10 \times 60) / (30 \times 4) = 5$ . Hence,  $P = \Pr \times m^* \times c = \Pr \times m \times k \times c = 0.055\% \times 5 \times 1 \times 2.33 = 0.64\%$  which means probability of microwave switch-on at current time step is 0.64%. When the simulation finishes the 1440 steps, i.e. covering the 24 hour period, results like those shown at the bottom of Figure 3.13 will be obtained. For this day of simulation, microwave is used for 5 times. The usage duration per time is 4 to 5 min, and total usage time is 21 min per day.

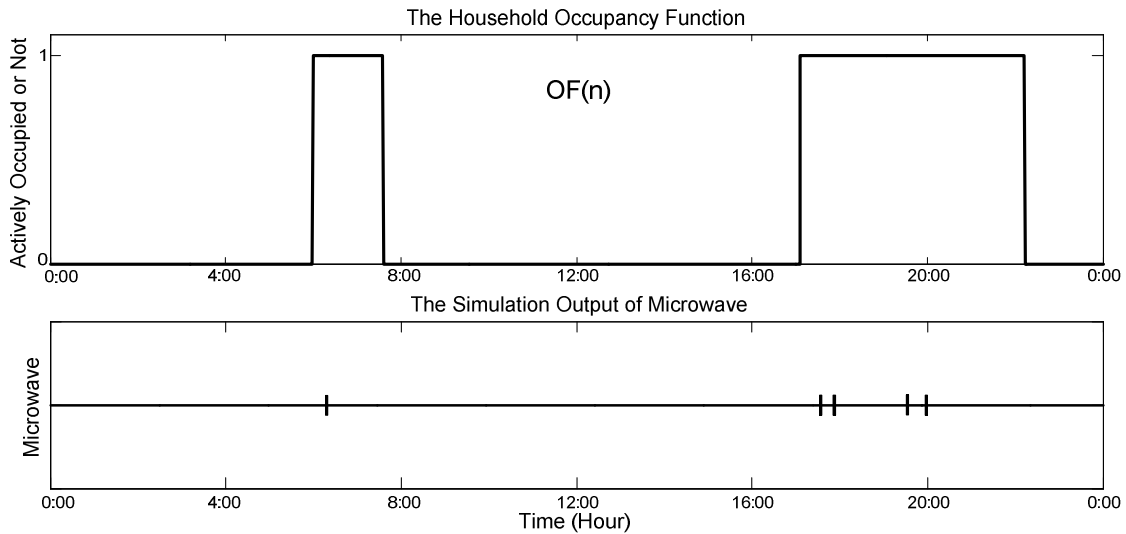


**Figure 3.13: Time of use probability profile for microwave.**

The same procedure is conducted for each installed residential load at each simulation step. An example use pattern of some loads as simulated by the procedure is showed in Figure 3.14. It is important to notice that the result shown in Figure 3.14 is obtained by Monte Carlo simulation by repeating the procedure shown Figure 3.11 several times. Monte Carlo methods are a class of computational algorithms that rely on repeated random sampling to compute their results [17], [52]. They are used to model phenomena with significant uncertainty in inputs, which is the case for the residential loads. The average between the experiments is used as convergence criterion, which means after the average does not change significantly the Monte Carlo simulation is ended. One can observe that the PC is used between 17:00 and 24:00 and washer and dryer are



not used throughout the day. Television and PC are used for a relatively long period throughout the day, while cooking loads are used for much shorter period but multiple times.

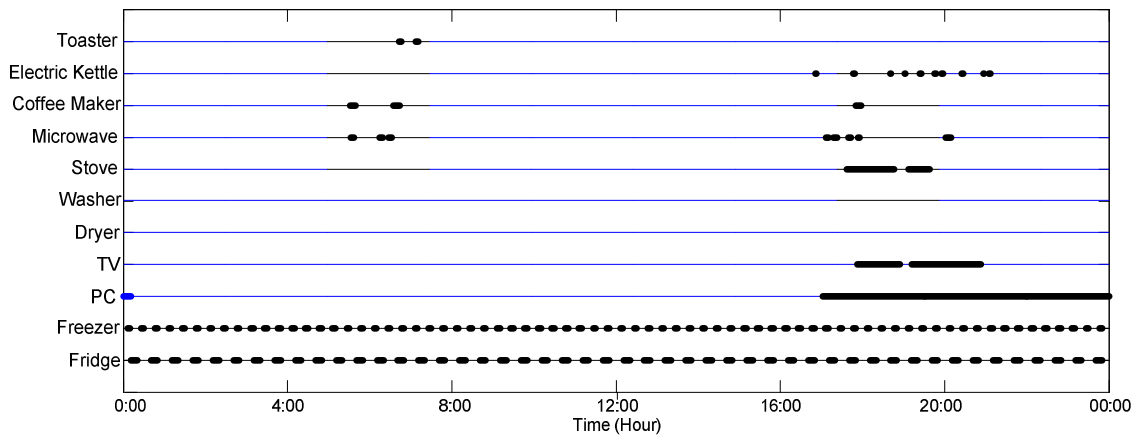


**Figure 3.14: Time of use probability profile for different residential loads.**

At the bottom of Figure 3.14, the fridge and freezer are activated periodically throughout the whole day and not associated with household occupancy pattern.

### 3.3. Single House Validation Studies

Once the residential load usage time information is derived, a load with ON state will be represented with its electrical model and be connected to the electric circuit of a house. Note that there could be different electrical models of the same load if one wants to consider different brands or consumer trends.

In North America, residential customers are usually supplied through three-wire single-phase distribution transformers, as shown in Figure 3.15. The secondary of these transformers have a neutral and two hot phases carrying 120V with respect to the neutral. In a residence, residential loads are connected in an essentially indeterminate way with respect to the circuits.

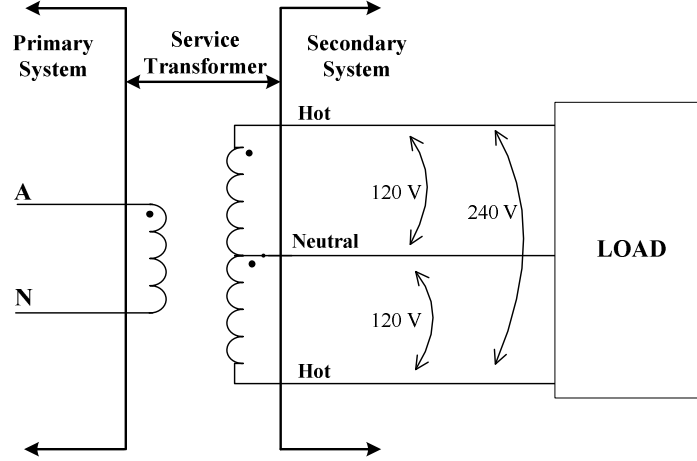


**Figure 3.15: Power distribution system for three-wire single-phase feeding systems.**

To conduct the validation analysis between the proposed methodology and real field measurement results, a simplified circuit model shown in Figure 3.16 is used. In this circuit,  $Z_{SYS} = 0.09 + j0.04$  ohm, which was obtained through real field measurements. In each simulation step, linear appliances are paralleled as total linear impedance ( $Z_{house}(h)$ ) and non-linear appliances are added up to combine a current source ( $I_{NL}(h)$ ). The proposed methodology discussed in Section 3.2 is used to determine which appliances are connected at each simulation step. The impedances and current sources of phase-to-phase (240 V) appliances are transferred to the 120 V circuit<sup>3</sup>. An example simulation output is shown in Figure 3.17, for the fundamental, 3<sup>rd</sup>, 5<sup>th</sup>, 7<sup>th</sup> and 9<sup>th</sup> harmonic components.

<sup>3</sup>Considering the measured phase-to-neutral voltage of phases A and B as  $\hat{V}_A$  and  $\hat{V}_B$ , and a phase-to-phase linear appliance with measured impedance  $Z$ , one could calculate the impedance of this appliance transferred to phase A ( $Z_A$ ) and phase B ( $Z_B$ ) using the expressions below:

$$Z_A = \frac{\hat{V}_A}{\hat{V}_A + \hat{V}_B} \times Z \quad \text{and} \quad Z_B = \frac{\hat{V}_B}{\hat{V}_A + \hat{V}_B} \times Z$$

Then, the single-phase equivalent impedance is  $Z_A // Z_B \approx Z/4$ .

A phase-to-phase nonlinear appliance with current source  $I_h$  shows up in the single-phase circuit as two current sources  $I_h$  in parallel (i.e.,  $2 \times I_h$ ). In this thesis, there are no current sources connected between phases because all measured phase-to-phase home appliances are linear (e.g., dryer, stove).

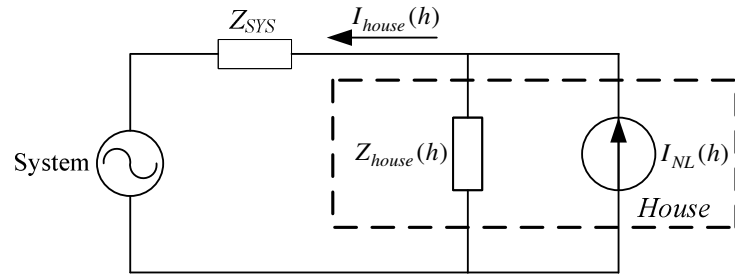
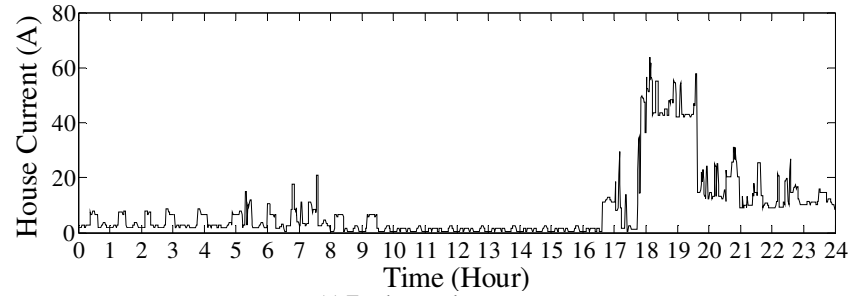
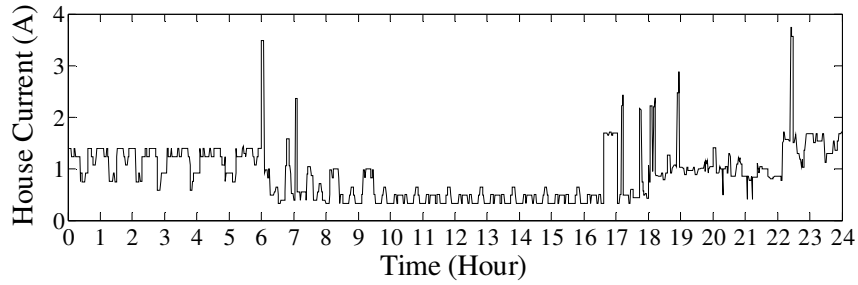


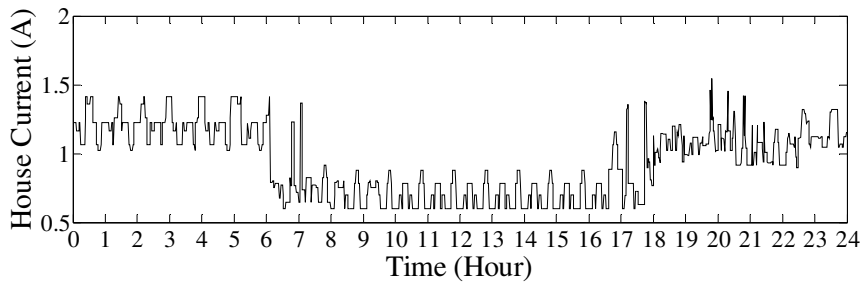
**Figure 3.16: Equivalent circuit model to represent a residential house.**



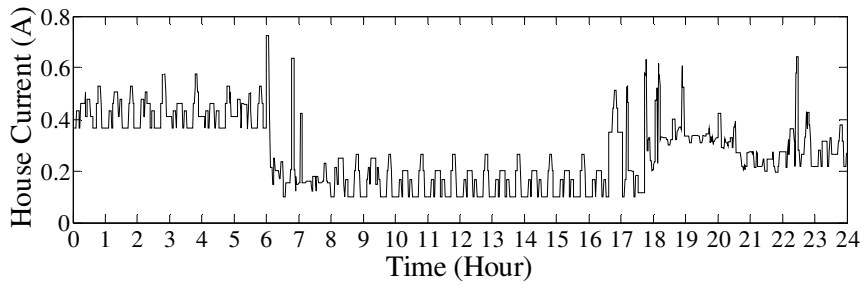
(a) Fundamental component



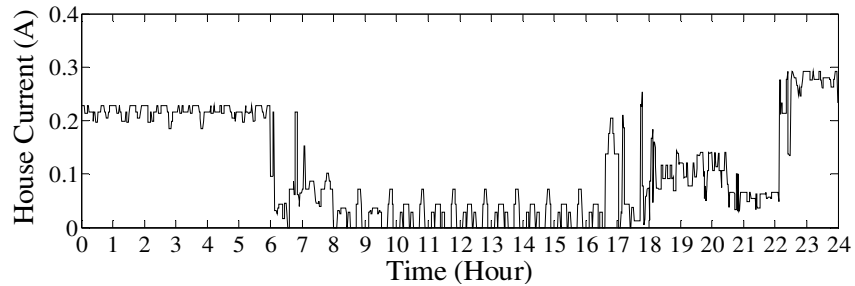
(b) Third harmonic component



(c) Fifth harmonic component



(d) Seventh harmonic component



(e) Ninth harmonic component

**Figure 3.17: The simulation output  $I_{\text{house}}(h)$  of a house during one day.**

The results of seven days simulation, which contains 5 weekdays and 2 weekend days, are shown in Table 3.4. The table lists the mean value and standard deviation of the total house fundamental, 3<sup>rd</sup> and 5<sup>th</sup> harmonic currents. In order to validate the simulation results, field measurements were conducted at the service entrance panel ( $\widehat{I}_A + \widehat{I}_B$ ) for typical residential houses and the results are shown in Table 3.5. The measured sample house has some occupants that do not need to go to work, so “not working” type occupancy pattern is chosen for simulation. Comparing Table 3.4 against Table 3.5, the mean and standard deviation (Std.) values of fundamental and each harmonic current matched quite well.

**Table 3.4: Simulation results of a residential house ( $I_{\text{house}}(\mathbf{h})$ ).**

Cases	Fundamental		3 <sup>rd</sup>		5 <sup>th</sup>		
	Mean	Std.	Mean	Std.	Mean	Std.	
Weekday	Case 1	7.4255	8.4936	1.4206	0.9767	1.1325	0.4134
	Case 2	12.0936	14.1378	0.9727	0.5012	1.0008	0.2513
	Case 3	6.3924	7.5214	1.3608	0.7513	1.0672	0.2648
	Case 4	5.9725	7.6786	1.0318	0.7756	0.9515	0.3326
	Case 5	9.6551	13.6628	1.0408	0.7182	0.9447	0.2982
	Average	8.3078	10.7166	1.1653	0.7599	1.0193	0.3174
Weekend	Case 6	7.2618	9.5808	1.2442	0.8669	1.047	0.3285
	Case 7	8.2197	9.7457	1.5898	0.8434	1.0189	0.2168
	Average	7.7408	9.6636	1.417	0.8552	1.033	0.2783

**Table 3.5: Field measurement results of a residential house.**

Date	Fundamental		3 <sup>rd</sup>		5 <sup>th</sup>		
	Mean	Std.	Mean	Std.	Mean	Std.	
Weekday	April, 02 2010 Friday	7.6203	6.1043	1.4647	0.6793	1.0056	0.281
	April, 05 2010 Monday	7.6898	4.8839	1.3404	0.6299	0.9733	0.2486
	April, 06 2010 Tuesday	11.3668	13.3124	1.195	0.555	0.9467	0.2483
	April, 07 2010 Wednesday	7.7067	6.8004	1.0466	0.5225	0.9215	0.1896
	Average	8.5959	8.4348	1.2617	0.5998	0.9618	0.2441
Weekend	April, 03 2010 Saturday	7.5689	4.9492	1.2367	0.5807	0.9793	0.2392
	April, 04 2010 Sunday	9.2585	8.4477	1.5668	0.772	1.072	0.2744
	Average	8.4137	6.9231	1.4018	0.6831	1.0257	0.2574

The simplified model shown in Figure 3.16 facilitates the estimation of the total impedance of the house  $Z_{\text{house}(h=1)}$ . Figure 3.18 shows the impedance obtained for the simulated house. In this figure, the impedance is not shown if linear loads are not in operation. From the profile, the operation of several significant appliances can be identified. The most power consuming appliances are dryer and stove, their impedance are  $2.74 + j0.56$  ohms and  $6 + j0.03$  ohms (transferred to 120V single-phase circuit), respectively. Since the impedance represents the harmonic absorption capability of a house, it is examined in more detail. Figure 3.19 shows the cumulative distribution function of the parallel impedance during one month (30 days, 22 weekdays and 8 weekends). It must be noticed that the maximum cumulative probability in Figure 3.19 is 44%. The other 56% probability, corresponding to no linear appliance working (infinite impedance), is not shown in the figure. The results show that the impedance is lower than 40 ohms for around 39% of the time.

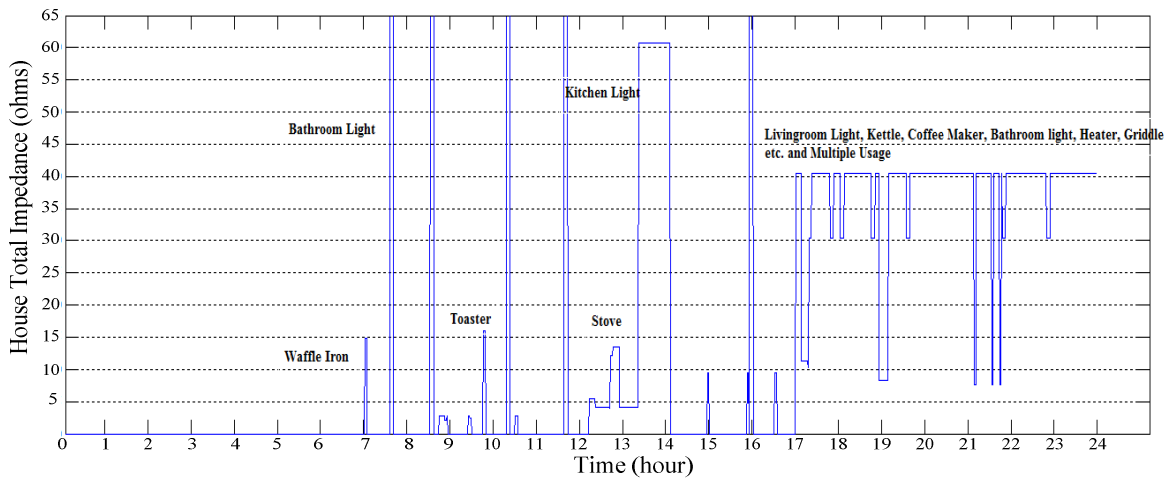


**Figure 3.18: House total impedance.**

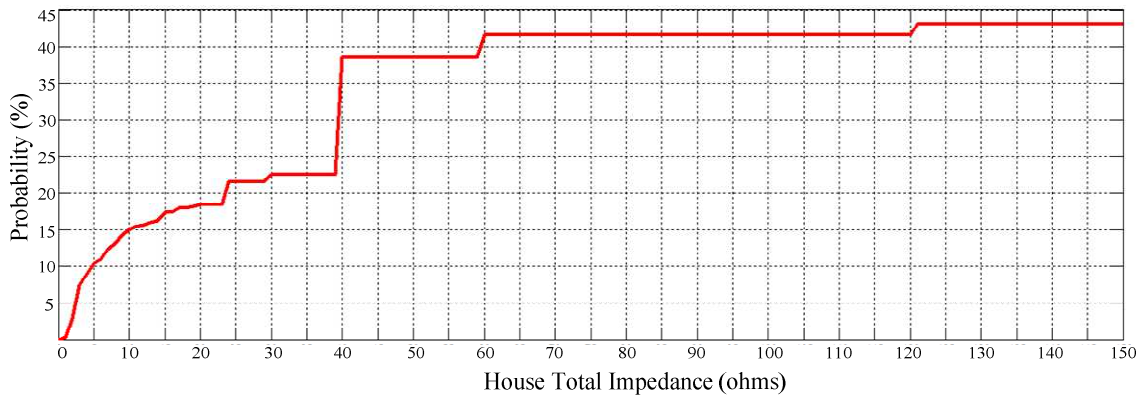


**Figure 3.19: Cumulative distribution of the house total impedance (30 days).**

### 3.4. Service Transformer Validation Studies

Residential houses are supplied through single-phase service transformers connecting the primary to the secondary system. The secondary is a 120/240V three-wire service. Each distribution transformer normally supplies ten to twenty houses. The loads are modeled collectively as one load connected to the secondary side of the service transformer (the "service transformer model"). This model is needed for studying the harmonic impact on primary distribution systems.

The steps for constructing such a model are as follows:

- 1) Generate harmonic models of 10-20 houses according to the proposed approach presented in Section 3.3;
- 2) Connect the house models into the circuit shown in Figure 3.20(a);
- 3) Build the equivalent circuit into the form shown in Figure 3.20(b).

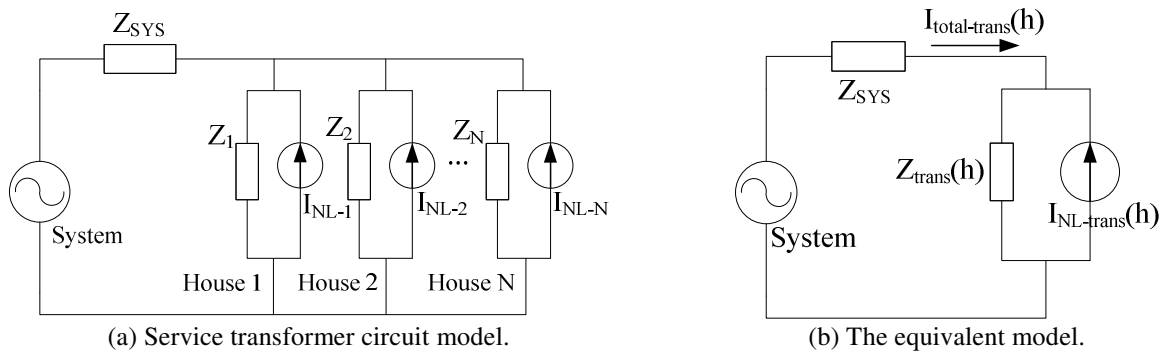


**Figure 3.20: The equivalent service transformer circuit model.**

The above service transformer model has been verified by comparing its results against those from field measurements. Field measurements of harmonic currents in a sample service transformer are shown in Figure 3.21. Such data were collected from ten different transformers serving residential loads in Edmonton, Canada in winter 2008. There is a total of 55 days measurement data. One can observe in Figure 3.21(a) that the fundamental current at 00:00 is not close to 23:59 and this is because transformer fundamental current pattern does not repeat cyclically every 24 hours. Moreover, current variation of each transformer is unique, so it is not easy to compare the results with those obtained from simulation which also exhibit random characteristics. The approach implemented in this thesis is to extract and compare the principal components (PCA) of the current profiles.

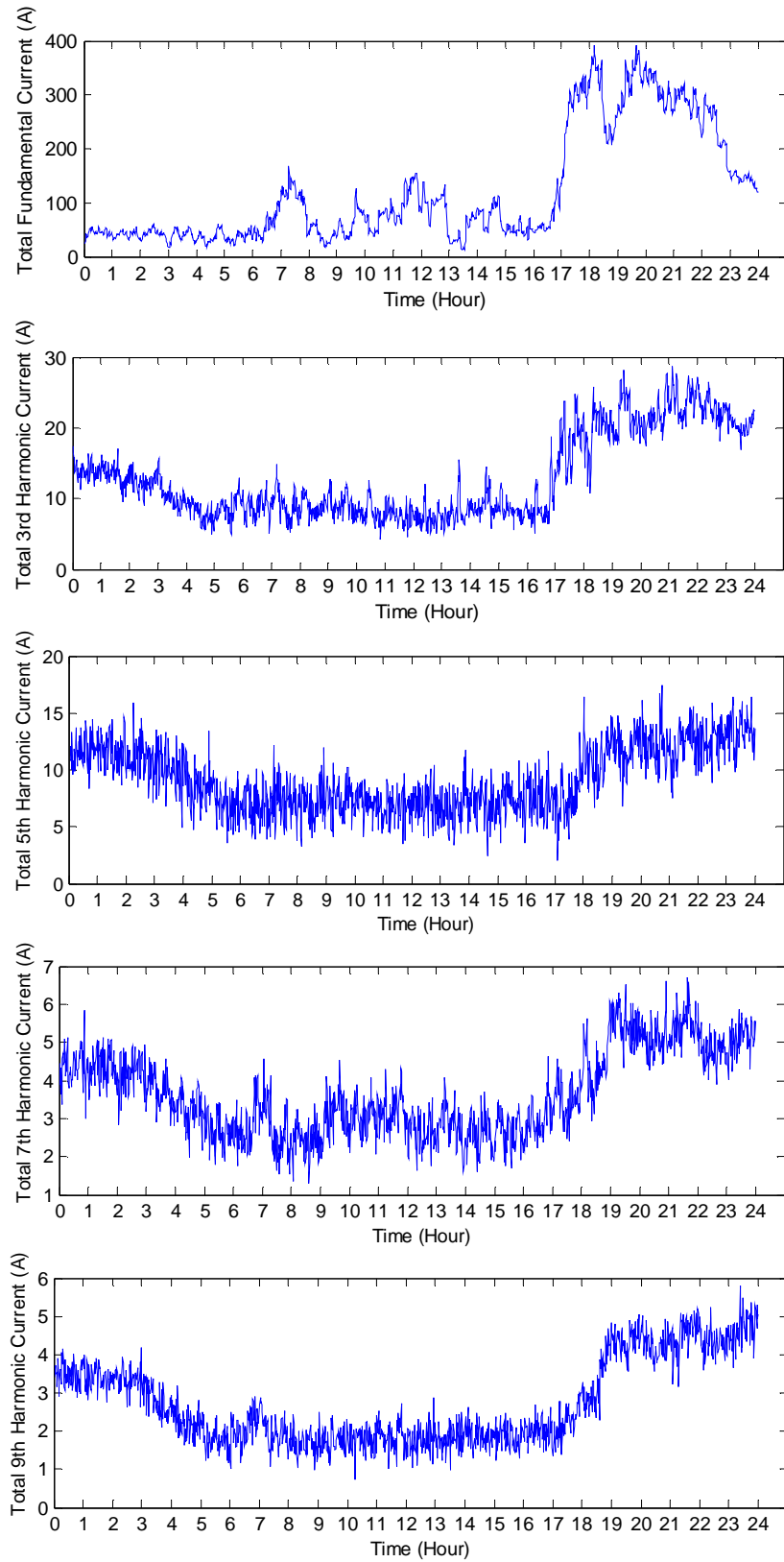


**Figure 3.21: Example of transformer current output during one weekday obtained from real field measurement.**



Principal Components Analysis (PCA) is a way of identifying patterns in data, and expressing the data in such a way as to highlight their similarities and differences. Since patterns in data can be hard to find in data of high dimension, where graphical representation is not available, PCA is a powerful tool for analysing data. More specifically, PCA is a computationally simple and fast technique that transforms a number of possibly correlated variables of the original data into a smaller number of uncorrelated variables called principal components (also known as loadings). These new variables are a linear combination of the original variables and are derived in decreasing order of importance so that, for example, the first principal component accounts for as much as possible of the variation in the original data. The usual objective of the analysis is to see if the first few components account for most of the variation in the original data. This way, one can choose not to use all the components and still capture the most important part of the data. More details can be found in [53]-[54] and the software Matlab (Statistics Toolbox) was used to conduct the PCA and other statistical studies.

The full set of principal components is as large as the original set of variables. But it is commonplace for the sum of the variances of the first few principal components to exceed 80% of the total variance of the original data. By examining plots of these few new variables, researchers often develop a deeper understanding of the **driving forces** that generated the original data [53]-[54]. The PCA technique has been applied for several power systems applications including switched capacitor location [55], transformer differential protection [56], identification of coherent generators [57], etc.

Table 3.6 lists the variance given by the first principal components for the magnitudes of measured transformers. Data are grouped into weekday and weekend. As it can be seen, for fundamental and 3rd harmonic current, first principal components can represent almost 60% of the original data; however, for higher harmonics these percentages drop to 20-30%. The reason is that higher harmonics are more difficult to predict and seem not show similar trends.

**Table 3.6: Percentage of variance of the first principal component of transformer current.**

	Fundamental	3 <sup>rd</sup> Harmonic	5 <sup>th</sup> Harmonic	7 <sup>th</sup> Harmonic	9 <sup>th</sup> Harmonic
Weekend Data	60.03	62.15	26.04	32.01	38.71
Weekday Data	54.87	60.76	27.73	36.21	42.06
Mixed Data	53.60	59.90	25.43	32.68	39.56

Based on the above analysis, two methods are proposed for the transformer model verification:

- 1) For fundamental and 3<sup>rd</sup> harmonic current, the verification method is to extract the first principal components from the field measurement data and the simulation results respectively. The components are then correlated to verify their consistency;
- 2) For higher order harmonic currents, the verification is to compare the probability distribution of the measured and calculated data. The measured and calculated harmonic current data was normalized relative to the respective average harmonic current during the day since we are interested to compare the tendency (e.g., standard deviation) between simulation and measurement results.

Figure 3.22 and Figure 3.23 show the daily variation of the first components of the fundamental and 3<sup>rd</sup> harmonic currents from both measurement and simulation on weekdays and weekends, respectively. The first component of simulated fundamental current fits quite well with that of measured one. The correlation factor is 0.94 for weekdays and 0.92 for weekend. There is an acceptable difference between the first components of 3<sup>rd</sup> harmonic current from simulation and measurements and the correlation factor is 0.73 and 0.85 for weekdays and weekends, respectively.

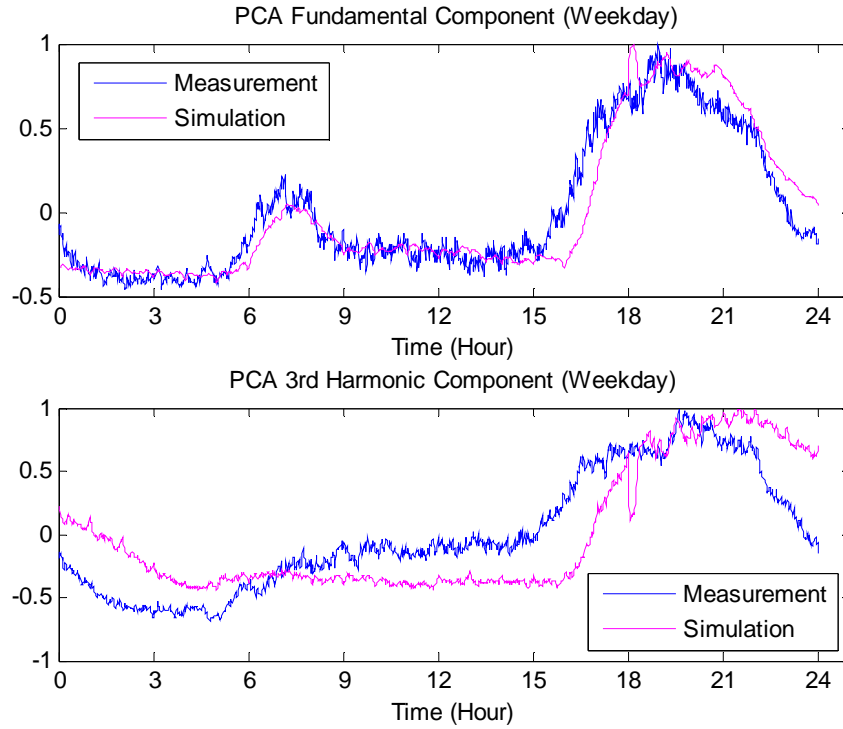


**Figure 3.22: Comparison of the first principal components (weekdays).**

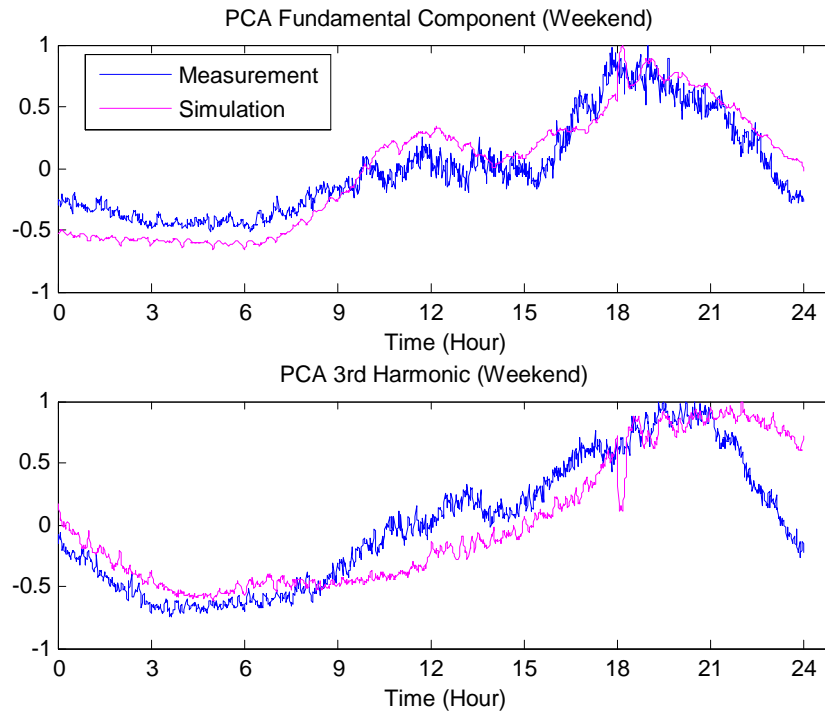


**Figure 3.23: Comparison of the first principal components (weekends).**

The remaining (residue) part of the fundamental and 3<sup>rd</sup> harmonic components contains almost 40% of the original data. A comparison is made in the form of statistical distributions in

Figure 3.24 for several weekdays. The distributions exhibit similar characteristics. Table 3.7 shows the standard deviation of the residue of both measured data and simulation results are quite close for fundamental and 3<sup>rd</sup> harmonic currents.

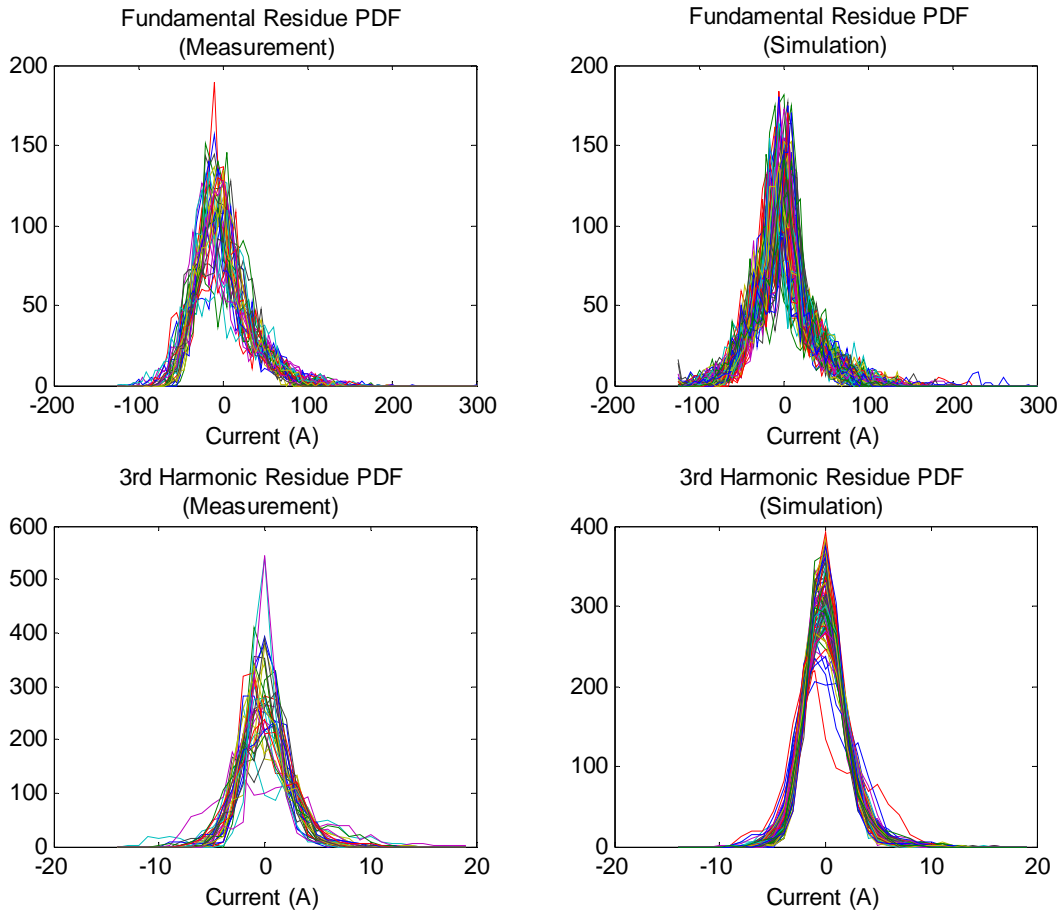


**Figure 3.24: Probability distribution of measured and simulated residue part for weekdays.**

**Table 3.7: Standard deviation of the residue of measured and simulated fundamental and 3<sup>rd</sup> harmonic current.**

	Fundamental Residue		3 <sup>rd</sup> Harmonic Residue	
	Measurements	Simulations	Measurements	Simulations
Weekend	33.29	33.34	2.43	2.01
Weekday	37.08	38.51	2.41	2.19

For higher order harmonics, their random variation is too strong for the principal components to yield meaningful results. So the components are not used for verification. Instead, harmonic probability distributions are used for comparison conducted in the software Matlab. Figure 3.25 shows the results for several weekdays. Table 3.8 shows the standard deviation of

the harmonics for both measurements and simulation results. The results show some form of consistency for both weekdays and weekends. Based on this verification analysis, it can be concluded that the proposed probabilistic residential house model is accurate and can be included in the modeling of distribution systems for harmonic impact assessment.

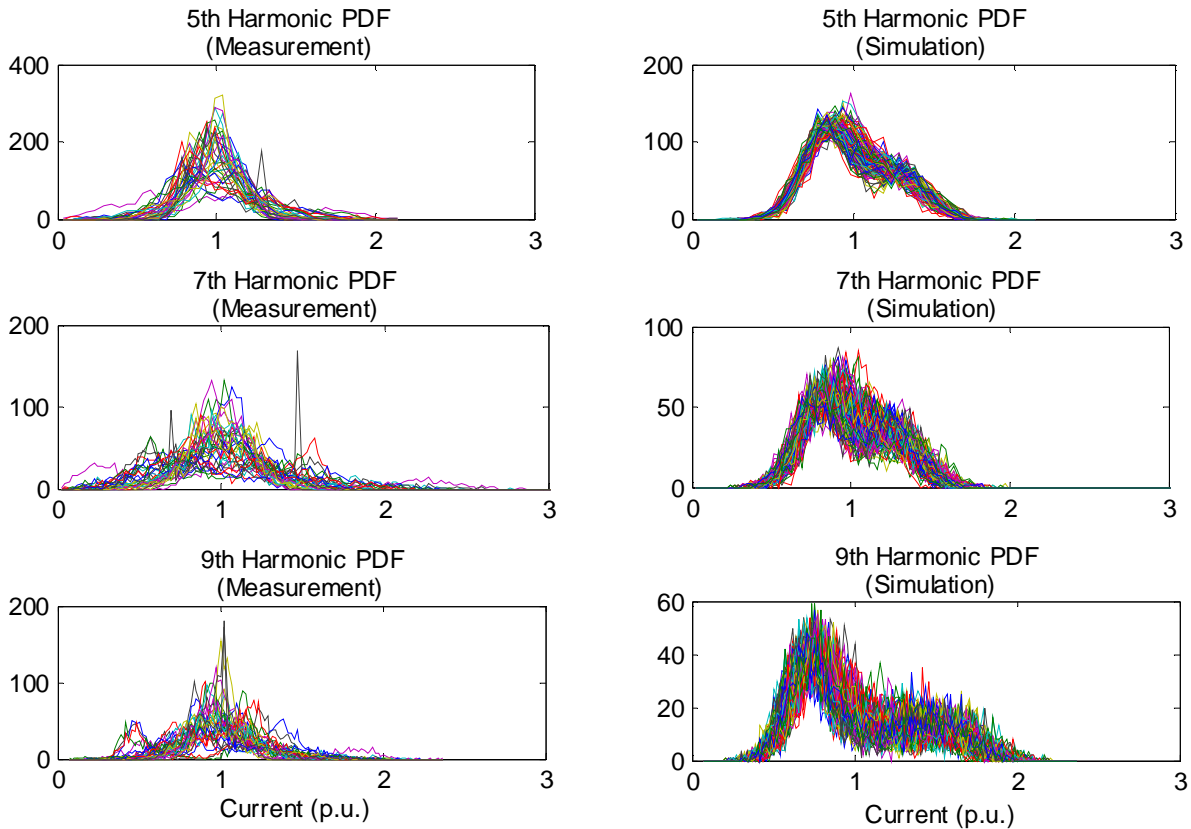


**Figure 3.25: Probability distribution curves of higher harmonics (weekdays).**

**Table 3.8: Average standard deviation of higher order harmonic currents.**

	5 <sup>th</sup> Harmonic		7 <sup>th</sup> Harmonic		9 <sup>th</sup> Harmonic	
	Measurements	Simulations	Measurements	Simulations	Measurements	Simulations
Weekend	0.22	0.26	0.31	0.27	0.30	0.39
Weekday	0.21	0.24	0.30	0.28	0.28	0.35

### 3.5. Summary

A probabilistic method to determine the harmonic impact of residential loads and houses has been presented in this chapter. The method models the random harmonic generations of residential loads by simulating the random operating states of the loads. This is done through determining the switching-on probability of a residential load based on the load research results.

The result is a randomly varying harmonic equivalent circuit representing a residential house. By combining multiple residential houses served by a service transformer, a model for service transformers is also derived. PCA and statistical analysis on the simulated and measurement results have confirmed the validity of the proposed modeling approach.

One of the attractive characteristics of the proposed method is its bottom-up approach. As a result, one can simulate the effect of market trends and policy changes. For example, the harmonic impact of CFLs can be studied by adjusting the composition of lighting fixtures in the residential load database. Applications of the proposed method to assess the harmonic impact of residential loads on the secondary and primary distribution systems will be presented in the following chapters.

---

## Chapter 4

# MODELING AND SIMULATION OF SECONDARY DISTRIBUTION SYSTEMS

---

One of the objectives of this thesis is to evaluate the impact of the nonlinear residential loads on the secondary distribution networks. This chapter presents the modeling and simulation techniques developed for this purpose.

In North America, the most common power distribution system is the multigrounded neutral (MGN) distribution system. An example is shown in Figure 4.1. The primary feeder delivers the electrical power from the source at the substation to the customers at various locations through secondary distribution systems. The secondary system consists of a service transformer, two phase wires and one neutral wire connecting the transformer to various houses, and several grounding points<sup>4</sup>. In each house, some loads are connected between the first phase and the neutral wires, some are connected between the second phase and the neutral wires, and the other loads are connected between the two phase wires [58].

---

<sup>4</sup> The multigrounded 4-wire distribution system is also common in Brazil. However, the three-wire (central tap) service transformer is not found in Brazil.

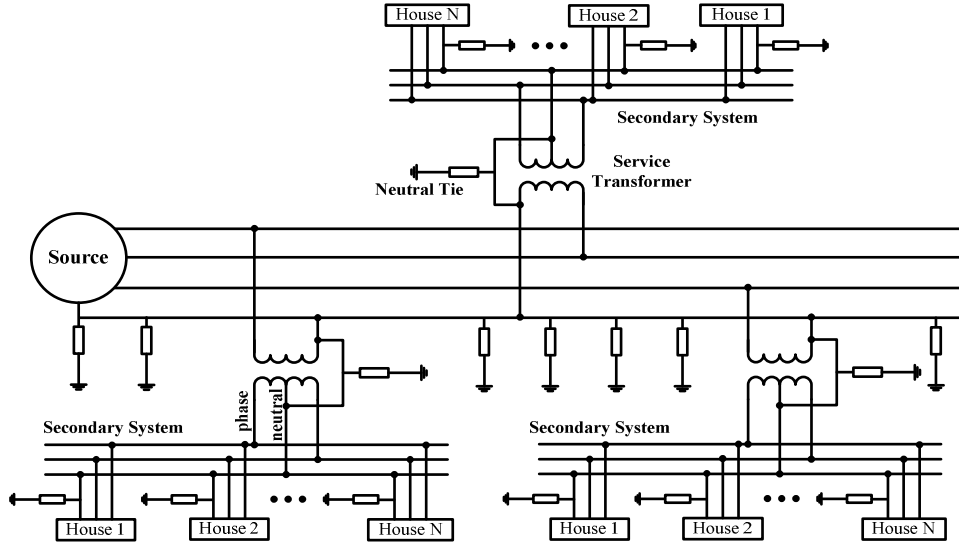


Figure 4.1: Layout of a MGN distribution system.

## 4.1. Distribution System Modeling

For studying the harmonic impact on the secondary system, the primary system will be modeled as an equivalent circuit. The service transformer will be modeled explicitly. The equivalent model to study the secondary system is shown in Figure 4.2.

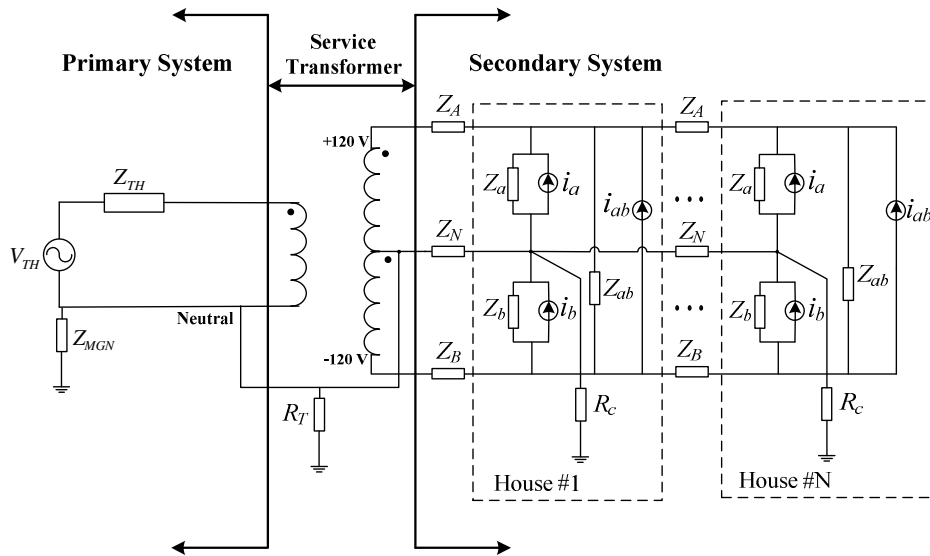


Figure 4.2: Schematic model to study secondary distribution systems.

### 4.1.1. Primary System Model

The primary system is a four-wire multi-grounded neutral (MGN) system. A general layout of a MGN distribution system was shown in Figure 4.1. The neutral of the primary feeder is grounded at regular intervals through resistances ( $R_{gn}$ ). In order to reduce the complexity of the



harmonic power flow simulations, an equivalent circuit model for the primary system is adopted, as shown in Figure 4.3.

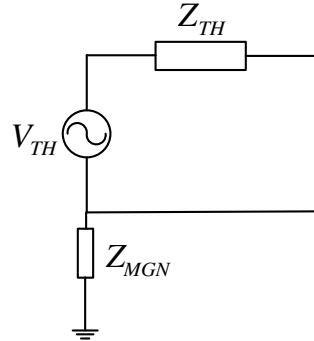


**Figure 4.3: Equivalent MGN primary distribution system.**

Because of the phase-to-neutral connection of the service transformer, the primary system is a one-phase Thévenin circuit. But for the proposed studies, there is also a need to model the neutral. The neutral is modeled as an equivalent neutral impedance based on the theory represented in [59]. Figure 4.4 shows a typical MGN ladder network, where  $z_{nn}$  is the self-impedance of a neutral segment between two grounding nodes and  $R_{gn}$  is the grounding resistance of the neutral conductor.

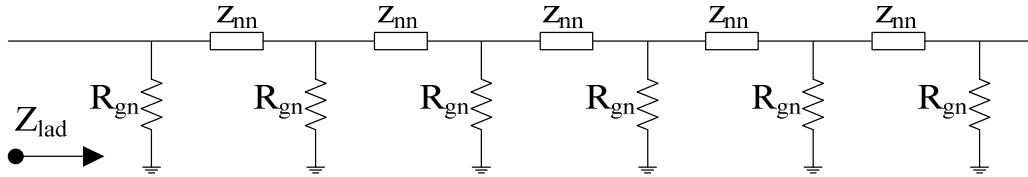


**Figure 4.4: Multigrounded neutral ladder network.**

The neutral impedance ( $Z_{MGN}$ ) can be estimated as [59]-[60]:

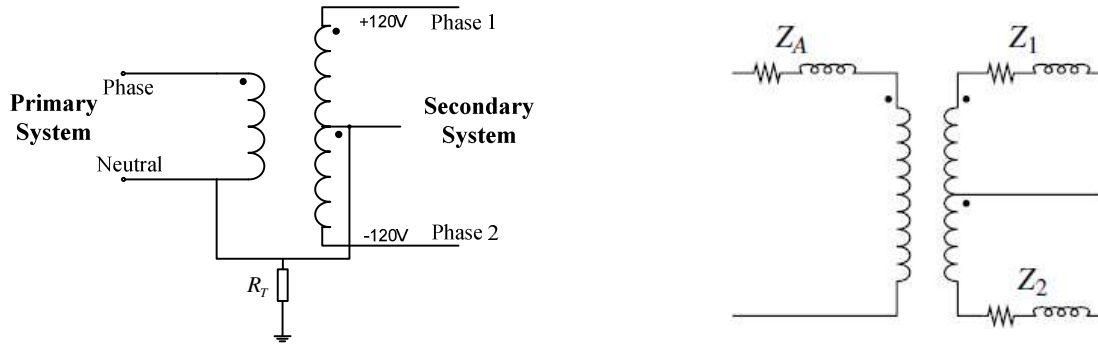
$$Z_{MGN} \approx Z_{lad1} // Z_{lad2} = \frac{1}{2} \sqrt{z_{nn} R_{gn} s} \quad (4.1)$$

$$Z_{lad} \approx \sqrt{z_{nn} R_{gn} s} \quad (4.2)$$

where,  $z_{nn}$  is the self-impedance of the primary system neutral wire ( $\Omega/\text{km}$ ),  $R_{gn}$  is the primary system neutral grounding resistance and  $s$  is the distance (km) between the grounding resistances ( $R_{gn}$ ). The parallel of  $Z_{lad1}$  with  $Z_{lad2}$  is due to the fact that there is an upstream and a downstream ladder at the point of the service transformer.

### 4.1.2. Service Transformer Model

In North America, the standard secondary load service is a 120/240 V three-wire service. This is accomplished with a single-phase, three-winding service transformers connecting the primary to the secondary system [61]. The model for this transformer is shown in Figure 4.5(a).



(a) Single-phase service transformer

(b) Model of a 120/240-V secondary winding with all impedances in percent

**Figure 4.5: Single-phase service transformer.**

Normally, the nameplate impedance of a single-phase transformer is the full-winding impedance, the impedance seen from the primary when the full secondary winding is shorted from “Phase 1” to “Phase 2”. If the full-winding nameplate impedance for the transformer is  $R + jX$ , the primary ( $Z_A$ ) and secondary impedances ( $Z_1$  and  $Z_2$ ), as shown in Figure 4.5(b), can be obtained through equation below [61]:

$$\begin{aligned} Z_A &= 0.5R + j0.8X \\ Z_1 &= Z_2 = R + j0.4X \end{aligned} \tag{4.3}$$

It is common practice to interconnect the primary and secondary neutrals and to use a single ground for these neutrals, which provides lower grounding resistance for both the primary and secondary systems.

### 4.1.3. Secondary System Model

The secondary feeder connects several houses (and other low voltage loads) to the service transformer. Loads of each house are connected between phases and neutral or between phases. Figure 4.6 shows an equivalent model of a residential house. Loads are supplied with phase-to-neutral 120V (modeled by  $Z_a, i_a$  and  $Z_b, i_b$ ) and phase-to-phase 240V (modeled by  $Z_{ab}, i_{ab}$ ).  $Z_N$  is the neutral impedance. Linear residential loads are modeled as constant power loads at the fundamental frequency and as impedance at harmonic frequencies [26]. The nonlinear residential

loads are modeled as constant power loads at the fundamental frequency and as current sources at harmonic frequencies [26].

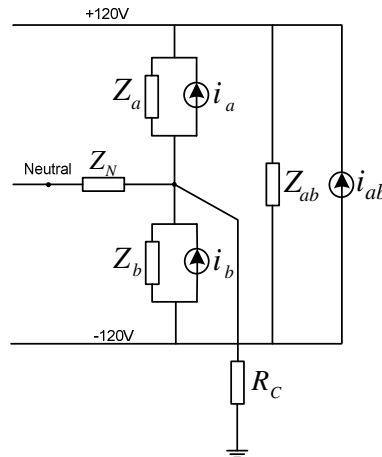


**Figure 4.6: Single house harmonic equivalent model.**

What is unique in this study is that the three impedances and harmonic currents sources vary throughout a 24 hour period according to the residential loads' switch-on probability distribution. In Chapter 3, a bottom-up probabilistic technique was proposed to create the impedances and current sources for each house. The approach can be summarized into the following steps:

- 1) Establish the types of residential loads;
- 2) Determine the number of loads per household;
- 3) From the probabilistic switch-on profile, the daily usage pattern for each load is determined;
- 4) Loads that are ON are modeled as current sources or impedances based on if they are nonlinear or linear;
- 5) Create the harmonic house aggregated model  $(Z_a, i_a, Z_b, i_b, Z_{ab}, i_{ab})$ , as shown in Figure 4.6. For example,  $i_a$  represents the summation of the harmonic current sources of all loads connected between phase A and neutral;
- 6) Connect each house model to the secondary side of the service transformer as shown in Figure 4.2.

## 4.2. Simulation Technique

A multiphase harmonic load flow (MHLF) program developed by Professor Wilsun Xu [19]-[20] and made available by the University of Alberta is used for the simulation studies. The

system must be modeled in multiphase due to the inclusion of the neutral conductor, grounding points and two-phase conductors. Basically, the MHLF technique consists of two major parts. The first part constructs harmonic Norton equivalent circuits for the nonlinear elements. The second part performs linear network solutions at fundamental and harmonic frequencies

The procedure to perform the harmonic power flow simulations is shown in Figure 4.7 and is summarized as follows:

- 1) Determine the type of appliances per household;
- 2) Determine the number of appliances per household;
- 3) Generate the model for the linear and nonlinear appliances;
- 4) Determine each appliance daily usage pattern and build the harmonic houses model (Figure 4.6);
- 5) For time snapshot T1, connect the fundamental frequency component of the houses model to the service transformer and the primary system and run power flow;
- 6) The harmonic spectrum of both magnitude and phase angle of the current sources are shifted to match the fundamental power flow results of Step 5;
- 7) Connect the harmonic current sources into the study system and run harmonic power flow. Save the results;
- 8) Go back to Step 5, and repeat it for another time snapshot (T2), until last snapshot;
- 9) Go back to Step 2 for another load penetration level (or residential load usage scenario).

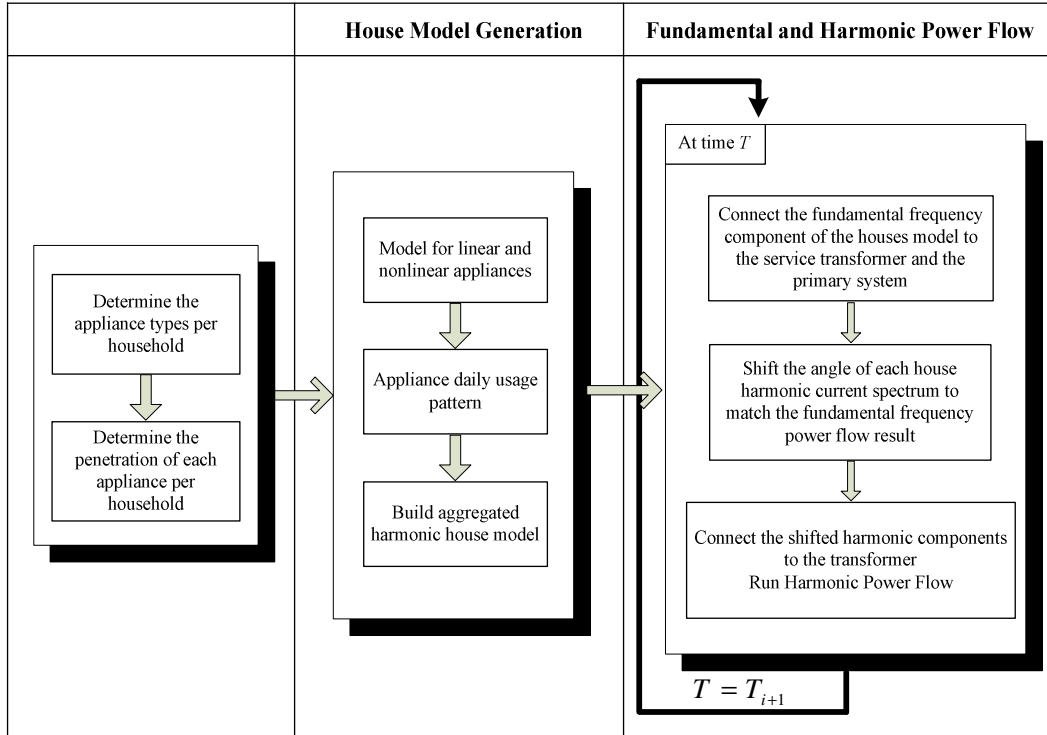


Figure 4.7: Harmonic power flow simulation procedure for the secondary system.

### 4.3. Model Parameters Used for Simulation Studies

Table 4.1 presents the system parameters for the base case harmonic power flow simulations considering the test system shown in Figure 4.2.

Table 4.1: Base case system parameters.

Base Case System Parameters		Values
Primary System	MGN grounding resistance ( $R_{gn}$ )	15 ohms
	Grounding span of the MGN neutral (s)	75 m
	Impedance of MGN neutral ( $z_{nn}$ )	$0.397 + j0.912$ ohm/km
	Voltage Source ( $V_{TH}$ )	14400 V (@ 60 Hz)
	Primary System Impedance ( $Z_{TH}$ )	$0.48 + j2.58$ ohm
Service Transformer	Voltage ( $V_H/V_L$ ) rating	14400/120 V
	KVA rating	37.5 kVA
	Impedance	2 %
	Resistance	1.293 %
	Grounding resistance ( $R_T$ )	12 ohms
Secondary System	Customer grounding resistance ( $R_C$ )	1 ohm
	Neutral impedance ( $Z_N$ )	$0.55 + j0.365$ ohm/km
	Phase impedance ( $Z_A$ and $Z_B$ )	$0.21 + j0.094$ ohm/km
	Number of houses (N) for each single-phase service transformer	10
	Distance between houses	20 m

Most single-phase service transformers in Alberta, Canada has a capacity of 37,5 kVA supplying 10-20 houses. It is important that in Table 4.1 the number of houses is 10 per each single-phase service transformer.

#### 4.4. Results of Interest for Secondary System Analysis

The harmonic power flow simulations yield massive amount of results for each time snapshot, feeder location, and power quality indices. For secondary system analysis, the following results are analyzed in this thesis:

- **Voltage and current distortions in the secondary system [62]:**

- Harmonic spectrum;
- Individual Harmonic Voltage Distortion (IHD<sub>V</sub>)

$$IHD_V(\%) = \frac{V_h}{V_1} \times 100 \quad (4.4)$$

- Total Harmonic Voltage Distortion (THD<sub>V</sub>)

$$THD_V(\%) = \frac{\sqrt{\sum_{h=3}^H V_h^2}}{V_1} \times 100 \quad (4.5)$$

- Individual Demand Distortion of Current (IDD):

$$IDD(\%) = \frac{I_h}{I_L} \times 100 \quad (4.6)$$

- Total Demand Distortion of Current (TDD):

$$TDD(\%) = \frac{\sqrt{\sum_{h=3}^H I_h^2}}{I_L} \times 100 \quad (4.7)$$

where  $I_L$  is the peak or maximum demand load current at the fundamental frequency.

The IDD or TDD factor is similar to IHD or THD except that the distortion is expressed as a percentage of maximum load current over a 24 hour period, rather than as a percentage of the fundamental current at the same instant. These indices are used to address the light load cases where a small fundamental frequency current may result in a large IHD or THD values.

- **Neutral conductor current/voltage rise:**
  - Neutral current and neutral-to-earth voltage harmonic spectrum
  - Neutral-to-earth voltage RMS:

$$V_{RMS} = \sqrt{\sum_{h=1}^H V_h^2} \quad (4.8)$$

- **Impact of harmonics on the secondary system losses:**
  - Fundamental and harmonic power losses at phases and neutral circuits

$$P_h = R(h) \times I_h^2 \quad (4.9)$$

- **Impact of harmonics on revenue meter errors**
  - Harmonic influence on the accuracy of residential revenue meter. This study is based on reference [8].
- **Overloading of the distribution transformer:**
  - Distribution transformer windings I<sup>2</sup>R losses for fundamental and harmonics
  - K-Factor: Transformers expected to supply non-linear loads must be oversized (derated) by a factor depending on the severity of the harmonics and the amount of eddy losses in the transformer. K-Factor is a standard unit of measure to describe the heating effects on a transformer of non-linear loads. It can be calculated from expression below:

$$K - factor = \frac{\sum_{h=1}^H h^2 (I_h / I_1)^2}{\sum_{h=1}^H (I_h / I_1)^2} \quad (4.10)$$

The above results can be quite different at different times of a day due to the varying nature of the loads. Therefore massive amount of results are available for analysis. In order to facilitate the interpretation of results, further processing is needed to produce summary information. The time variation of the results can be condensed using histograms and cumulative distribution curves. For example, instead of providing the 24 hours profile of a harmonic result, a single index showing the average value or the value that is not exceeded by 95% of the time (called “95% index”) can be more useful. On the other hand, for 5% of the time (around 1.2 hours), the harmonics should be expected to be more severe than the 95% index value. However, IEEE 519-1992 [62] states that the steady state harmonic limits can be exceeded by 50% for short periods of time (up to one hour per day).

The results obtained at different locations can also be condensed through averaging. In this

thesis, the “95% index” is adopted. This index is explained using Figure 4.8. In this case, the simulation studies will yield the 3<sup>rd</sup> harmonic voltage profiles for different houses (i.e. nodes in the simulation model) over a 24 hour period. These profiles are averaged first to create a 3<sup>rd</sup> harmonic voltage profile representing the secondary system. The average profile is then transformed into an accumulative probability curve. This curve allows extraction of a 3<sup>rd</sup> harmonic voltage value that will not be exceeded by 95% of the time. This value (showed as 0.81V in the Figure) is the “95% index” value of interest.

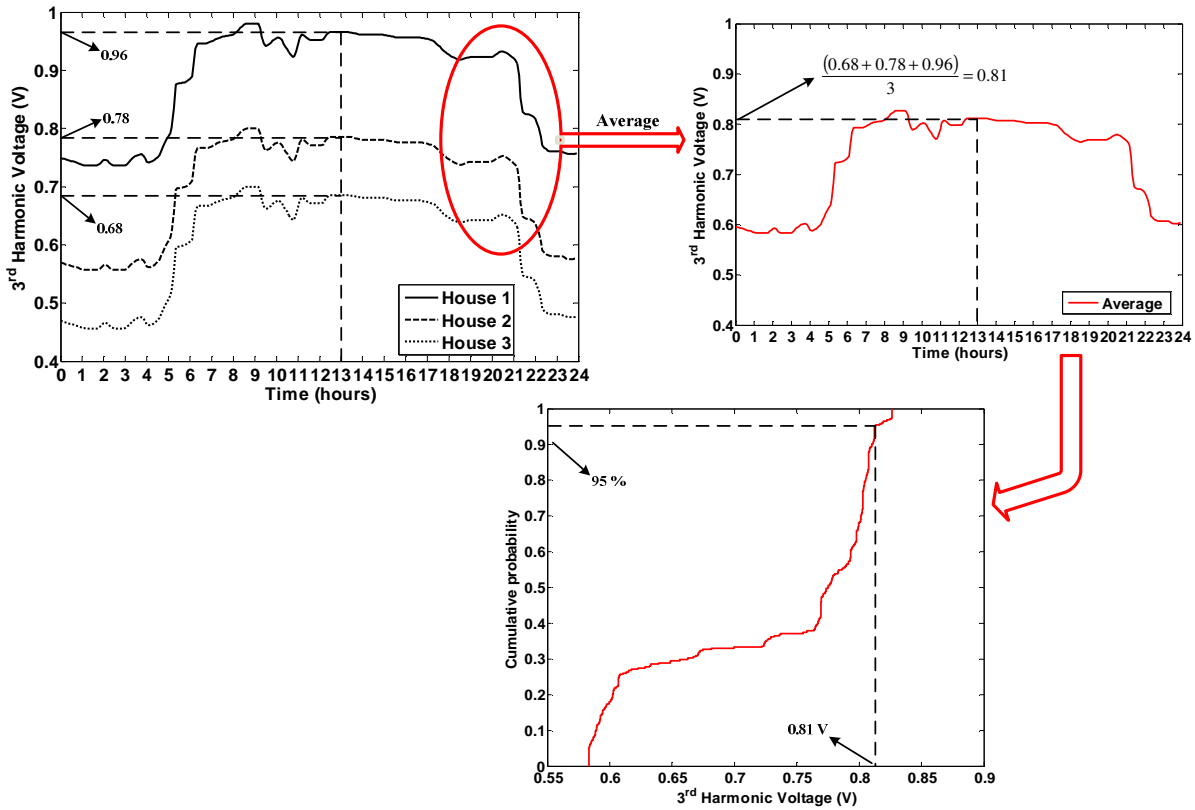


Figure 4.8: Definition of and procedure to determine the “95% index”.



---

## Chapter 5

# MODELING AND SIMULATION OF PRIMARY DISTRIBUTION SYSTEMS

---

In the previous chapter, a modeling approach to perform the harmonic analysis on the secondary system was presented. In the present chapter, the objective is to develop a distribution network model to analyze the impact of the distributed nonlinear loads on the primary distribution system. Depending on the type of the study and on the location of interest, the primary and the secondary distribution systems can be modeled differently. In this chapter, the objective is to analyze the impact of the harmonic loads on the *primary system* so that a detailed model for this system is necessary. On the other hand, the *secondary system* is represented by a simplified model. An ideal feeder and an actual feeder have been used for this study. The configuration of the ideal feeder is shown in Figure 5.1. The actual feeder and its study results are described in Appendix D.

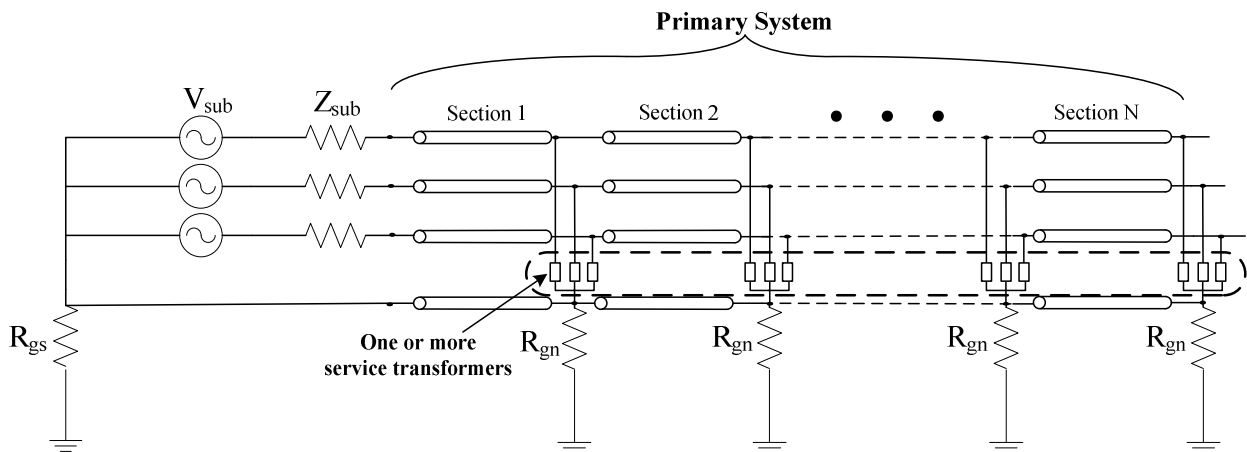


Figure 5.1: Multigrounded 4-wire distribution system.

In Figure 5.1, the portion of the network inside the dashed rectangle represents one or more service transformers connected to the secondary system composed of several residential homes. The service transformer model in this case is an equivalent circuit representing the entire

secondary distribution systems served by that transformer.

## 5.1. Primary System Model

As shown in Figure 5.1, the general configuration of the primary distribution system adopted for simulations is a four-wire, multigrounded system (three-phase conductors plus a multigrounded neutral). The loading of a distribution feeder is inherently unbalanced because of the large number of unequal single-phase loads that must be served. The supply system (substation) is represented by a three-phase voltage (fundamental frequency) source in star connection. The equivalent impedance  $Z_{\text{sub}}$  includes the impedances of high voltage system and the substation transformer.  $R_{\text{gs}}$  is the grounding resistance at the substation.

The feeder itself is represented using a four-phase line model, meaning the coupling among the phase and neutral conductors are represented. For the harmonic impact analysis, the line is represented by the lumped PI model, as shown in Figure 5.2. In order to facilitate the visualization of Figure 5.2, not all mutual impedances are represented, but they are taken into account as shown in equations below. Applying the Kirchhoff Current Law (KCL) in the node  $k$  of the line segment illustrated below, the following relationship can be found:

$$\begin{bmatrix} I_a^{\text{line}} \\ I_b^{\text{line}} \\ I_c^{\text{line}} \\ I_n^{\text{line}} \end{bmatrix} = \begin{bmatrix} I_a^k \\ I_b^k \\ I_c^k \\ I_n^k \end{bmatrix} - \frac{1}{2} \times \begin{bmatrix} Y_{aa} & Y_{ab} & Y_{ac} & Y_{an} \\ Y_{ba} & Y_{bb} & Y_{bc} & Y_{bn} \\ Y_{ca} & Y_{cb} & Y_{cc} & Y_{cn} \\ Y_{na} & Y_{nb} & Y_{nc} & Y_{nn} \end{bmatrix} \times \begin{bmatrix} V_{ag}^k \\ V_{bg}^k \\ V_{cg}^k \\ V_{ng}^k \end{bmatrix} \quad (5.1)$$

And by applying the Kirchhoff Voltage Law (KVL) between nodes  $k$  and  $m$ , we have:

$$\begin{bmatrix} V_{ag}^k \\ V_{bg}^k \\ V_{cg}^k \\ V_{ng}^k \end{bmatrix} = \begin{bmatrix} V_{ag}^m \\ V_{bg}^m \\ V_{cg}^m \\ V_{ng}^m \end{bmatrix} + \begin{bmatrix} Z_{aa} & Z_{ab} & Z_{ac} & Z_{an} \\ Z_{ba} & Z_{bb} & Z_{bc} & Z_{bn} \\ Z_{ca} & Z_{cb} & Z_{cc} & Z_{cn} \\ Z_{na} & Z_{nb} & Z_{nc} & Z_{nn} \end{bmatrix} \times \begin{bmatrix} I_a^{\text{line}} \\ I_b^{\text{line}} \\ I_c^{\text{line}} \\ I_n^{\text{line}} \end{bmatrix} \quad (5.2)$$

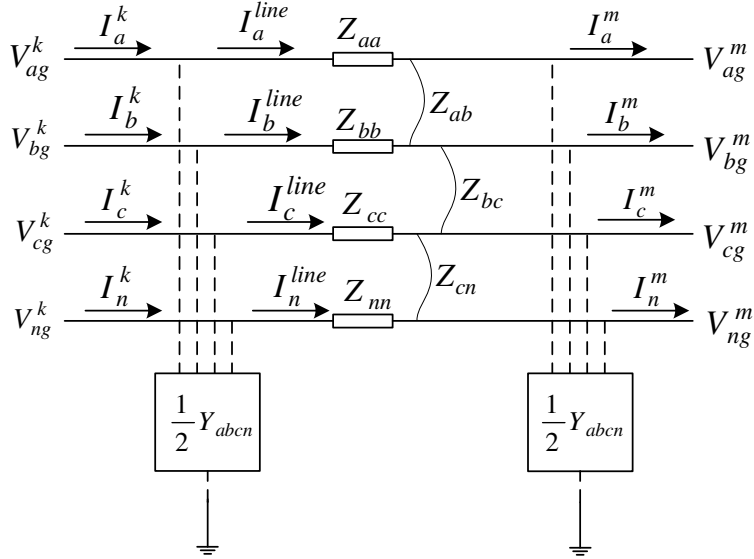


**Figure 5.2: Four-wire (four-phase) feeder model.**

Furthermore, the neutral of the primary feeder is grounded at regular intervals with identical resistances ( $R_{gn}$ ). In one of the studies to be presented later, a 5<sup>th</sup> wire is introduced to model a conductor that runs in parallel with the feeder. This conductor simulates the probe-wire<sup>5</sup> in telephone interference measurement. The voltage induced in this conductor is a useful index to estimate the level of telephone interference.

From the primary system, several houses (and other low voltage loads) are connected through multiple distribution (service) transformers whose modeling will be discussed in the next subsection.

## 5.2. Service Transformer and Secondary System Model

For studying the primary systems, instead of using the full service transformer model (Figure 5.3(a)) in the multiphase harmonic power flow simulations, an equivalent circuit model is proposed to represent the service transformers and their loads, as shown in Figure 5.3(b). The process to derive the model is presented in Appendix C, including validation studies. The proposed simplified transformer model reduces both the time and the complexity of the simulations.

<sup>5</sup>One standard procedure to measure the levels of telephone interference is to place a 100 feet probe wire, grounded on both ends, under and parallel to an overhead power line. This procedure is commonly adopted by power utilities and telephone companies. This wire is used to get measurements of the induced voltage from the resultant magnetic field produced by harmonic currents flowing in the above overhead power line (phases and neutral). From the induced harmonic voltage on the probe wire, it is possible to observe which are the highest harmonic components contributing to the telephone line noise [63].

In Figure 5.3(b), N and G represent the common points connected to primary system phase, neutral and ground respectively. The impedances and current sources are determined from the probabilistic bottom-up approach presented in Chapter 3 and summarized in Section 4.1.3. So the model parameters are different at different simulation steps.

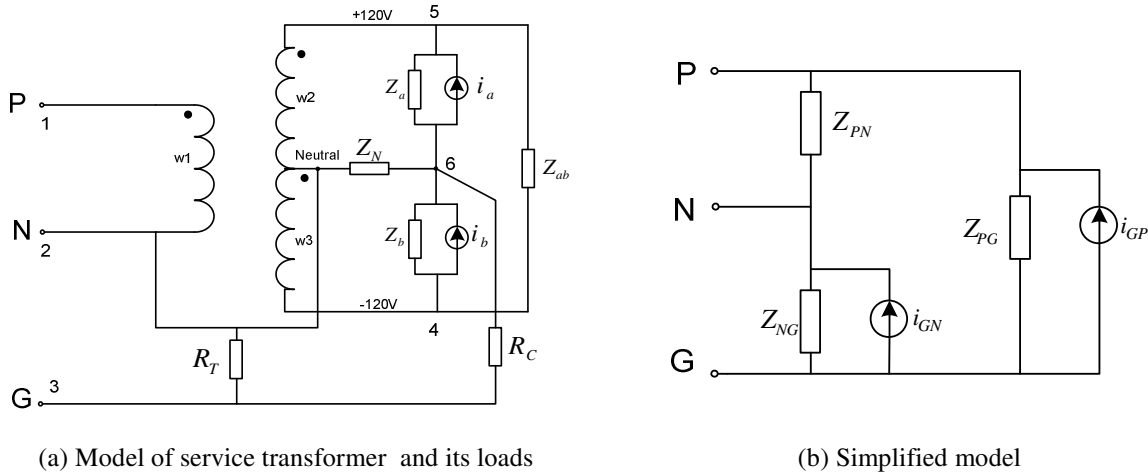


**Figure 5.3: Simplified model of the service transformer and its loads.**

### 5.3. Simulation Procedure for Primary System Analysis

This section describes the steps necessary to perform the multiphase harmonic power flow simulations to study the impact of distributed nonlinear residential loads on the primary system. The procedure to perform the harmonic power flow simulations is shown in Figure 5.4 and is summarized as follows:

- 1) Determine the type of appliances per household;
- 2) Determine the number of appliances per household;
- 3) Generate the model for the linear and nonlinear appliances;
- 4) Determine each appliance daily usage pattern and build the harmonic houses model (Figure 4.6);
- 5) Connect the houses to the service transformer and build simplified model for all service transformers per the procedure of Appendix C;
- 6) For time snapshot T1, connect the fundamental frequency component of the simplified transformers model to the primary system and run power flow;
- 7) The phase angle of the harmonic current sources of the simplified transformers are shifted

to match the fundamental power flow results of Step 6;

- 8) Connect the shifted harmonic components of the simplified transformer models and run harmonic power flow. Save the results;
- 9) Go back to Step 6, and repeat it for another time snapshot (T2), until last snapshot;
- 10) Go back to Step 2 for another load penetration level (or residential load usage scenario);

It is worthwhile to point out that Steps 1 to 4 are similar to those used in the secondary system studies. The difference is that these steps are used to create an equivalent service transformer model (Step 5) suitable for studying the primary systems. In the secondary system study, steps 1 to 4 are used to create models for each house.

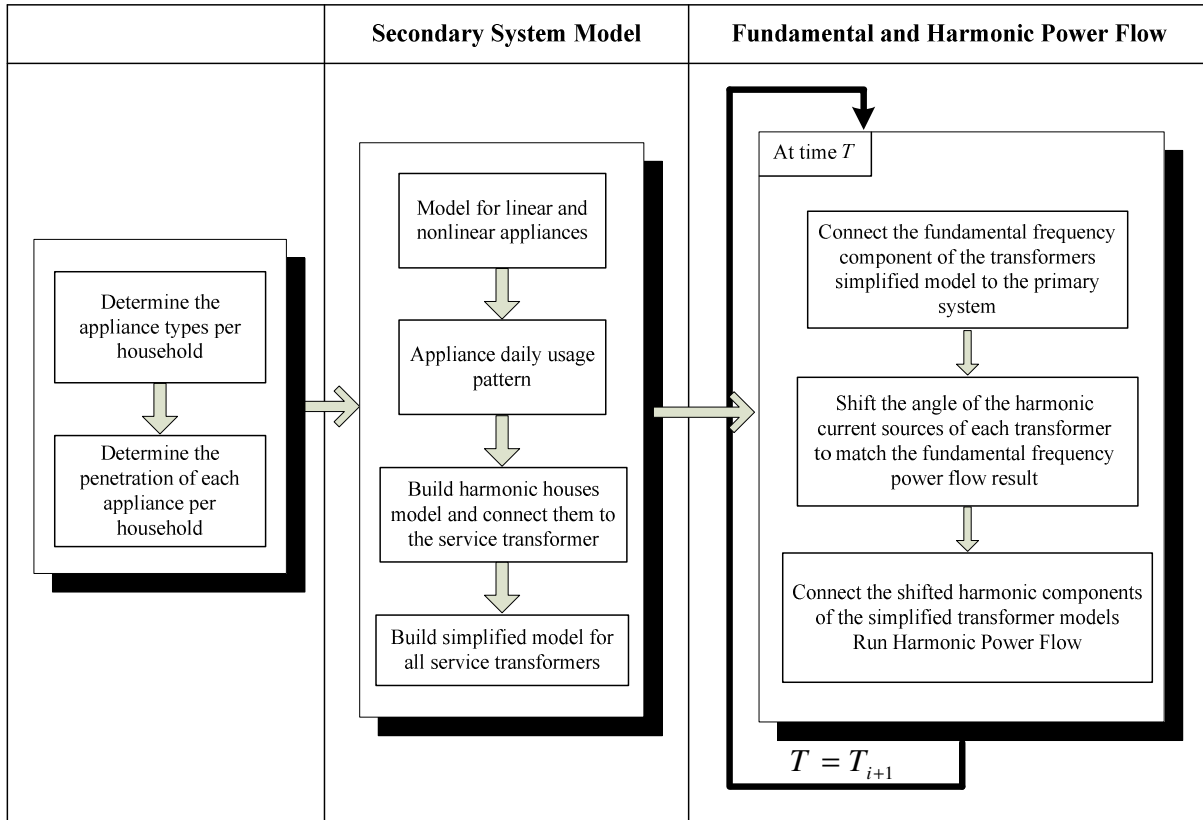


Figure 5.4: Harmonic power flow simulation procedure for the primary system.

## 5.4. Model Parameters Used for Simulation Studies

Figure 5.5 shows the distribution network employed to study the impact of residential loads on the primary systems. This network is referred in this thesis as an ideal feeder. Model parameters of the ideal feeder are summarized in Table 5.1. The feeder under analysis has 12 service transformers per kilometer and for each phase. Then, the total number of service

transformers is 12 x 3 phases x 15 km = 540. Each of the service transformers represents the random power demand of approximately 10 houses.

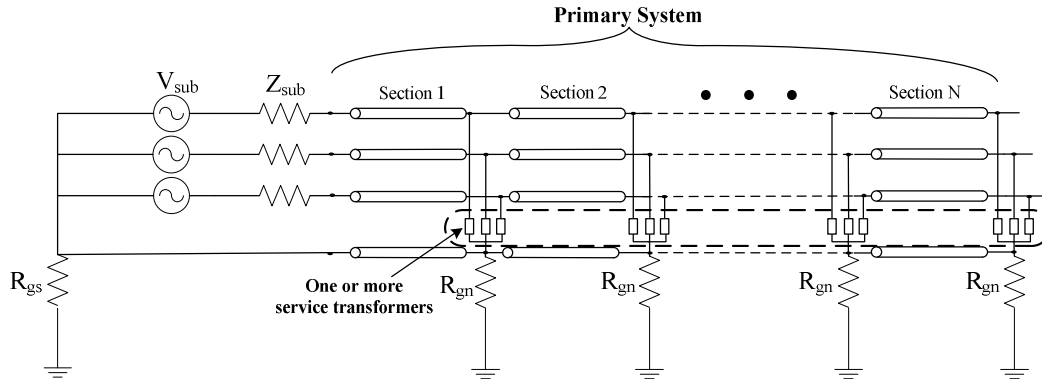


Figure 5.5: Distribution network model for primary system analysis.

Table 5.1: Base case system parameters.

Base Case System Parameters		Values
Primary System	Supply system voltage	14400 V @ 60 Hz
	Substation MVA level	242 MVA
	Substation positive sequence impedance	0.688 + j2.470 ohms
	Substation zero sequence impedance	0.065 + j2.814 ohms
	Substation grounding ( $R_{gs}$ )	0.15 ohms
	MGN grounding resistance ( $R_{gn}$ )	15 ohms
	Grounding span of the MGN neutral (s)	75 m
	Feeder length	15 km
Feeder conductor type	4 - 336.4 ACSR	
Services Transformer	Number of transformers per phase	12 per km
	Voltage ( $V_H/V_L$ ) rating	14400/120 V
	KVA rating	37.5 kVA
	Impedance	2 %
	Resistance	1.293 %
	Grounding resistance ( $R_T$ )	12 ohms
Secondary System	Customer grounding resistance ( $R_C$ )	1 ohm
	Neutral impedance ( $Z_N$ )	0.55 + j0.365 ohm/km
	Phase impedance ( $Z_A$ and $Z_B$ )	0.21 + j0.094 ohm/km
	Number of houses (N)	10
	Distance between houses	20 m

## 5.5. Results of Interest for Primary System Analysis

For studying the harmonic impact of residential loads on the primary systems, the following results are analyzed in this thesis:

- **Harmonic voltage and current distortion levels in the primary system:**
  - Harmonic spectrum (and THD) of voltage on both phase and sequence domain;
  - Harmonic spectrum (and THD/TDD) of current on both phase and sequence domain;

- **Telephone interference in the form of IT factors:** One of the consequences of increasing harmonic current levels is audible noise on telephones lines that run in parallel with distribution feeders. [6]. Telephone circuits are more affected by zero-sequence harmonics because these are in phase in the three phases and add arithmetically. The impact on the telephone line is normally measured by calculating the residual IT factors given by equations below.

- Total residual IT product

$$IT_{total} = \sqrt{\sum_{h=1}^H (w_h \times I_h^o)^2} \quad (5.3)$$

where  $I_h^o$  is the zero sequence current at harmonic  $h$  (only odd harmonics),  $H$  is the maximum harmonic order (in this thesis,  $H = 15$ ).

- Contribution of each harmonic to the residual IT:

$$IT_h = w_h \times I_h^o \quad (5.4)$$

where  $w_h$  is the telephone interference factor (TIF) weighting and is used to take into account the response of the telephone equipment and the sensitivity of the human ear to the harmonic frequencies [6]. Table 5.2 shows the value of this weight for different frequencies. Normally, the main contributors to telephone interference (i.e., highest individual IT) are the 9<sup>th</sup> and 15<sup>th</sup> harmonic orders since they are dominated by zero sequence components and have significant weights (i.e., human ear is significantly susceptible to these frequencies). 3<sup>rd</sup> harmonic component is also dominated by zero sequence components and its magnitude is higher than 9<sup>th</sup> and 15<sup>th</sup>, however the associated TIF weighting is much lower.

**Table 5.2: Telephone interference factor (TIF) weighting at different frequencies [6].**

Frequency (Hz)	Harmonic order #	$w_h$ (TIF)
60	1	0.5
120	2	10
180	3	30
240	4	105
300	5	225
360	6	400
420	7	650
480	8	950
540	9	1320
600	10	1790
660	11	2260
720	12	2760
780	13	3360
840	14	3830
900	15	4350
960	16	4690
1020	17	5100
1080	18	5400
1140	19	5630
1200	20	5860
1260	21	6050
1320	22	6230
1380	23	6370
1440	24	6650
1500	25	6680

- **Neutral conductor current/voltage rise:**
  - Harmonic spectrum (and THD) of neutral to ground voltage
  - Harmonic spectrum (and THD) of neutral current
- **Impact of harmonics on the primary system losses**
  - Fundamental and total active power loss of the primary feeder
- **Overload of substation capacitor**
  - Harmonic spectrum and RMS voltage and current at capacitor location

The primary system studies will also yield massive amount of data. Again the results are



condensed using average values of different locations and the “95% index”, as explained in Chapter 4.

In the next chapters, the harmonic analysis simulations are performed to analyze the impact of the distributed harmonic residential loads on the primary and secondary systems. The results will be useful to answer important questions like:

- What are the potential power quality impacts of mass distributed nonlinear loads on primary and secondary power distribution systems?
- How serious the impacts will become when more and more energy efficient appliances and consumer electronics penetrates into the residential loads?
- If the consequence is of concern, what are the strategies and options available for utilities to manage the problem? The strategies may include the establishment of connection standards and limits.



---

## Chapter 6

# HARMONIC IMPACTS ON SECONDARY DISTRIBUTION SYSTEMS

---

This chapter presents the harmonic study results with respect to the impact of nonlinear residential loads on the secondary distribution systems. Several study scenarios are investigated in order to understand the mechanisms of harmonic build up in residential feeders. Indices are employed to quantify the distortion in voltages and currents at various locations on the secondary system. To assess the impact of nonlinear loads into the future, a load evolution study is conducted.

More specifically, for the secondary distribution system, there are several issues that concern utilities, such as:

- Neutral-to-earth voltage (NEV): Will the harmonics contribute to increase NEV? NEV is a main contributor to stray voltages [64]-[65]
- Service transformer overloading: What is the impact of the harmonic currents on service transformers?
- Revenue meter error: Can high harmonic currents from a house cause unacceptable revenue meter errors?
- Harmonic caused losses: Will the losses in the secondary system increase significantly because of the harmonic currents injected by residential loads?
- How worse the situation can get if more and more appliances are adopted?
- Adopting IEC device level limits: What is the evidence to support the need to limit harmonic emissions from individual residential loads?

## 6.1. Study Scenarios

As the goal of this thesis is to determine the impact of nonlinear home appliances into the future, the studies are conducted for each year over the next several years considering the market trends established in Chapter 2. The following study scenarios are evaluated:

- **Base Case:** The base case scenario uses a current year nonlinear load penetration situation. Its results are used to check if there are any inconsistencies in the simulation results and to serve as the baseline results for comparative studies.
- **Load Evolution Cases:** The appliance loads are “evolved” or “grown” according to the market data. Four load evolution cases are studied:
  - *Case 1: Natural Load Evolution.* This case considers the evolution or change of all major home appliances per the market trend.
  - *Case 2: CFL Load Evolution.* This case considers the replacement of lighting loads by the CFL only. The other loads remain the same as the base case. This is a hypothetical case that helps to understand the impact of CFL.
  - *Case 3: PC Load Evolution.* This case considers the situation where only PC related appliances are changed. Again this is a hypothetical case useful to understand the specific impact of PC loads.
  - *Case 4: TV Load Evolution.* This case considers the situation where only TVs are changed. The results help to understand the specific impact of TV loads.

It shall be noted that the same distribution network is used for all case studies. The number of customers remains the same as in the base case. Only thing that is changed is the appliances under study. The appliances are changed according to the market trend.

## 6.2. Base Case Results

### 6.2.1. Voltage and current distortions in the secondary system

The harmonic phase-to-neutral voltages for all the 10 houses connected to Phase A of the secondary system are obtained. For simplicity, phase-to-neutral voltage will be referred to as phase voltage. The daily average profile include THD<sub>V</sub> is determined and shown in Figure 6.1(a). The “95% index” of the phase voltage is shown in Figure 6.1(b). The results associated to Phase B are not shown because they are similar to Phase A.

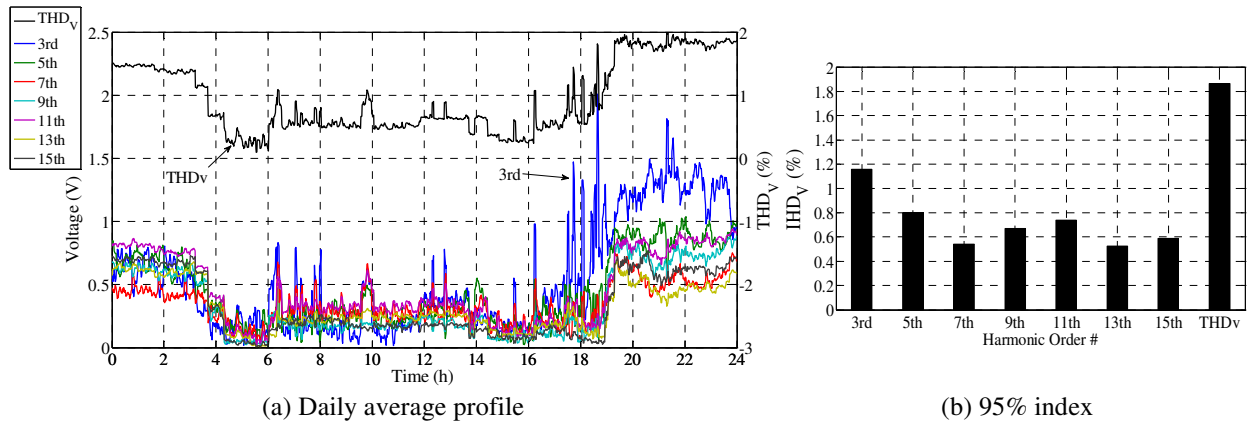


**Figure 6.1: Average harmonic phase voltages of all houses.**

Likewise, the harmonic phase A currents between the houses are obtained. Then, the daily average profile is determined and shown in Figure 6.2(a). The daily average profile of the TDD is shown as well. Finally, from Figure 6.2(a), the 95% index of the individual demand distortion (IDD) and TDD are determined and are shown in Figure 6.2(b).

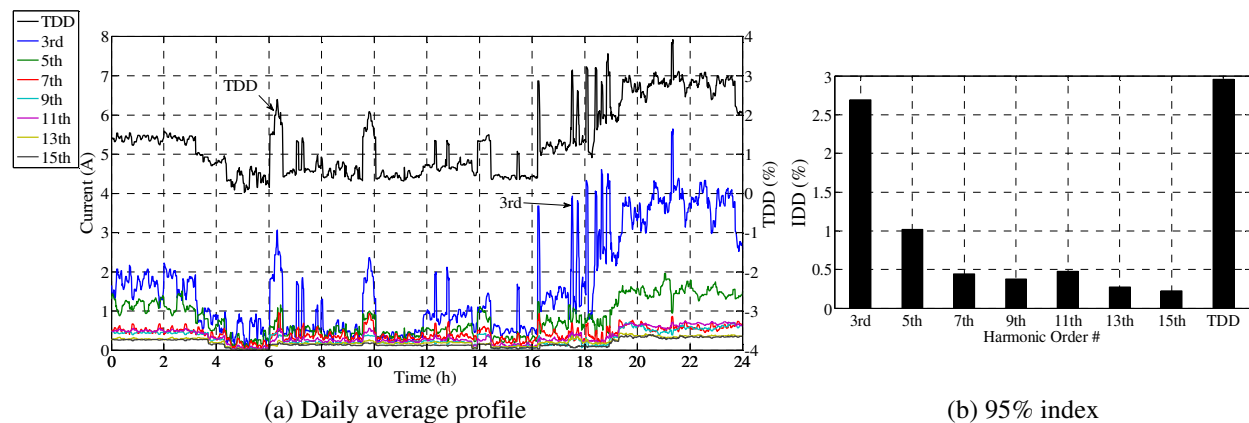


**Figure 6.2: Average harmonic phase current of all houses.**

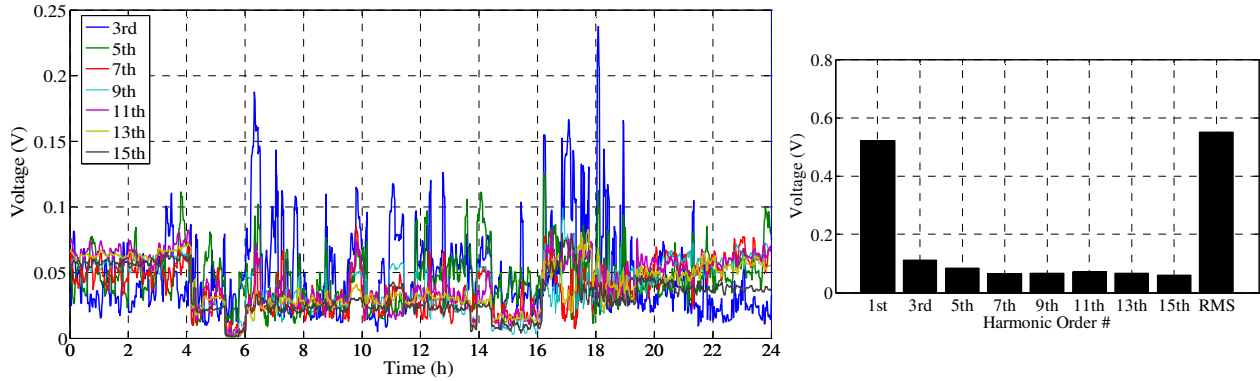
The results show that the 3<sup>rd</sup> harmonic is the dominant component, followed by the 5<sup>th</sup> and 7<sup>th</sup> components. The period during which the harmonic levels are the highest is between 18:00

and 24:00 because more nonlinear load usage occurs during this time such as desktop computers, CFLs, and TVs. From 00:00 to 05:00, most working loads are non-linear, such as fridges and furnaces. The decrease of the harmonic levels from 02:00 can be attributed to people using PCs and CFLs until that late.

### **6.2.2. Neutral conductor current & voltage rise**

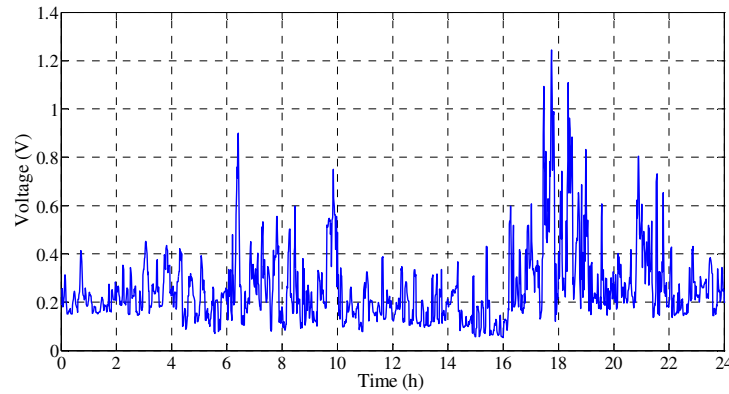
Figure 6.3(a) shows the daily profile of the neutral-to-earth harmonic voltage averaged over all the secondary system houses. Figure 6.3(b) shows the 95% index of the neutral harmonic voltage and its RMS value. Figure 6.4(a) shows the daily profile of the average harmonic neutral current circulating between the houses of the secondary system. Figure 6.4(b) shows the 95% index of the harmonic neutral current. The fundamental component daily profile is not shown so that the figures do not become too crowded.

The results show that the neutral voltage is still dominated by the fundamental frequency component. These are caused by the load imbalance between the two phases. *The implication is that the harmonics produced by nonlinear loads don't have a major impact on neutral-to-earth voltage rise (a major component of stray voltage).* The results also show that 3<sup>rd</sup> harmonic component is the main component of the neutral current. It is important to emphasize that the residential systems considered in this paper are not 3-phase, so there is no accumulation effect for the 3<sup>rd</sup> harmonic current in the neutral due to 120 degree fundamental phase shift.



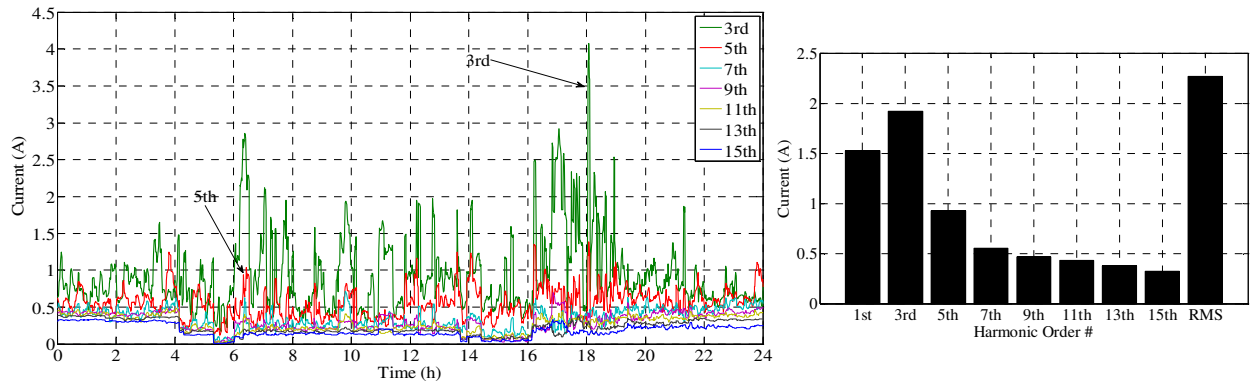
(a) Neutral voltage daily average profile.

(b) 95% index



(c) RMS neutral voltage daily average profile

**Figure 6.3: Average neutral to ground voltage.**



(a) Daily average profile

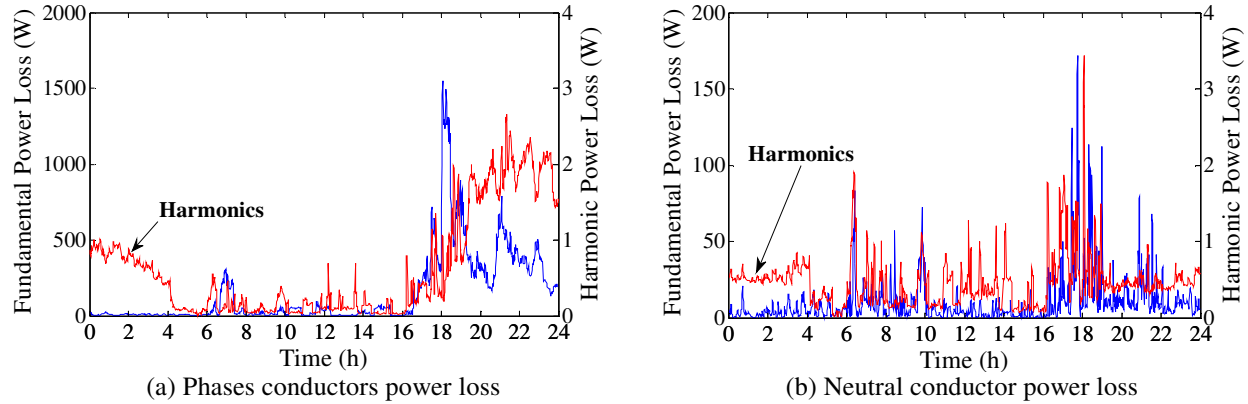
(b) 95% index (fundamental and RMS divided by 10)

**Figure 6.4: Average neutral current circulating between the houses.**

### 6.2.3. Impact of harmonics on the secondary system losses

Figure 6.5 shows the daily total fundamental and harmonic losses of the phase and neutral circuits of the secondary system. The 95% index over the daily phase and neutral losses is also provided. The main finding is that the majority of losses are caused by the fundamental

frequency component and they occur in the phase conductors. The conclusion is that harmonic-caused losses in 3-wire single phase secondary systems should not be a concern to utility companies.



95% index of Power Loss			
Conductor	Phases	Neutral	Total
<b>Fundamental</b>	618.16 W	35.22 W	656.77 W
<b>Harmonic</b>	2.91 W	0.83 W	4.35 W
<b>Total</b>	621.07 W	36.05 W	661.13 W

Figure 6.5: Secondary system power losses.

#### 6.2.4. Overloading of distribution transformers

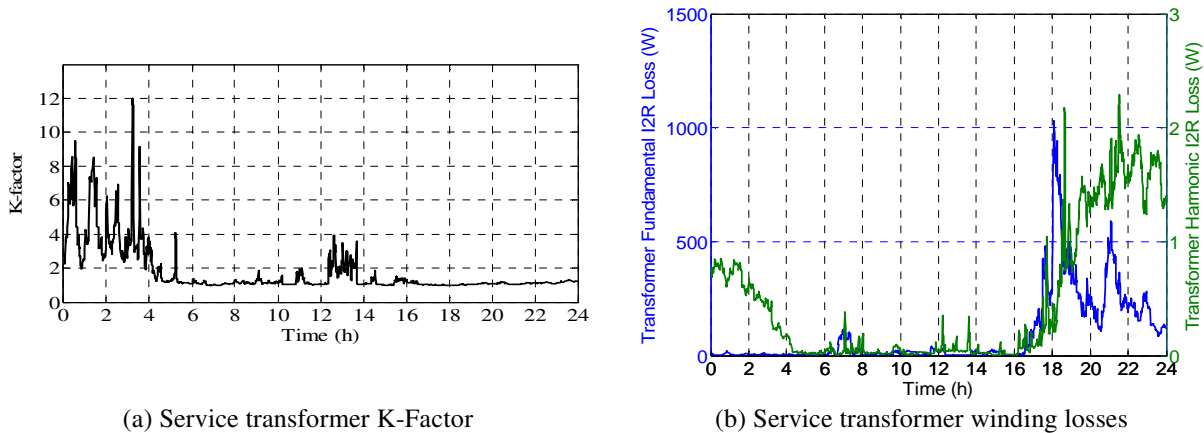
Losses in transformers are due to stray magnetic losses in the core, and eddy current and resistive losses in the windings. Transformers expected to supply non-linear loads must be oversized (derated) by a factor depending on the severity of the harmonics and the amount of eddy losses in the transformer. K-Factor is a standard unit of measure to describe the heating effects on a transformer of non-linear loads [66].

Figure 6.6(a) shows that the K-Factor is high between 00:00 a.m. to 04:00 a.m., which is due to the fact that mainly nonlinear appliances are operating, such as fridge and freezer, and also the transformer loading (fundamental component) is very low during this period, which makes the K-Factor very high, however this should not be a concern because during this period the fundamental current is low. A high K-factor should be of concern if the TDD is also high. On the other hand, beyond this period, the K-Factor is around 1.2 showing that harmonic heating effect is lower. The implication is that the overloading of service transformer could be a concern depending on its 60Hz load level. Here the factor is used as an indicator to assess the increased



loading on the service transformers. How to include harmonics in estimating the total loading of a service transformer needs more research.

The winding losses shown in Figure 6-6 reveal that the fundamental frequency winding loss is still much higher than the harmonic loss.



**Figure 6.6: Service transformer power losses.**

### 6.3. Load Evolution Results

One of contributions of this thesis is to assist the utility distribution companies to evaluate how serious the harmonic impacts will become when more and more energy efficient appliances and consumer electronics penetrates into the residential loads. Therefore, the objective of this section is to investigate the impact of changing the penetration of different residential appliances on the secondary system harmonic level. It must be noticed that the distribution network from the base case is used. Moreover, the number of customers remains the same as in the base case, only the appliances penetration for each existing customer will change.

As mentioned before, to facilitate the interpretation and comparison of the results, all the results are represented by their “95% index” values. Two different charts are provided. The first type of charts shows the index values over the study period (5 years). The second type of charts shows the average annual growth rate of the indices. The growth rate is obtained from the arithmetic mean of the percentage increase obtained for each year relative to the previous year. The annual growth rate is the most useful parameter to predict the future harmonic conditions of a residential feeder.

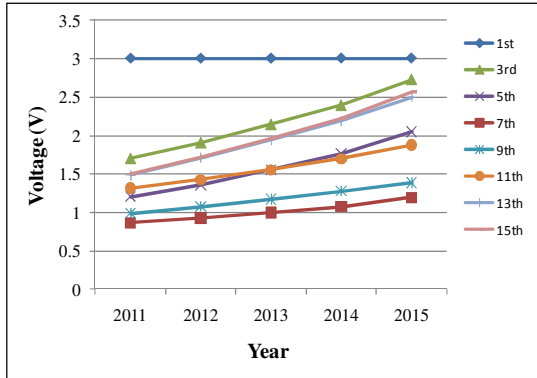
### 6.3.1. Harmonic voltage and current distortions

Figure 6.7(a) shows harmonic voltage in the next 5 years. From the curves, one can calculate the average annual growth rate associated to the index, which is shown in Figure 6.7(c). For example, the 3<sup>rd</sup> harmonic index will grow at the rate of 15% per year. Figure 6.7(c) also shows the individual impact of CFL, PC and TV loads on the annual harmonic growth rate. The harmonic current results are shown in Figure 6.8. The main findings are

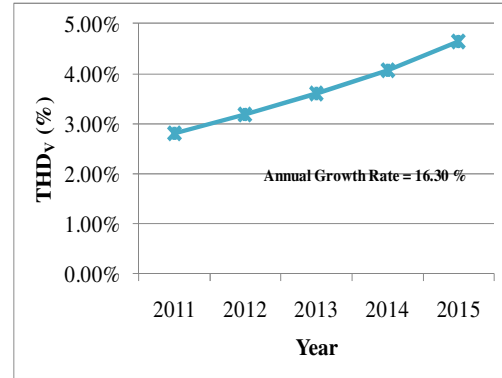
- The phase harmonic currents presented average annual growth rates similar to those of phases harmonic voltages;
- The harmonic growth rates are generally high (above 10%). Among them, the 3<sup>rd</sup>, 5<sup>th</sup>, 13<sup>th</sup> and 15<sup>th</sup> harmonics have the highest growth rates;
- The CFLs have more contributions to the harmonic increase. The LCD TVs has insignificant impact on harmonic increases<sup>6</sup>.

---

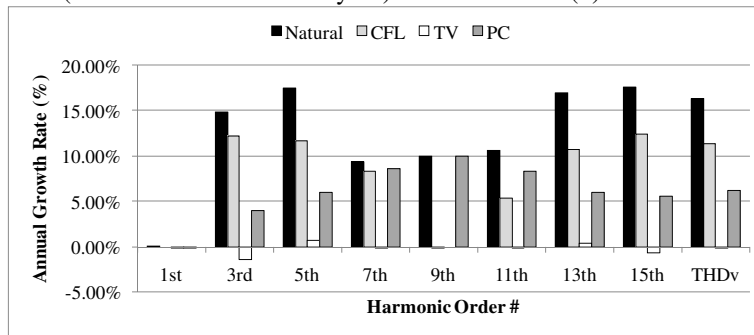
<sup>6</sup> A report entitled “Currents Status of Harmonic in Japan” described the status of harmonics in Japan between 1989 and 2001. It showed that there is a high correlation between the usage of TV and the level of voltage distortion. The larger the number of TVs used, the greater the voltage distortion. Furthermore, the report also showed that the main harmonic of concern is the 5<sup>th</sup>. It shall be noted that during the period of the Japanese study, most TVs were CRT types. This study shows that the replacement of the CRT TVs by the LCD TVs will not cause significant harmonic problems. TVs used, the greater the voltage distortion. Furthermore, the report also showed that the main harmonic of concern is the 5<sup>th</sup>. It shall be noted that during the period of the Japanese study, most TVs were CRT types. This study shows that the replacement of the CRT TVs by the LCD TVs will not cause significant harmonic problems.



(a) Natural load evolution (fundamental is divided by 40)

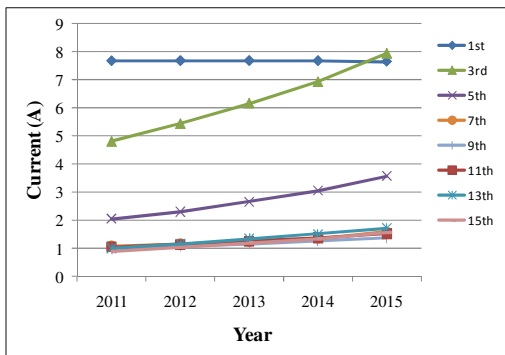


(b) Natural load evolution

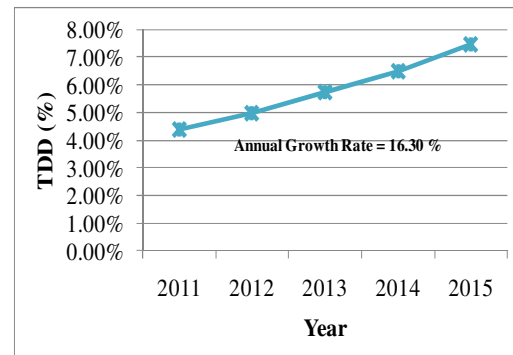


(c) Average annual growth rate

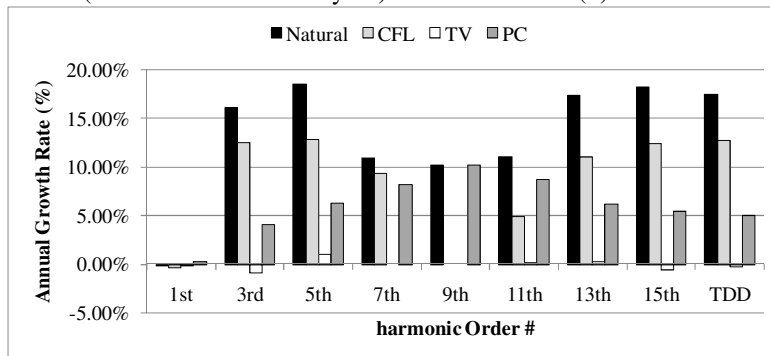
**Figure 6.7: Average phase A voltage.**



(a) Natural load evolution (fundamental is divided by 10)



(b) Natural load evolution



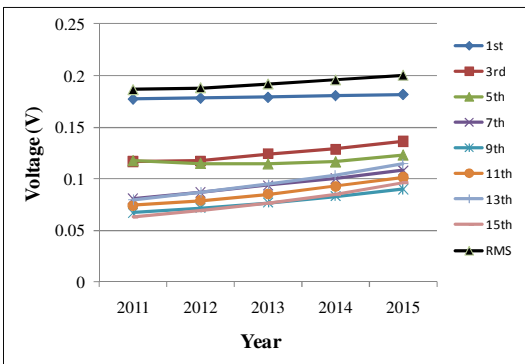
(c) Average annual growth rate

**Figure 6.8: Average phase A current.**

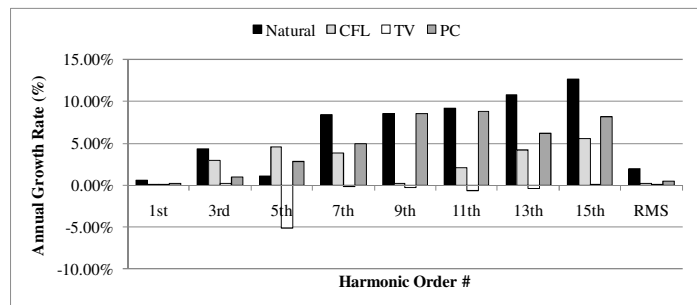
### 6.3.2. Neutral harmonic voltage and current

Figure 6.9 shows the average neutral-to-earth voltage in the next 5 years and the associated average annual growth rate. The results of neutral current are shown in Figure 6.10. The main findings are as follows:

- The neutral voltage and current harmonics have similar growth rates. They are generally lower than that of the phase harmonics;
- The PCs and CFLs are the main contributors for the increase of the neutral harmonics in the coming years. From 3<sup>rd</sup> to 5<sup>th</sup> harmonic component, the CFLs are the main sources and for higher harmonics PCs devices are more influential;
- The neutral RMS voltage levels still remain very low and its average annual growth rate is less than 3%, so home appliances are not expected to create problems associated with neutral voltages. Similar behaviour can be noticed for the RMS current levels, shown in Figure 6.10(b), in which the average growth rate is also less than 3%. This means the increasing penetration usage of nonlinear appliances is not expected to create problems associated to neutral currents, including neutral losses.

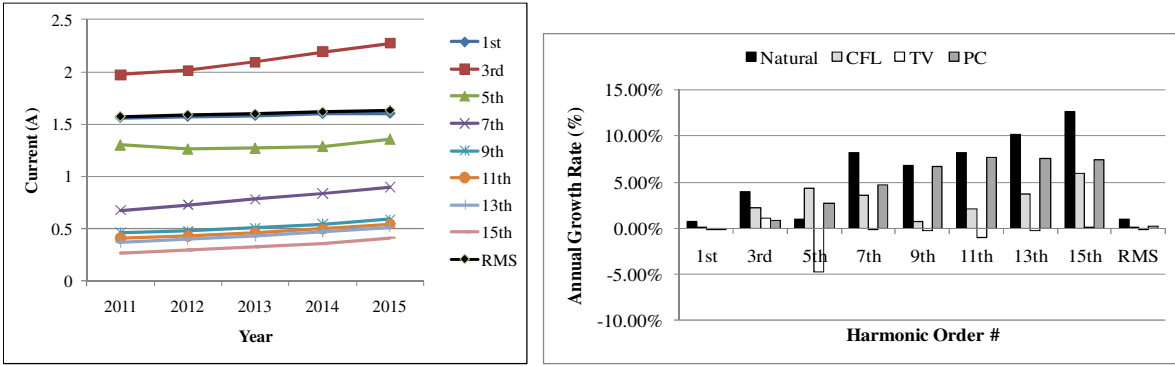


(a) Natural load evolution (fundamental and RMS divided by 3)



(b) Average annual growth rate

**Figure 6.9: Average neutral voltage level.**



(a) Natural load evolution (fundamental and RMS divided by 10)

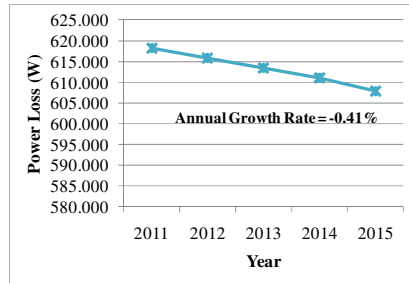
(b) Average annual growth rate

**Figure 6.10: Average neutral current circulating between the houses.**

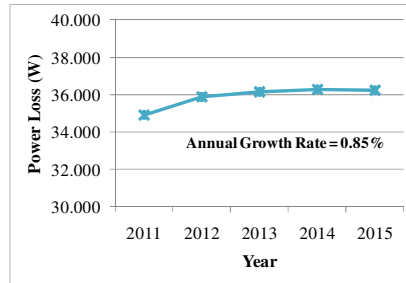
### 6.3.3. Power losses

Figure 6.11 and Figure 6.12 show the total fundamental and harmonic power losses, respectively, on the phases and neutral circuits of the secondary system for the next five years and correspondent average annual growth rate. Figure 6.11 shows a small decrease on the fundamental power losses, which is caused by the use for of more energy efficient appliances, such as CFLs. Although Figure 6.12 shows a relatively higher growth rate of harmonic power losses, it does not represent a concern because the harmonic power losses are very low in comparison with those caused by the fundamental frequency component.

### Natural Load Evolution

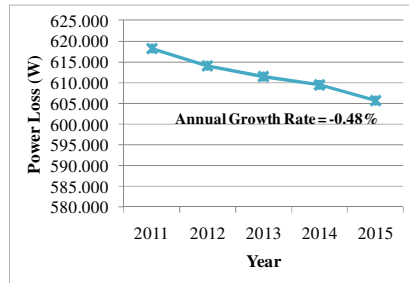


(a) Phases conductors power loss

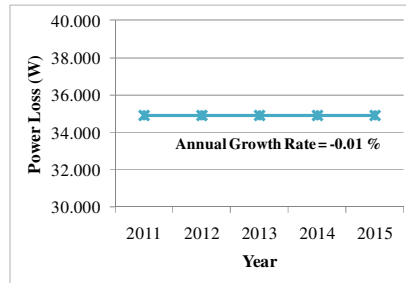


(b) Neutral conductors power loss

### CFL Load Evolution

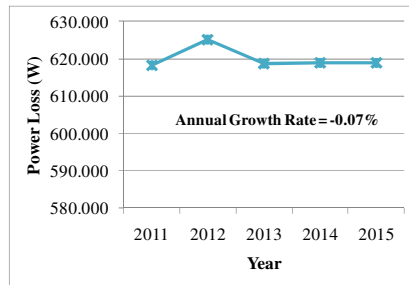


(c) Phases conductors power loss

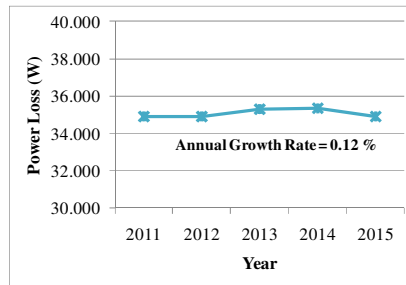


(d) Neutral conductors power loss

### TV Load Evolution

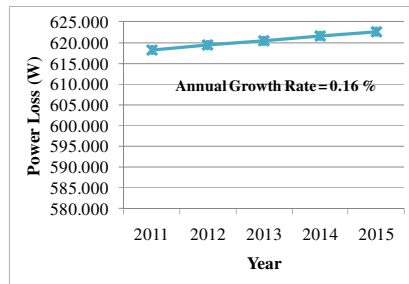


(e) Phases conductors power loss

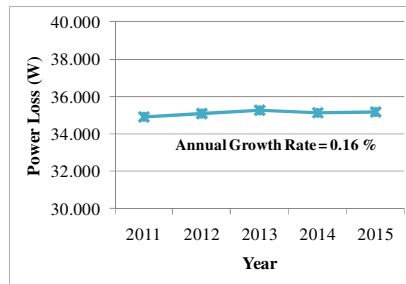


(f) Neutral conductors power loss

### PC Load Evolution



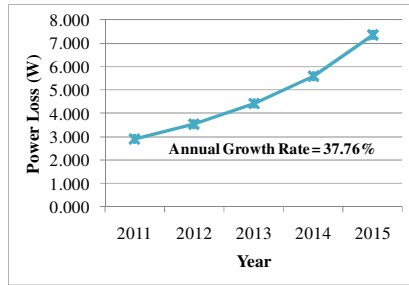
(g) Phases conductors power loss



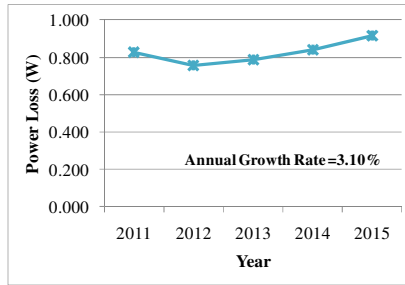
(h) Neutral conductors power loss

**Figure 6.11: Total fundamental power losses at the secondary system.**

### Natural Load Evolution

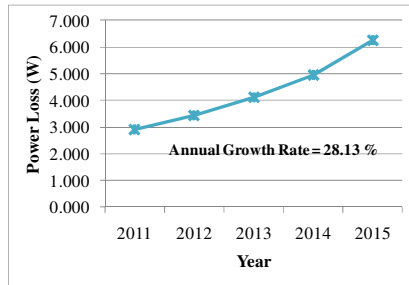


(a) Phases conductors power loss

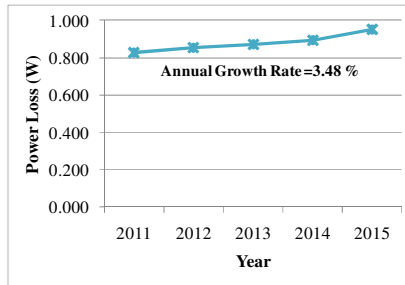


(b) Neutral conductors power loss

### CFL Load Evolution

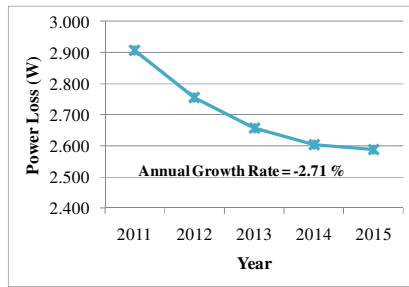


(c) Phases conductors power loss

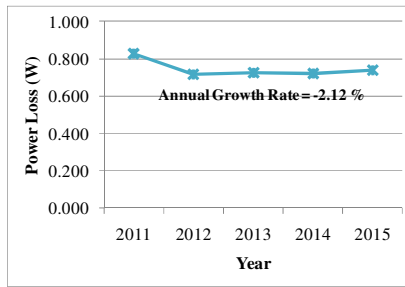


(d) Neutral conductors power loss

### TV Load Evolution

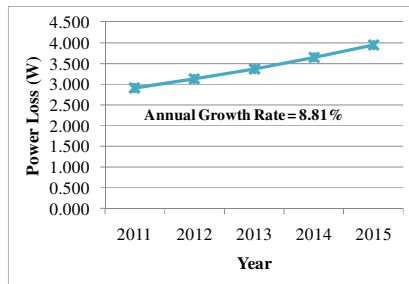


(e) Phases conductors power loss

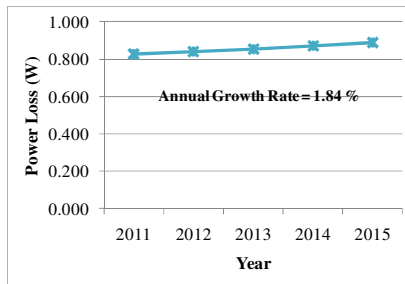


(f) Neutral conductors power loss

### PC Load Evolution



(g) Phases conductors power loss



(h) Neutral conductors power loss

**Figure 6.12: Total harmonic power losses at the secondary system.**

#### **6.3.4. Impact of harmonics on revenue meter errors**

Reference [8] investigated the billing accuracy of three residential revenue meters of different designs (inductive, digital sampling and time division) under both sinusoidal and distorted conditions. The results indicated that if the voltage distortion limits of IEEE Standard 519-1992 ([62], limit of 5%  $THD_V$ ) are not violated, the harmonic power of the load is small and does not significantly affect the overall accuracy of the energy meters. Six conditions with different harmonic levels were considered in the analysis. Even with the worst condition of  $THD_V = 4.1\%$  and  $TDD_I = 28.8\%$ , the energy measured by each meter was very accurate. For example, we can apply the load growth shown in Figure 6.7 to a real scenario.

Our field measurements of some residential houses in Canada showed that the 95% index of  $THD_V$  at the metering point is between 4.3% and 4.5%. If these levels are compared to the analysis of [8], one can conclude that the harmonic levels would not affect the accuracy of the energy meters at present. However, according to the results shown in Figure 6.7 (c), i.e., the average growth rate of  $THD_V$  is about 16% per year, the  $THD_V$  could exceed the IEEE limit of 5% in two years. Higher distortion levels may affect the performance of revenue meters and lead to billing inequities. This situation not only applies to existing mechanical revenue meters, it may also apply to the low end smart meters if the meters are designed without considering the impact of harmonics on the errors of energy calculation [8],[67]-[68].

#### **6.3.5. Impact on service transformer**

Figure 6.13 shows the fundamental, harmonic power losses and the K-Factor of the service transformer on the next five years and correspondent average annual growth rate. It is noted that the Personal Computers (PC) are the responsible for most of the K-factor increase in the coming years. The Natural Load Evolution case reveals that the K-factor will increase at the rate of 10% per year. This is one area that needs the attention by utility companies. The results also show the harmonic caused losses in service transformers are insignificant in comparison with those produced by the 60Hz component.



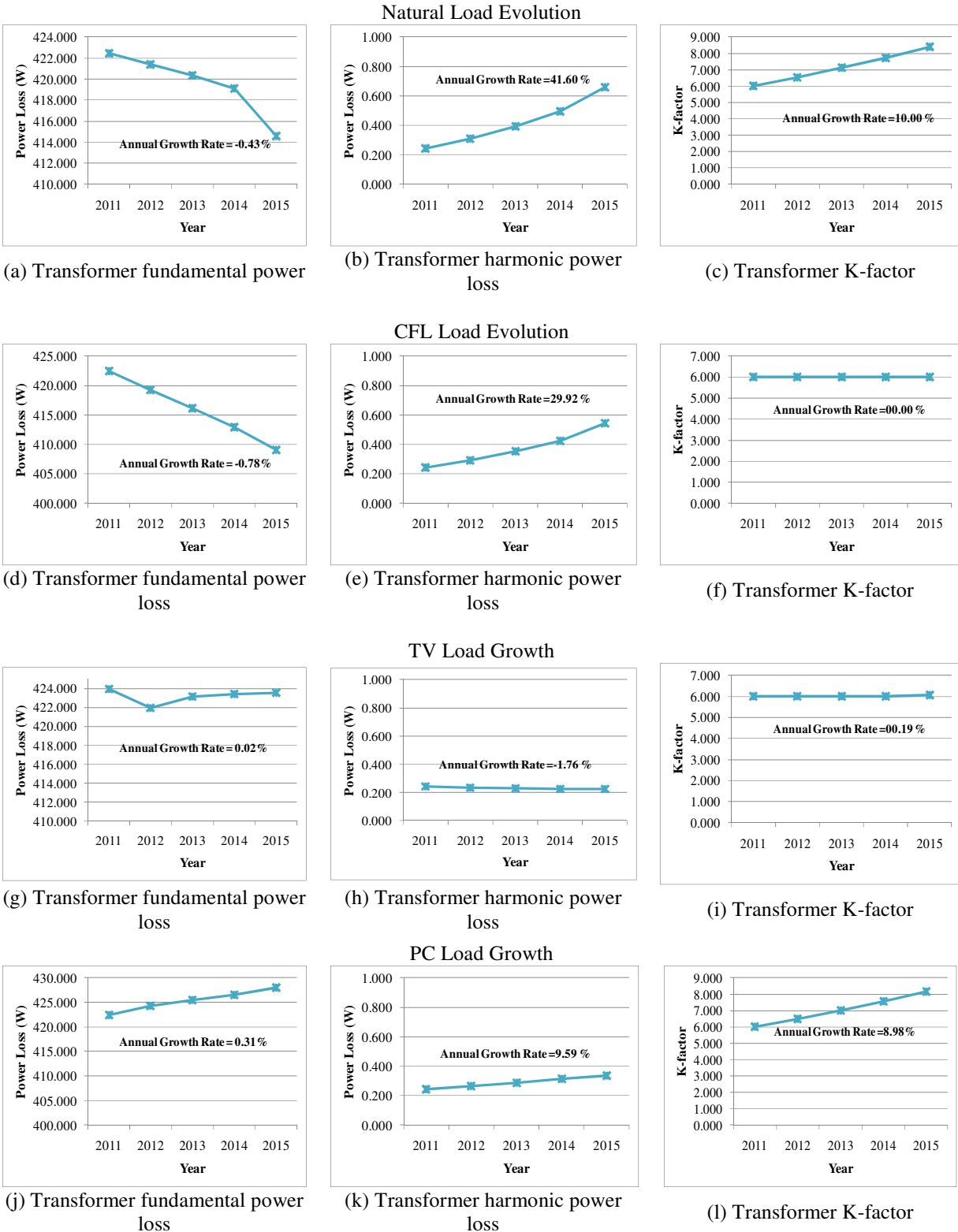


**Figure 6.13: Power loss and K-factor of service transformer.**

Figure 6.13(f) shows that the annual growth rate associated to the K-factor is close to zero. The main reason is that the increasing penetration of CFLs affects the K-Factor level mainly

during the period between 6 p.m and midnight. As a result, one can observe from the base case result (Figure 6.6(a)) that the 95% index remains unchanged with the CFL increase. Considering the period only from 6 p.m. to midnight, the K-factor has an average annual growth of 8%. So, CFLs are unlikely to be a problem regarding transformer overloading in the coming years.

#### 6.4. Summary of Findings

Figure 6.14 shows a summary of the load evolution results for the various indices. The value in parenthesis and the one without above each bar refer to index level at the year 2011 and the average annual growth rate, respectively. The main findings are summarized below:

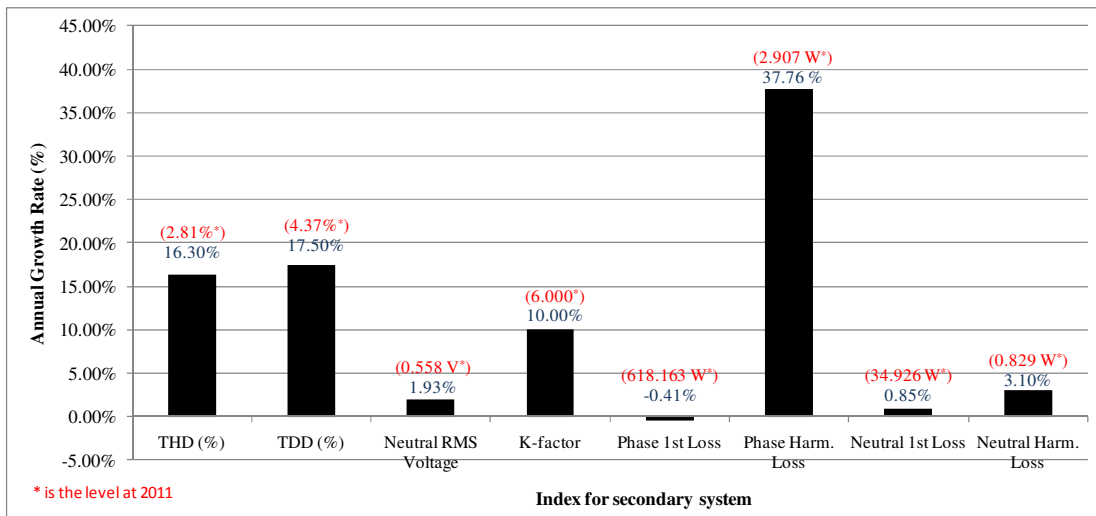


Figure 6.14: Average annual growth for main power quality indices.

- The increased use of electronic home appliances is likely to create concerns in the following areas: (1) increased phase voltage and current harmonics, (2) increased loading on service transformers, and (3) revenue meter errors. The following areas are not of significant concern: (1) harmonic-caused neutral voltage and current rises (2) harmonic-caused losses;
- Revenue meter error: The results also showed that the average growth rate of  $THD_V$  is about 12% per year. As a consequence, considering the present levels of  $THD_V$  of residential houses, this index could exceed the IEEE limit of 5% in two years. According to [8],[67]-[68], the accuracy of revenue meter is not guaranteed when

voltage distortion exceeds 5%;

- Neutral-to-earth voltage (NEV) rise: The results revealed that the RMS NEV levels still remain very low and its average annual growth rate is less than 1%, so CFLs and other modern residential loads are not expected to contribute to the NEV rise problem;
- Harmonic caused losses: The base case results showed that the harmonic power losses on residential 3-wire single-phase secondary systems are very low in comparison with those caused by the fundamental frequency component so that this type of loss should not be a concern to utilities;
- The typical annual growth rates of the indices of concern are in the range of 10% to 15%. The main harmonic components that are of concerns are: 3<sup>rd</sup>, 5<sup>th</sup>, 13<sup>th</sup> and 15<sup>th</sup> due to their relatively high growth rate;
- In terms of major home appliances, CFLs and computing devices are major sources of harmonic increase while the CFL as the most significant. The new generation TVs (LCD TV) are not a concern since they don't contribute to harmonic increase in the system.

It is important to note that the results reported here are based on the load composition characteristics of Canada and United States. Using the previous results directly for other countries will basically depend if they have similar socio-economic scenario, residential loads usage habits and on the characteristics of the secondary distribution networks. Some of the residential loads included in the methodology are not common in other countries. Results for other locations can be obtained using the proposed technique but one needs to consider relevant regional load characteristics. The main purpose of this thesis is to show how to use this information to study the evolution of the harmonic distortion in residential feeders in the coming years.



---

## Chapter 7

# HARMONIC IMPACTS ON PRIMARY DISTRIBUTION SYSTEMS

---

This chapter investigates the impact of the distributed nonlinear residential loads on the primary distribution system. A procedure similar to that of the secondary system study is followed in this investigation, though the focus of this study is different. Several study scenarios are investigated in order to understand the mechanisms of harmonic build up in residential feeders. For the primary distribution system in particular, there are several issues that concern utilities, such as:

- Telephone interference: What is the impact of the harmonic currents on the noise at the telephone lines running in parallel with power lines?
- What is the impact of the harmonic currents on the overloading of substation capacitors
- Harmonic caused losses: Will the losses in the primary system increase significantly because of the harmonic currents injected by residential loads?
- Neutral-to-earth voltage (NEV): Will the harmonics contribute to increase NEV? Stray voltage originates from the contributions of NEV at the secondary and primary distribution systems [64]-[65]
- How the amount of harmonic current injected into the supply transmission system is affected?

### 7.1. Study Scenarios

The four study scenarios used in the secondary system studies are also adopted for primary system study as follows:

- **Base Case:** The base case scenario uses a current year nonlinear load penetration situation. Its results are used to check if there are any inconsistencies in the simulation results and to serve as the baseline results for comparative studies.
- **Load Evolution Cases:** The appliance loads are “evolved” or “grown” according to the market data. Four load evolution cases are studied:
  - *Case 1: Natural Load Evolution.* This case considers the evolution or change of all major home appliances per the market trend.
  - *Case 2: CFL Load Evolution.* This case considers the replacement of lighting loads by the CFL only. The other loads remain the same as the base case. This is a hypothetical case that helps to understand the impact of CFL.
  - *Case 3: PC Load Evolution.* This case considers the situation where only PC related appliances are changed. Again this is a hypothetical case useful to understand the specific impact of PC loads.
  - *Case 4: TV Load Evolution.* This case considers the situation where only TVs are changed. The results help to understand the specific impact of TV loads.

The ideal distribution network shown in Figure 5.5 is used to conduct the case studies in this chapter. The actual feeder and its study results are described in Appendix D. It shall be noted that the same distribution network is used all case studied. The number of customers remains the same as in the base case. Only thing changed is the appliances under study. The appliances are changed according to the market trend.

## 7.2. Base Case Results

Before proceeding to the results, Figure 7.1 provides the average level of load imbalance on the distribution system shown in Figure 5.1, considering the base case parameters. The negative and zero sequence load imbalance ratios are given by equations (7.7) and (7.8), respectively.

$$\text{Negative Sequence Load Imbalance Ratio} = \frac{I_{\text{negative sequence}}}{I_{\text{positive sequence}}} \quad (7.1)$$

$$\text{Zero Sequence Load Imbalance Ratio} = \frac{I_{\text{zero sequence}}}{I_{\text{positive sequence}}} \quad (7.2)$$

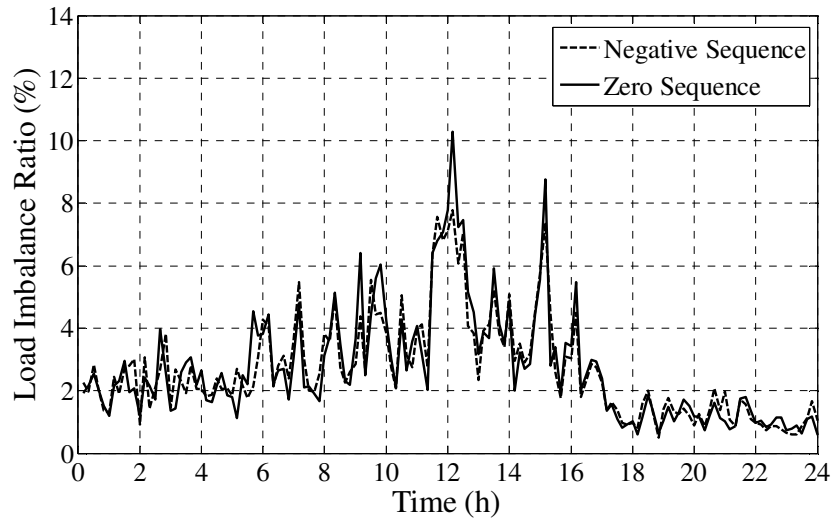
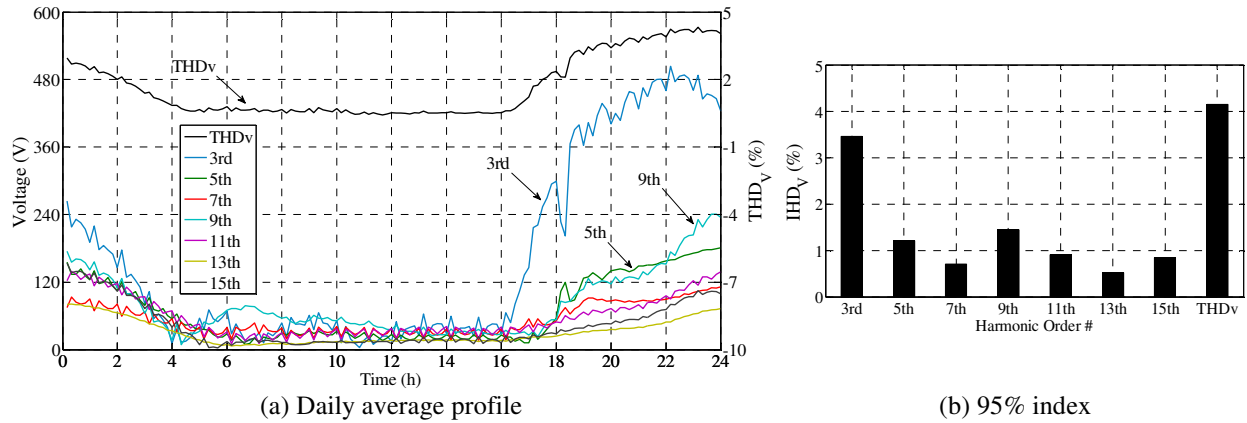


Figure 7.1: Average imbalance level on the distribution network.

### 7.2.1. Voltage and current distortions in the primary system

For quantifying the harmonic distortions, the three phase voltages at every 1 km along the primary feeder are obtained first. The sequence components are calculated and for each harmonic the dominant sequence is determined. Then, the procedure of condensing the data discussed in Chapter 4 is applied. The daily average profile associated to the dominant sequence voltage of each harmonic is determined and shown in Figure 7.2(a). The daily average profile of the  $THD_V$  is shown as well. Finally, from Figure 7.2(a), the 95% index of the dominant sequence voltage individual harmonic distortion ( $IHD_V$ ) and  $THD_V$  can be determined and are shown in Figure 7.2(b). The daily average profile associated to the zero sequence voltage of each harmonic is shown in Figure 7.3 along with the 95% index associated to the zero sequence voltage  $IHD_V$ . The results show that the harmonic levels are more prominent during the period between 18:00 and 24:00 as there is a high usage of nonlinear appliances during this period. The harmonics with high magnitudes are the 3<sup>rd</sup>, 5<sup>th</sup>, and 9<sup>th</sup>.



**Figure 7.2: Average dominant sequence voltage.**

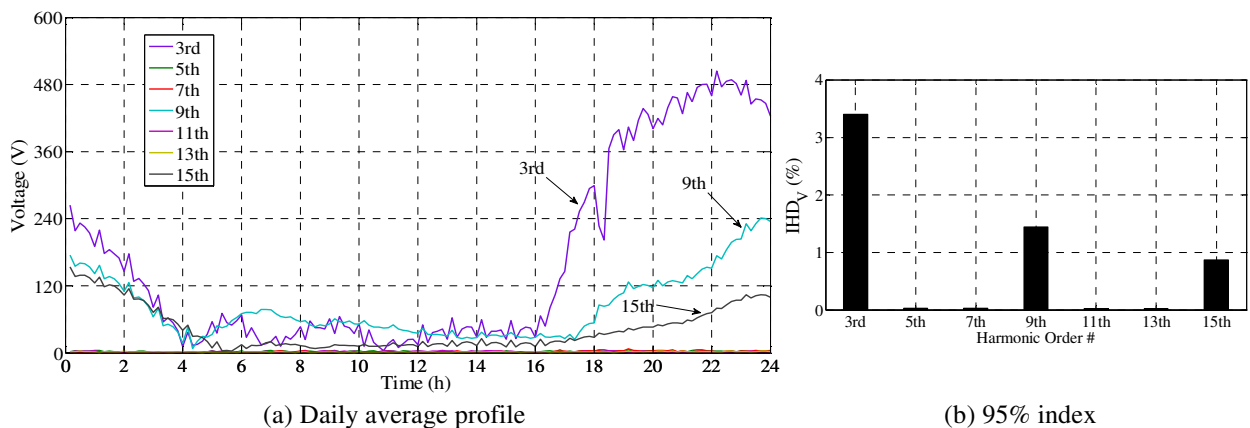
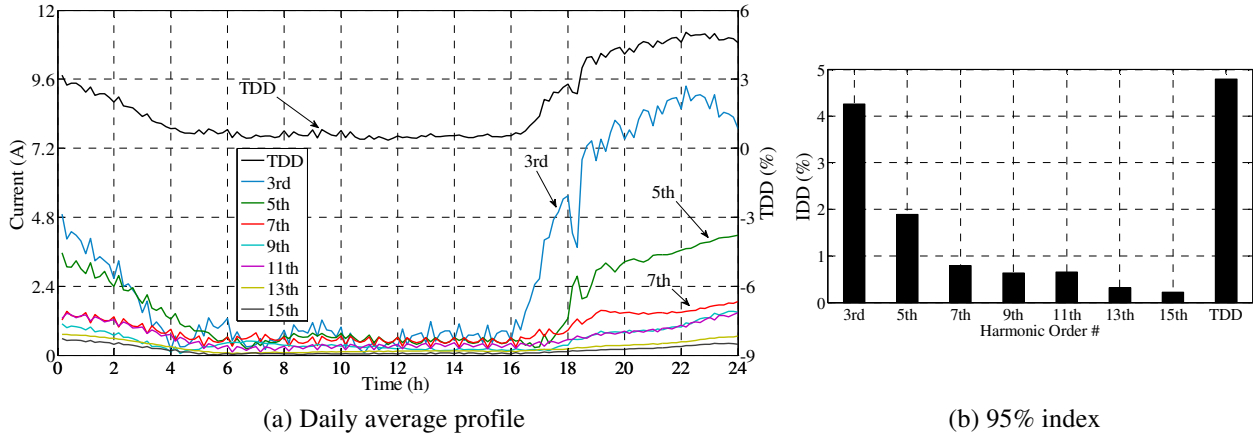


**Figure 7.3: Average zero sequence voltage.**

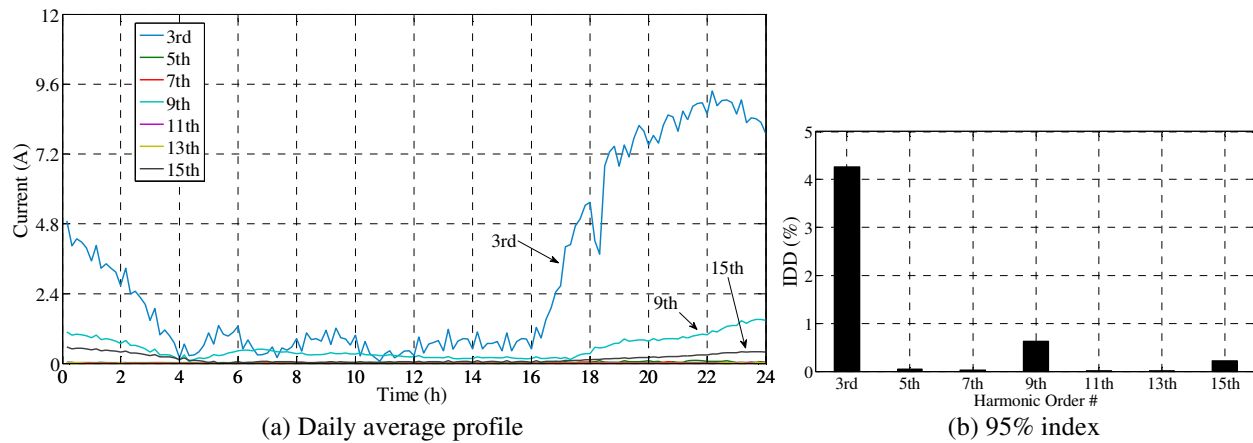
Likewise, the harmonic phase currents at each section of the primary feeder and the respective sequence components are obtained. Then, the daily average profile associated to the dominant sequence current of each harmonic is determined and shown in Figure 7.4(a). The daily average profile of the TDD is shown as well. Finally, from Figure 7.4(a), the time 95% index of the individual demand distortion (IDD) and TDD can be determined and are shown in Figure 7.4(b). The daily average profile associated to the zero sequence current of each harmonic is shown in Figure 7.5 along with the index associated to the zero sequence voltage  $IHD_v$ .

Figure 7.2 to Figure 7.5 show that the 3<sup>rd</sup> harmonic is the most dominant component. Furthermore, from Figure 7.2, one can observe that the dominant (zero) sequence 9<sup>th</sup> harmonic voltage is higher than the dominant (negative) sequence 5<sup>th</sup> harmonic. Figure 7.5 shows that the zero sequence current is dominated by the triplen harmonics (3<sup>rd</sup>, 9<sup>th</sup> and 15<sup>th</sup>), which are related to the telephone interference, increased system losses, high neutral current (overload), etc.





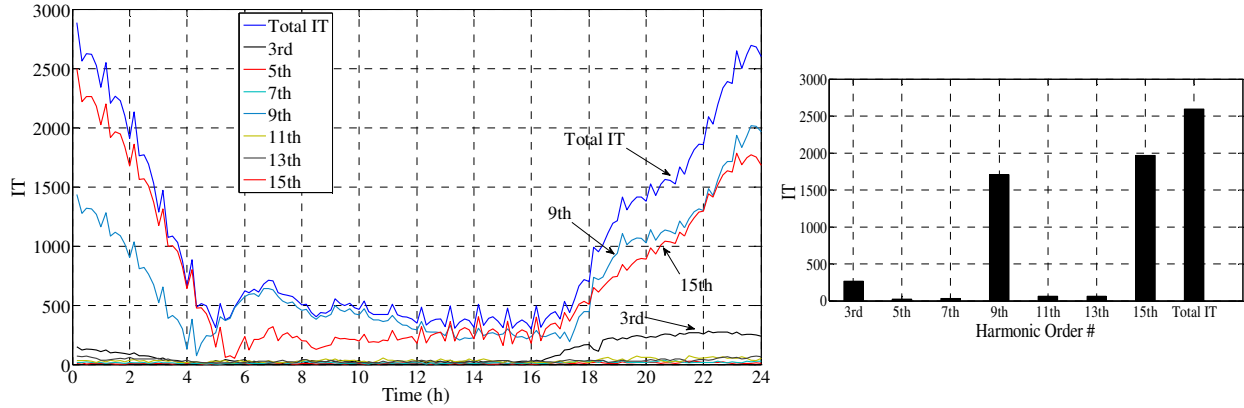
**Figure 7.4: Average dominant sequence current.**



**Figure 7.5: Average zero sequence current.**

### 7.2.2. Telephone interference level

One of the consequences of increasing harmonic current levels is audible noise on telephones lines that run in parallel with distribution feeders. The impact on the telephone line is normally measured by calculating the IT factors given in Chapter 5. The results are shown in Figure 7.6. The results confirm that the 9<sup>th</sup> and 15<sup>th</sup> harmonics are the main contributors of the residual IT level.



(a) Daily average profile (b) 95% index  
**Figure 7.6: Average individual and total IT levels at the primary system.**

This section also investigates the impact of the nonlinear residential loads on the voltage induced at a telephone line. The voltage induced at the end of a (75m) conductor parallel to the primary feeder is determined, as shown in Figure 7.7. This voltage is a more useful indicator on the telephone interference level since the effect of neutral current is included. The results are shown in Figure 7.8. This induced voltage is roughly proportional to the difference of the zero sequence and the neutral current. The voltage consists of mainly the 3<sup>rd</sup>, 9<sup>th</sup> and 15<sup>th</sup> harmonics.

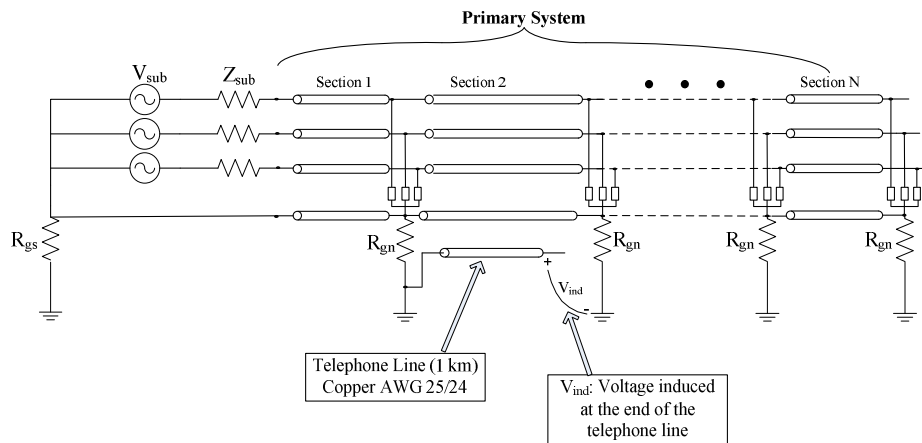
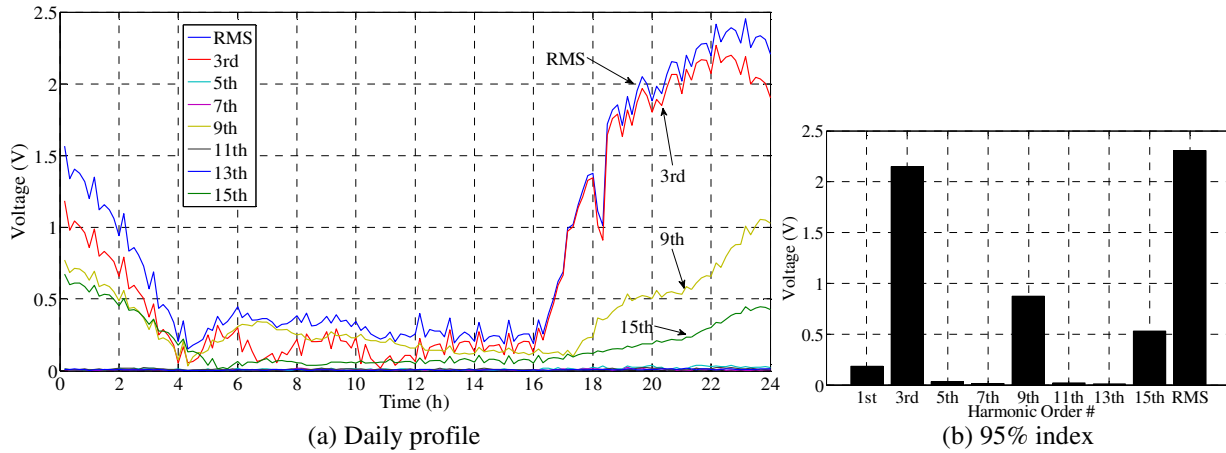


**Figure 7.7: Schematic representation of the telephone line in parallel to the primary system.**

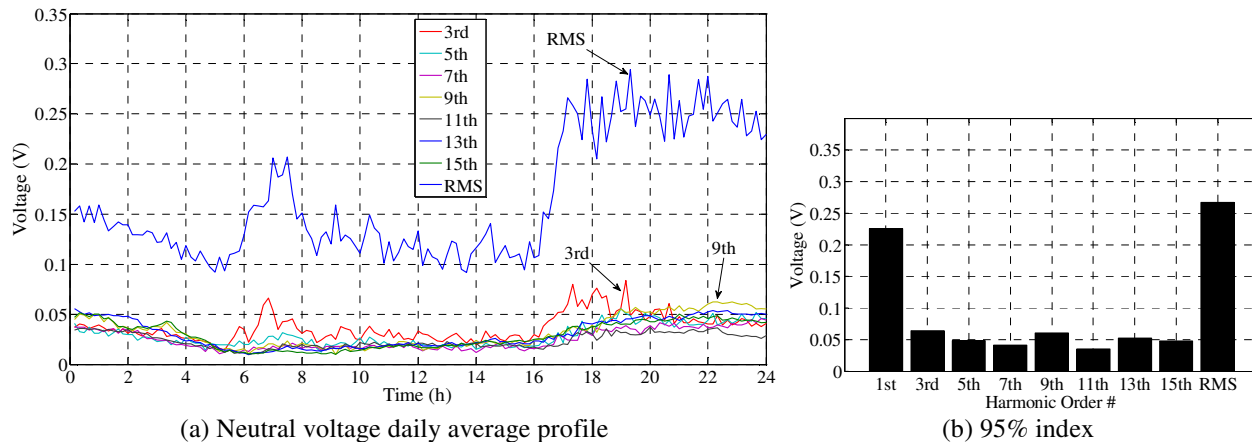


(a) Daily profile  
**Figure 7.8: Voltage induced at the end of a telephone line.**

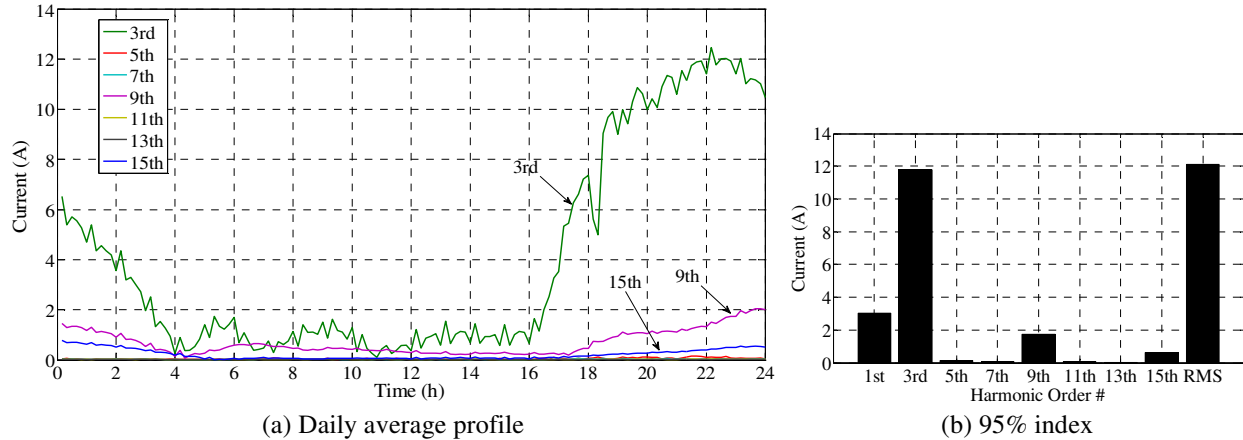
### 7.2.3. Neutral conductor current/voltage rise

The impact of the nonlinear residential loads on the average neutral current and voltage levels at the primary distribution system has been investigated. The results are shown in Figure 7.9 and Figure 7.10. The main findings are:

- The neutral voltage rise is quite small and is mainly dominated by the fundamental component. The conclusion is that harmonic-caused neutral voltage rise shall not be a concern. The contribution of each harmonic to neutral voltage rise is roughly the same.
- The neutral current can be as large as 10Amps and it is mainly caused by the triplen (3<sup>rd</sup>, 9<sup>th</sup> and 15<sup>th</sup>) harmonics, especially the 3<sup>rd</sup> harmonic. The contribution of fundamental current is small due to the relatively good phase balance of the study case. Depending on the issues involved, a high neutral current might be a concern to utility companies.



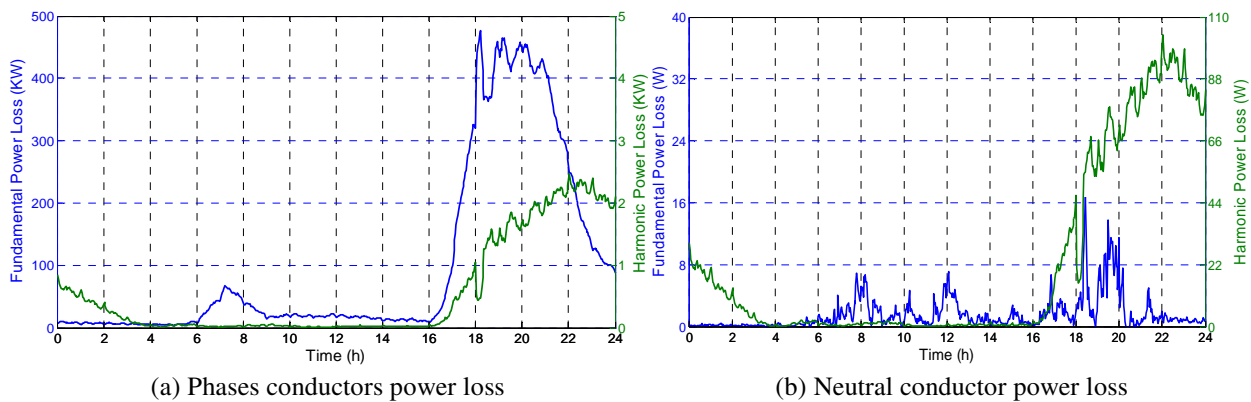
(a) Neutral voltage daily average profile  
**Figure 7.9: Average neutral voltage level at the primary system.**



(a) Daily average profile  
 (b) 95% index  
**Figure 7.10: Average neutral current level at the primary system.**

### 7.2.4. Harmonic-caused losses

The impact of harmonics on the system losses are shown in Figure 7.11. The losses shown are total losses of the study feeder. The results show that the fundamental frequency current caused losses are much higher than that caused by the harmonic currents for the phase conductors. The harmonics cause more losses in the neutral conductor. However, the amount of loss is still small. One can therefore conclude the harmonic-caused energy losses on the feeder conductors and neutrals are not a concern.



(a) Phases conductors power loss  
 (b) Neutral conductor power loss

95% index of Power Losses			
Circuit	Fundamental	Harmonic	Total
Phases	439.50 kW	2.19 kW	441.69 kW
Neutral	5.74 W	90.99 W	96.73 W
Total	439.52 kW	2.39 kW	441.91 kW

**Figure 7.11: Daily profile of the total active power losses at the primary system.**

On the load evolution studies presented in the next section, it will be evaluated the impact of increasing usage of nonlinear residential loads on the power losses. The use of energy efficient appliances may lead to the decrease of the fundamental current on the phase circuit and,

consequently, fundamental power losses reduction.

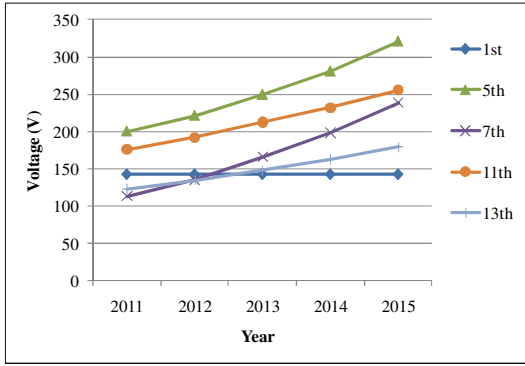
### **7.3. Load Evolution Results**

The load evolution studies are done using the market trend data. In order to facilitate the interpretation and comparison of the results, all the results are represented by their “95% index” values. Two different charts are provided. The first type of charts shows the index values over the study period (5 years). The second type of charts shows the average annual growth rate of the indices. The annual growth rate is the most useful parameter to predict the future harmonic conditions of a residential feeder.

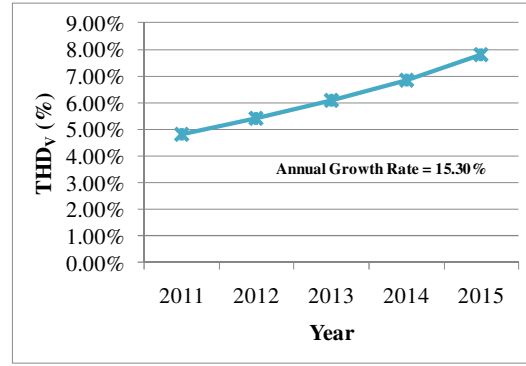
It must be noticed that the distribution network from the base case is used. Moreover, the number of customers remains the same as in the base case, only the appliances penetration for each existing customer will change.

#### **7.3.1. Harmonic voltage and current distortions**

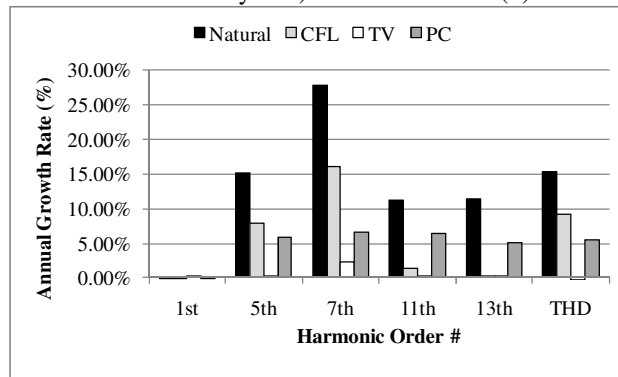
Figure 7.12(a) shows the 95% index of the harmonic dominant sequence voltages in the next 5 years. From the data provided in Figure 7.12(a), it is possible to calculate the average annual growth rate associated to the phase voltage index, which is shown in Figure 7.12(b). The results reveal that the growth rate of voltage harmonics is between 10% and 15% per year. The 7<sup>th</sup> and 5<sup>th</sup> harmonics have the highest growth rate. This is mainly caused by the CFL devices. In term of the zero sequence components, the 9<sup>th</sup> harmonic has a slightly higher growth rate.



(a) Natural load evolution (fundamental divided by 100)

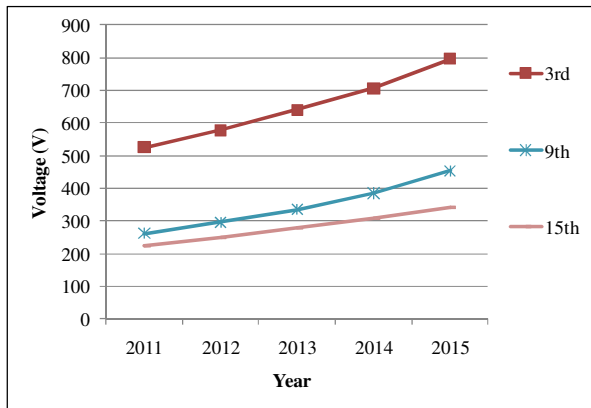


(b) Natural load evolution

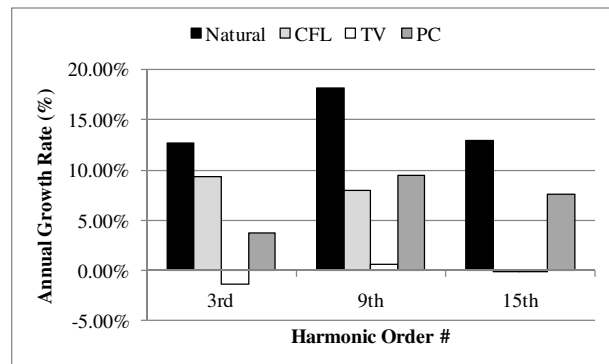


(c) Annual growth rate

**Figure 7.12: Growth characteristics of dominant sequence voltages in the primary system.**



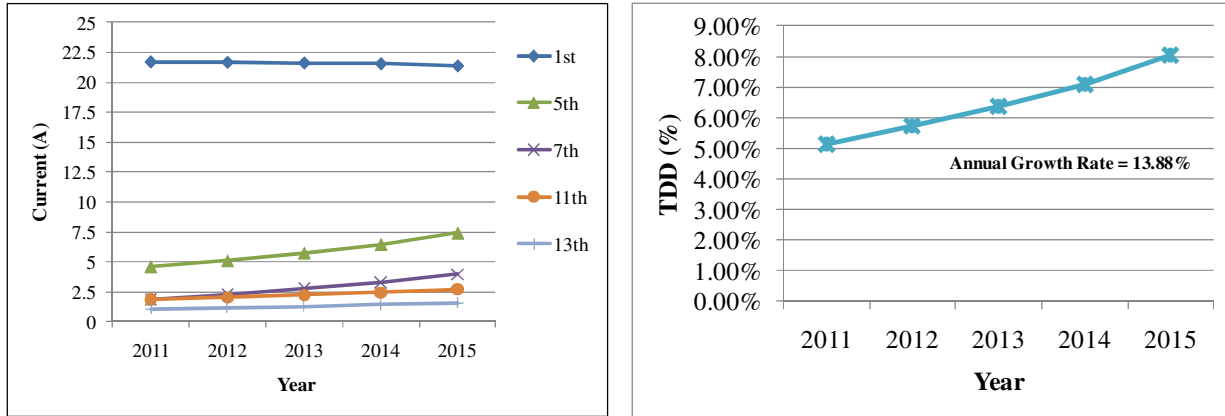
(a) Natural load evolution



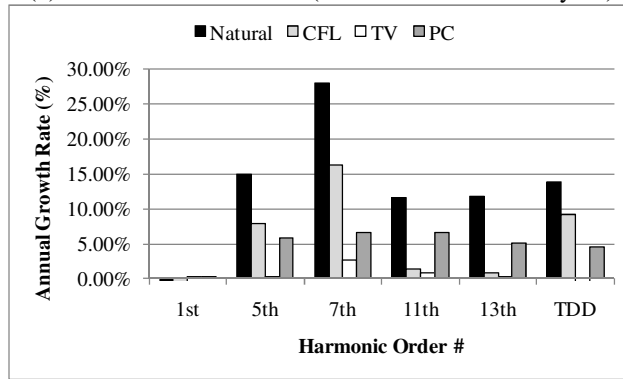
(b) Annual growth rate

**Figure 7.13: Growth characteristics of zero sequence voltages in the primary system.**

Similarly, Figure 7.14 and Figure 7.15 show the 95% index associated to the dominant and zero sequences of the average current along the primary feeder in the next 5 years and the associated average annual growth rate. The results reveal a growth pattern similar to that of the harmonic voltage. Note that there is a slight drop on fundamental frequency current. This is due to the adoption of energy efficient home appliances.

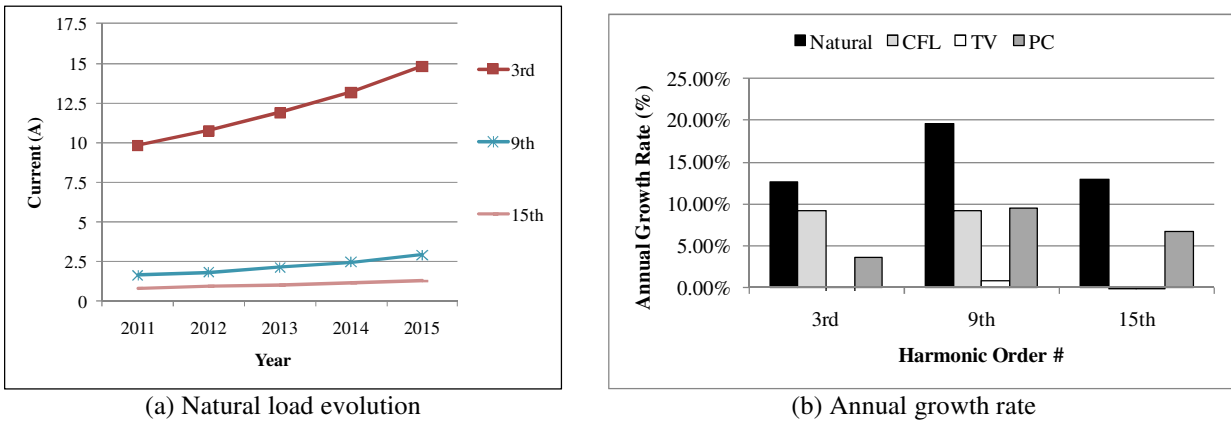


(a) Natural load evolution (fundamental divided by 10)



(b) Annual growth rate

Figure 7.14: Growth characteristics of dominant sequence currents in the primary system.



(a) Natural load evolution

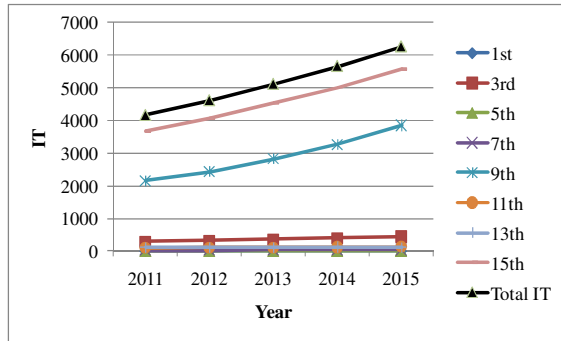
(b) Annual growth rate

Figure 7.15: Growth characteristics of zero sequence currents in the primary system.

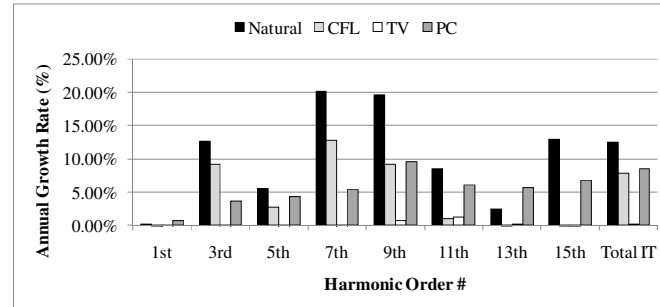
### 7.3.2. Telephone interference in the form of IT factors

The annual growth of IT levels and voltage induced on a parallel conductor are shown in Figure 7.16 and Figure 7.17 respectively. It is found that total IT level and induced voltage will increase at the rate of 10% to 15% per year, with the 9<sup>th</sup> harmonic as the most significant contributor. This high growth rate is mainly caused by the adoption of personal computing

devices and CFLs.

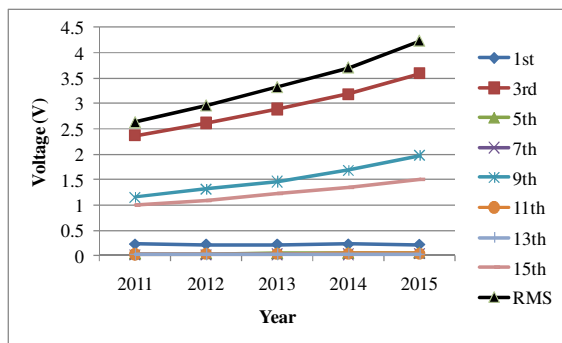


(a) Natural load evolution

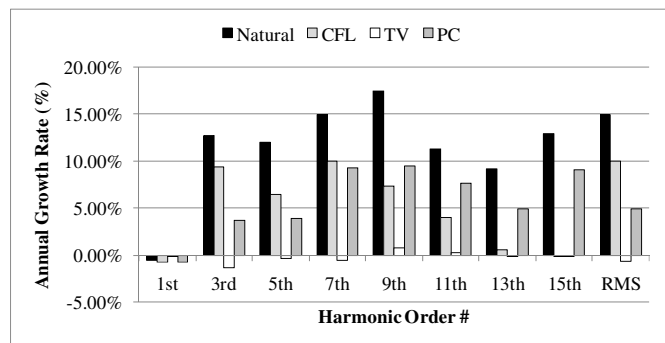


(b) Annual growth rate

**Figure 7.16: Growth characteristics of IT index in the primary system.**



(a) Natural load evolution

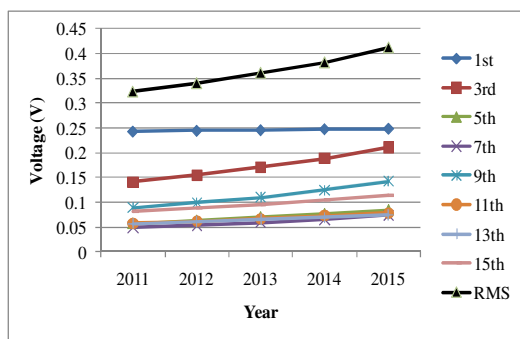


(b) Annual growth rate

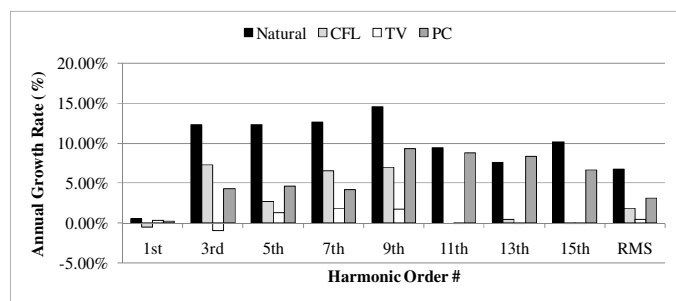
**Figure 7.17: Growth characteristics of induced voltage on a parallel conductor.**

### 7.3.3. Neutral conductor current/voltage rise

The results of neutral voltage and current growth are shown in Figure 7.18 and Figure 7.19 respectively. Although the growth rate of neutral voltage is relative high, this is not a concern since its base value is very low.



(a) Natural load evolution



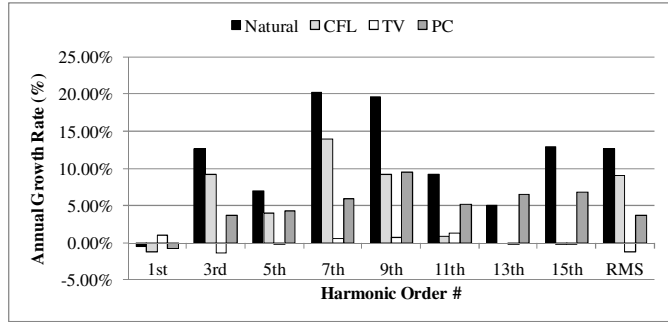
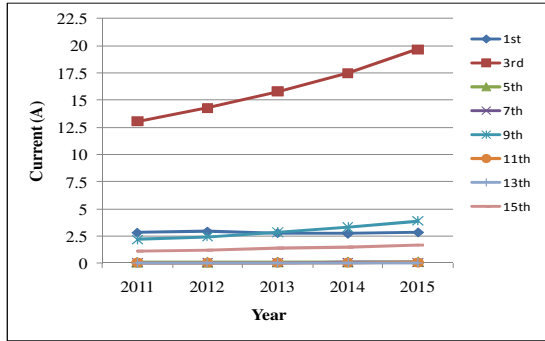
(b) Annual growth rate

**Figure 7.18: Growth characteristics of neutral voltage in the primary system.**

The main contributors for the neutral voltage and current growth in the coming years are the CFLs and PCs appliances. The 3<sup>rd</sup> harmonic is the main contributor to the neutral current. Its



growth rate is over 10%.



(a) Natural load evolution

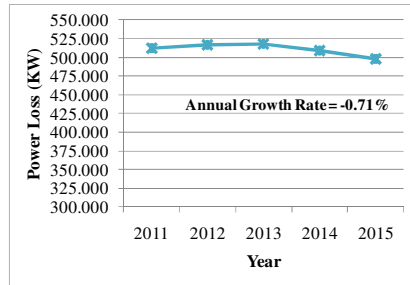
(b) Annual growth rate

**Figure 7.19: Growth characteristics of neutral current in the primary system.**

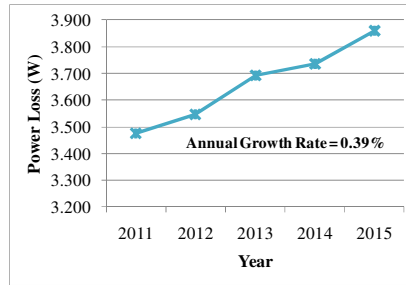
### 7.3.4. Harmonic-caused losses

As discussed in the base case section, the harmonic-caused losses are not a concern. For completeness, the growth characteristics of various loss components are shown in this section.

### Natural Load Evolution

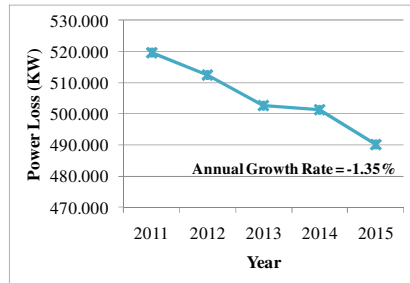


(a) Phases conductors power loss

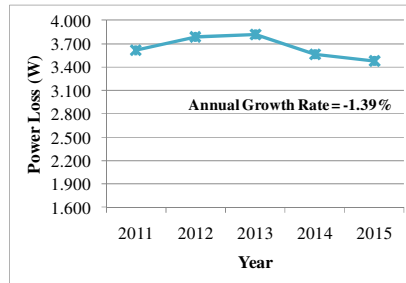


(b) Neutral conductors power loss

### CFL Load Evolution

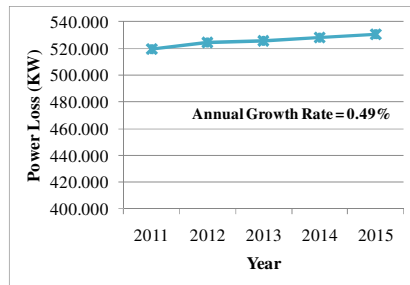


(c) Phases conductors power loss

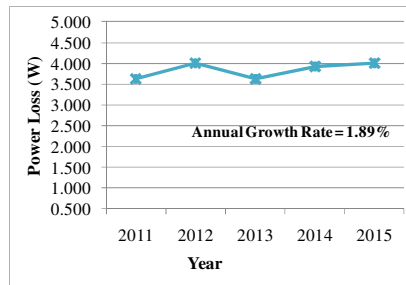


(d) Neutral conductors power loss

### TV Load Evolution

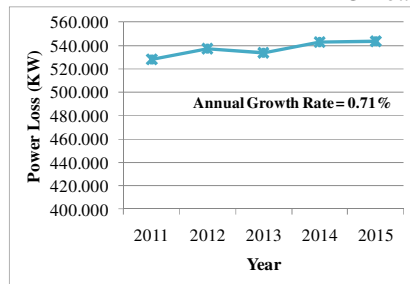


(e) Phases conductors power loss

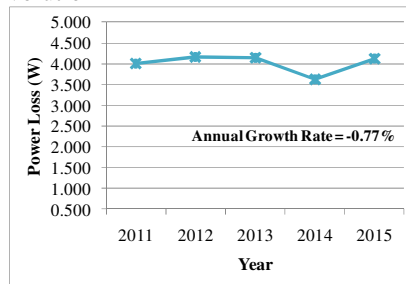


(f) Neutral conductors power loss

### PC Load Evolution



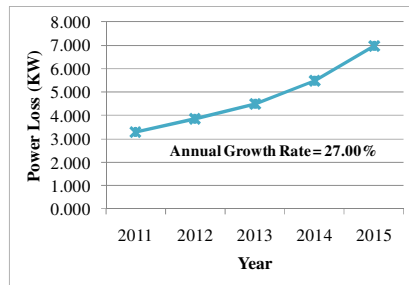
(g) Phases conductors power loss



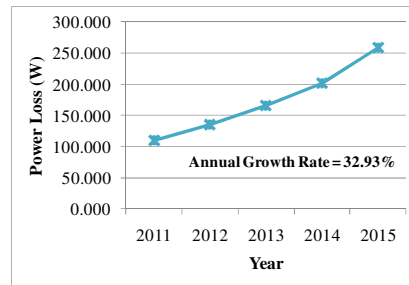
(h) Neutral conductors power loss

**Figure 7.20: Total fundamental power losses at the primary system.**

### Natural Load Evolution

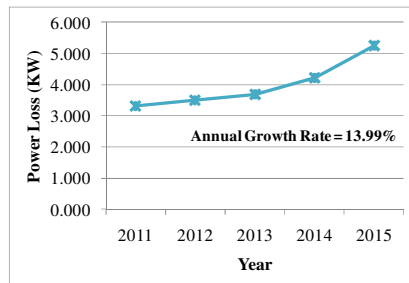


(a) Phases conductors power loss

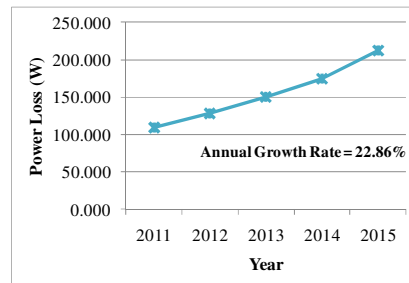


(b) Neutral conductors power loss

### CFL Load Evolution

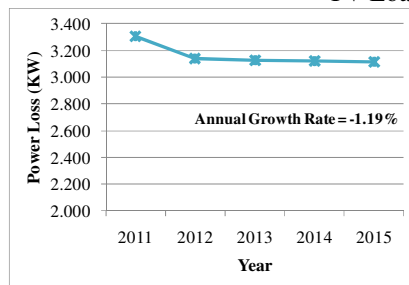


(c) Phases conductors power loss

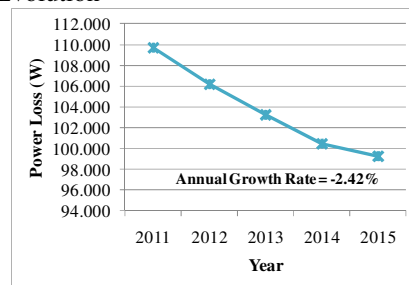


(d) Neutral conductors power loss

### TV Load Evolution

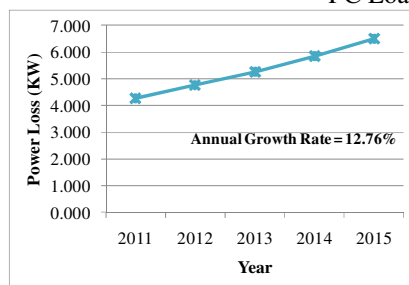


(e) Phases conductors power loss

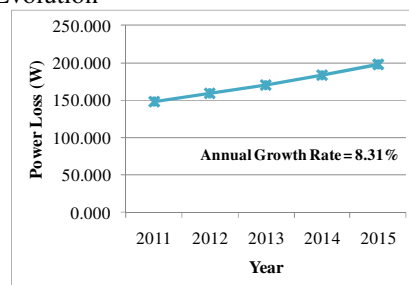


(f) Neutral conductors power loss

### PC Load Evolution



(h) Phases conductors power loss



(g) Neutral conductors power loss

**Figure 7.21: Harmonic power losses at the primary system.**

### 7.3.5. Substation capacitor loading

The impact of the load evolution on the loading of a substation shunt capacitor commonly used for reactive power compensation has also been evaluated. It shall be noted that there is no shunt capacitor connected at the substation for all of the previous study results. For this study, a

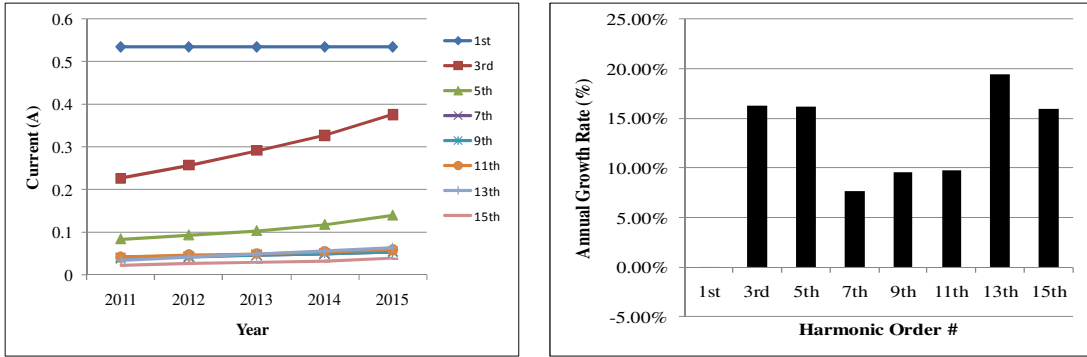
capacitor of 2.3Mvar is added to the secondary side of the substation transformer. The size is selected in such a way that there is no capacitor-caused harmonic resonance. To evaluate the impact of harmonics on the capacitor, the capacitor loading indices shown in Table 7.1 is used:

**Table 7.1: Capacitor loading limits (related to its rating).**

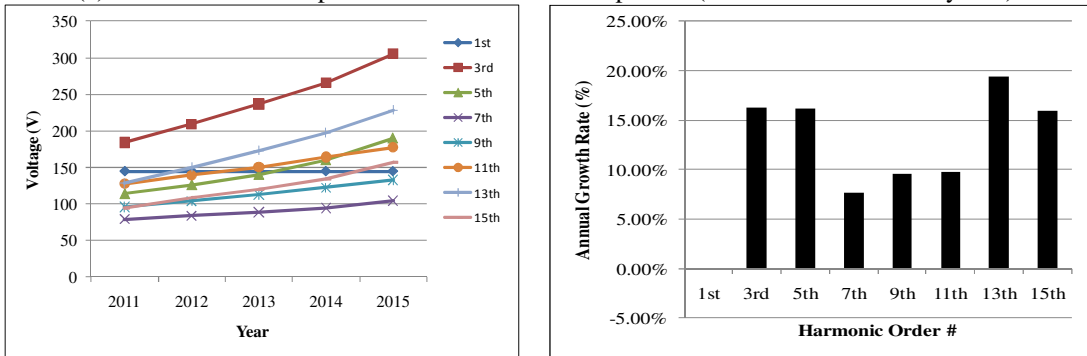
Index	Explanation	Limit
kvar	Apparent power of the capacitor ( $kvar = I_{rms} \times V_{rms}$ )	135%
$V_{rms}$	RMS voltage of the capacitor	110%
$V_{peak}$	Peak voltage of the capacitor	120%
$I_{rms}$	RMS current of the capacitor	180%

The results on capacitor harmonic voltage and current are shown in Figure 7.22. It is observed that although there is an increase on the harmonic levels in the coming years, these harmonics do not affect the capacitor loading indices (Figure 7.23) in a meaningful way. This is caused by the fact that capacitor loading indices are dominated by the fundamental frequency component. Since the fundamental frequency component does not change over the simulation years, the growth rate of the indices is close to zero. We can therefore conclude the load evolution in the coming years does not represent a concern in terms of substation shunt capacitor loading levels. However, the lifetime of the capacitors will likely to be reduced because of the expected increase on the harmonic current distortion in the coming years reported in the previous subsections.

Moreover, it is important to note, however, the results do not mean that a capacitor will not experience harmonic-caused problem. They only show that the adoption of new loads is not likely to cause overloading problem to capacitors. If a capacitor is close to resonance conditions, harmonic-caused problems will occur. So the issues faced by the capacitors are the same regardless the characteristics of the home appliances.

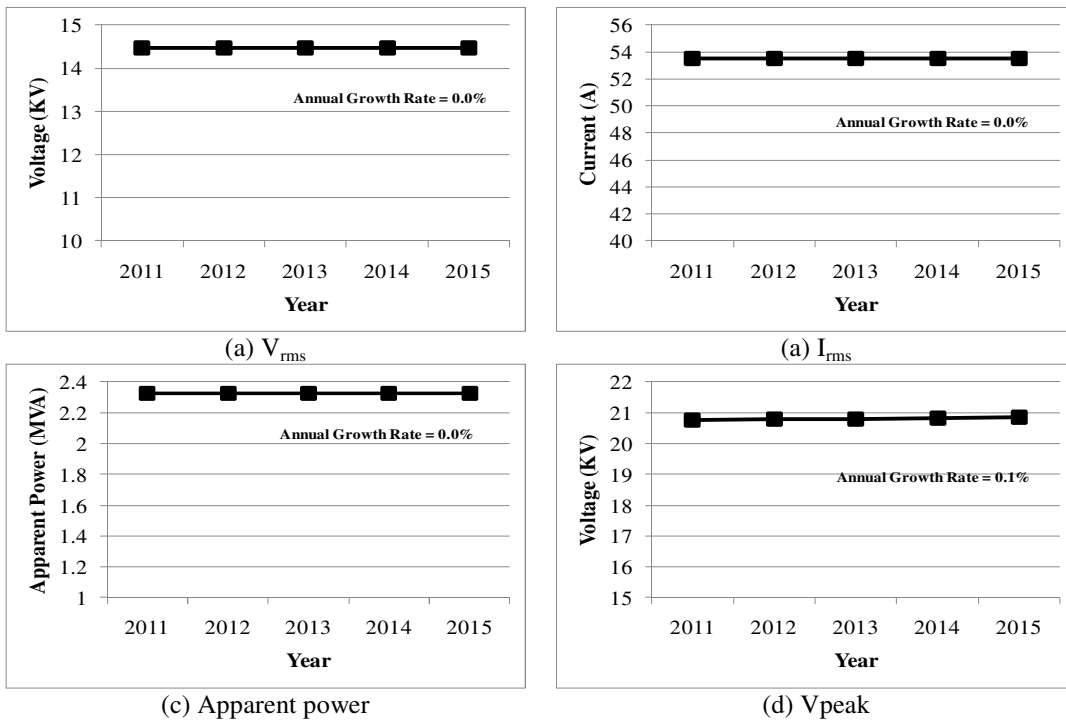


(a) Harmonic current spectrum at the substation capacitor (fundamental divided by 100).



(b) Harmonic voltage spectrum at the substation capacitor (fundamental divided by 100).

**Figure 7.22: Harmonic voltage and current levels at the substation capacitor.**



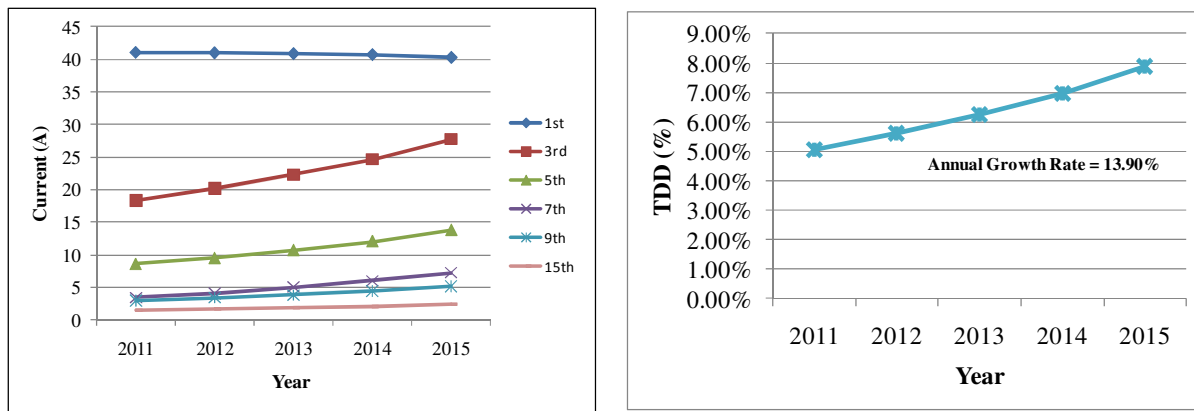
(c) Apparent power

(d)  $V_{peak}$

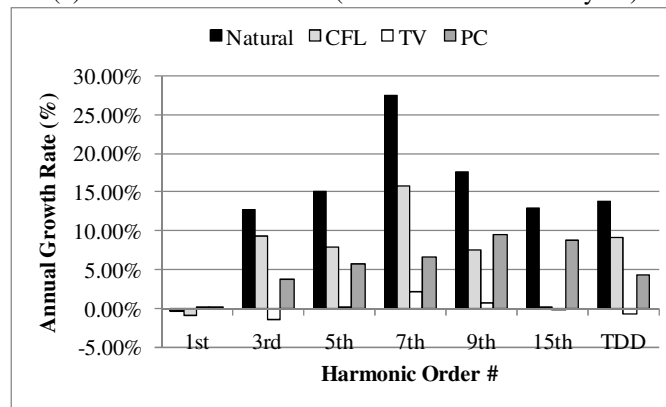
**Figure 7.23: Capacitor loading indices.**

### 7.3.6. Harmonic current penetration into the transmission system

The amount of harmonic current injected into the supply transmission system has also been studied. This harmonic current is defined as that at the sending end of the study feeder. Figure 7.24 shows the growth characteristics of the various harmonics entering into the transmission system. The results reveal that the 7<sup>th</sup> and 9<sup>th</sup> harmonics have a relatively higher growth rate. The typical growth rate is about 15% for different harmonics. This growth rate is very similar to that reported in Section 7.3.1. That section shows the growth characteristics of average harmonic currents inside the feeder.



(a) Natural load evolution (fundamental divided by 10)



(b) Annual growth rate

Figure 7.24: Growth characteristics of the harmonics entering into transmission system.

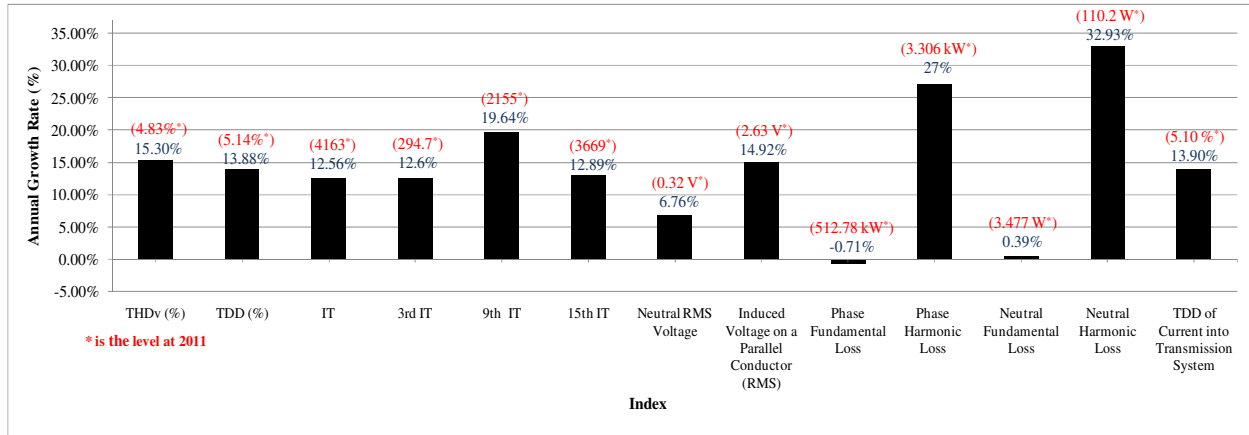
## 7.4. Summary of Findings

Figure 7.25 shows a summary of the load evolution results for the various indices. The value between parenthesis and the one without above each bar refer to index level at the year 2011 and the average annual growth rate, respectively. The main findings are summarized below:

- For feeders supplying residential loads, the most significant voltage distortions occur

at the 3<sup>rd</sup>, 9<sup>th</sup> and 5<sup>th</sup> harmonics. The most significant current distortions occur at 3<sup>rd</sup>, 5<sup>th</sup>, 7<sup>th</sup> etc. The high 9<sup>th</sup> harmonic voltage is caused by a higher feeder impedance at the 9<sup>th</sup> harmonic frequency. Over the next five years, the annual growth rate of harmonic distortions is around 10% to 15%, with the 9<sup>th</sup> and 7<sup>th</sup> harmonics show the highest growth rate. This is mainly caused by the adoption of CFLs and home computing devices.

- Significant telephone interference level exists in residential feeders. The residual IT level can reach 2500A for the study feeder, much higher than 300A generally allowed when there is a parallel telephone circuit. The growth rates of telephone interference indices are about 15% per year.
- The voltage rise at feeder grounding points (neutral voltage rise) is dominated by the fundamental frequency component. The harmonic-caused neutral voltage rise is quite small and shall not be a concern.
- Feeder neutral current can be as high as 10Amps and it is mainly caused by the triplen (3rd, 9th and 15th) harmonics, especially the 3rd harmonic. The contribution of fundamental current is small due to the relatively good phase balance of the study case. Growth rate of neutral current is about 10% which is closely related to the growth rate of the third harmonic current in the system.
- Harmonic caused losses in the primary conductors are small and shall not be a concern.
- The adoption of new home appliances is not likely to cause overloading problems to feeder and substation capacitors as the loading level is dominated by the fundamental frequency component. However, capacitor caused harmonic resonance problem is a known concern to utility companies.
- The harmonic currents produced by home appliances are getting into the supplying transmission system in a noticeable way. The annual growth rate of the harmonic currents is about 10% to 15%.



**Figure 7.25: Average annual growth rate of key power quality indices.**

It is important to note that the results reported here are based on the load composition characteristics of Canada and United States. Using the previous results directly for other countries will basically depend if they have similar socio-economic scenario, residential loads usage habits and on the characteristics of the primary distribution networks. Some of the residential loads included in the methodology are not common in other countries. Results for other locations can be obtained using the proposed technique but one needs to consider relevant regional load characteristics. The main purpose of this thesis is to show how to use this information to study the evolution of the harmonic distortion in residential feeders in the coming years.



---

## Chapter 8

# HARMONIC MITIGATION STUDIES

---

The results presented in the previous chapters have shown that the harmonics resulted from home appliances are increasing rapidly at a rate of 10% to 15% per year. Several areas of concern such as service transformer overloading and telephone interference have been identified. There is, therefore, a great need to identify possible ways to manage the situation. For this purpose, a high-level feasibility and effectiveness study on two harmonic mitigation options has been conducted. These options are (1) imposing the IEC 61000-3-2 device level harmonic emission limits on home appliances and (2) installing feeder level harmonic filters. The findings are presented in this chapter.

### 8.1. The Need for Mitigating Harmonics from Residential Customers

It is useful to establish a perspective on the harmonic situation associated with residential customers before studying the mitigation options. In North America, residential customers are often scattered in the form of suburban community or neighborhood clusters as illustrated in Figure 8.1<sup>7</sup>. Each neighborhood may contain, for example, about 100 service transformers or 500 to 1000 single detached homes. As a result, the total load of each neighborhood can be about 3MW or 70A (at 25kV). Through simulations and field measurements, we have established the harmonic current characteristics of typical neighborhood loads, as shown in Figure 8.2. Therefore, each neighborhood can be viewed as a harmonic-producing load. The point labeled as “PCC” can be considered as the interconnection point (point of common-coupling) of this aggregate load with the system.

---

<sup>7</sup> Similar trend can also be found in Brazil with the increasing number of residential neighbourhoods called *condomínios* in portuguese.

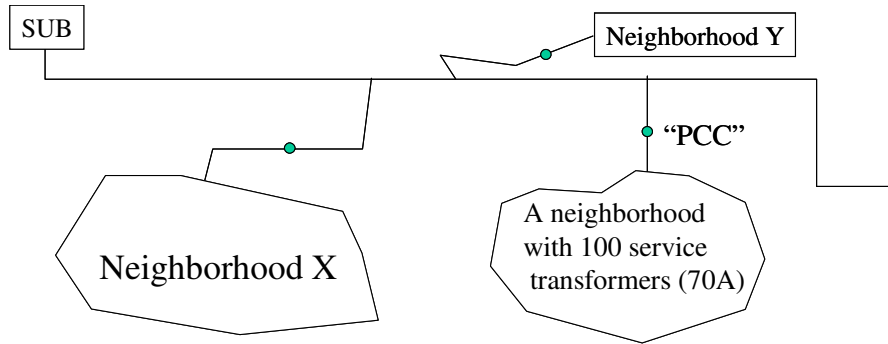


Figure 8.1: Suburban residential customer clusters supplied by one distribution feeder.

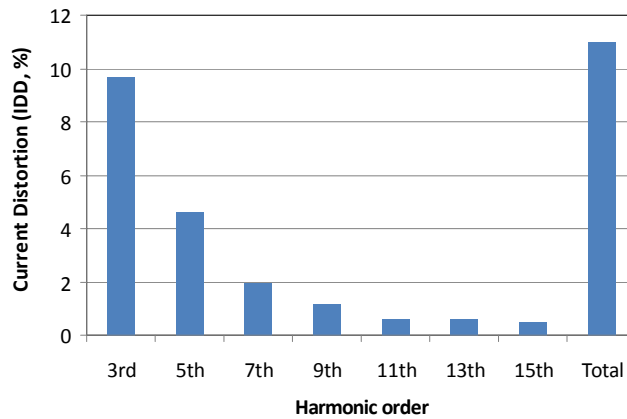


Figure 8.2: Harmonic current spectrum of neighborhood loads.

Now, suppose an industrial customer of 3.7MW with a similar harmonic characteristics requesting interconnection to the feeder. It is clear that such a load must meet the utility harmonic limits. Figure 8.3 shows the IEEE Std. 519 limits [62]. One can easily see that if the system fault level at the “PCC” is less than 300MVA ( $I_{sc}/I_L < 100$ ), some of the harmonic limits would be violated. Examples are the 3<sup>rd</sup> and 5<sup>th</sup> harmonics and the TDD limits. Furthermore, this load will produce a residual IT of 1000A, which far exceeds the typical limits of 500A<sup>8</sup>. As a result, the customer must equip itself with harmonic mitigation means such as installing harmonic filters within its facility.

Figure 8.3: Harmonic current limits of IEEE Std. 519.

$I_{sc}/I_L$	Individual Harmonic Order (Odd Harmonics)					
	<11	11≤h<17	17≤h<23	23≤h<25	35≤h	TDD
<20	4.0	2.0	1.5	0.6	0.3	5.0
20<50	7.0	3.5	2.5	1.0	0.5	8.0
50<100	10.0	4.5	4.0	1.5	0.7	12.0
100<1000	12.0	5.5	5.0	2.0	1.0	15.0
>1000	15.0	7.0	6.0	2.5	1.4	20.0
Even harmonics are limited to 25% of the odd harmonic limits above.						

<sup>8</sup>Distribution power companies in Canada typically adopts 500 A as the limit for the total IT.

The above comparison between the residential neighborhood load and an industrial customer early shows that there is a need to deal with the harmonics produced by neighborhood loads if utilities want to maintain acceptable harmonic levels in the system. Furthermore, it yields a consistent harmonic control standard on all customers. The challenge, however, is that there is no single owner for the neighborhood loads. Utility cannot impose harmonic limits to such loads (i.e. residential customer clusters). Another challenge is that there are no transformers separating the neighborhood loads. So harmonic filters added to one neighborhood could affect the harmonics from another neighborhood<sup>9</sup>. In summary, this illustration has shown that there is a need to mitigate harmonics from residential loads. Doing nothing is not a proper option from a number of perspectives.

## **8.2. Harmonic Mitigation Using IEC Limits**

One method to mitigate the harmonic levels on both primary and secondary distribution systems is to make the home appliances comply with the harmonic compatibility levels defined in the standard IEC 61000-3-2 [10]. This has been done in Europe with the consequence of slightly increased costs of home appliances. The objective of this section is to determine how the harmonic levels on the distribution system are affected if the harmonic emissions of all appliances under analysis in this thesis comply with the IEC limits. In the following subsections, the IEC standard is briefly described and the procedure to alter the harmonic spectrum of each appliance to meet this standard is also explained.

### **8.2.1. IEC Standard 61000-3-2**

The IEC 61000-3-2 standard assesses and sets the limit for equipment that draws input current less than or equal to 16A per phase. According to the standard, the harmonic emission limits are defined for four different classes (A to D) of equipments. Three of these classes are of interest according to the appliances analyzed in this thesis:

- Class A:
  - household appliances, excluding equipment identified as class D
- Class C:

---

<sup>9</sup> For the case of industrial customers, there is always a service transformer. Harmonic filters are installed at the secondary side of the transformer. The transformer's relatively high impedance will help contain the filtering effects within the customer's facility.

- lighting equipment
- Class D:
  - personal computers and personal computer monitors
  - television receivers

Table 8.1 to Table 8.3 present the harmonic emission limits for each class type. It must be noticed that the limits defined in IEC 61000-2-2 are for 230V (phase-to-neutral) equipments only. According to this standard, the limits have not yet been considered for systems with nominal voltages less than 230 V (phase-to-neutral). As the limits for Class D are presented in mA per Watt, they are converted to percentage to represent 120V devices<sup>10</sup>.

**Table 8.1: Limits for Class A equipment.**

Harmonic order (n)	Maximum permissible harmonic current (A)
3	2.30
5	1.14
7	0.77
9	0.40
11	0.33
13	0.21
$15 \leq n \leq 39$	$0.15 \times 15/n$

**Table 8.2: Limits for Class C equipment.**

Harmonic order (n)	Maximum permissible harmonic current expressed as a percentage of the input current at the fundamental frequency (%)
2	2
3	$30 \times \lambda^*$
5	10
7	7
9	5
$11 \leq n \leq 39$	3
* $\lambda$ is the circuit power factor	

<sup>10</sup>To calculate the harmonic limits in percentage for class D, it is assumed that the fundamental current is equal to  $I_1 = (1W)/(230V) = 4.3mA$  (unitary power factor). The original 3<sup>rd</sup> harmonic limit value in the standard 61000-3-2 is 3.4 mA/W. Therefore, the limit in percentage is assumed equal to  $3.4/4.3 = 79\%$ . Similar procedure was done for the other harmonic components.

**Table 8.3: Limits for Class D equipment.**

Harmonic order (n)	Maximum permissible harmonic current expressed as a percentage of the input current at the fundamental frequency (%) $75 \text{ W} < P < 600 \text{ W}$
3	79
5	43
7	23
9	11
11	8
$13 \leq n \leq 39$	$88/n$

To determine the effects of imposing the IEC limits, the harmonic spectrum of each appliance presented on Appendix A is scaled down to meet the limits defined on tables above. For example, Figure 8.4 shows the real measured harmonic current spectrum of four appliances and the modified spectrum if the IEC limits are enforced. Only the 3<sup>rd</sup> to 15<sup>th</sup> harmonic orders are shown in Figure 8.4 since the change on higher harmonics is very small.

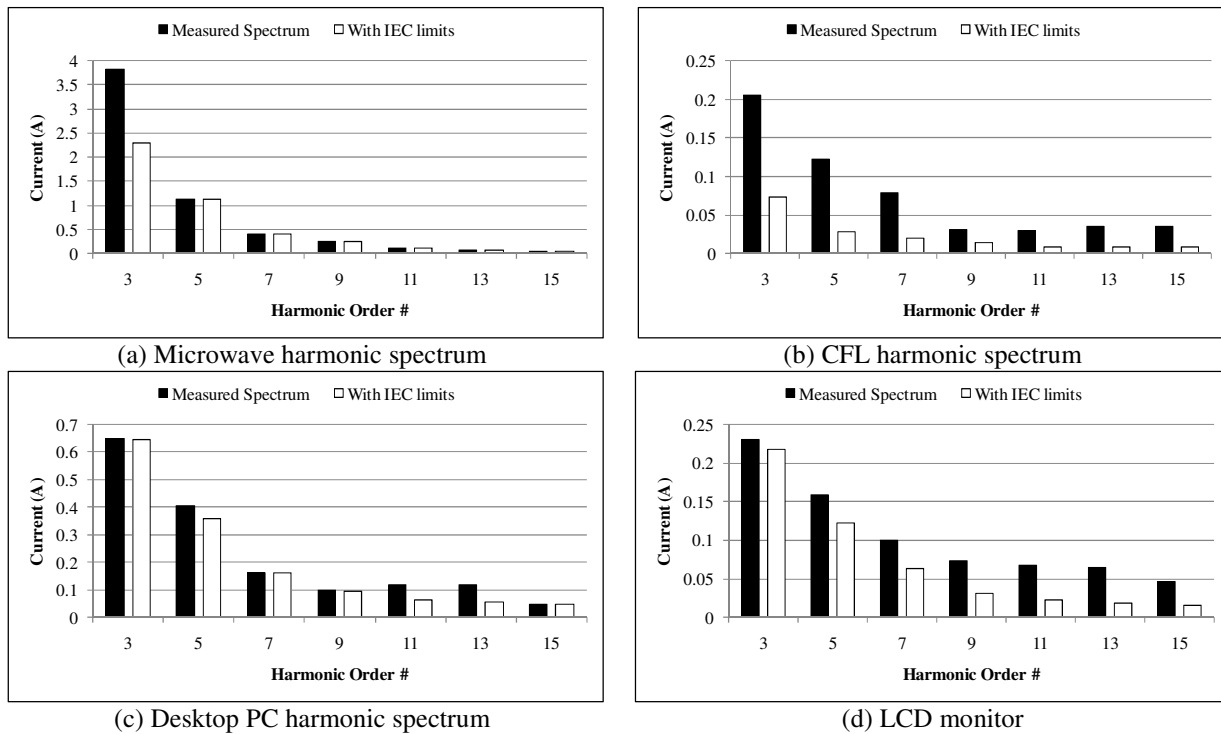


**Figure 8.4: Measured and modified (IEC limits) harmonic spectra for four appliances.**

### 8.2.2. Case Study Description

The simulation procedure including the IEC limits is similar to the case studies for the secondary and primary system analysis carried out on Chapter 6 and 7, respectively. In this

study, the distribution networks for the secondary and primary system analysis remain the same as the base case. The number of residential houses is also the same. The only difference is that the harmonic spectrums of all appliances are scaled down to satisfy the IEC limits.

The simulation results are shown in the following sections, which show the impact of the IEC limits on the secondary distribution system. Similar to the natural load evolution case study analyzed on Chapter 6, the PQ index values are determined at the coming years considering the IEC limits. From these results, two different charts are provided for each power quality index:

- **Index average decrease:** The PQ index levels without and with the IEC limits are compared year by year and the PQ index average decrease is calculated.
- **Annual growth rate:** The average annual growth of each PQ index can be determined providing an estimation of how much the PQ index level will increase at every year, considering the IEC limits. These results are compared to the annual growth rate obtained on Chapter 6 and 7.

### 8.2.3. Results of the Secondary System

Figure 8.5 shows the 95% index of the phase A voltage at the next five years for the case study without and with the IEC limits. The annual growth rates of the indices are shown in Figure 8.6. One can observe that when the IEC limits are enforced, the average 3<sup>rd</sup> harmonic component of the phase voltage drops approximately 35%. Moreover, the IEC limits decrease the annual growth rate of this index from 15% to around 7.5%.

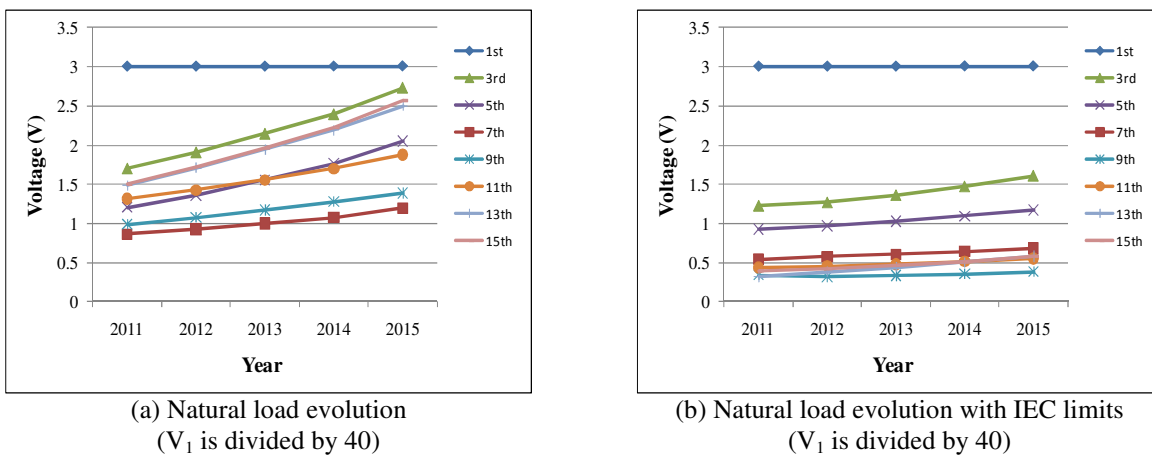


**Figure 8.5: Impact of IEC limits on secondary system voltage.**

The results show that the adopting the IEC limits will cut the growth rate of key harmonics

(3<sup>rd</sup>, 5<sup>th</sup>, 7<sup>th</sup> and 9<sup>th</sup>) by about half<sup>11</sup>.

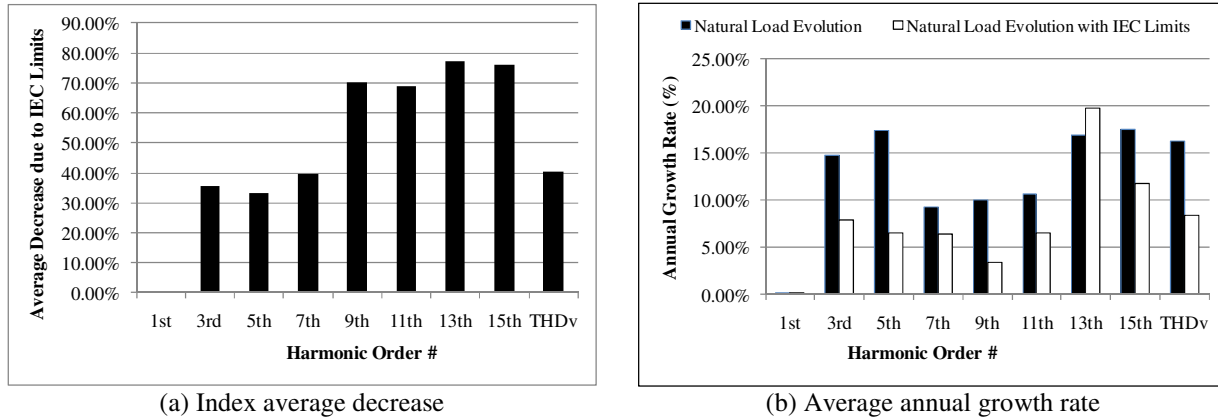


Figure 8.6: Impact of IEC limits on phase voltage of the secondary system.

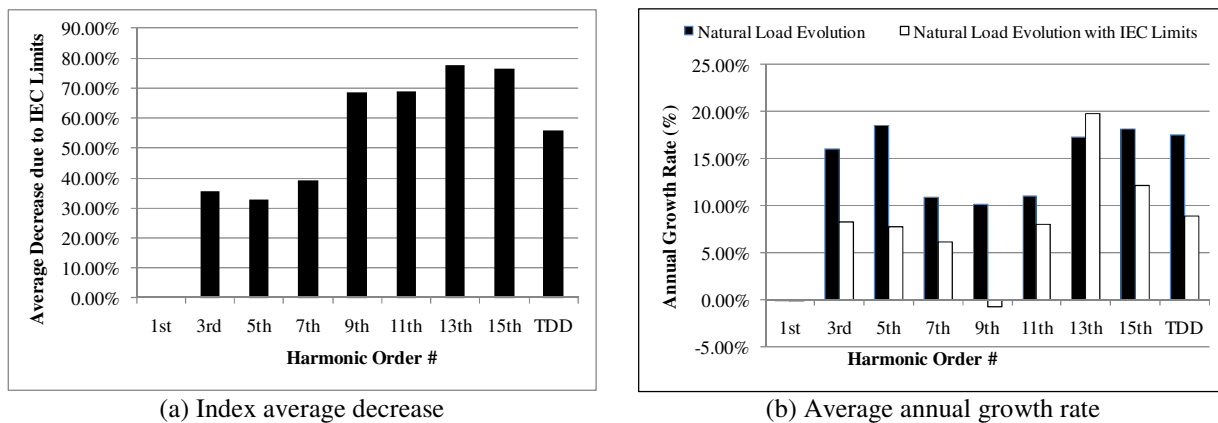


Figure 8.7: Impact of IEC limits on phase current of the secondary system.

Table 8.4 shows how the service transformer K-factor decreases if the IEC limits are enforced. One can also observe that the annual growth rate is reduced by half by imposing the IEC limits. The main idea of the annual growth rate is to see if any mitigation technique can

<sup>11</sup> One may observe from Figures in Figure 8.6(b) that the growth rate of 13<sup>th</sup> harmonic is higher when IEC limit is imposed. This is caused by the smaller starting value of the 13<sup>th</sup> harmonic index as explained below:

- Figure 8.5(a) shows that the 13<sup>th</sup> harmonic voltage at 2011 is 1.484V and increases in average 0.251V per year.
- Figure 8.5(b) shows that the 13<sup>th</sup> harmonic voltage at 2011 decreased to 0.321V and the growth rate decreased to 0.06V per year when the IEC limits are considered.
- So, the growth rate in absolute value is *smaller* for the IEC case study.
- However, Figure 8.5(a) also shows that the 13<sup>th</sup> harmonic voltage increases 68% from 2011 to 2015, while Figure 8.5(b) shows 81% of increase in the same period considering the IEC limits.

To provide a meaningful growth rate, the absolute growth rate is normalized to the value at first year (base value). So, for this case, the 13<sup>th</sup> harmonic voltage growth rate of the case without IEC limits is  $0.251/1.484 = 16.9\%$  and with IEC is  $0.063/0.321 = 19.6\%$ , which are provided in Figure 8.6(b). This normalized annual growth rate is useful to estimate what will be the PQ index level on the following years. For example, the 13<sup>th</sup> harmonic voltage in 2014 for the IEC case study can be obtained from the base year as follows;  $0.321V * (1 + 3 \text{ years} * 19.6\%) = 0.509V$ , which is very close to the value shown in Figure 8.5(b).

Therefore, the normalized growth rate for the case study with IEC can in some cases be *larger* than the case without IEC because the base value of IEC case study can be much smaller. Nonetheless, the IEC limits will always cause a large decrease on the indices absolute levels, as can be seen in Figure 8.6(a).

decrease it and, if so, it might postpone any improvements on the distribution system. For example, it was previously shown that the K-factor for the base case study is around 1.2 for most of the time. Considering the Natural Load Evolution without the IEC limits, the annual growth rate is at 10% which means that in five years the K-factor will reach around 1.8 ( $1.2 \times (1 + 10\% \times 5 \text{ years})$ ). This might require the derating of the service transformer after this time. However, with the IEC limits the annual growth rate decreases to 5%, which means the K-factor will take at least 10 years to reach 9.

**Table 8.4: Impact of IEC limits on the transformer loading.**

Index	Average Decrease due to IEC Limit	Annual Growth Rate	
		Natural Load Evolution	Natural Load Evolution with IEC Limits
Transformer K-Factor	48.76%	10.00%	5.09%

The effects of enforcing the IEC limits on the primary system are shown in Section 8.4 along with the effects of adding harmonic filters to the system.

### 8.3. Harmonic Mitigation Using Passive Filters

Another potential solution for managing the harmonic distortion situation is to install a few harmonic filters in the primary system, especially the passive shunt filters. One filter topology considered in this thesis is the single-tuned filter which is a series combination of an inductance and a capacitance shown in Figure 8.8(a). The inductor is sized in such a way that the branch resonates at a particular harmonic frequency called tuning (resonance) frequency,  $h_i$  on Figure 8.8(b). So the branch impedance approaches zero at the tuning frequency, enabling the branch to bypass harmonic current at that frequency. This is the most common filter. To filter multiple harmonics, multiple single-tuned filters are used, each tuned to a specific harmonic number.

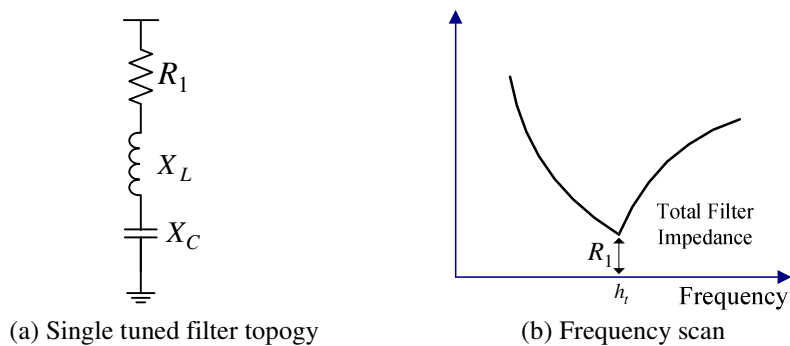


**Figure 8.8: Single tuned filter and associated frequency response.**

To tune the above filter for the 5<sup>th</sup> harmonic, the following relationship can be used:



$$hX_L = \frac{X_C}{h} \Rightarrow X_L = \frac{X_C}{h^2} = \frac{V_{rated}^2}{Q_C \times 25}$$

where  $Q_C$  is the capacitor size (var),  $V_{rated}$  is the capacitor voltage rating (equal to the line-to-line voltage).

As mentioned before, the 3<sup>rd</sup> harmonic has become a main contributor to the feeder voltage distortion and the 9<sup>th</sup> harmonic has caused telephone interference in a number of cases. Since these harmonics are mainly in zero sequence, the so-called zero sequence harmonic filters can also be considered. One type of zero sequence filter is proposed in [71], which is a combination of a Yg/Δ transformer and one capacitor in the secondary winding, as shown in Figure 8.9(a). By tuning the capacitor with the zero sequence impedance of the transformer, it is possible to create a low zero-sequence impedance circuit, thereby sinking the zero sequence harmonics. The zero-sequence filters have no impact on the positive and negative sequence harmonics in the system. Thus, an advantage of this topology is that there is no possibility of causing resonance at non-zero sequence harmonics.

The steps necessary to tune a Yg/Δ transformer based filter shown in Figure 8.9(a) are described as follows:

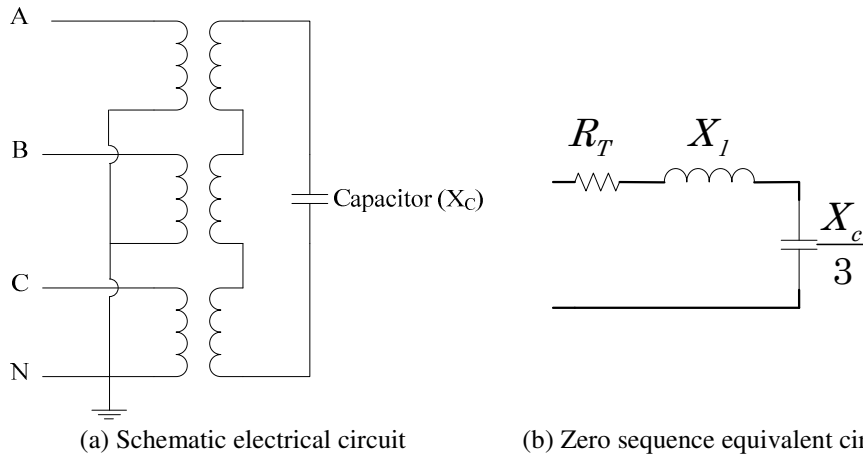


Figure 8.9: The Yg/Δ transformer based filter.

- 1) Build the zero sequence equivalent circuit of the Yg/Δ transformer based filter, as shown in Figure 8.9(b).  $X_l$  is the leakage reactance of transformer and  $X_C$  is the capacitor reactance.
- 2) The zero sequence impedance ( $Z_{f0}$ ) of the filter can be derived as follows:

$$Z_{f0} = Z_T + \frac{X_C}{3} = R_T + jhX_l - j\frac{X_C}{3h}$$

- 3) To tune the filter for the 3<sup>th</sup> harmonic, the corresponding capacitor size can be found as follows:

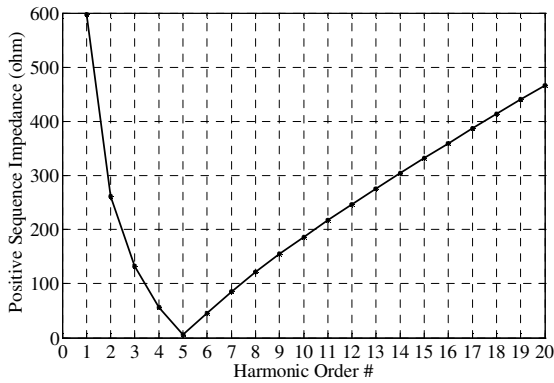
$$X_c = 27 \times X_l \quad \text{or} \quad Q_c = \frac{V_{rated}^2}{27 \times X_l}$$

where  $Q_c$  is the capacitor size (var),  $V_{rated}$  is the capacitor voltage rating (equal to the transformer line-to-line secondary voltage).

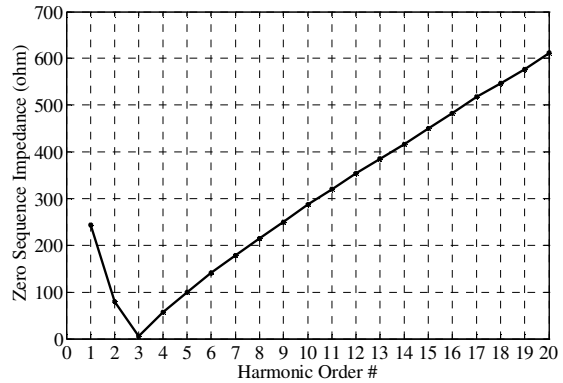
The single tuned filter adopted in this study uses a 1 Mvar capacitor (commonly connected at the substation for reactive power compensation) at 25 kV and is designed to filter the 5<sup>th</sup> harmonic. A typical Yg/Δ three-phase service transformer is employed to build the zero sequence filter tuned for the 3<sup>rd</sup> harmonic. Such a transformer's specification is 1 MVA, 25/0.480 kV with a reactance of 5%. Parameters of the filters are shown in Table 8.5. The filters' frequency responses are shown in Figure 8.10.

**Table 8.5: Parameters of harmonic filters.**

Filter	Tuned Capacitor	Tuned Inductor
3 <sup>rd</sup> Zero Sequence	740 kvar	-
5 <sup>th</sup> Single Tuned	1000 kVar	66 mH



(a) 5th harmonic single tuned filter



(b) 3rd harmonic zero sequence filter

**Figure 8.10: Frequency scan for each individual tuned harmonic filter.**

The location of the above filter package (one 3<sup>rd</sup> filter and one 5<sup>th</sup> filter) is determined through sensitivity studies. In this study, 5 potential locations are evaluated, which are 1, 5, 8, 11 and 15 kilometers from the substation. The index used to compare the location effect is the average harmonic current along the feeder. The results are shown in Figure 8.11, which show that the best location to install the filters is at 11 kilometers from the substation.

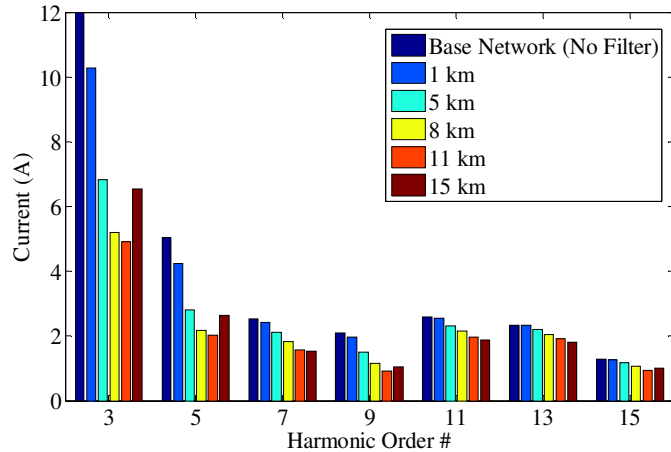


**Figure 8.11: Feeder harmonic currents as affected by filters locations.**

Since the filters are connected to the primary feeder and the supply system has much low impedance, it is useful to check if the filters have sufficiently low impedances that can “compete” harmonic currents with the supply system at the 11 km location, i.e. preventing the 3<sup>rd</sup> and 5<sup>th</sup> harmonic flowing into the supply system. For this purpose, a system frequency scan is performed. The results are shown in Figure 8.12. The solid line represents the system impedance and the dashed line represents the 3<sup>rd</sup> and the 5<sup>th</sup> filters combined impedance. One can observe that the system impedance is higher than the filters impedance at the 3<sup>rd</sup> and 5<sup>th</sup> harmonics which are close to zero even if realistic resistances of the filter components are considered. This explains why the low impedance of the supply system shall not be a concern.

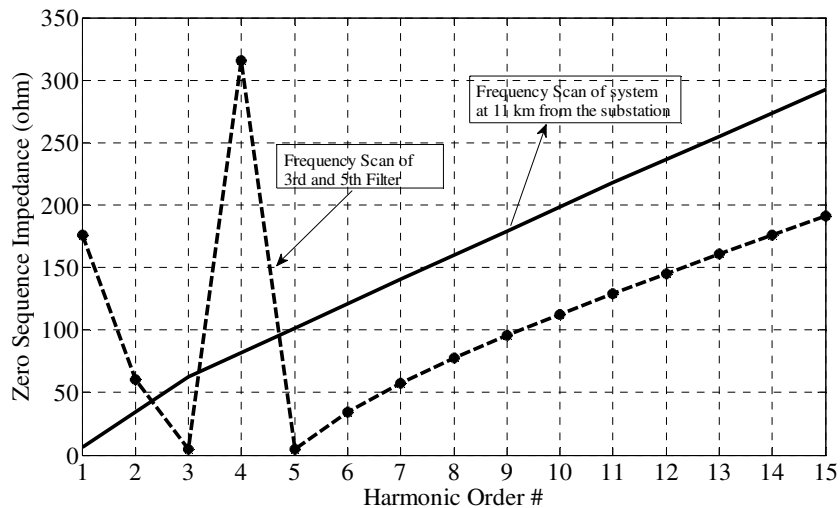


**Figure 8.12: System and 3rd and 5th filters frequency scan.**

#### 8.4. Harmonic Mitigation Effectiveness for Primary System

This section presents the effectiveness of the two harmonic mitigation options (imposing

IEC limits and adding harmonic filters) on controlling the harmonic distortions in the primary system. The effectiveness is evaluated from the following two perspectives:

- **Index average decrease:** The PQ index levels without and with the IEC limits are compared year by year and the PQ index average decrease is calculated. The same is done with and without filters. Therefore, we have two useful numbers; one shows the average decrease of the PQ index due to the IEC limits and the other shows the average decrease due to the filter placement.
- **Annual growth rate:** The annual growth rate is determined considering the IEC limits and the filters placement. They are compared against those obtained from the base case of Chapter 7.

#### 8.4.1. Harmonic voltage and current distortions

Figure 8.13 shows that if the house appliances comply with the IEC standards the phase voltage THD level decreases significantly by an average of 30%. The average annual growth rate of most harmonic components decreases when the IEC limits are enforced. Even though there is an increase of the average annual growth rate associated to the 13<sup>th</sup> harmonic component, one can observe, from Figure 8.13(a) and Figure 8.14(a), that there is a large decrease on the level 13<sup>th</sup> harmonic component of both dominant sequence voltage and current at the primary system. The reduction on the THD level is even larger, at around 60%, when the 3<sup>rd</sup> and the 5<sup>th</sup> filters are connected at the primary distribution system.

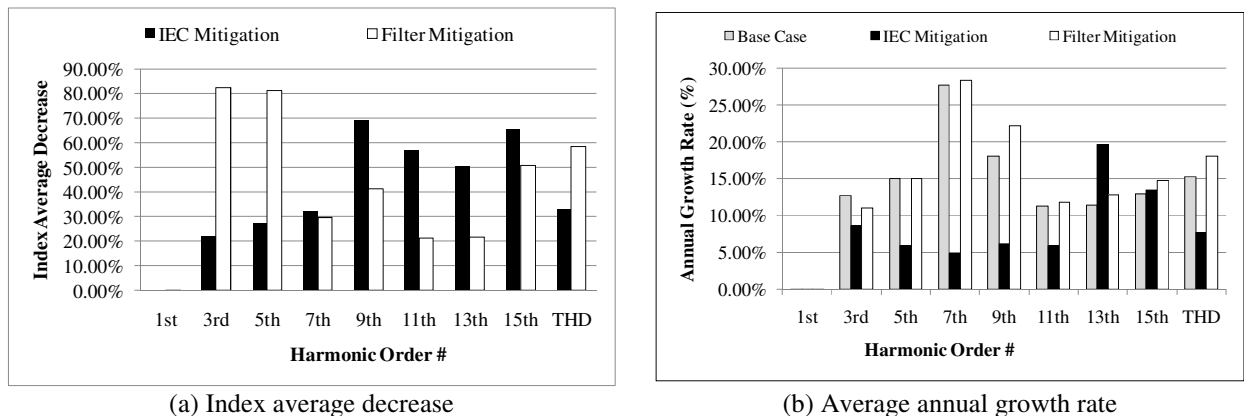
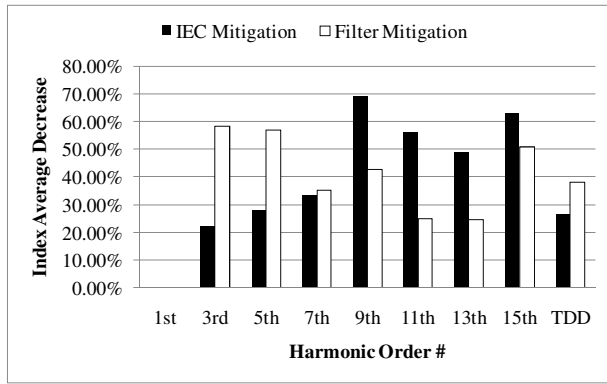


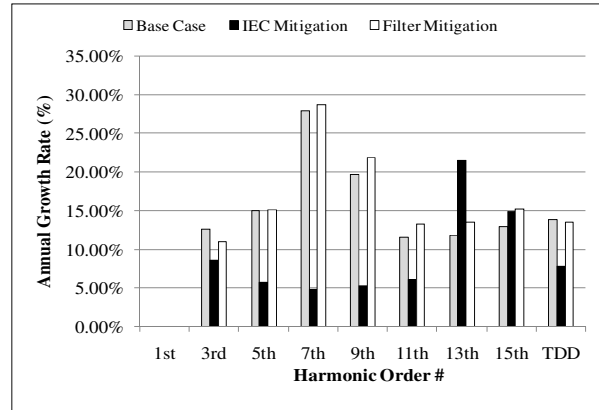
**Figure 8.13: Effects of mitigation options on feeder harmonic voltage.**

In terms of annual growth rate, the IEC option can reduce the growth rate of key harmonics such as 5<sup>th</sup>, 7<sup>th</sup> and 9<sup>th</sup> by about half. The impact on the 3<sup>rd</sup> harmonic growth rate is not as

significant. This is partial due to the fact that there is a significant reduction of the 3<sup>rd</sup> harmonic in the first year already. As expected that the filter has no impact on the annual growth rate. Figure 8.14(a) shows that even though the filters are tuned at the 3<sup>rd</sup> and 5<sup>th</sup> resonance frequencies, they also help to decrease other harmonics like the 9<sup>th</sup> and 15<sup>th</sup> harmonics.



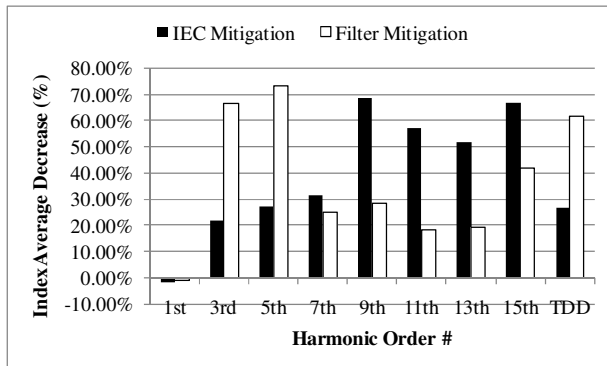
(a) Index average decrease



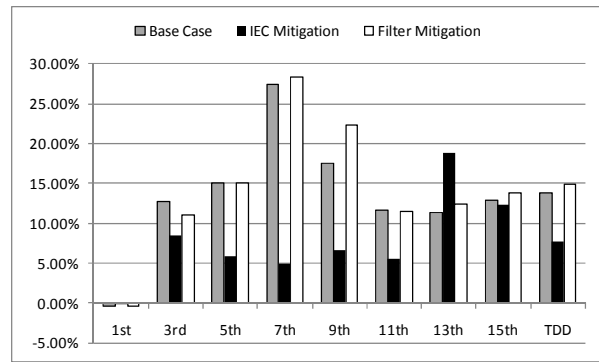
(b) Average annual growth rate

**Figure 8.14: Effects of mitigation options on feeder harmonic current.**

The above conclusions are also applicable to the harmonic currents injected into the transmission system from the feeder, as can be shown in Figure 8.15.



(a) Index average decrease



(b) Average annual growth rate

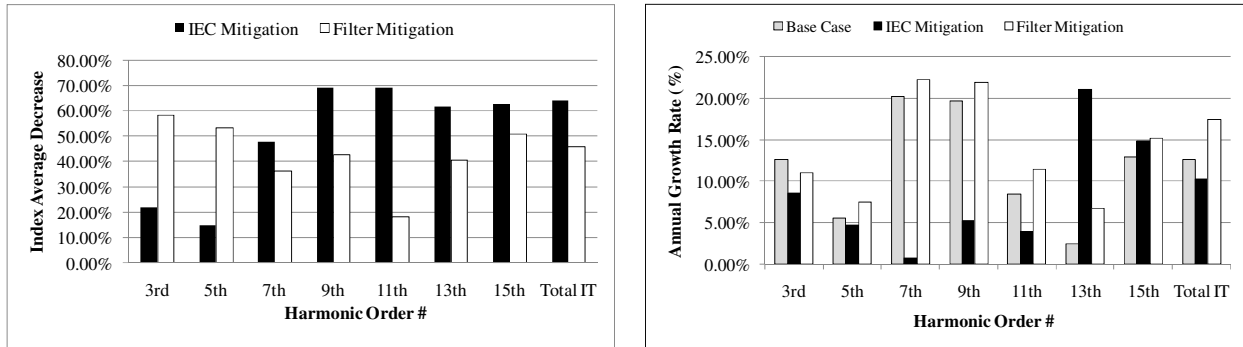
**Figure 8.15: Effects of mitigation options on the harmonics entering into transmission system.**

### 8.4.2. Telephone interference levels

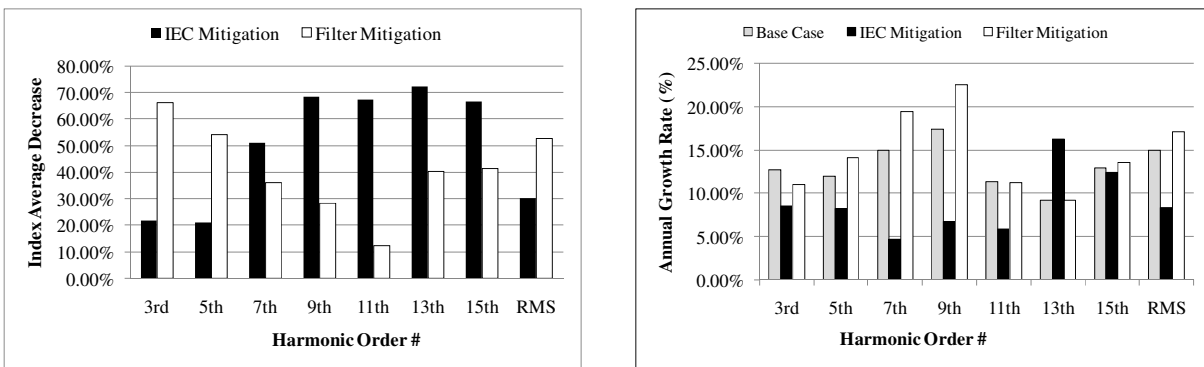
The effects of two mitigation options on telephone interference levels are shown in Figure 8.16 and Figure 8.18. The option of imposing IEC limits can yield significant reduction (60% to 80%) on the telephone interference level. The annual growth rate of the 9<sup>th</sup> harmonic contribution to the telephone interference is cut by approximately half. This is also quite significant.

The option of installing 3<sup>rd</sup> and 5<sup>th</sup> harmonic filters also results in large reductions on the

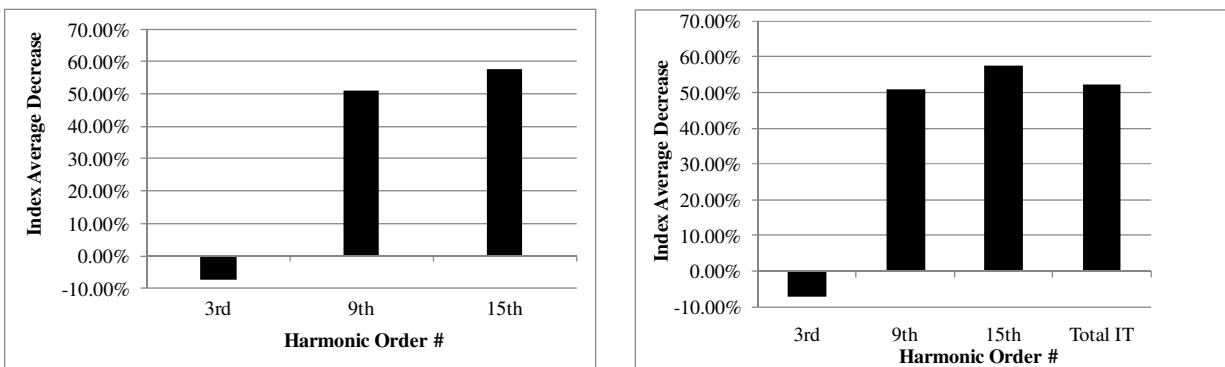
contributions of the 3<sup>rd</sup> and 5<sup>th</sup> harmonics to the telephone interference level. Additional studies have shown that the telephone interference level can be reduced further if 9<sup>th</sup> and 15<sup>th</sup> harmonic filters are installed. Sample results are shown in Figure 8.18. Note that there is a slight increase of 3<sup>rd</sup> harmonic in this case. This is due to the lack of a 3<sup>rd</sup> harmonic filter and the interaction between the installed filters and the supply system. As expected, installing filters has little impact on the annual growth rate of the telephone interference level.



(a) Index average decrease (b) Average annual growth rate  
**Figure 8.16: Effects of mitigation options on the IT levels at the primary system.**



(a) Index average decrease (b) Average annual growth rate  
**Figure 8.17: Effects of mitigation options on the voltage induced in a parallel conductor.**



(a) Average zero sequence current (b) Average total and individual IT  
**Figure 8.18: Effects of installing 9th and 15th filters on telephone interference.**

### 8.4.3. Neutral conductor current

Figure 8.19 shows the effects of the mitigation options on the neutral current. The IEC limits have a significant effect on reducing the 7<sup>th</sup>, 9<sup>th</sup>, 11<sup>th</sup> and 13<sup>th</sup> harmonics. The reduction is more than 50%. It has some impact on the 3<sup>rd</sup> and 5<sup>th</sup> harmonics. The annual growth rates of harmonics have also been reduced. The reason for increased growth rate of the 13<sup>th</sup> harmonic is related to the definition of the index which was explained before. The filter option is very effective to reducing the 3<sup>rd</sup> and 5<sup>th</sup> harmonics.

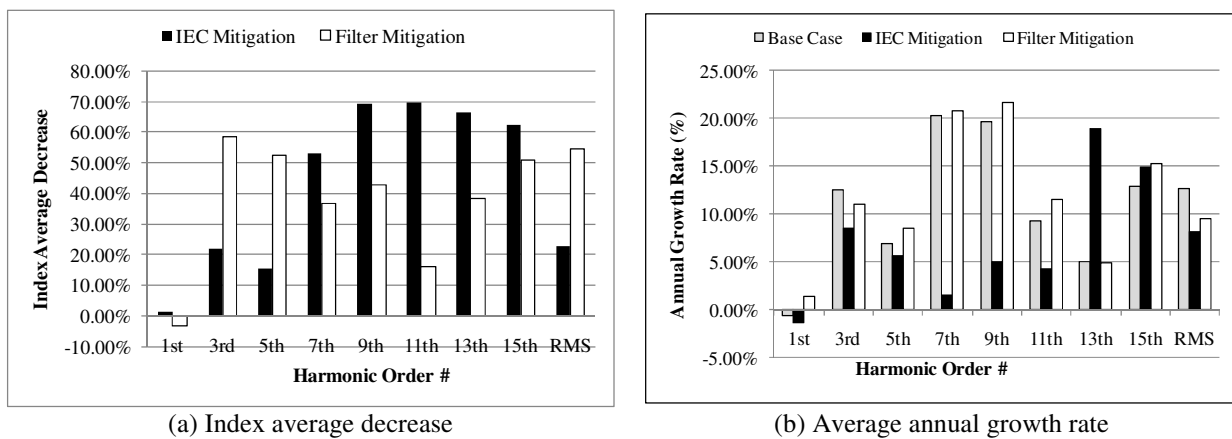


Figure 8.19: Effects of mitigation options on the average neutral current levels.

### 8.5. Summary

This chapter has shown that both harmonic mitigation options are quite effective in improving the power quality of the system. The effectiveness adopting the IEC limits has been quantified. This option can reduce many of the key harmonic components by about 50% and decrease their annual growth rate by about half. This option has some effectiveness in reducing the 3<sup>rd</sup> harmonic in the system. The reduction rate is about 20%. The filter option study has shown that it is definitely feasible to use feeder level harmonic filters to mitigate the harmonics. The effectiveness of harmonic filters can be quite high, but it is dependent on the locations and parameters of the filters. In summary, we can conclude that utilities do have solution options to manage the power quality situations caused by modern residential loads.

In the particular case of North America and other countries that do not adopt the standard IEC 61000-3-2, the harmonic filter option is a more viable option. Industry manufacturers largely oppose enforcing harmonic emission limits on equipments due to economic reasons and

electric utilities have different viewpoints on what harmonic limits should be set for the equipments. It will take some time to implement a standard similar to the IEC on North America and other countries. However, there is a renewed interest for discussions with the intense use of CFLs and the increasing penetration of electric vehicles (particularly the plug-in hybrid electric vehicles). On the other hand, the mitigation of the harmonic distortion caused by residential loads can be very difficult once in the network due to the dispersed nature. It is impractical to place filters to all these dispersed sources once installed and installing system harmonic filters has its own issues. Therefore, prevention, for example with an IEC 61000-3-2 standard, might be an easier solution from the technical point of view.



---

## Chapter 9

# CONCLUSIONS AND FUTURE WORK

---

A probabilistic method to determine the harmonic impact of residential loads and houses has been presented in this thesis. The method models the random harmonic generations of residential loads by simulating the random operating states of the loads. This is done through determining the switching-on probability of a residential load based on the load research results. The result is a randomly varying harmonic equivalent circuit representing a residential house. By combining multiple residential houses served by a service transformer, a model for service transformers is also derived. PCA and statistical analysis on the simulated and measurement results have confirmed the validity of the proposed modeling approach. One of the attractive characteristics of the proposed method is its bottom-up approach. As a result, one can simulate the effect of market trends and policy changes. For example, the harmonic impact of CFLs can be studied by adjusting the composition of lighting fixtures in the residential load database.

Moreover, this thesis conducted an extensive investigation on the potential harmonic impacts of modern residential loads such as energy efficient lightings and consumer electronic devices. A set of techniques and algorithms on studying the impacts have been developed and applied. The impacts have been assessed from many perspectives with the help of a set of indices. Both primary and secondary distribution systems are analyzed. The main findings of this thesis are summarized as follows:

- The harmonic-producing home appliances or modern residential loads can affect the secondary and primary residential feeders in the following areas: (1) harmonic voltage and current distortion levels, (2) loading of service transformers, (3) telephone interference, (4) neutral current of the primary feeder, (5) harmonic currents injected into the transmission system and (6) potentially revenue meter accuracy if the situation is not managed properly.

- The harmonics produced by these loads have negligible effects in the following subjects: (1) harmonic-caused neutral voltage rise in both secondary and primary systems, (2) neutral current rise in the secondary systems, (3) losses in either the primary or the secondary systems, and (4) capacitor overloading under non-resonant condition.
- The main harmonics of concern are the 3<sup>rd</sup>, 9<sup>th</sup>, 5<sup>th</sup>, 7<sup>th</sup> and 15<sup>th</sup>. Among them, the 3<sup>rd</sup>, 9<sup>th</sup> and 15<sup>th</sup> harmonics are dominantly in zero sequence. They create new problems such as telephone interference and neutral current rise that were not commonly experienced in the past when most harmonic sources are three-phase industrial customers.
- With the adoption of new home appliances such as the compact fluorescent lights and home computing devices, the indices characterizing the harmonic impacts will grow at an annual rate of 10% to 15% over the next several years. The growth of harmonic impact is mainly caused by the adoption of CFL and home computing devices. The replacement of CRT TV by the LCD TV does not cause negative harmonic impact.
- An illustration using calculated and measured data of harmonic currents injected by single-detached homes has shown that clusters of residential homes can inject into primary distribution systems harmonic currents that exceed the limits established for individual industrial customers of comparable MW sizes. In view of this situation and the growing trending of harmonic distortions in residential feeders, there is a need for utility companies to manage the situation.
- The investigation on the solution options to mitigate harmonic distortion has shown that imposing the IEC device-level limits on home appliances have a significant impact on reducing the harmonic levels in both primary and secondary distribution systems. The degree of harmonic reduction ranges from 20% to 70% depending on the harmonic order and indices of interest. The option of installing feeder level harmonic filters can also be quite effective. The effectiveness is dependent on the locations, parameters and tuning frequency of the filters.

In summary, the overall conclusion of the thesis is that modern residential loads with energy efficient and consumer electronic appliances have emerged as a significant harmonic source in

power distribution systems. Harmonics injected by clusters of such loads can exceed the limits established for industrial facilities of similar power demands. Furthermore, the harmonic impacts are growing at a relatively high rate of 10% to 15% per year and this trend is expected to continue. Since the harmonic-producing loads are small in size, large in numbers and distributed in locations, there are challenges for utility companies to manage the situation. However, solution options are available. As utility companies pay more attention to the issue, more solutions could be developed.

The following outlines suggestions for future work:

- A similar approach can be adopted to study the impact of electric cars, distributed generation (e.g., photovoltaic generation) and/or other residential appliances;
- More realistic considerations can be added into the probabilistic bottom-up residential house model, such as weather or season effect etc.;
- Investigate other electrical models for the residential appliances (e.g., norton equivalent, voltage source model);
- Develop a theory or guidelines to decide the best locations for harmonic filters.



---

## Chapter 10

### REFERENCES

---

- [1] A. E. Emanuel and et al., "Voltage distortion in distribution feeders with nonlinear loads," IEEE Trans. Power Delivery, 1994, 9, (1), pp. 79–87.
- [2] N. R. Watson, T. L. Scott, and S. Hirsch, "Implications for Distribution Networks of High Penetration of Compact Fluorescent Lamps," IEEE Trans. Power Delivery, vol.24, no.3, pp.1521-1528, July 2009.
- [3] D. J. Pileggi and et al, "The Effect of Modern Compact Fluorescent Lights on Voltage Distortion", IEEE Transactions on Power Delivery, v. 8, no. 3, July 1993, pp. 1451-59.
- [4] J. A. Pomilio and S. M. Deckmann, "Characterization and Compensation of Harmonics and Reactive Power of Residential and Commercial Loads," IEEE Trans. Power Delivery, vol.22, no.2, pp.1049-1055, April 2007.
- [5] A. Nassif, "Modeling, Measurement and Mitigation of Power System Harmonics", PhD Thesis, University of Alberta, Canada, 2008.
- [6] J. Arrillaga, and R. W. Neville, Power System Harmonics, 2nd Edition, 2003, John Wiley & Sons.
- [7] IEEE Working Group, "Power Line Harmonic Effects on Communication on Line Interference," IEEE Trans. on Power Apparatus and Systems, vol.PAS-104, no.9, pp.2578-2587, Sept. 1985.
- [8] R. Arseneau, G. T. Heydt, and M. J. Kempker, "Application of IEEE standard 519-1992 harmonic limits for revenue billing meters", IEEE Trans. Power Delivery, vol.12, no.1, pp.346-353, Jan 1997.
- [9] E. F. Fuchs, D. J. Roesler, K. P. Kovacs, "Sensitivity of Electrical Appliances to Harmonics and Fractional Harmonics of the Power System Voltage. Part II: Television

- Sets, Induction Watthour Meters and Universal Machines”, IEEE Transactions on Power Delivery, vol 2, no. 2, April 1987. pp. 445-453.
- [10] Electromagnetic compatibility (EMC) – Part 3-2: Limits – Limits for harmonic current emissions (equipment input current  $\leq 16$  A per phase), IEC 61000-3-2, International Standard, 2005.
- [11] *Draft Guide for Harmonic Limits for Single-Phase Equipment*, P1495/D2, Jan. 2001. [Online]. Available: [grouper.ieee.org/groups/harmonic/single/docs/P1495D2.doc](http://grouper.ieee.org/groups/harmonic/single/docs/P1495D2.doc) [Accessed: 23 Jan. 2010].
- [12] Probabilistic Aspects Task Force of the Harmonics Working Group, “Time-Varying Harmonics: Part II– Harmonic Summation and Propagation”, IEEE Trans. Power Delivery, vol. 17, no. 1, January 2002, pp. 279-285.
- [13] M. Lehtonen, “A General Solution to the Harmonics Summation Problem”, European Trans. Electrical Power Engineering, vol. 3, no. 4, July/Aug. 1993, pp. 293-297.
- [14] A Cavallini and G. C. Montanari, “A Deterministic/Stochastic Framework for Power System Harmonics Modeling”, IEEE Trans. Power Systems, Vol. 12, No. 1, February, 1997, pp. 407-415.
- [15] S. R. Kaprielian, A. E. Emanuel, R. V. Dwyer and H. Mehta, “Prediction Voltage Distortion in a System with Multiple Random Harmonic Sources”, IEEE Trans. Power Delivery, vol. 9, no. 3, July 1994, pp. 1632-1638.
- [16] G. Zhang and W. Xu, "Estimating harmonic distortion levels for systems with random-varying distributed harmonic-producing loads," IET Generation, Transmission & Distribution , vol.2, no.6, pp.847-855, November 2008.
- [17] Time-Varying Waveform Distortions in Power Systems Edited by Paulo F. Ribeiro 2009 John Wiley & Sons, Ltd.
- [18] Y. Rubinstein, Simulation and the Monte Carlo method, John Wiley and Sons, Inc., New York, USA, 1981.
- [19] W. Xu, J. R. Marti, and H. W. Dommel , "A multiphase harmonic load flow solution technique," IEEE Trans. on Power Systems, vol.6, no.1, pp.174-182, Feb 1991.

- [20] W. Xu, "A multiphase harmonic load flow solution technique", PhD Thesis, University of British Columbia, 1989.
- [21] C. Walker and J. Pokoski, "Residential load shape modelling based on customer behavior," IEEE Trans. Power Apparatus and Systems, 1703-1711, 1985.
- [22] A. Capasso, W. Grattieri, R. Lamedica, and A. Prudenzi, "A bottom-up approach to residential load modeling," IEEE Trans. Power System, vol. 9, pp. 957–964, May 1994.
- [23] I. Richardson, M. Thomson, et al, "Domestic electricity use: A high-resolution energy demand model", Energy and Buildings 42(10): 1878-1887, 2010.
- [24] M. Armstrong, M. Swinton, H. Ribberink, I. Beausoleil-Morrison, and J. Millette, "Synthetically derived profiles for representing occupant driven electric loads in canadian housing," Building Performance Simulation, vol. 2, pp. 15–30, 2009.
- [25] IEEE Standard Definitions for the Measurement of Electric Power Quantities Under Sinusoidal, Nonsinusoidal, Balanced, or Unbalanced Conditions, IEEE Std 1459-2010 (Revision of IEEE Std 1459-2000) , vol., no., pp.1-40, March 19 2010.
- [26] Task Force on Harmonics Modeling and Simulation, Modeling and Simulation of the Propagation of Harmonics in Electric Power Networks, Part I: Concepts, Models, and Simulation Techniques, IEEE Transactions on Power Delivery, vol. 11, no. 1, January 1996.
- [27] A. Mansoor, W. M. Grady, A. H. Chowdhury, and M. J. Samotyj, "An Investigation of Harmonics Attenuation and Diversity Among Distributed Single-Phase Power Electronic Loads", IEEE Trans. Power Delivery, vol. 10, no. 1, Jan. 1995, pp. 467-473.
- [28] A.B. Nassif and W. Xu, "Characterizing the Harmonic Attenuation Effect of Compact Fluorescent Lamps," IEEE Trans. Power Delivery, vol.24, no.3, pp.1748-1749, July 2009.
- [29] B. C. Smith, N.R. Watson, A.R. Wood, and J. Arrillaga, "A Newton solution for the harmonic phasor analysis of AC/DC converters," IEEE Trans. Power Delivery, 1996, 11, (2), pp. 965–97.

- [30] R. Dwyer, A. K. Khan, M. McGranaghan, L. Tang, R. K. McCluskey, R. Sung, T. Houy, "Evaluation of Harmonic Impacts from Compact Fluorescent Lights on Distribution Systems", IEEE Trans. Power Systems, vol. 10, no. 4, Nov. 1995, pp. 1772-1779.
- [31] V. Letschert, Potential Impact of Adopting Maximum Technologies as Minimum Efficiency Performance Standards in the U.S. Residential Sector, eScholarship, 2010.
- [32] IEA, Light's Labour's Lost, International Energy Agency, OECD, Paris, 2006.
- [33] ESource, Who's Buying CFLs? Who's Not Buying Them? Findings from a Large-Scale, Nationwide Survey, 2008 ACEEE Summer Study.
- [34] LCD TV Market Growing Despite Weakness in North America; LED-Backlit Set to Take Lead in 2011, available online at: <http://www.displaysearch.com/>
- [35] The Economist, Pocket World in Figures 2006 and 2010.
- [36] World Development Indicators, World Bank Group, 2010.
- [37] Canadian laptop ownership, IPSOS, 2009, available online at <http://www.ipsos-na.com/news-polls/>.
- [38] 2008 could be the year laptop sales eclipse desktops in US, January 2008, available online at: <http://arstechnica.com>
- [39] Gartner Says Worldwide PC Market Grew 13 Percent in 2007, January 2008, available online at: <http://www.gartner.com/it/page.jsp?id=584210>
- [40] Natural Resources Canada, Energy Consumption of Major Household Appliances Shipped in Canada-Trends for 1990-2006, December 2008.
- [41] M. Jungreis, A. W. Kelley, Adjustable Speed Drive for Residential Applications, IEEE Transactions on Industry Applications, vol. 31, no. 6, Nov./Dec. 1995, pp. 1315-1322.
- [42] Clément C. Lefebvre, Electric Power: Generation, Transmission And Efficiency, Nova Science Publishers, Inc, 2008.
- [43] Ipsos-RSL and Office for National Statistics, United Kingdom Time Use Survey, 3rd ed., UK Data Archive, Colchester, Essex, September 2003.



- [44] R. Hendron, Building America Research Benchmark Definition Updated December 2009 Robert Hendron and Cheryn Engebrecht.
- [45] Bell, M. Swinton, M.C. Entchev, E. Gusdorf, J. Kalbfleisch, W. Marchand, R.G. Szadkowski, F., Development of Micro Combined Heat and Power Technology Assessment Capability at the Canadian Centre for Housing Technology, pp. 48. 2003-12-08.
- [46] CSA, Energy Consumption Test Methods for Household Dishwashers, CSA Standard CAN/CSA-C373-92, 1992.
- [47] CSA, Test Method for Measuring Energy Consumption and Drum Volume of Electrically Heated Household Tumble-Type Clothes Dryers, CSA Standard CAN/CSA-C361-92, 1992.
- [48] CSA, Energy Performance, Water Consumption and Capacity of Automatic Household Clothes Washers, CSA Standard CAN/CSA-C360-98, 1998.
- [49] Natural Resources Canada, Photovoltaic Systems – A Buyer’s Guide, ISBN 0-662-31120-5, 2002.
- [50] Natural Resources Canada, Micro-Hydropower Systems – A Buyer’s Guide, ISBN 0-662-35880-5, 2004.
- [51] Statistics Canada, Selected dwelling characteristics and household equipment, available online at: <http://www40.statcan.gc.ca/l01/cst01/famil09b-eng.htm>.
- [52] M. H. Kalos and A. P. Whitlock, Monte Carlo Methods, Wiley-VCH, 2008.
- [53] I.T. Jolliffe, Principal Component Analysis, by Springer-Verlag New York Inc, 1986.
- [54] Jackson, J. E., A User's Guide to Principal Components, John Wiley and Sons, 1991, p. 92.
- [55] Ying-Yi Hong and Bo-Yuan Chen, "Locating Switched Capacitor Using Wavelet Transform and Hybrid Principal Component Analysis Network," IEEE Trans. Power Delivery, vol.22, no.2, pp.1145-1152, April 2007.
- [56] E. Vazquez, I. I. Mijares, O. L. Chacon, and A. Conde, "Transformer Differential Protection Using Principal Component Analysis," IEEE Trans. Power Delivery, , vol.23, no.1, pp.67-72, Jan. 2008.

- [57] K.K. Anaparthi, B. Chaudhuri, N. F. Thornhill, and B. C. Pal, "Coherency Identification in Power Systems Through Principal Component Analysis," *IEEE Trans. Power Systems*, vol.20, no.3, pp. 1658- 1660, Aug. 2005.
- [58] J. J. Burke, *Power Distribution Engineering—Fundamentals and Applications*, New York: Marcel Dekker, 1994, pp. 16–17.
- [59] L. Levey, "Calculation of ground fault currents using an equivalent circuit and a simplified ladder network," *IEEE Trans. Power App. Syst.*, vol. PAS-101, no. 8, pp. 2491–2497, Aug. 1982.
- [60] J.R. Acharya, Y. Wang, and W. Xu, "Temporary Overvoltage and GPR Characteristics of Distribution Feeders With Multigrounded Neutral," *IEEE Trans. Power Delivery*, vol.25, no.2, pp.1036-1044, April 2010.
- [61] T .A. Short, *Electric Power Distribution Handbook* CRC Press 2003.
- [62] *IEEE Recommended Practices and Requirements for Harmonic Control in Electrical Power Systems*, IEEE Standard 519-1992, 1992.
- [63] *IEEE Recommended Practice for Inductive Coordination of Electric Supply and Communication Lines*, IEEE Standard 776-1992, 2012.
- [64] J. Burke, "The Confusion Over Stray Voltage", *IEEE Industry Applications Magazine*, May/June 2008, p. 63-66.
- [65] E. R. Collins and J. Jiang, "Analysis of Elevated Neutral-to-Earth Voltage in Distribution Systems with Harmonic Distortion," *IEEE Trans. Power Delivery*, vol.24, no.3, pp.1696-1702, Jul. 2009.
- [66] *IEEE Recommended Practice for Establishing Transformer Capability When Supplying Non-sinusoidal Load Currents*, IEEE Std C57.110-1998 , vol., no., pp.i, 1998
- [67] *IEEE Working Group on Nonsinusoidal Situations*, "A Survey of North American Electric Utility Concerns Regarding Nonsinusoidal Waveforms," *IEEE Trans. Power Delivery*, Vol. 11, No. 1, January 1996, pp 73-78.

- [68] CEA 043-D-610, "Optimum Metering Systems for Loads with High Harmonic Distortion," Prepared by Precision Measurement Group, Division of Electrical Engineering, National Research Council, May 1988.
- [69] IEEE C62.92.4-1991, Guide for the Application of Neutral Grounding in Electrical Utility Systems, Part IV-Distribution, 1992.
- [70] A. P. Meliopoulos, "Impact of Grounding System Design on Power Quality", IEEE Power Engineering Review, Nov 2001, p. 3-7.
- [71] US patent 5914540 "Filter for removing harmonic current from a neutral conductor", published June 22, 1999.
- [72] H. E. Mazin and W. Xu, "Harmonic Cancellation Characteristics of Specially Connected Transformers," Electric Power Systems Research, Vol. 79, No. 12, 2009, pp. 1689-1697.
- [73] Distribution System Modeling and Analysis William H. Kersting, 2001, CRC edition.



# Appendix A Harmonic Data of Home Appliances

This appendix presents the harmonic spectrum data of various home appliances that were used in the simulation studies. Note that each brand of an appliance has slightly different spectrum and the simulation study used all measured spectrums. For the sake of space, the spectrum for only one brand is shown here. More measurements results and details about the different brands can be found in [5].

**Table A.1: Characteristics of measured appliances.**

Appliances	CFL Lamp		Electronic Ballast Lamp		Desktop PC		LCD Monitor		Laptop	
Operating Power (W)	15		17		94		31.2		55.5	
THD <sub>1</sub> (%)	120		145.36		99.5		118		127	
	Mag. (A)	Angle (deg)	Mag. (A)	Angle (deg)	Mag. (A)	Angle (deg)	Mag. (A)	Angle (deg)	Mag. (A)	Angle (deg)
H1	0.156	26.44	0.153	21.2	0.823	0.5	0.279	14.4	0.496	16.2
H3	0.125	81.39	0.124	53.9	0.65	1.6	0.230	34.7	0.397	47.1
H5	0.091	148.04	0.087	105.5	0.407	3.6	0.159	63.5	0.256	89.1
H7	0.070	-137.53	0.069	169.4	0.161	8.6	0.100	108.7	0.173	154.1
H9	0.050	-66.75	0.067	-134.8	0.099	58.1	0.073	167.6	0.172	-135.9
H11	0.030	10.19	0.054	-84.2	0.12	168.7	0.068	-141.7	0.178	-82.9
H13	0.020	110.40	0.039	-21.8	0.118	178	0.065	-105.5	0.149	-37.4
H15	0.018	-154.24	0.031	51.1	0.05	-170.2	0.047	-59.8	0.124	21.3
H17	0.013	-60.78	0.031	118.6	0.05	-64.8	0.031	1.2	0.116	77.4
H19	0.012	41.66	0.026	-172.7	0.07	-17.7	0.032	44	0.095	134
H21	0.014	133.14	0.019	-95.7	0.041	-7.9	0.026	88.5	0.081	-171.7
H23	0.015	-130.98	0.024	-31.5	0.025	12.6	0.018	139.6	0.067	-110.1
H25	0.018	-50.13	0.025	61.8	0.031	144.6	0.012	-167.6	0.063	-50.6
H27	0.018	26.01	0.025	142.1	0.031	161.6	0.011	-97.8	0.055	6.11

**Table A.2: Characteristics of measured appliances.**

Appliances	LCD TV		CRT TV		Microwave		ASD* Fridge		Freezer	
Operating Power (W)	95.3		48.5		1097		1100		114	
THD <sub>1</sub> (%)	6.24		145.8		41.3		5.8		19.6	
	Mag. (A)	Angle (deg)	Mag. (A)	Angle (deg)	Mag. (A)	Angle (deg)	Mag. (A)	Angle (deg)	Mag. (A)	Angle (deg)
H1	0.797	4	0.398	5.2	9.770	-11.4	2.32	-7.0	1.101	-29.22
H3	0.027	-22.2	0.356	10.8	3.808	43.4	0.09	-131.3	0.175	-128.22
H5	0.019	-155.6	0.309	18.4	1.130	-72.6	0.06	-131.1	0.097	-169.94
H7	0.017	-24.3	0.246	26	0.417	156.3	0.08	64.4	0.068	113.99
H9	0.022	-148.5	0.184	33.5	0.257	85	0.02	-3.0	0.029	79.26
H11	0.004	3.75	0.123	43.1	0.131	-4.9	0.01	-88.5	0.026	-128.5
H13	0.009	-162	0.066	55.2	0.071	-102.8	0.03	-4.2	0.007	4.06
H15	0.009	56.2	0.022	81.1	0.061	-169.2	0.01	-51.5	0.011	-136.54
H17	0.002	146.7	0.011	-174.5	0.037	75.1	0.00	-44.6	0.007	-141.82
H19	0.003	40.5	0.022	-136.2	0.041	-21.1	0.00	1.2	0.005	84.33
H21	0.005	-61.4	0.024	-118.5	0.039	-123.4	0.00	-12.9	0.005	14.27
H23	0.004	-99.3	0.018	-112.9	0.033	131.8	0.00	32.52	0.001	-56.41
H25	0.002	-81.6	0.008	-101.1	0.030	50.9	0.00	-55.8	0.002	-15.15
H27	0.003	148.3	0.001	-112.5	0.028	-42.6	0.00	52.6	0.001	163.04

**Table A.3: Characteristics of measured appliances.**

Appliances	Regular Fridge		Washer		ASD* Dryer		Regular Dryer		Furnace	
Operating Power (W)	150		123		871		4180		535	
THD <sub>1</sub> (%)	18		75.4		53.2		1.37		10.5	
	Mag. (A)	Angle (deg)	Mag. (A)	Angle (deg)	Mag. (A)	Angle (deg)	Mag. (A)	Angle (deg)	Mag. (A)	Angle (deg)
H1	1.275	-19.7	2.310	-63.6	4.235	11.266	20.2	38.7	5.160	-33
H3	0.060	-131.6	1.538	164.5	1.293	114.795	0.1936	110.1	0.505	-159.4
H5	0.170	173.5	0.528	19.2	1.141	192.033	0.1673	-176.1	0.199	78.6
H7	0.076	34.4	0.289	126.1	0.988	-90.863	0.0504	-101.7	0.049	141.5
H9	0.007	5	0.380	-19.7	0.796	-12.060	0.0060	-26.6	0.027	-30.8
H11	0.034	-129	0.118	174.3	0.590	67.979	0.0544	49.9	0.020	-131.7
H13	0.022	76	0.180	-76.5	0.415	150.708	0.0464	129.9	0.006	-78.7
H15	0.004	145.1	0.192	147.5	0.259	237.409	0.0060	-145.7	0.004	125.7
H17	0.012	-37.9	0.042	-91.1	0.163	-26.460	0.0181	-51.4	0.006	-0.1
H19	0.007	146	0.122	88.6	0.120	81.412	0.0121	52.6	0.002	-179.2
H21	0.002	-155.3	0.105	-41.1	0.104	189.139	0.0101	153.6	0.001	45
H23	0.004	34.4	0.021	25.6	0.091	284.774	0.0121	-115.3	0.003	-120.9
H25	0.002	-126.1	0.082	-101.9	0.070	14.073	0.0121	-30.8	0.001	94.1
H27	0.001	-100.6	0.057	-63.5	0.044	103.498	0.0121	57.1	0.004	55

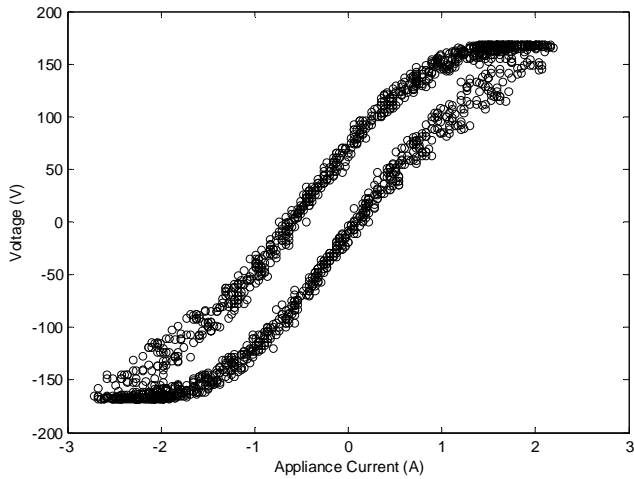
\*ASD - Adjustable speed drive

**Table A.4: Characteristics of measured appliances.**

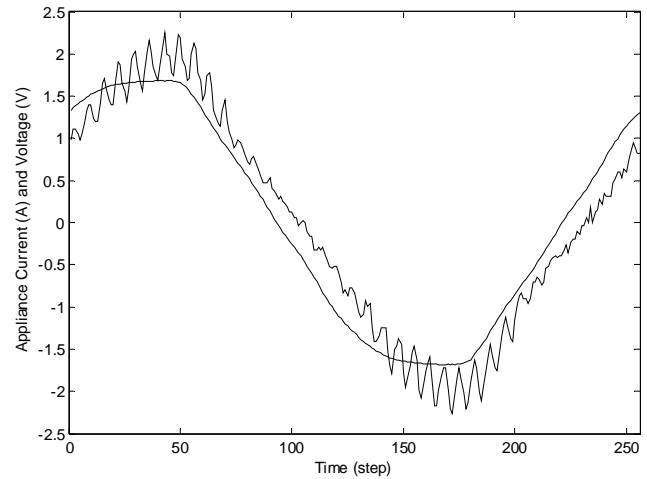
Appliances	Vacuum		Garage Door		Blender		Bread Maker		Food Processor	
Operating Power (W)	1237		472		157		80.1		193	
THD <sub>1</sub> (%)	13.7		14		10		12.4		15.8	
	Mag. (A)	Angle (deg)	Mag. (A)	Angle (deg)	Mag. (A)	Angle (deg)	Mag. (A)	Angle (deg)	Mag. (A)	Angle (deg)
H1	10.512	-10.52	4.768	-30.776	1.313	-13.653	0.936	-45.508	1.616	-11.229
H3	1.374	-45.02	0.589	-85.841	0.119	-54.903	0.110	-104.759	0.233	-54.345
H5	0.283	-165.33	0.301	163.040	0.047	-170.710	0.029	162.250	0.076	-160.517
H7	0.251	106.28	0.017	22.706	0.017	100.132	0.017	91.345	0.068	121.548
H9	0.138	61.16	0.082	92.863	0.015	55.727	0.013	24.952	0.018	59.528
H11	0.044	-65.05	0.032	-162.285	0.002	-68.559	0.003	-48.582	0.011	-48.599
H13	0.043	-134.5	0.026	-1.617	0.005	-94.084	0.003	-112.668	0.005	-135.050
H15	0.036	149.92	0.026	-164.442	0.002	-2.936	0.001	141.331	0.005	-144.892
H17	0.027	52.77	0.012	-118.912	0.002	163.616	0.002	136.419	0.004	178.461
H19	0.003	-51.99	0.012	100.608	0.001	-83.484	0.002	-126.746	0.002	-19.907
H21	0.009	87.38	0.010	44.382	0.004	86.865	0.000	86.950	0.002	71.692
H23	0.005	95.82	0.007	30.899	0.003	-95.907	0.001	-91.599	0.007	28.168
H25	0.009	71.12	0.007	-119.932	0.004	-74.727	0.001	-1.68401	0.004	-41.975
H27	0.025	7.81	0.002	166.935	0.002	40.389	0.001	-40.409	0.004	-14.503

# Appendix B V x I Characteristics of Home Appliances

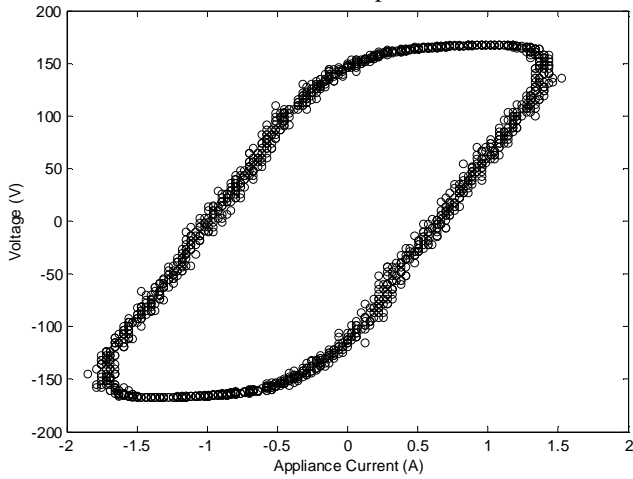
In this appendix, the correlation between the supply instantaneous voltage and current drawn by each appliance (V x I plot) analyzed in this thesis is presented. The voltage and current waveforms shown in the figures on the right side are normalized to facilitate visualization. On the other hand, the V x I plot results shown on the left side are obtained from the real instantaneous values without any normalization. Moreover, the sampling rate adopted for the measurements is 256 samples per cycle.



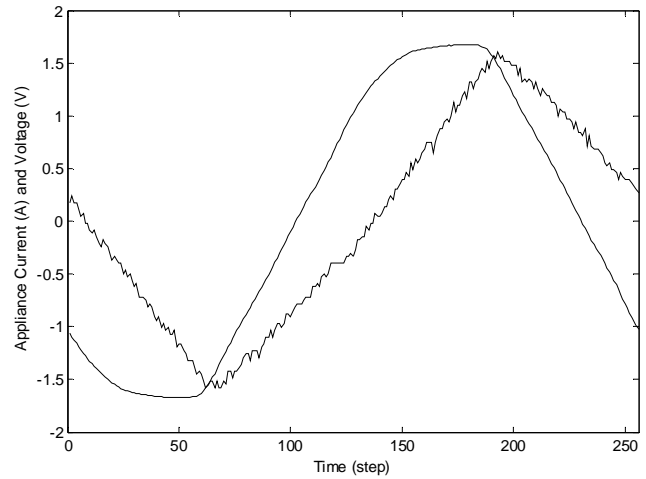
Blender V x I plot



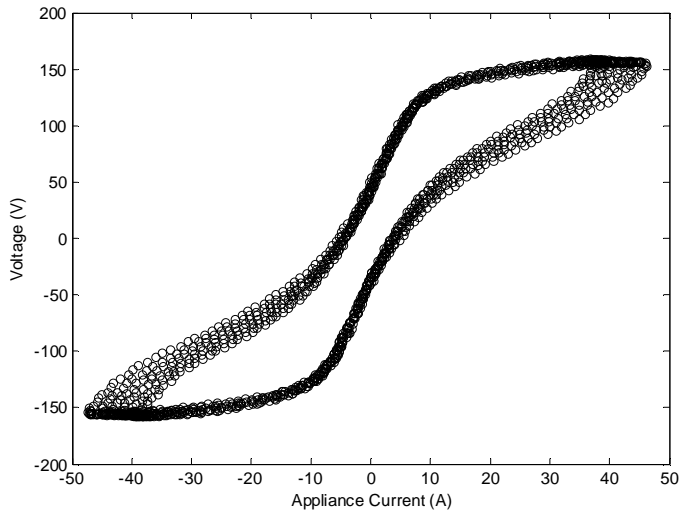
Blender V and I waveforms.



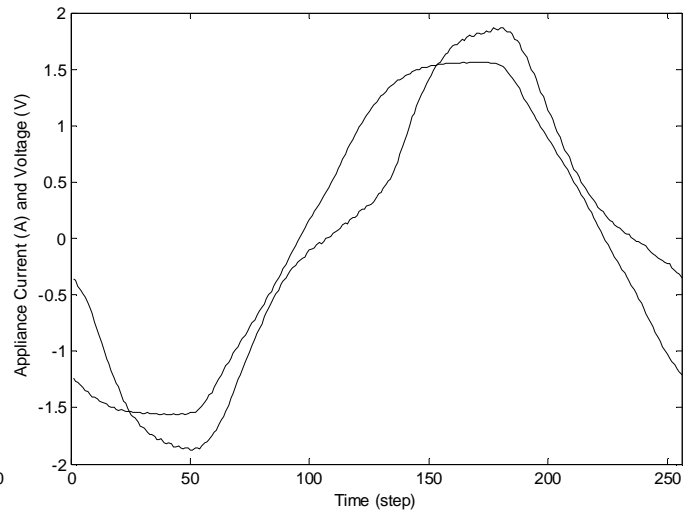
Bread maker V x I plot



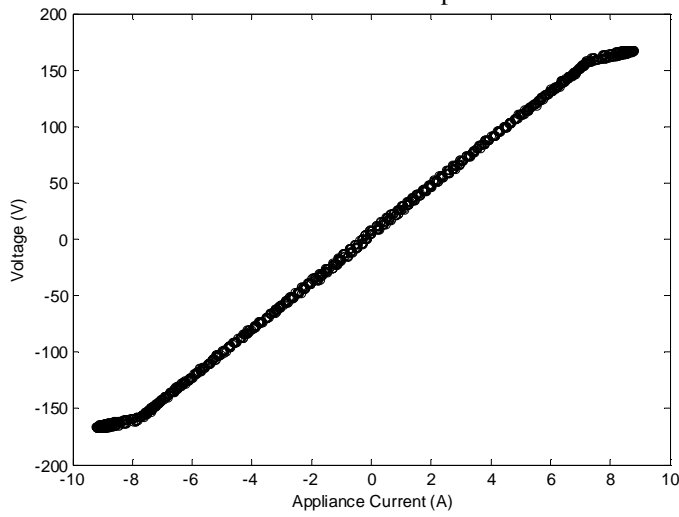
Bread maker V and I waveforms.



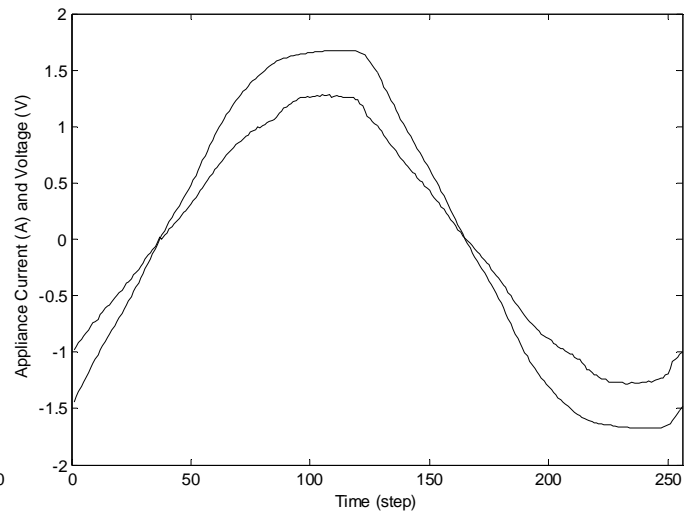
Central vacuum V x I plot



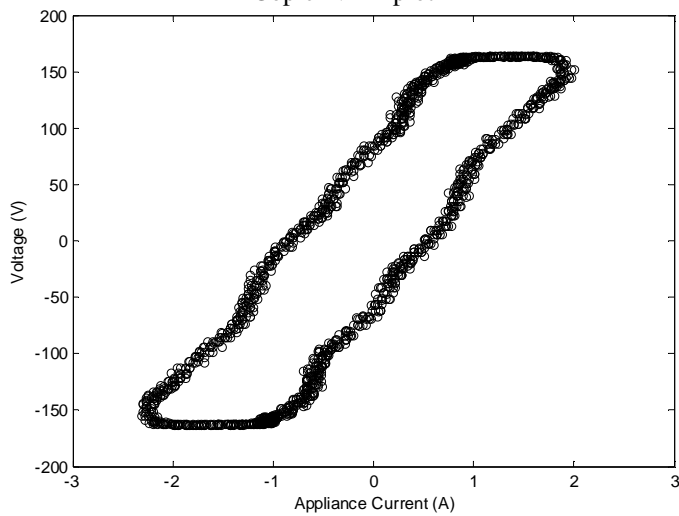
Central vacuum V and I waveforms.



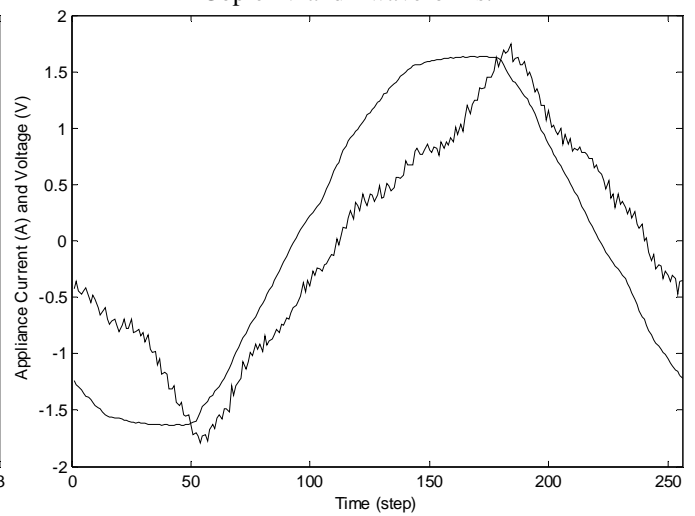
Copier V x I plot



Copier V and I waveforms.

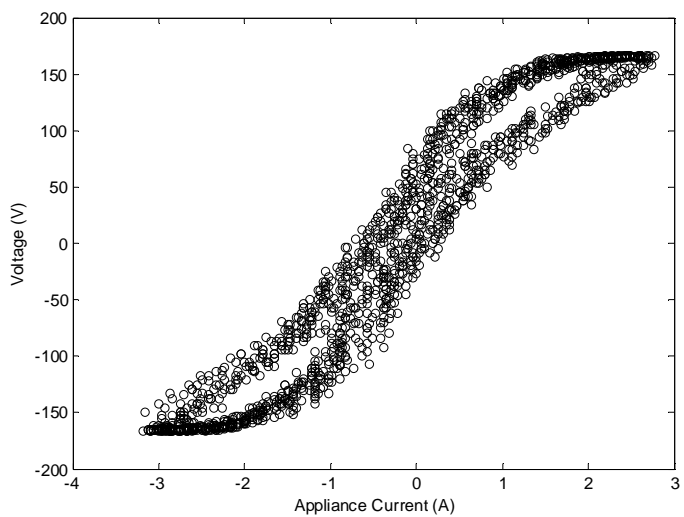


Freezer V x I plot

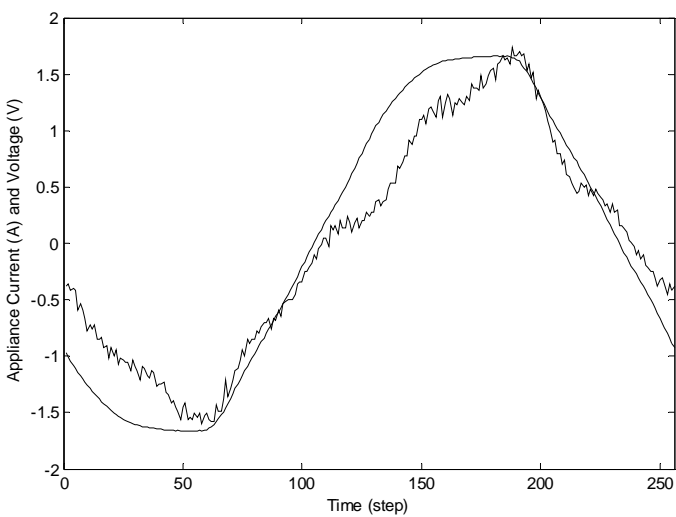


Freezer V and I waveforms

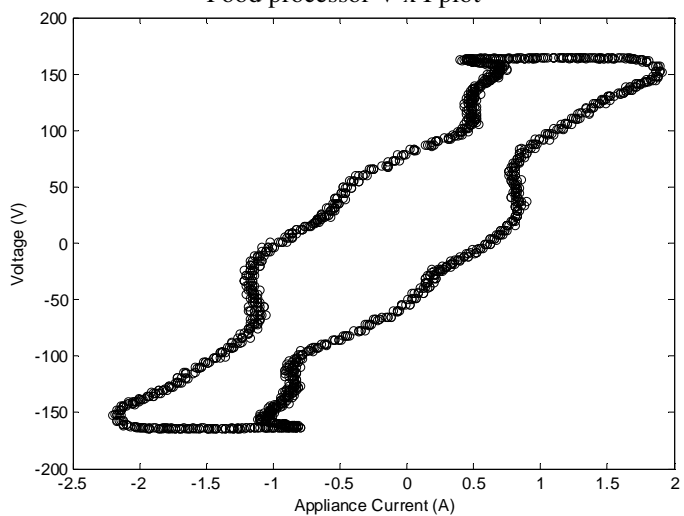




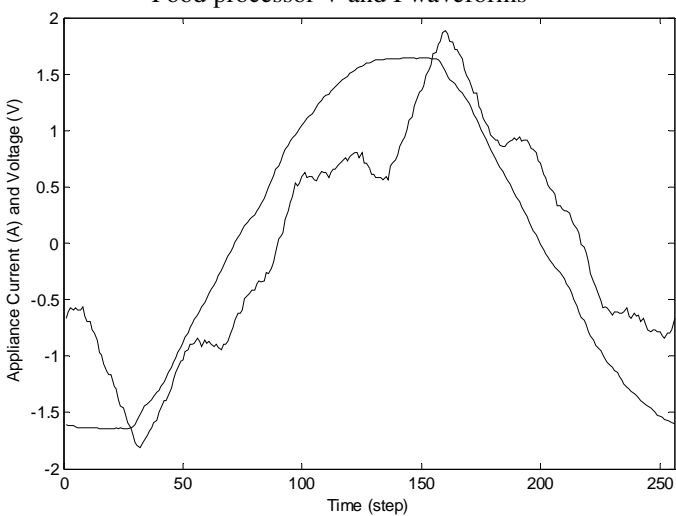
Food processor V x I plot



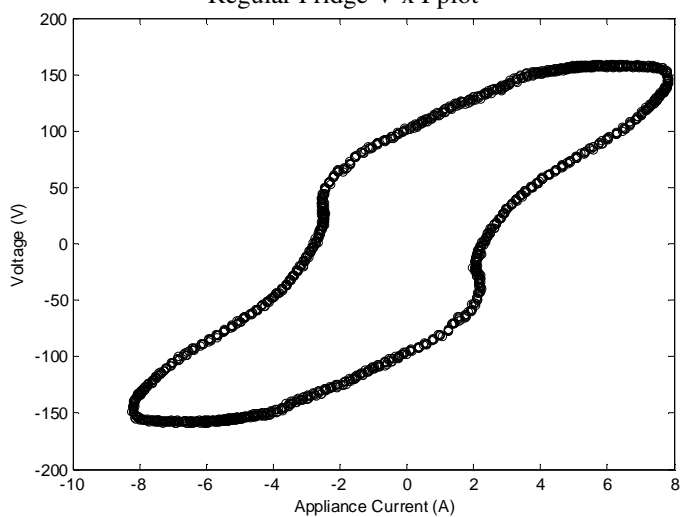
Food processor V and I waveforms



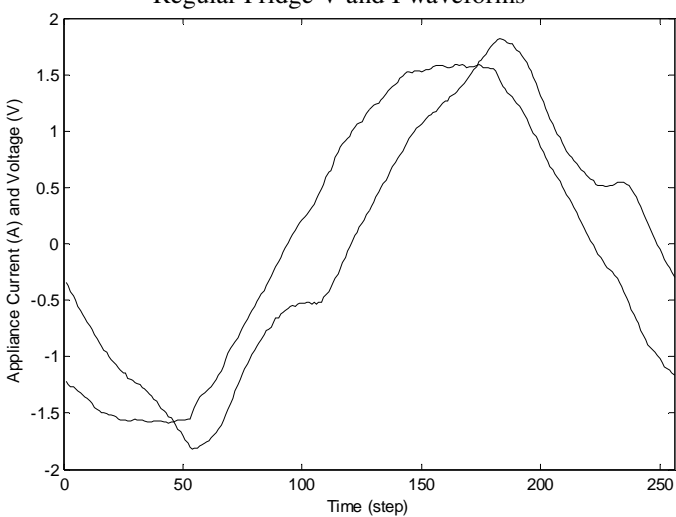
Regular Fridge V x I plot



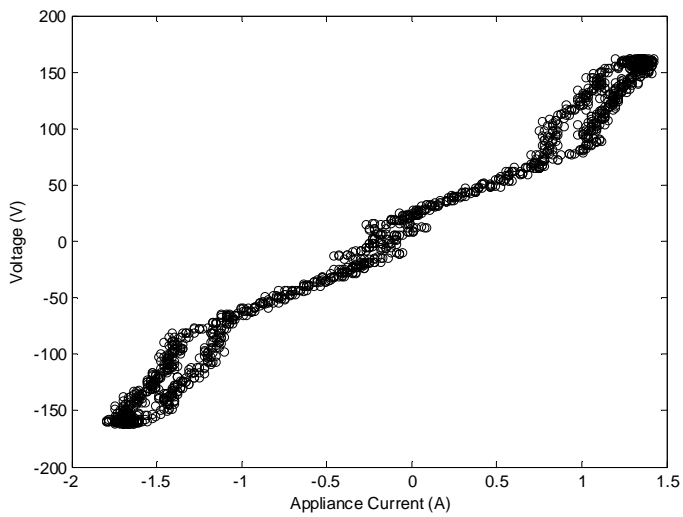
Regular Fridge V and I waveforms



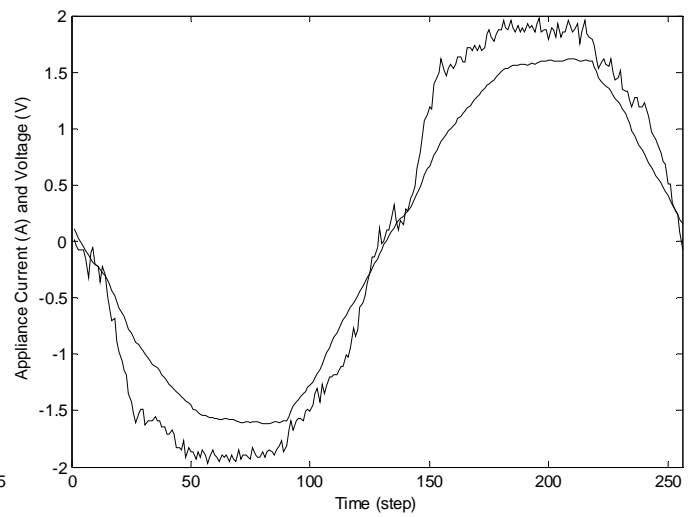
Garage door V x I plot



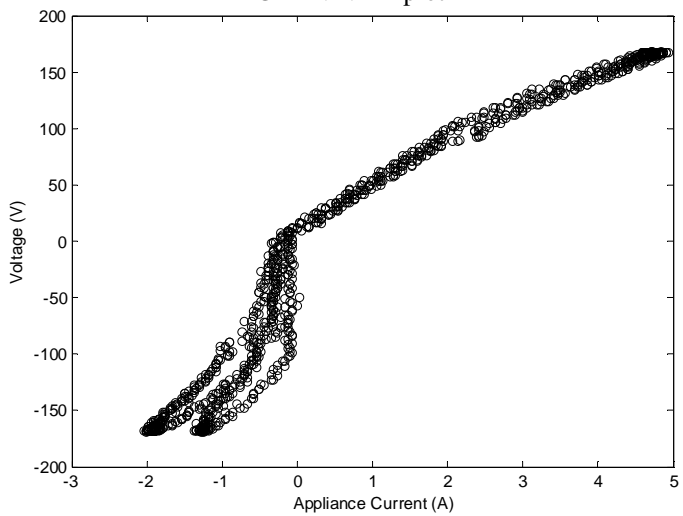
Garage door V and I waveforms



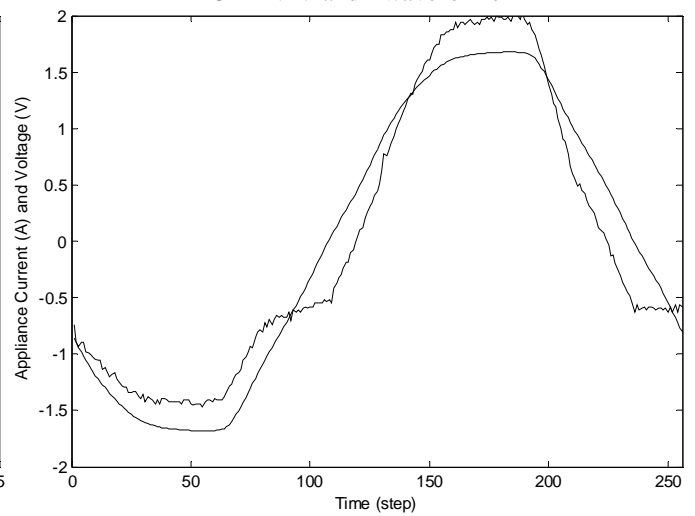
LCD TV V x I plot



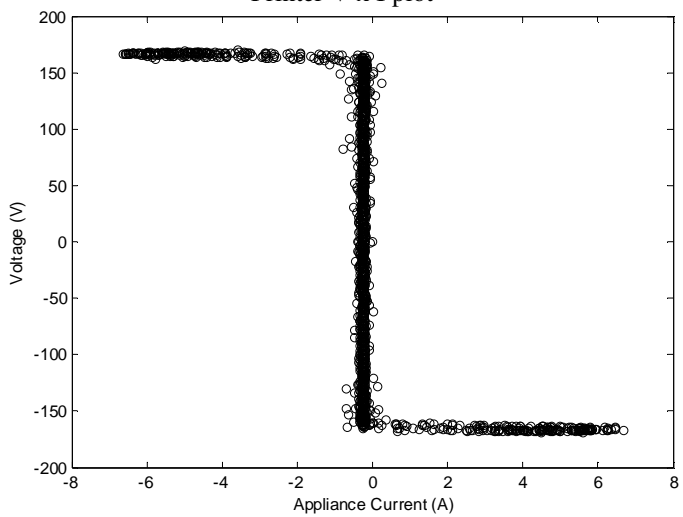
LCD TV V and I waveforms



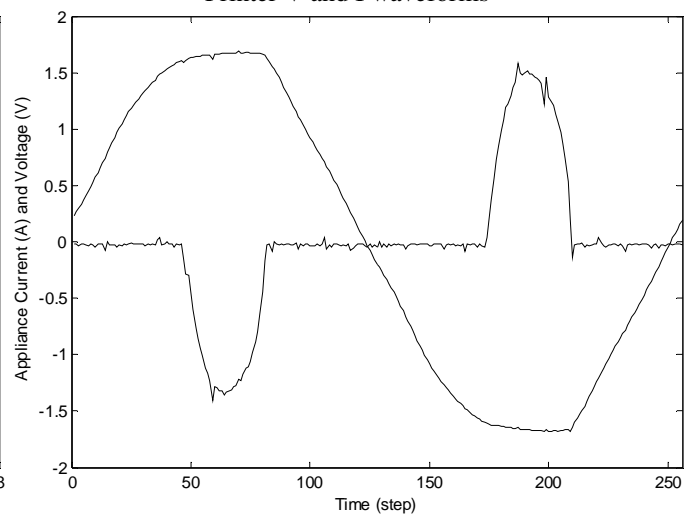
Printer V x I plot



Printer V and I waveforms



Treadmill V x I plot



Treadmill V and I waveforms

## Appendix C Service Transformer Model

Figure C.1 shows the circuit configuration of a typical service transformer. The neutral line of primary side and secondary side are short circuited, and further grounded with a resistor  $R_T$ .  $Z_N$  is the secondary neutral line impedance.  $R_C$  is the house grounding impedance. Loads are connected between +120V line, -120V line and neutral. The harmonic model (i.e.  $Z_a$ ,  $i_a$  and  $Z_b$ ,  $i_b$  and  $Z_{ab}$ ) can be acquired from the bottom-up harmonic source model discussed on Chapter 3. They are treated as known variables here. P, N and G on the left hand represent the common points connected to primary system's phase, neutral and ground respectively.

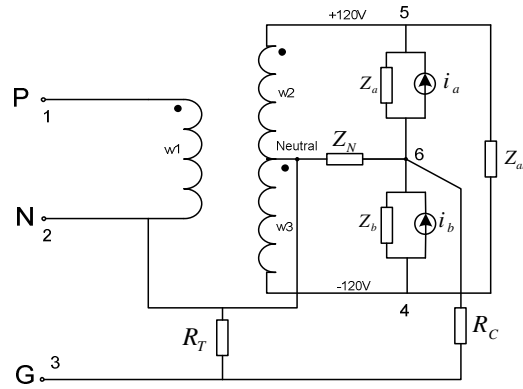


Figure C.1: Service transformer connected to the harmonic house model.

The three-winding service transformer can be mathematically represented by the following equation:

$$V_W^{pu} = Z_W^{pu} I_W^{pu} \quad (C.1)$$

where  $V_W^{pu}$ ,  $I_W^{pu}$  and  $Z_W^{pu}$  are per-unit values of the voltage, current and impedance of windings  $w_1, w_2$  and  $w_3$ , as shown by equations below [72]:

$$V_W^{pu} = [V_{w2}^{pu} \ V_{w2}^{pu} \ V_{w3}^{pu}]^T \quad (C.2)$$

$$I_W^{pu} = [I_{w2}^{pu} \ I_{w2}^{pu} \ I_{w3}^{pu}]^T \quad (C.3)$$

$$Z_W^{pu} = \begin{bmatrix} Z_P^{pu} + Z_m^{pu} & Z_m^{pu} & Z_m^{pu} \\ Z_m^{pu} & Z_S^{pu} + Z_m^{pu} & Z_m^{pu} \\ Z_m^{pu} & Z_m^{pu} & Z_S^{pu} + Z_m^{pu} \end{bmatrix} \quad (C.4)$$

Where  $Z_P^{pu}$  and  $Z_S^{pu}$  are the leakage impedance in per unit of the primary and secondary side of the transformer, respectively.  $Z_m^{pu}$  is the magnetizing impedance, which can be neglected since it is much

larger compared to  $Z_P^{pu}$  and  $Z_S^{pu}$ .

The parameters  $Z_P^{pu}$  and  $Z_S^{pu}$  can be obtained from the nameplate impedance of the transformer ( $R_T^{pu} + jX_T^{pu}$ ) through the following equations:

$$Z_P^{pu} = 0.5R_T^{pu} + j0.8X_T^{pu} \quad (C.5)$$

$$Z_S^{pu} = R_T^{pu} + j0.4X_T^{pu} \quad (C.6)$$

To transform these per unit values into physical ones, the following transformation needs to be used:

$$I_w^{pu} = U_I I_W \quad (C.7)$$

$$V_w^{pu} = U_V V_W \quad (C.8)$$

where

$$U_I = \text{diag} \left\{ \frac{1}{I_{w1}}, \frac{1}{I_{w2}}, \frac{1}{I_{w3}} \right\} \quad (C.9)$$

$$U_V = \text{diag} \left\{ \frac{1}{V_{w1}}, \frac{1}{V_{w2}}, \frac{1}{V_{w3}} \right\} \quad (C.10)$$

where  $I_{wk}$  and  $V_{wk}$  are the current and voltage base values of the  $k^{\text{th}}$  winding. Therefore,

$$V_W = Z_W I_W \quad (C.11)$$

$$Z_W = U_V^{-1} Z_W^{pu} U_I \quad (C.12)$$

The admittance matrix of three windings then would be as follows:

$$Y_W = Z_W^{-1} \quad (C.13)$$

Apart from the three branches of the transformer (three windings), there are six other branches, represented by  $R_T$ ,  $Z_N$ ,  $R_C$ ,  $Z_a$ ,  $i_a$ ,  $Z_b$ ,  $i_b$  and  $Z_{ab}$ . Therefore, without considering the branch connections, the  $Y$  matrix of all branches is as follows [72]:

$$Y_B = \begin{bmatrix} Y_W & & & & & & & & \\ 0 & \text{diag} \left\{ \left[ \frac{1}{R_T} \frac{1}{Z_N} \frac{1}{Z_a} \frac{1}{Z_b} \frac{1}{Z_{ab}} \frac{1}{R_C} \right] \right\} & & & & & & & \\ & & & & & & & & \end{bmatrix}_{9 \times 9} \quad (C.14)$$

To transform branch equation (C.14) into nodal equation (there are totally 6 nodes, as marked in Figure C.1), the incidence matrix is defined:

$$T_v = [t_{ij}]_{b \times n} \quad (C.15)$$

where  $m$  and  $n$  stand for the number of nodes and branches, respectively. The values of  $t_{ij}$  are defined as follows:

$$t_{ij} = \begin{cases} 1 & \text{if node } j \text{ is connected to branch } i \text{ and the branch current flows to } j \\ -1 & \text{if node } j \text{ is connected to branch } i \text{ and the branch current flows from } j \\ 0 & \text{otherwise} \end{cases}$$

Therefore, for the transformer configuration shown in Figure C.1:

$$T_v = \begin{bmatrix} -1 & 1 & 0 & 0 & 0 & 0 \\ 0 & 1 & 0 & 0 & -1 & 0 \\ 0 & -1 & 0 & 1 & 0 & 0 \\ 0 & 1 & -1 & 0 & 0 & 0 \\ 0 & 1 & 0 & 0 & 0 & -1 \\ 0 & 0 & 0 & 0 & 1 & -1 \\ 0 & 0 & 0 & -1 & 0 & 1 \\ 0 & 0 & 0 & -1 & 1 & 0 \\ 0 & 0 & -1 & 0 & 0 & 1 \end{bmatrix} \quad (C.16)$$

Nodes voltage and current can be obtained by using the incident matrix, as follows:

$$V_B = T_v V_N \quad (C.17)$$

$$I_N = T_v^T I_B \quad (C.18)$$

where the subscript  $B$  refers to branch and the subscript  $N$  to node. Finally, the admittance nodal matrix can be represented as follows:

$$Y_N = T_v^T Y_B T_v \quad (C.19)$$

In order to investigate the equivalent circuit seen from primary system (i.e. P, N and G ports), we need to eliminate the internal three nodes (node 4, 5 and 6). The nodal equations are:

$$\begin{bmatrix} I_{PN} \\ I_{inter} \end{bmatrix} = \begin{bmatrix} Y_{11}^{2 \times 2} & Y_{12}^{2 \times 3} \\ Y_{21}^{3 \times 2} & Y_{22}^{3 \times 3} \end{bmatrix} \begin{bmatrix} V_{PN} \\ V_{inter} \end{bmatrix} \quad (C.20)$$

where,  $Y_{11}$ ,  $Y_{12}$ ,  $Y_{21}$  and  $Y_{22}$  are the sub-matrix of  $Y_N$ ,  $V_{PN} = [V_P \ V_N]^T$ ,  $V_{inter} = [V_4 \ V_5 \ V_6]^T$ ,  $I_{PN} = [I_P \ I_N]^T$ ,  $I_{inter} = [I_4 \ I_5 \ I_6]^T$ .

According to Figure C.1,  $I_{inter}$  is known,

$$I_{inter} = \begin{bmatrix} -i_b \\ i_a \\ -i_a + i_b \end{bmatrix} \quad (C.21)$$

Eliminating  $V_{inter}$ , equation (C.20) can be simplified to:

$$[Y_{11} - Y_{12}Y_{22}^{-1}Y_{21}]V_{PN} = I_{PN} - [Y_{12}Y_{22}^{-1}]I_{inter} \quad (C.22)$$

Equation (C.22) gives the matrix format of nodes P and N (G is the reference node, so it is not included in the matrix). A new equivalent Y matrix can be defined as:

$$Y_{eq} = Y_{11} - Y_{12}Y_{22}^{-1}Y_{21} \quad (C.23)$$

and the current source:

$$I_S = [Y_{12}Y_{22}^{-1}]I_{inter} \quad (C.24)$$

In order to separate harmonic current source  $i_a$  and  $i_b$ , the following expression can be obtained:

$$I_P = Y_{12}Y_{22}^{-1} \left( \begin{bmatrix} 0 \\ 1 \\ -1 \end{bmatrix} i_a + \begin{bmatrix} -1 \\ 0 \\ 1 \end{bmatrix} i_b \right) = \alpha \bullet i_a + \beta \bullet i_b \quad (C.25)$$

From the mathematical development above, the equivalent circuit shown in Figure C.2 is then proposed.

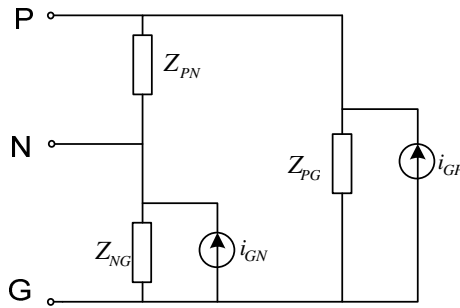


**Figure C.2: Simplified model of the distribution transformer.**

There are five parameters in this model, which are  $Z_{PN}$ ,  $Z_{PG}$ ,  $Z_{NG}$ ,  $i_{PG}$ ,  $i_{NG}$ . The nodal admittance matrix of the simplified model circuit is given by:

$$\begin{bmatrix} I_P + i_{GP} \\ I_N + i_{GN} \end{bmatrix} = Y_{SM} \begin{bmatrix} V_P \\ V_N \end{bmatrix} = \begin{bmatrix} \frac{1}{z_{PN}} + \frac{1}{z_{PG}} & -\frac{1}{z_{PN}} \\ -\frac{1}{z_{PN}} & \frac{1}{z_{PN}} + \frac{1}{z_{NG}} \end{bmatrix} \begin{bmatrix} V_P \\ V_N \end{bmatrix} \quad (C.26)$$

Comparing admittance matrix  $Y_{eq}$  in equation (C.23) and  $Y_{SM}$  in equation (C.26), we have:

$$Y_{SM}(1,1) = Y_{eq}(1,1) \quad (C.27)$$

$$Y_{SM}(2,2) = Y_{eq}(2,2) \quad (C.28)$$

$$Y_{SM}(1,2) = -Y_{eq}(1,2) \quad (C.29)$$

According to the Kirchhoff's circuit law at nodes in the simplified model:

$$i_{GP} = -[\alpha(1) \bullet i_a + \beta(1) \bullet i_b] \quad (C.30)$$

$$i_{GN} = -[\alpha(2) \bullet i_a + \beta(2) \bullet i_b] \quad (C.31)$$

Therefore, from the service transformer impedance ( $R_T^{pu} + jX_T^{pu}$ ) and from the data of the target harmonic source, the five parameters in the simplified model can be acquired from equations (C.27) to (C.31).

The service transformer simplified model previously developed is compared against the complete configuration in order to validate its accuracy. Both circuits are built on the toolbox *Simulink* from Matlab, as shown in figure below.

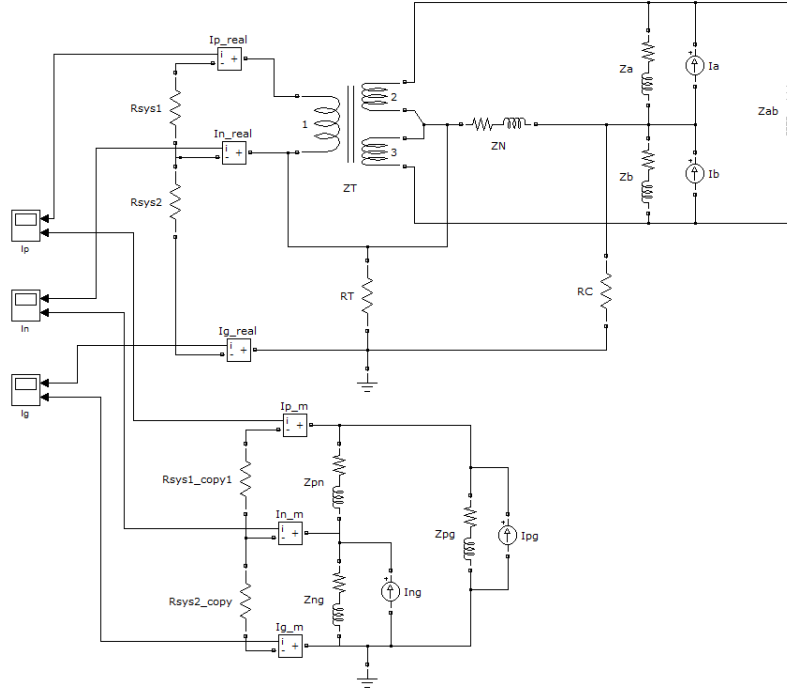


**Figure C.3: Complete and simplified service transformer models in Simulink.**

One case scenario is chosen for simulation. Table C.1 shows the values of  $Z_a$ ,  $Z_b$ ,  $Z_c$ ,  $i_a$ ,  $i_b$  for that scenario:

**Table C.1: Parameters for the validation scenario.**

Parameters	Values
$Z_a$	20.2417+0.0525i (ohm)
$Z_b$	26.9889+0.07i (ohm)
$Z_{ab}$	23.98+0.39i (ohm)
$i_a$	-2.8624 (A)
$i_b$	24.0308 (A)

Based on the mathematical development for the simplified transformer model, the corresponding parameters (i.e.  $Z_{PN}$ ,  $Z_{PG}$ ,  $Z_{NG}$ ,  $i_{PG}$ ,  $i_{NG}$ ) in the simplified model can be found and are shown in Table C.2:

**Table C.2: Parameters for the simplified model.**

Parameters	Values
$Z_{PN}$	6.0632e4+3.5123e3i (ohm)
$Z_{NG}$	3.7808+0.0202i (ohm)
$Z_{PG}$	6.2975e5-4.0495e5i (ohm)
$i_{PG}$	0.1763-0.0002i (A)
$i_{NG}$	-0.4695-0.1901i (A)

Figure C.4 shows the validation results by comparing the currents  $I_p$ ,  $I_n$  and  $I_g$  for both complete



and simplified transformer models. The simulations show that the simplified circuit gives out the same output currents as the complete model. Furthermore, the impedance seen from port P, N and G show the same value for both circuits.

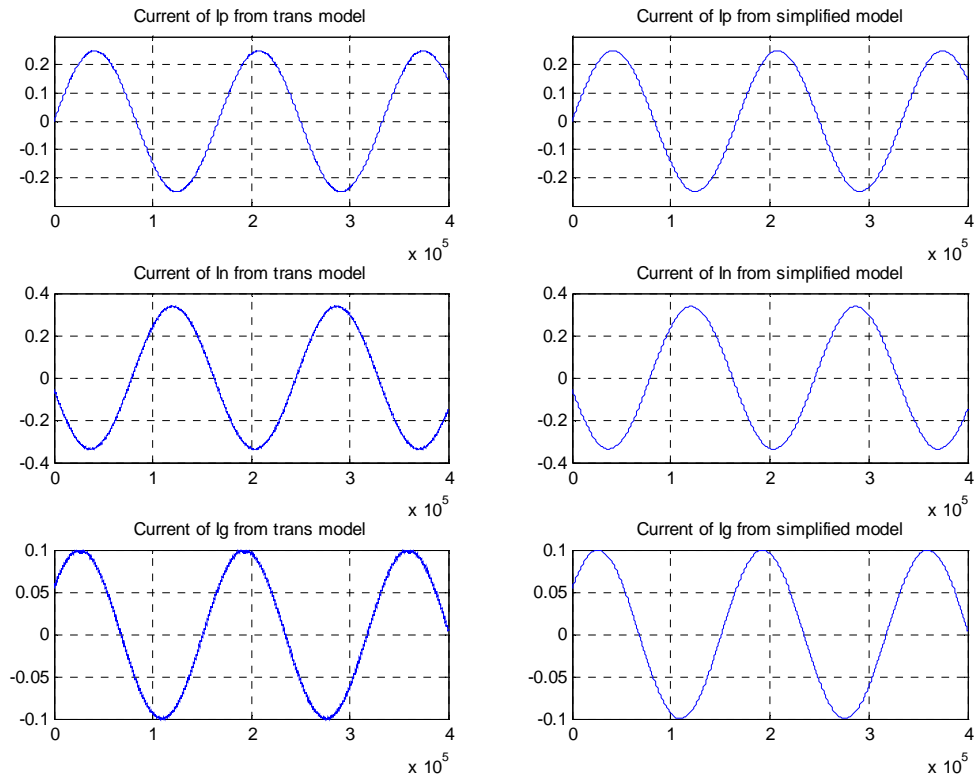


**Figure C.4: Validation results.**



# Appendix D Case Study Using an Actual System

Two feeder cases have been used to analyze the impact of nonlinear residential loads on primary distribution systems. Chapter 7 presents the results obtained from an ideal feeder. Results obtained from simulation studies on a real feeder are presented in this Appendix. This study has confirmed that the conclusions derived from the ideal feeder are applicable to real feeders.

## D.1 Description of the System

Figure D.1 shows a real feeder supplying mainly residential customers in the city of Edmonton, Canada. The data was provided by the utility company that manages this feeder. It is supplied by a 240/25 kV substation and has a main trunk<sup>12</sup> (in red) and three-phase, two-phase and single phase lateral branches (in black). In this thesis, the branches that do not belong to the main trunk will be referred to as *lateral branches*. Table D.1 provides the data associated with the feeder.

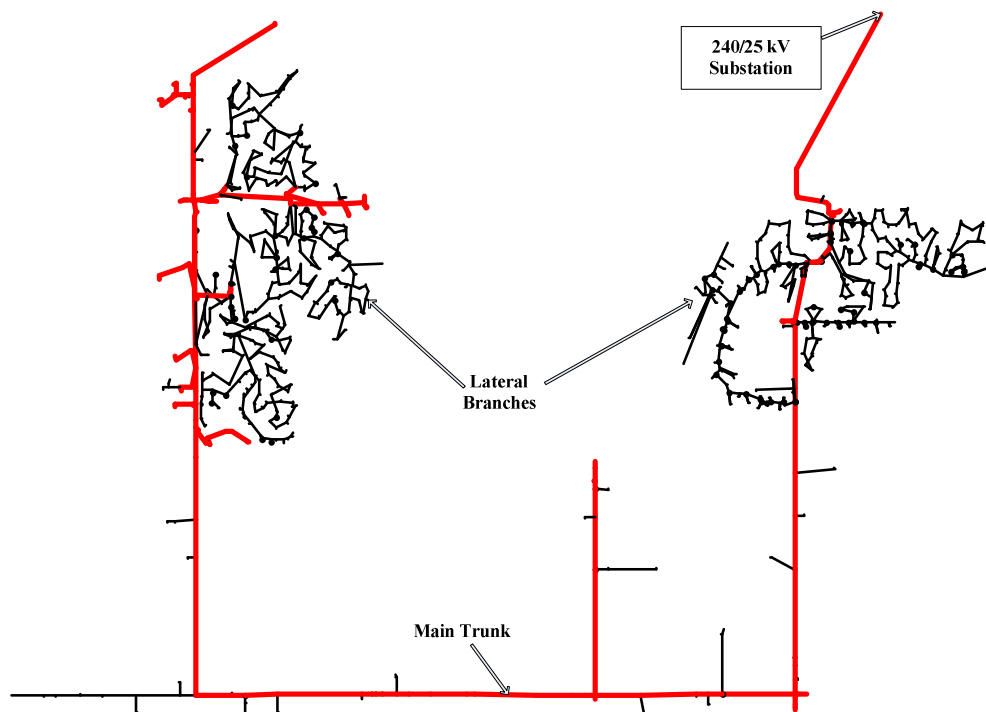


Figure D.1: Real distribution feeder.

In order to perform the harmonic power flow simulations over the real feeder the following modifications/inclusions were done:

- The data provided by the utility do not contain information about the multigrounded neutral circuit (MGN) grounding circuit (*i.e.*, grounding span and resistance). Therefore, it is adopted a

<sup>12</sup>The main trunk consists of the three-phase branches directly connected to the source (substation). Due to the large number of nodes and branches ( $\approx 1550$  branches), a simple graph path algorithm available in the Matlab software was used to find the main trunk.

grounding resistance of 15 ohms and a grounding span of 100 meters. The substation grounding resistance is 0.15 ohms.

- Both the main trunk and branches of the feeder shown in Figure D.1 consist of various types of overhead and underground conductors. In order to facilitate the analysis, one type of overhead line and one type of underground cable are adopted for the harmonic power flow simulations. The criteria used to choose the types is based on those with the longest length in the system:
  - The overhead line was modeled as a three-phase, four-wire line segment model and with a *conductor type 336.4 ACSR* [73].
  - The underground cable was modeled as a three-phase, six-wire line segment model [73]. *The cable type adopted for the simulations is the 500Al XLPE 25kV DBUR.* Underground cable conductors present a much higher shunt capacitance if compared to overhead lines.
- There is only information about the fundamental active power load connected at each service transformer of the feeder. In order to include the harmonic characteristics of the residential loads, the houses connected to each service transformer is modeled by the proposed bottom up approach (Chapter 3) as it was done for the ideal feeder. It is assumed that the active power associated with each house is approximately 1kW. Hence, number of houses connected per each transformer is obtained by dividing active power load of that service transformer by 1kW.

**Table D.1: Parameters of the actual system.**

Actual Feeder Parameters		Values
Primary System	Main trunk overhead line length	12.00 km
	Main trunk underground cable length	10.85 km
	Total length of three-phase lateral branches	8.02 km
	Total length of two-phase lateral branches	4.81 km
	Total length of single-phase lateral branches	54.89 km
	Substation voltage level	25kV <sub>rms</sub> (LL)
	Substation short-circuit level	305 MVA
	Substation equivalent impedance (including substation transformer)	$Z_+ = 0.035 + j2.05 \Omega$ $Z_0 = 0.053 + j2.161 \Omega$
	Overhead line type	336.4 ACSR
	Underground cable type	500Al XLPE 25kV DBUR
	MGN grounding resistance	15 $\Omega$
	MGN grounding span	100 m
	Substation grounding resistance	0.15 $\Omega$
	Secondary System	Number of service transformers
Total active power load		8.79 MW

All lateral branches are underground cables since they are located in the residential areas. The main trunk has also some sections of underground cables and the associated length is shown in table below.

## D.2 Aggregate Load Modeling

Figure D.1 shows several residential areas composed by single and two-phase branches (and a few three-phase branches that do not belong to the main trunk) and service transformers supplying several houses. From a detailed analysis of that network it was possible to identify five residential areas, each one supplied by one main trunk branch, as shown in Figure D.2. Each dashed circle encompasses a group of branches and service transformers connected to one branch of the main trunk. Each group is denoted as a “Neighborhood”.

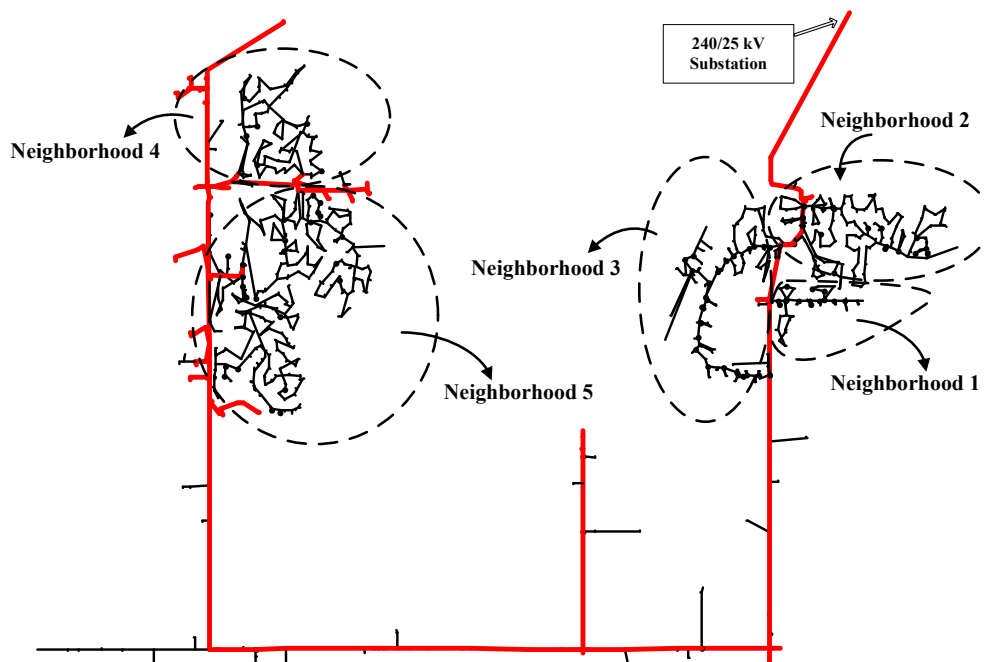


Figure D.2: Location of the five “Neighborhoods” on the distribution feeder.

Since we are interested in analyzing the harmonic levels on the main trunk feeder, each “Neighborhood” is represented as an *aggregate load model*. This procedure significantly reduces the complexity and the time duration of the multiphase harmonic power flow simulations. The steps to build the aggregated model are summarized below:

1. Identify the neighborhoods, which consists of locating the branches (and the service transformers) connected to one main trunk branch. It must be highlighted that there is no “Neighborhoods” connected to more than one main trunk branch since this would characterize a loop in the system;
2. Then, each service transformer with the respective bottom-up house models are represented by the simplified model (discussed on Chapter 5), as it was done for the ideal feeder on Chapter 7;

3. Build the admittance matrix for each neighborhood including the lateral branches, service transformer and the main trunk branch feeding the respective neighborhood;
4. All of the harmonic current sources introduced by the service transformers are also aggregated and reduced to four current sources each one connected to one of the phases. Therefore, the complexity of the simulations is reduced;
5. Finally, the substation supply source, the main trunk admittance matrix, the neighborhoods aggregated 4x4 admittance matrices, the grounding circuit are represented in a multiphase harmonic power flow program in the same way it was explained for the ideal feeder on Chapter 5.

The following sections present key results regarding two scenarios:

- ***Ideal and Actual Feeder Comparison:*** The harmonic components of voltage and current injected at the substation of both ideal and actual feeder are compared in order to verify if there is some similarity at least regarding the distribution of the harmonic components. As the ideal feeder is only composed by overhead lines, the underground cables of the main trunk of the actual feeder are replaced by overhead lines.
- ***Impact of Underground Cables:*** The objective is to compare the harmonic levels of the current calculated at the substation of the actual feeder for two cases; original feeder and modified feeder, in which the main trunk cables are replaced by overhead lines.

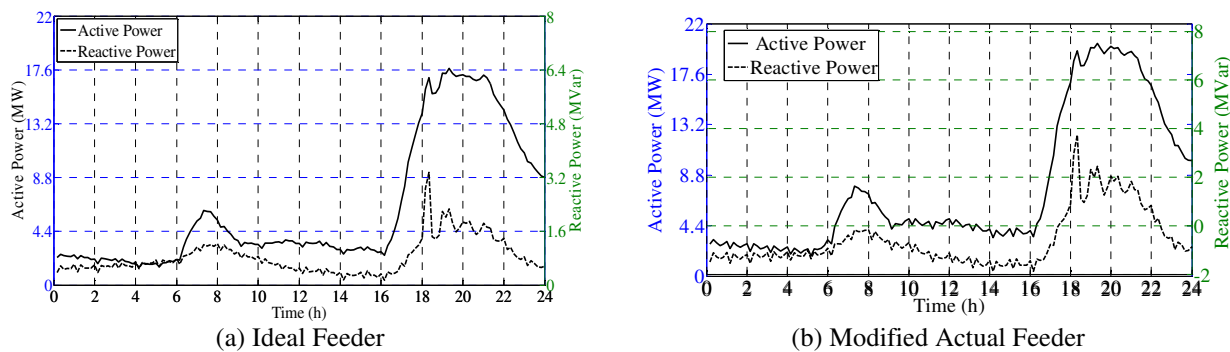
### **D.3 Ideal and Actual Feeder Comparison: Base Case**

The objective of this section is to determine if the results regarding the ideal feeder presented on Chapter 7 are adequate. Therefore, some key results related to the ideal feeder are compared to the actual feeder shown in Figure D.1. First, the base case study is analyzed and, then, the natural load evolution case study is evaluated in the next subsection. The only modification over the actual feeder is that the underground cables of the *main trunk* are replaced by overhead lines. It must be noticed the *lateral branches* (i.e., the branches that do not belong to the main trunk) remain unchanged even if those that are cables. Because of these changes, the actual feeder will be referred to as “Modified Actual Feeder” in the following results.

Since, the topology of the ideal and actual feeders are significantly different, the location of analysis is at the substation of both feeders. As it was done before, first the phase voltage to neutral (or

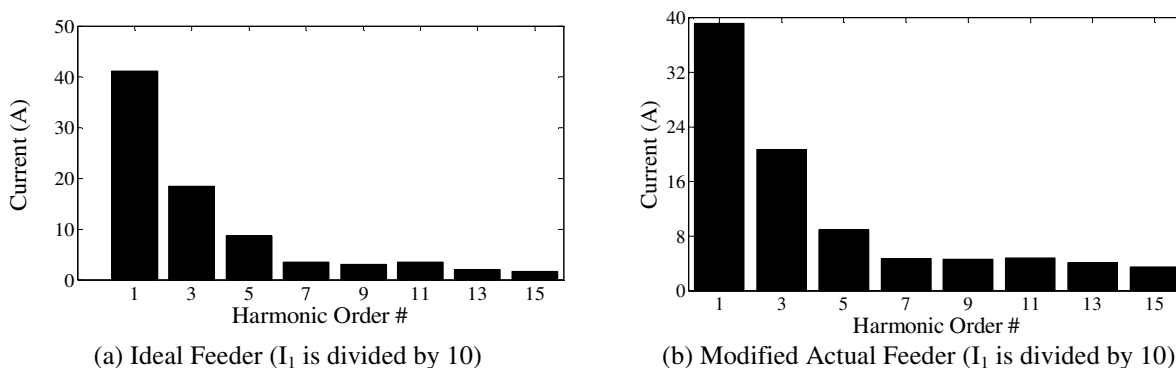
current) at the substation location are obtained, for a 24 hours period (to take into account different appliance usage), from the harmonic power simulations. Then the 95% cumulative distribution function (95% index) of this 24 hours period is determined and used for the comparison.

Figure D.3 shows the daily active and reactive power calculated at the substation location of both ideal and modified actual feeder (i.e., only overhead lines). One can observe a good correlation between Figure D.3(a) and Figure D.3(b), which is expected because the loads for both case are modeled through the bottom-up approach and the topology of the networks does not impact significantly in the results. This suggests that the results presented on Section 7.3 associated to the ideal feeder can be used with confidence. This is also corroborated by the results associated to other indices as shown below.



**Figure D.3: Daily active and reactive power at the substation.**

Figure D.4 shows the 95% index of the dominant sequence harmonic current calculated at the substation of both ideal and modified actual feeder. One can observe a good correlation between the results, which reveals that the ideal feeder can produce representative results.



**Figure D.4: 95% index of the dominant sequence harmonic current at the substation.**

Figure D.5 illustrates the average zero sequence harmonic current calculated at the substation. One can observe that the fundamental current associated to the modified actual feeder is higher than the one associated to the ideal feeder revealing that the actual feeder loads are more unbalanced. Furthermore, there is a good correlation between harmonic components.

It can also be observed that the fundamental component of the zero sequence current for the modified actual feeder is higher if compared to the ideal feeder revealing a more unbalanced system, which is expected because in the ideal feeder the loads are evenly distributed.

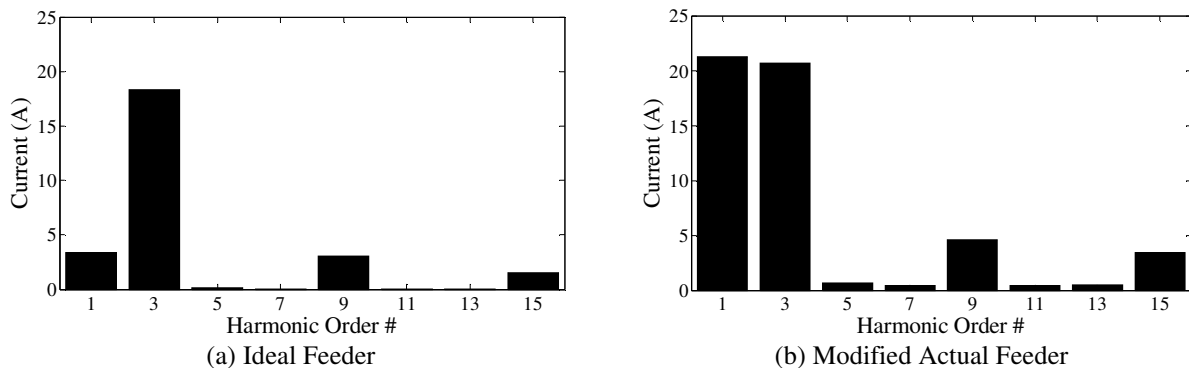


**Figure D.5: 95% index of the zero sequence harmonic current at the substation.**

Two important indices that can be used to compare different networks are the TDD and the THD since they are normalized to the loading of each network. Figure D.6 and Figure D.7 show the daily TDD and voltage THD at the substation of both feeders, respectively. One can observe a good correlation between the results associated to the ideal and actual feeders.

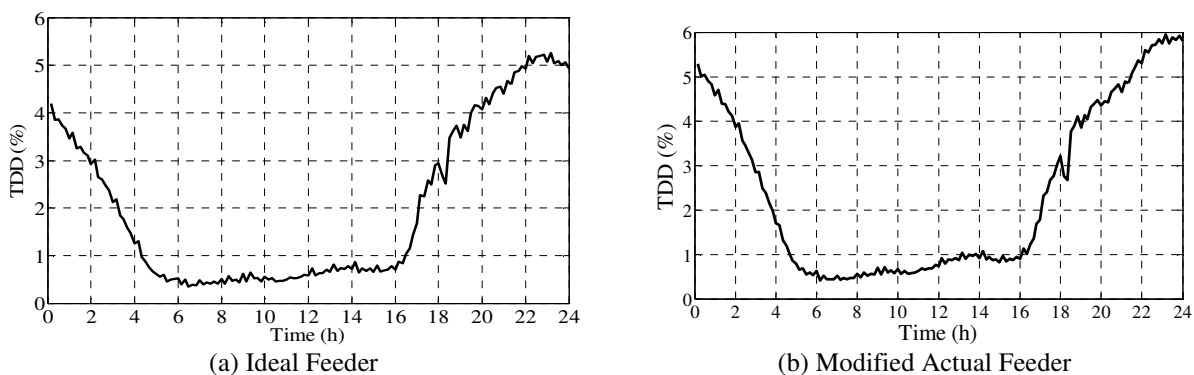


**Figure D.6: Daily TDD at the substation.**

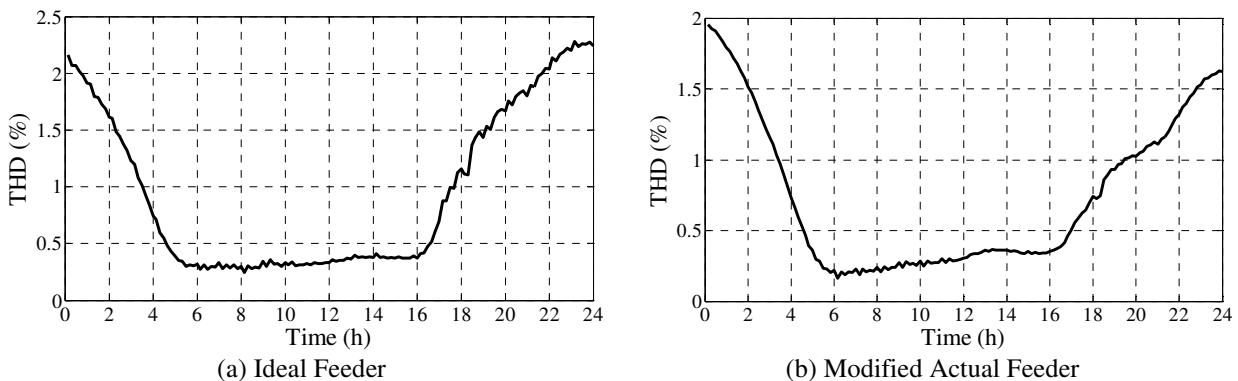


**Figure D.7: Daily voltage THD at the substation.**

Figure D.8 shows the average neutral to ground voltage calculated at the substation of both ideal



and modified actual feeders. Again, one can observe a good correlation between the results. The higher fundamental component associated to the modified actual feeder can be explained by the irregular distribution of the loads on that system. Again, the high fundamental component of the neutral to ground voltage shown in Figure D.8(b) reveals the unbalance level of the actual feeder.

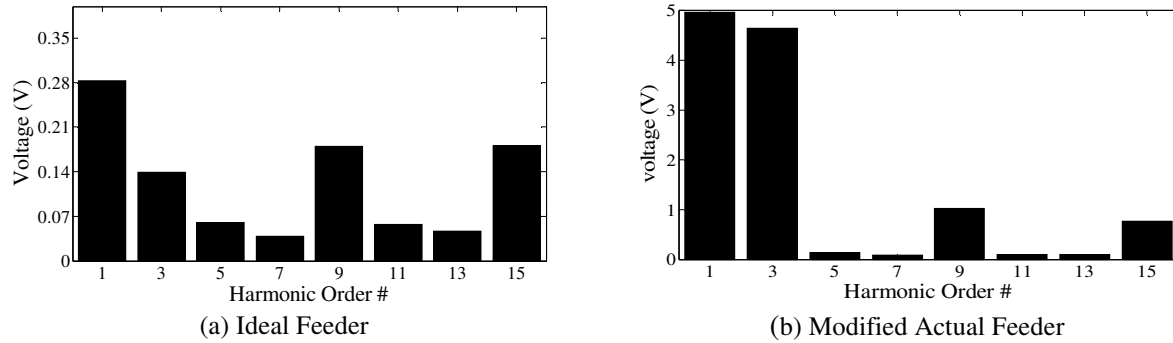


**Figure D.8: 95% index of the neutral to ground voltage at the substation.**

Figure D.9 and Figure D.10 show the average individual IT and the daily total IT calculated at the substation of both feeders, respectively. Figure D.9(b) illustrates that the results associated to the modified actual feeder confirm the conclusions obtained for the ideal feeder, which is that the individual 3<sup>rd</sup>, 9<sup>th</sup> and 15<sup>th</sup> harmonic orders are the components that most contribute for the IT level on the system.

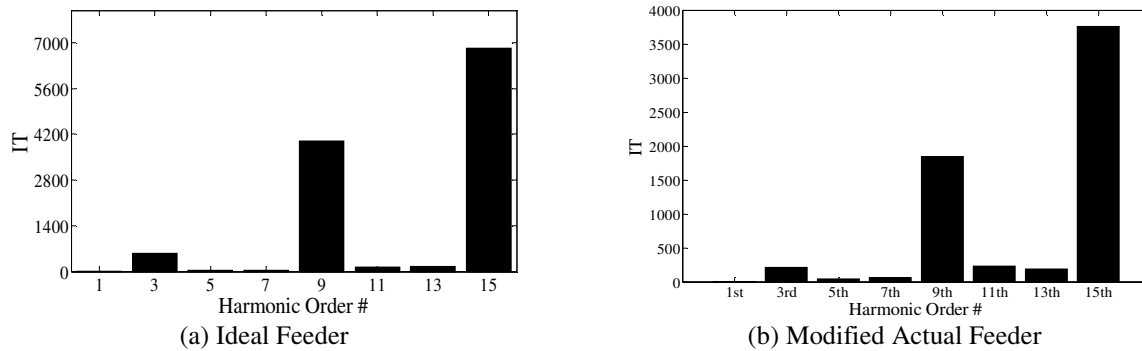


**Figure D.9: 95% index of the individual IT at the substation.**

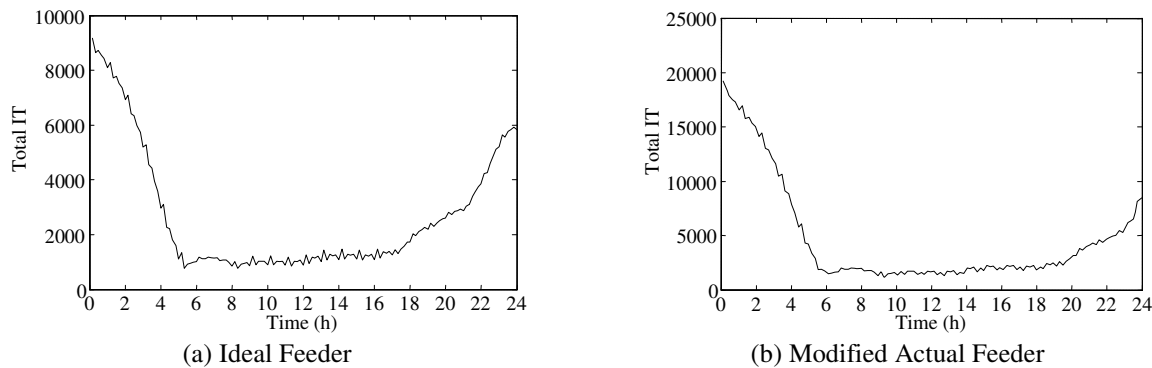


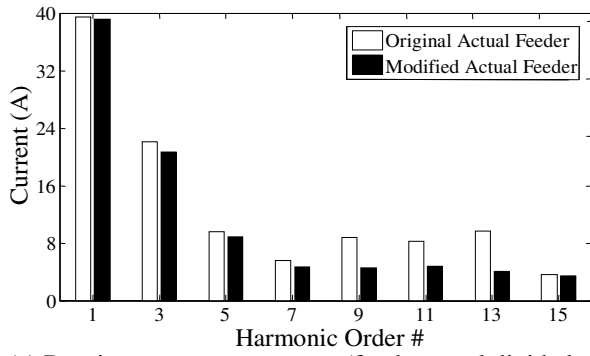
**Figure D.10: Daily Total IT at the substation.**

## D.4 Impact of Underground Cables on the Distribution System

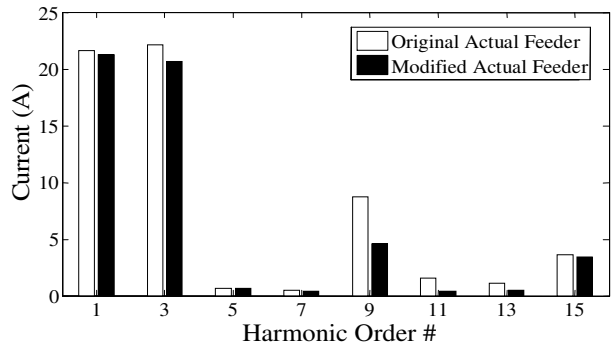
It is known that the underground cables have higher shunt capacitances if compared with overhead lines, which might impact significantly on the harmonic levels of the system. In this context, the objective of this section is to verify the impact of different types of conductors on the harmonic levels at the substation. In order to perform this comparison, two network scenarios are considered:

- **Original Actual Feeder:** The original feeder contains a mix of underground cables and overhead lines composing the main trunk
- **Modified Actual Feeder:** This is the same network analyzed on previous section, which consists of the original actual feeder, but the underground cables of the main trunk are replaced by overhead lines.

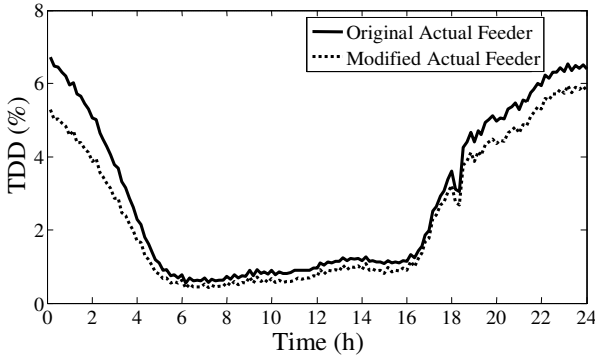
Figure D.11 shows the comparison between the original actual feeder and modified actual feeder (i.e., only overhead lines at the main trunk) for the 95% index of the dominant and zero sequence harmonic current, daily phase TDD and voltage THD and average individual IT and total IT calculated at the substation.



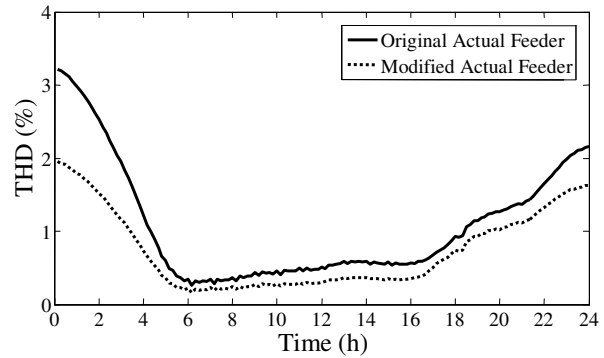
(a) Dominant sequence current (fundamental divided by 10).



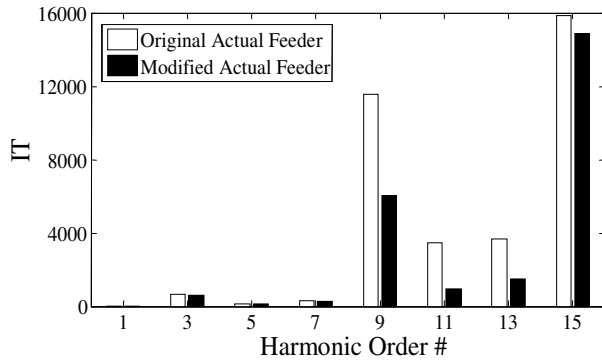
(b) Average zero sequence current



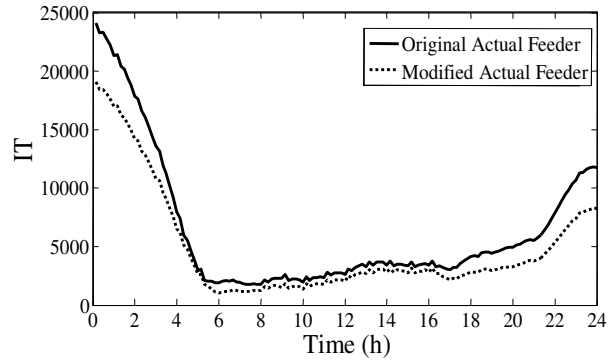
(c) Daily Phase A TDD



(d) Daily Phase A voltage THD



(e) Average individual IT



(f) Daily Total IT

**Figure D.11: Impact of underground cables on the harmonic levels at the substation.**

The main findings are as follows:

- One can observe that the presence of underground cables lead to more distortion at the network since practically all harmonic components increased.
- The increasing distortion caused by the underground cables can also be seen by the TDD and voltage THD levels shown in Figure D.11(c) and Figure D.11(d).

Figure D.11(e) shows that the presence of underground cables led to an increase of the 3<sup>rd</sup> and 9<sup>th</sup> and 15<sup>th</sup> individual IT levels. Eventually, most of the time, during the period of 24 hours, the total IT is higher when the underground cables are considered in the main trunk, as can be shown in Figure D.11(f).



# Appendix E Publications

The publications resulting directly from this research are shown below:

## *Journal publications:*

1. D. Salles, C. Jiang, W. Xu, W. Freitas, and H. E. Mazin “Assessing the Collective Harmonic Impact of Modern Residential Loads – Part I: Method”, accepted by **IEEE Transactions on Power Delivery**, 2012.
2. C. Jiang, D. Salles, W. Xu, and W. Freitas, “Assessing the Collective Harmonic Impact of Modern Residential Loads – Part II: Applications”, accepted by **IEEE Transactions on Power Delivery**, 2012.
3. S. Lin, D. Salles, W. Freitas, and W. Xu, “An Intelligent Control Strategy for Power Factor Compensation on Distorted Low Voltage Power Systems”, accepted by **IEEE Transactions on Smart Grid**, 2012.
4. S. Salas, L. C P da Silva, R. Romero, D. Salles, “Strategic Capacitor Placement in Distribution Systems by Minimization of Harmonics Amplification Due to Resonance”, accepted by **IET Generation, Transmission and Distribution**, 2012.

## *Conference publications:*

5. D. Salles, W. Xu, “Information Extraction from PQ Disturbances An Emerging Direction of Power Quality Research”, in **Proc. 15th IEEE International Conference on Harmonics and Quality of Power**, Hong Kong, 2012.
6. S. Lin, D. Salles, “A Novel Control Method for Power Factor Compensation on Harmonic Distorted Low Voltage Power Systems”, in **Proc. 15th IEEE International Conference on Harmonics and Quality of Power**, Hong Kong, 2012.
7. D. Salles, Telephone interference problems in modern residential feeders. in **Proc. Power & Energy Innovation Forum**, Edmonton, 2011.
8. T. Barbosa, D. Salles, W. Freitas, “Fluxo de Carga Harmônico Multifásico”, in **Proc. SISPOL - Encontro de Pesquisadores de Sistemas de Potência**, Campinas, 2012.

Other publications indirectly related to this PhD include:

***Journal publications:***

9. D. Salles, W. Freitas, J. C. M. Vieira, W. Xu, “Nondetection Index of Anti-Islanding Passive Protection of Synchronous Distributed Generators”, accepted by **IEEE Transactions on Power Delivery**, 2012.
10. J. C. M. Vieira, D. Salles, W. Freitas, “Power imbalance application region method for distributed synchronous generator anti-islanding protection design and evaluation”, **Electric Power Systems Research (Print)**, v. 81, p. 1952-1960, 2011.
11. D. Salles and W. Freitas, “Integrated Voltage and Reactive Power Control in Distribution Power Systems through Support Vector Machine”, in review by **IEEE Transactions on Industrial Informatics**, 2012.

***Conference publications:***

12. T. R. Ricciardi; D. Salles, R. T. Borges, W. Freitas, “Sustainable Energy and Distributed Generation Scenario in the Brazilian Electricity Sector”, In: **IEEE Power & Energy Society General Meeting**, 2012, San Diego.
13. R. T. Borges, D. Salles, T. R. Ricciardi, T. Barbosa, H. F. F. Costa, “Review of International Guides for the Interconnection of Distributed Generation into Low Voltage Distribution Networks”, In: **IEEE Power & Energy Society General Meeting**, 2012, San Diego.
14. D. Salles, “Integrated Voltage and Reactive Power Control in Modern Distribution Systems” In: **Power & Energy Innovation Forum**, 2010, Edmonton, Canada.
15. C. F. Morais, D. Salles, P. C. M. Meira A. G. P. Pavani, W. Freitas, W. Xu, “Método Prático Para a Avaliação do Impacto da Partida Direta de Motores de Indução no Afundamento de Tensão”. In: **Congresso Brasileiro de Automática**, 2010, Bonito.
16. D. Salles, “Technical Impact of Distributed Generation on Modern Power Distribution Systems”. **Invited Presentation for IV Conference for the Next Generation of Researchers in Power Systems**, Zurich, Switzerland, 2009.